An integrated method for the assessment of the seismic vulnerability of historic buildings

Speranza, Elena

Award date:
2003

Awarding institution:
University of Bath

AN INTEGRATED METHOD FOR THE ASSESSMENT OF

THE SEISMIC VULNERABILITY OF HISTORIC BUILDINGS

Submitted by Elena Speranza

for the Degree of PhD
of the University of Bath
2003

ProQuest LLC
789 East Eisenhower Parkway
P.O. Box 1346
Ann Arbor, MI 48106-1346

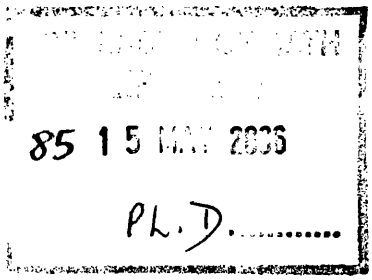
85 15 MAY 2006
PL. D.

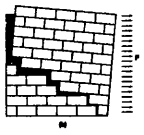

List of contents

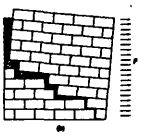

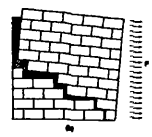

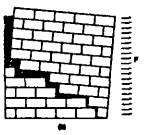

List of notations

Ai	*Instantaneous centre of rotation at a variable storey;*
C_i	*Maximum shear strength developed at a generic level;*
C_{qr}	*Horizontal restraining action due to frictional effect of the roof;*
C_{qf}	*Horizontal restraining action due to frictional effect of horizontal structures;*
C_{tot}	*Total Shear Strength along vertical crack;*
$C_{tot(1)}$	*Total Shear Strength along the upper wall portion of height H_1 involved in failure mechanism F;*
$C_{tot(2)}$	*Total Shear Strength along the lower wall portion of height H_2 involved in failure mechanism F;*
$C_{tot(\alpha c)}$	*Total Shear Strength along inclined cracks;*
$C_{tot(\beta i)}$	*Total Shear Strength developed by internal bearing walls;*
d_{fi}	*Lever harm of W_{fi};*
d_{si}	*Lever harm of W_{si};*
F	*Horizontal force distributed along the height H;*
f	*Friction coefficient along bedding surfaces;*
G_{fi}	*Centre of mass of a triangular portion of wall identified by angle α_{fi};*
G_{si}	*Centre of mass of a triangular portion of side wall identified by angle α_{si};*
H	*Total height of the wall;*
H_i	*Height of the wall including a variable number of storeys;*
H/N	*Average height of each individual storey of the wall;*
H_u	*Height of the wall portion above top horizontal hinge of failure mechanism F;*
H_{var}	*Variable height of the wall involved in failure mechanism F;*
H_b	*Height of the wall portion which does not take part to failure mechanism F;*
H_1	*Height of the upper wall portion taking part to failure mechanism F;*
H_2	*Height of the lower wall portion taking part to failure mechanism F;*
H_g	*Height of gable end;*
H_v	*Height of vertical addition;*
H_g	*Height of gable end;*
h_i	*Height of the wall (from top) above generic bedding surface;*
l_o, h_o	*Average length and height of openings;*
ℓ, h, b	*Length, height, thickness of a regular stone block;*
ℓ_α	*Variable length defining the wall portion involved in failure mechanism G;*
I_s	*Structural index;*
I_f	*Failure extent index;*
$I_{s(-)}; I_{s(+)}$	*Lower and upper boundaries of the structural index;*
$I_{f(-)}; I_{f(+)}$	*Lower and upper boundaries of the failure extent index;*
L	*Length of the wall;*
L_{var}	*Variable length of the wall;*
N	*Number of storeys of the wall;*
n	*Number of layers in a wall of total height H;*
Op_1	*Percentage of openings at a variable storey of the wall;*
Op_i	*Cumulative percentage of openings and chimney flues at a variable storey of the wall;*
Q_{fi}	*Total vertical weight of horizontal structures acting on each intermediate storey of the wall;*
Q_r	*Total vertical weight of roof acting on top of the wall;*
Q_u	*Vertical load simulating the weight of the wall portion identified by H_u;*
Q_{rs}	*Total vertical weight of roof acting on top of side walls;*
Q_{fs}	*Total vertical weight of horizontal structures acting on each intermediate storey of side walls;*
q_{r_1}	*Vertical weight of roof distributed over the total length of the wall;*

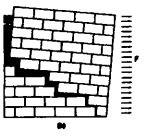

q_f *Vertical weight of horizontal structures distributed over the total length of the wall;*
q_{rs} *Vertical weight of roof distributed over the total length of side walls;*
q_{fs} *Vertical weight of horizontal structures distributed over the total length of side walls;*
R_{lim} *Frictional resistance developed by triangular edges of failure mechanism G;*
R_L *Reliability level of information;*
R_T *Total reliability of information;*
R_w *Weight factor assumed for each field of the survey form;*
s *Stagger ratio of an opus quadratum fabric;*
T_b *Wall thickness at top of the wall;*
T_u *Wall thickness at bottom of the wall;*
T_i *Wall thickness at generic storey of the wall;*
T_k *Wall thickness at level k corresponding to intermediate hinge of failure mechanism F ;*
T_m *Average wall thickness of the wall;*
T_{ri} *Reduced wall thickness at a generic storey of the building;*
T_v *Thickness of vertical addition;*
V_{ij} *Seismic vulnerability;*
W_{tot} *Total weight of the wall;*
W_i *Weight of a generic storey of the wall;*
$W_{tot(\alpha c)}$ *Weight of the wall portion identified by the crack angle* α_c ;
$W_{(\alpha j)}$ *Weight of the portion of side wall identified by the angle* α_j;
W_{fi} *Weight of a triangular portion of wall identified by angle* α_{fi};
W_{si} *Weight of a triangular portion of the side wall identified by angle* α_{si};
W_v *Weight of the vertical addition;*
W_g *Weight of gable end;*
W_F *Weight factor in relation to the type of failure mechanism;*
w *Weight of a generic stone block;*
X_{ij} *Seismic risk;*
Y_j *Hazard for ground motion of severity j;*
α_b *Geometric ratio of the wall defined by arctan s/h;*
α_c *Crack angle;*
α_{fi} *Crack angle of the wall defining the failure mechanism C;*
α_p *Stagger ratio of stones defined by arctan L/H;*
α_{si} *Crack angle of the side wall defining the failure mechanism C;*
β *Number of internal bearing walls orthogonal to the wall under exam;*
γ *Specific weight;*
$\Delta x_{i,j}$ *Horizontal lever harm for rotational equilibrium;*
$\Delta y_{i,j}$ *Vertical lever harm for rotational equilibrium;*
ε *Number of edge side walls strongly connected with the wall under exam;*
η *Number of regular side piers due to openings layout;*
λ, λ_c *load factor described by the ratio between lateral acceleration a and the gravital acceleration g;*
λ_o *Overturning load factor;*
λ_s *Sliding load factor;*
$\lambda_{(m,i)}$ *Load factor relative to a given failure mechanism at a variable storey of the wall;*
μ *Critical load factor;*
ν *Variable governing the position of the intermediate hinge of failure mechanism F;*
$\mathcal{D}$ *Domain of existence;*
$\%tr_1$ *Percentage of wall thickness reduction as function of the level of maintenance of masonry;*
$\%tr_2$ *Percentage of wall thickness reduction as function of the lack of verticality;*
$\%tr_3$ *Percentage of thickness reduction on the top storey;*
$\%tr_4$ *Percentage of effective sliding surface along masonry fabric layers;*
$\%tr_5$ *Additional percentage of openings due to chimney flue;*
$\%F_w$ *Percentage of wall surface involved in the failure mechanism;*
$\%F_{rf}$ *Extent percentage of failure of roof and/or horizontal structure;*

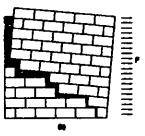

$\%F_f$ *Percentage taking into account the collapse of horizontal structures;*
$\%F_r$ *Percentage taking into account the collapse of roof;*
$\%R$ *Percentage taking into account the reliability of information;*

List of figures

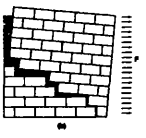

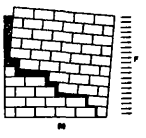

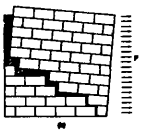

List of tables

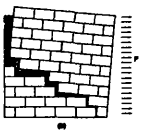

Acknowledgements

This work is dedicated to Prof. Antonino Giuffrè, who first encouraged me to undertake research in the field of seismic vulnerability of historic centres. Although his premature death has not allowed him to see this work, I sincerely hope that he would be proud of what I have attempted to do.

My deepest thanks go to my supervisor, Dr. Dina D'Ayala, who has supported me during these years. Her suggestions, critical comments, and inspired discussions have been essential to carrying out the entire work.

I also wish to thank Prof. Alberto Bernardini, with whom I have carried out other parallel work in the same field, and who has followed the developments of this study, with continual interest. Prof. Mauro Dolce and Dr. Agostino Goretti have been invaluable in providing data and documentary material concerning the 1997 earthquake in Umbria-Marche, Italy.

I also express all my gratitude to my mother, my father, my husband, for having been so understanding and having supported and encouraged me in overcoming any difficulties. Without their invaluable help I could not have concluded my research.

Finally my special and dearest thanks go to Veronica and Myles Metcalfe, who I had the pleasure and luck to meet during my first year in Bath, and who have become dearest friends. Their kindness and affection during my stay in Bath, have allowed wonderful memories of that period of my life.

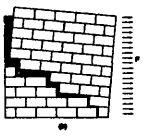

Summary

The study of the seismic vulnerability of historic buildings has become an autonomous research field, mainly in the wake of some catastrophic seismic events which occurred in Europe in the 80's. These events and the damage caused to buildings, particularly when historical, highlighted the need for suitable and reliable tools to calibrate the intrinsic vulnerability of buildings, the associated seismic risk and to develop appropriate strategies for mitigating their damage.

Although many different approaches have been developed over the years, the seismic vulnerability of existing buildings has so far focused mainly on monumental or individual historic buildings, while ordinary "anonymous" buildings making up the bulk of historic European centres have been almost neglected. One of the reasons for this neglect is the difficulty of modelling the wide heterogeneity and complexity of a typical historic centre in a reliable and at the same time extensive way. Most procedures developed so far are based on drastic simplification and generalisation of the construction characteristics, and hence are inadequate for predicting the mechanical performance.

The objective of this work is the evaluation of the seismic vulnerability of masonry buildings with a focus on ordinary historic buildings.

The method proposed, named FaMIVE (*Failure Mechanisms Identification for Vulnerability Evaluation*), enables analysis of medium-size samples of buildings without foregoing a detailed understanding of their constructive and structural layout.

The approach pursued is based on the identification of feasible collapse mechanisms and on the calculation of their associated load factors. The mechanical performance is defined by a model of frictional behaviour developed specifically, on the basis of which the failure mechanisms are formulated.

This formulation gives rise to a new definition of seismic vulnerability by predicting not only the extent of expected damage but also the associated feasible failure modes.

The work is organised by introducing in Chapter 1 a review on the state of the art in this research field outlining results achieved and general limits of the available literature. This

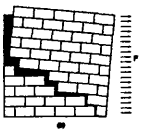

preliminary review enables a possible way to develop the research to be sketched out, and also to introduce the methodological assumptions for the new procedure.

Chapter 2 introduces the theoretical basis of the work, by formulating a model for the frictional behaviour of stone ashlars masonry, followed by the analytical developments of failure mechanisms. Chapter 3 describes the general framework of the procedure, ranging from the survey phase and criteria of data collection to the final evaluation of vulnerability. Chapter 4 presents the results of a survey carried out in the historic town of Nocera Umbra (Italy), hit by several seismic shocks in September-October 1997. This Chapter illustrates the damage investigated as well as the constructive features recorded according to the investigation criteria presented in Chapter 3.

Finally, in Chapter 5 the results of applying the method, in terms of expected damage and vulnerability, enable the approach proposed to be validated and its limits to be highlighted.

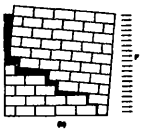

CHAPTER 1
INTRODUCTION TO THE RESEARCH TOPIC

1.1 Introduction

This Chapter presents the state of the art on the research topic, in order to outline the methodological assumptions of the new method.

Once the seismic vulnerability has been presented in a general context, as one of the factors defining the seismic risk, together with some associated physical entities, a critical discussion on the literature available on the topic is pursued. Particular attention is paid to methods based on structural approaches, with a special section dedicated to those based on failure mechanisms and limit states.

Using this review process some conclusions can be drawn about the effectiveness of the various approaches, so that the theoretical framework for developing the research can be outlined.

A final section is devoted to a survey, carried out using photographic material from different earthquakes, aimed at recognising common failure mechanisms occurring in historic centres, following a seismic event. The results achieved, are assumed as operative tool for developing the new method.

1.2 Seismic Risk and Vulnerability: definitions

The seismic risk, defined by an international convention agreed upon in 1979, refers to the expected losses, following catastrophic events, in a region or population, or a settlement of buildings, over a specified time period (UNDRO, 1979).

According to the definition of the element at risk, the risk may be measured in terms of expected economic loss, in terms of the numbers of lives lost, or the extent of physical damage to property, where appropriate damage assessment is available (Coburn et al., 1992). The damage severity, and therefore the risk itself, depends on three orders of factors:

- Nature, number and intensity of earthquake which could occur in a given area;

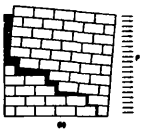

- Distribution of resources and population exposed;
- Capacity of the resources to survive the event, measured by the effects which earthquakes could produce on settlements;

These aspects are strictly linked to three variables named *hazard, exposure* and *vulnerability.*

Hazard is the probability of an earthquake or earthquake effects of a certain severity occurring within a specific period of time in a given area. Therefore it is strictly linked to the physical characteristics of seismic events.

Exposure and *vulnerability* refer to the quantity and quality of resources exposed to the seismic hazard, and also to the number of people involved and their ability to react (CNR-GNDT, 1993).

These three variables all refer to a given territorial area, clearly located and defined, and can be related by the following formulation of seismic risk (UNDRO, 1979):

$$[X_{ij}] = [Y_j] \cdot [V_{ij}] \qquad (1\text{-}1)$$

where, for each element *i* for which the risk is to be evaluated:

[Xij] is the risk; the probability of loss of element *i* due to earthquake ground motion of severity *j*;

[Yj] is the hazard; the probability of experiencing earthquake ground motion of severity *j*;

[Vij] is the vulnerability, the level of loss that element *i* would undergo as a result of experiencing earthquake ground motion of severity *j*;

1.3 Earthquake characteristics and damage

An effective and synthetic definition, proposed by Sandi, compares the seismic vulnerability of a building to its seismic performance, by means of a cause-effect law, according to which the earthquake is the cause while the damage is effect (Sandi, 1986).

Vulnerability can be most easily defined by the degree of loss of a given element at risk resulting from the occurrence of a specified earthquake (EERI,1984).

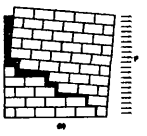

These two definitions clearly illustrate that seismic vulnerability is strictly linked on the one hand to the physical event (*earthquake*), on the other hand to *damage*, while the relation between these two variables has to be assessed.

As the definition of these parameters usually changes from method to method, a clarification of their nature is required.

The *earthquake* characteristics are generally described in terms of either macro-seismic intensity I, or in terms of peak ground acceleration *PGA*, sometimes measured as a ratio to the gravitational acceleration *g*. Although hard to assess, the passage from one parameter to the other can be carried out using specific methods, proposed by several authors (Murphy et al., 1977, Margottini et al., 1993). The weak point of macro-seismic intensities is that they are based on damage effects, and hence can be influenced by a subjective component. On the contrary, the peak ground acceleration *PGA* is a physical entity, though strictly related to a limited geographic area, as deeply influenced by soil characteristics .

A more rigorous way to describe the seismic action is represented by the amount of energy released by the earthquake at its focus, known as the magnitude, M. However, this variable is rarely used for vulnerability evaluations, as rather difficult to correlate with the structural performance of buildings.

The *damage* can be described in several ways, i.e. based on economical estimates, or scales with qualitative descriptions, or by the use of structural parameters.

The first criterion usually expresses the cost of repairs of the damaged item in comparison with the total reconstruction costs. The main problem with this method is how to compare the variable, working in a continuous interval (0,1), between different areas because this is strictly linked to the social-economical characteristics of the place in question. Moreover, it is extremely variable with time and location, so that a comparison between damage occurred in different areas hit by different earthquakes is not possible (CNR-GNDT, 1993).

Damage as defined by the Italian Group for Defence against Earthquakes (GNDT), is also based on economic estimates, and defined by a hybrid variable, depending both on the extent and gravity of the damage in the different parts of the building together with their economic weight (Benedetti et al, 1984a).

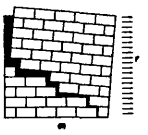

When defined by qualitative descriptions (light, heavy etc), such as the damage scenarios of macro-seismic scales, every damage level is described with accuracy and is associated with a given extent. The disadvantage of this method is that it does not work on a numerical scale, and hence the damage assessment can be influenced subjectively by the surveyor.

Finally, the damage can also be expressed in structural terms. In this case the performance of the building in terms of evaluation of its structural "response" has to be taken into account.

The problem is basically dynamic in nature, since the response of a structure can be defined by comparing the frequency content of the earthquake with the natural frequency of the building, its energy dissipation and its deformation capacity.

1.3.1 Vulnerability functions: general purposes and common formulations

The relation between earthquake and damage forms the crucial issue around which this field of research has developed for several years.

As a matter of fact, only after formulating appropriate functions establishing a relation between earthquake and damage is it possible in general to move on from the *observed vulnerability* to the *predicted vulnerability.*

While the former one refers to assessments deriving from direct observations of damage, or based on statistics of past earthquake damage, the latter one refers to the estimates of expected behaviour of buildings based on calculations and forecasting criteria.

For a vulnerability function to be reliable, it must fit the observed vulnerability data, that is past earthquake damage information.

A vulnerability function can be defined according to either probabilistic or deterministic approaches. Because of the uncertainty of the variables dealt with, a proper way to define a vulnerability function is the probabilistic criterion, according to which every value of the earthquake (y), corresponds to infinite possible values of damage (d). A value of conditioned probability density $p \cdot dy$ function is associated to each of them.

In the same way, for each value y it is possible to express two functions $p\{y|0\}$ and $p\{y|1\}$ which determine the probability density of y as regards the value 0 and 1 of the damage index, ranging from 0 and 1. Figure 1- 1 shows a generic vulnerability function

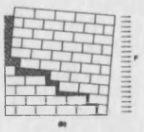

defined by a probabilistic approach. In the same figure y_i and y_c refer to the earthquake parameters respectively at the beginning and at the end of damage.

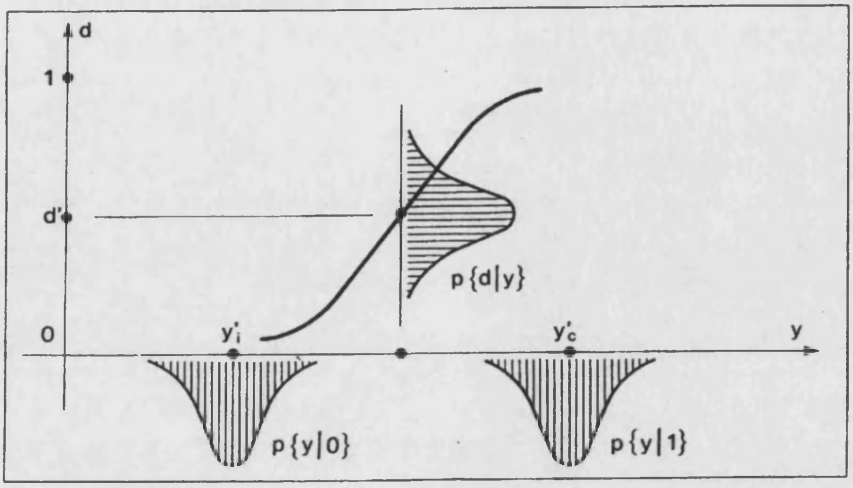

Figure 1- 1 – Vulnerability function defined by probabilistic approach (CNR-GNDT, 1993)

If, in place of a probability function, a non-continuous function is assumed, the conditioned probabilities P{d | y} refer to a finite number of couples d_h, y_k.

In this case Damage Distribution Diagrams or Damage Probability Matrix (DPM) can be produced, whose generic element is P{ d_h | y_k.}.

The DPMs, first used by Whitman (Whitman, 1973), show the probability distribution of damage among different damage states, for each level of ground shaking. A separate matrix is defined for each class of building or vulnerable facility.

This criterion was first used following the San Fernando earthquake of 9 February 1971, which caused damage to approximately 1600 buildings, with 5 or more storeys.

The basic assumption of this procedure is that in any location hit by destructive earthquakes, buildings generally suffer different states of damage. Once the buildings are divided into representative structural classes, the damage distribution for each class, relative to a given macro-seismic intensity, can be described by means of histograms or matrix.

This kind of distribution is strictly related to the severity of ground motion so that, generally, where high intensities have been experienced, the damage probability distribution peaks for high levels of damage (Coburn, et al., 1992).

This format of a damage probability matrix has become the most widely used criterion to define the probable distribution of damage, adapted by several authors for different purposes.

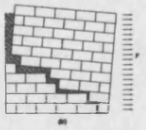

The advantage of DPMs is that they can be used for forecasting purposes, by predicting the damage levels for similar classes of buildings at any given level of intensity of ground shaking. However, their validity is restricted to a specific geographic area, so that their application to other different sites is arbitrary and scarcely reliable.

An alternative set of vulnerability functions related to commonly observed building types in earthquake prone areas, has been developed by Spence et al. (1991). The novelty of this approach is the definition a new intensity scale associated to damage distribution, avoiding the use of macro seismic intensities. The procedure is based on data collected during different case studies of damage caused by a number of earthquakes from a range of different countries. Five different damage grades are considered. For each building type the scatter of the intensity at which each individual structure passes a given damage threshold is assumed to be normally distributed. The damage distribution is expressed graphically by the probability of going beyond a certain damage grade given the seismic input defined by a parameterless scale of intensity, named PSI (*Parameterless Seismic Intensity*), (Spence et al. 1991, 1992b). Figure 1- 2 shows an example of PSI for earthen brick masonry.

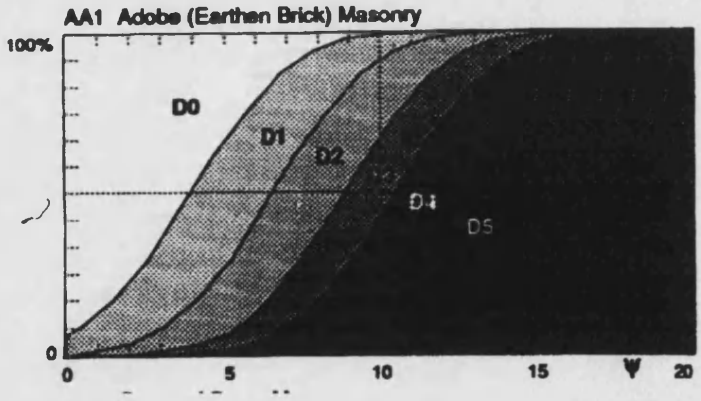

Figure 1- 2 – Example of PSI curve for earthen brick masonry (Cobourn et al., 1992)

The drawback of probability methods like DPM, or PSI is that, in order to carry out probability processing, they require a considerable amount of data on past earthquakes damage and building classes.

Where data are missing or inadequate, other methods giving reasonable and sufficiently reliable results are required. In most cases, in place of earthquake-damage probabilistic

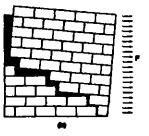

relationships, deterministic functions are used, formulated using a more restricted data set, more often obtained from one or a few damaged locations.

The approach pursued by GNDT in Italy (Benedetti et al., 1984a), is based on deterministic functions between earthquake and damage. These relations are characterised by a tri-linear pattern in the interval (y_i, y_c), where y_i and y_c are the same as in Figure 1- 1.

According to this criterion, every given curve *d(y)*, depends on the structural characteristics of the building, which are summarised by a vulnerability index.

1.4 Review on the seismic vulnerability studies

The issue of how different classes of buildings resist earthquakes, and also how their seismic performance can be improved, first emerged clearly, following some events which occurred in Europe, particularly in Romania (1977), Montenegro (1979) and Italy (1974, 1980).

These seismic events found the countries totally unprepared to face emergency situations and without proper criteria to evaluate damage on retrofitting strategies.

One common problem was the lack of clear and suitable specific codes aimed at strengthening or rebuilding damaged structures.

In Italy, the earthquakes occurring in the 70's particularly stressed the urgent need for appropriate criteria aimed at seismic risk evaluation. Most of the districts, damaged by the 1974 (Friuli) and the 1980 (Irpinia) events, were not included in the national seismic list, and this meant that constructions there did not need to comply with seismic codes. The reconstruction and retrofitting interventions, in the absence of any kind of guidelines, were left to the individual decisions of technicians, without general supervision. Other towns, even if listed in the national catalogue, also suffered heavy damage, even in buildings designed in accordance with the seismic codes.

A first step attempting a radical change in the strategic policy, shifting the emphasis from the management of emergency situations to forecasting of damage likelihood, was the so called Geodynamics Project. This Project, developed in 1980 by the Italian National Research Centre, (CNR), created a new seismic catalogue for Italy, a new method able to evaluate the

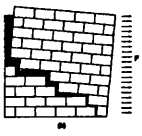

seismic risk for listed areas, general criteria to mitigate risk, and a new seismic code. One of the most important objectives reached consists of specific Seismic Risk Maps, recently upgraded (Slejko, 1999), whose purpose was to map the level of risk, hazard, and vulnerability due to seismic events, over the whole Italian territory (Postpischl, 1986).

These important experiences, which likewise characterised other countries, rapidly led to a process of specialisation of some aspects linked to seismic risk. Around this time, the vulnerability, until then strictly linked to risk analysis, became a separate field of research.

This general context, highlighted the urgent need to set up proper strategies of analysis for predicting and mitigating the effects of earthquakes on historic heritage, so far neglected.

1.4.1 Possible targets in the vulnerability assessment

Vulnerability assessment is generally characterized by a great diversity due to its different possible objectives: decisions in the post-earthquake emergency, strategies to reduce seismic risk, predictions for seismic upgrading, territorial planning, macro-seismic mapping, the property insurance market.

A second reason for this variety arises from the extreme variability of the resources and time available for the investigation, especially when dealing with very extensive applications.

A consequence of this is that the present state of the art shows a wide range of methods, without considering anyone of them as being suitable for all cases (Corsanego, 1985).

Undoubtedly one of the crucial aspects influencing vulnerability evaluation is represented by the scale of the assessment. Large scale assessments, involving whole urban area or large regions, require speedy methods, and these are generally based on observed vulnerability or expert opinion. Large scale assessments are carried out for different objectives, ranging from the seismic performance to property insurance market.

When the assessment involves a block of buildings or even a single building, the vulnerability evaluation is based on more accurate analysis obtained by detailed inspections. In this case methods based on score assignments are commonly used, or procedures focusing on the structural performance of buildings.

The crucial issue is that each method, independently from the approach pursued, necessarily has to find its own compromises between the scale of the assessment and the accuracy of results produced.

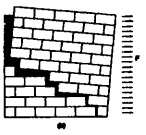

The criterion followed in presenting and critically discussing the available literature on the topic, is based on the level of accuracy of each method, the time expenditure required, and the reliability of results produced. Starting from criteria relying on observed vulnerability or experts opinion, progressive levels of detail of analysis are introduced and some final conclusion are drawn at the end of each section.

1.4.2 Methods based on observed vulnerability or experts opinion

One of the first attempts to codify the seismic vulnerability at a large scale, is undertaken in the U.S. by the Applied Technology Council (organisation born in 1971 for the assistance of practising structural engineers), founded by the Federal Emergency Management Agency (FEMA). Among the works carried out by the ATC, it can be mentioned the so called ATC-13, aimed at the damage evaluation in California (ATC-13, 1985).

The results achieved by ATC-13 are the creation of damage probability matrices, for 78 different structures types, 40 of which are buildings. The particularity of the method is that the DPM, relative to different structural types as well as to different seismic intensity are defined throughout the opinion of 78 experts, which are asked to give an estimate of the most likely damage level which would occur for each specific structural type in occasion of a given earthquake severity. The weak point of this method is clearly represented by the subjective component which cannot enable reliable results. However this method has represented one of the most common operative tools, during the 80's.

A similar approach is pursued by macro-seismic scales, as MSK and EMS (Medvedev, 1977, Grunthal, 1993,1998), in defining vulnerability classes, in order to speed up and improve post-earthquake macro-seismic surveys.

The EMS 92 scale, upgraded in 98, is intended as an improvement of the MSK in the classes definition, as it is characterised by a wider range of classes, passing from 3 of the MSK (A,B,C) to a total of 6 (A,B,C,D,E,F). These additional classes refer to buildings designed in accordance to seismic codes. The criterion is based on the assignment of vulnerability classes to different building types, which can be carried out by experts whose subjectivity represents the basic limit of this approach.

The prediction of damage is carried out by providing damage distribution over the 6 levels considered (from 0 to 5) for each vulnerability class and each macro seismic intensity.

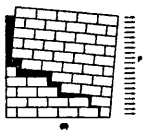

Evaluations of vulnerability at urban or even regional scales, using EMS or MSK, have been carried out in many applications worldwide. Recent research has been conducted in the city of Barcelona, Spain. In this case the old vulnerability classes of MSK are used, and the wide variety of building types is grouped into the 3 MSK classes (Pujades et al., 2000).

Another work with similar aim has been carried out on the city of Basel, which has been considered as test-site for a wider application aimed at creating damage scenarios for Switzerland (Fah et al, 2001). In this case EMS 98 classes are used and vulnerability curves are obtained for each class as function of the earthquake intensity.

An attempt to improve the capability of the macro seismic scales, as far as vulnerability evaluations are concerned, has been recently carried out by Dolce et al. (2000). The authors propose a criterion for upgrading the EMS 98 vulnerability classes by taking into account the reinforcments which a structure can undergone during its lifetime.

The novelty of the work, applied to the town of Potenza, Italy, lies in the fact that a double vulnerability class is associated with the 21 building types considered, according to the case of absence/presence respectively of strengthening devices.

Notwithstanding the huge subjectivity of vulnerability classes, the official method used in Italy for vulnerability evaluations, developed by GNDT in 1983 (Benedetti et al., 1984a), is characterised by two levels of screening (known as level 1 and level 2). The first of the two is basically aimed at assessing vulnerability classes. The purpose of this level is to obtain general information about the location, geometry and type of buildings and is suitable for all kinds of structures. Moreover, the observed damage, mentioned in §1.3, is registered throughout its severity and extent percentage.

In 1980, following the earthquake which occurred in Irpinia, Italy, a wide survey on the damaged buildings was carried out using a pilot version of GNDT level 1.

The work was based on a preliminary classification of the buildings according to a pre defined range of 13 construction types. Thanks to the large amount of data collected in the post earthquake phase, during which 41 towns and about 38.000 buildings were surveyed, diagrams providing damage probability values for each MCS macro seismic intensity and for each structural type were created.

By assembling these diagrams it was possible to create DPMs, for each of the 13 building types. These distributions were then compared with others developed as function of the MSK

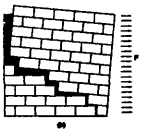

scale, where the gaps due to incomplete data were filled by binomial distributions (Braga., et al., 1982 a,b).

One of the limits of this approach, as underlined by some authors, is that the vastness of the building classes usually considered, and also the rough way in which they are defined, can yield ineffective probability curves (Carocci,1996).

Other authors have underlined that aggregating data on the basis of assigned intensities can lead to large distribution error. Macro seismic intensities are considered, by the same authors to be scarcely reliable and hence a poor model of vulnerability (Coubum et al., 1992).

An interesting recent application carried out by the Italian Seismic Service (Orsini, 1999), using the Irpinia earthquake data, has enabled the uncertainty of the damage evaluation performed with DPM expressed in MCS intensity to be estimated. This objective has been achieved by using the Parameterless Scale of Intensity (Spence et al., 1991), which has been compared to the MSK and MCS degrees resulting from the Italian seismic catalogue. A good correlation has been found with the MSK intensities, while a scatter is evident with the MCS intensities.

A rapid method for the assessment of vulnerability buildings was carried out by the FEMA (Federal Emergency Management Agency) in 1988 (FEMA 154, FEMA 155). The procedure requires a rather rapid survey of the building, carried out from the street, aimed at recording data for assessing the vulnerability index, governed by an appropriate score. In this case the method is based on a first association of the building under examination to a pre-defined range of building types; a different *structural hazard score* (BSH) is associated to each of them. This score can be then modified according to the peculiarities (improving or worsening the seismic performance) of the single building. The value of BSH is linked to the probability of exceeding damage to 60% of the building for a specified earthquake severity, and is directly derived from ATC-13 probability matrices. However, while the BSH is expressed as function of peak ground acceleration, the DPMs of the ATC-13 use macro-seismic intensities, so a conversion between the two factors is also required. As for ATC-13, the weak point of this procedure is the subjective component, as the modification factors are evaluated by expert opinions.

A new and highly sophisticated research field, is the application of neural networks to seismic vulnerability assessment (Sanchez et al. 2001). This method, combined with the use

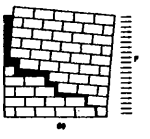

of fuzzy logic (Blockley, 1992, Carpignano et al.2002, Ballocco et al.2003) and system theory, is used to assess the structural damage for a given earthquake. The model is able to synthesize multiple factors to reach an overall evaluation considering the dependence and interaction between all system components. The ten variables implemented as input data (ranging from ground motion to construction qualities of the building), are expressed by linguistic values of expert opinion based on linguistic variables associated to fuzzy sets. These are then transformed into numeric values by carrying out a "defuzzification" process as a transfer function. Values resulting from this process are then used to define the damage. This method was applied by comparing the damage observed in Central California following the earthquake of 1999 to forecast damage, as results of the neural network computer software ERS-99. The capability of the program is that it is characterised by a "learning process" of encoding information. This means that the system compares the expected output of any input data, to the data set within the system. If the two sets of data do not match, the system is able to adapt its internal structure to include a new pattern and hence widen the "knowledge" of the system. Despite the big effort made to improve the reliability of information from experts opinion, the extreme generality of the method (suitable for any structure type) does not enable all the variables qualifying all structural systems to be considered, and this leads to unreliable evaluations of the seismic performance of buildings and hence of damage prediction.

All the methods mentioned have features in common, which can be summarised as follows:

- Most of them are based on the definition of building types and classes, suitable for any location worldwide;
- Building types and classes are too general all-inclusive;
- The subjectivity of the operator (usually an expert) in the class assignment process can cause results to be somewhat unreliable;
- In the absence of pre-defined classes the information required to describe the building type is very general and scarcely able to identify the aspects qualifying the seismic performance of the building;
- The earthquake characteristics, as outlined in §1.3, are described by macro seismic intensities which rely on damage effects and hence are poor models of vulnerability (Coburn et al., 1992).

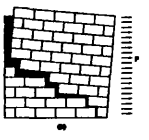

- The damage is evaluated by its severity and in some cases by its extent, but no effort is made to give an interpretation from a structural point of view.

1.4.3 Methods based on score assignment

Observation-based, statistical methods that assign a seismic vulnerability score to buildings are among those most widely used. This category also includes the approach developed by GNDT, level 2, based on a detailed survey of the building. This level of screening produces a measure of the level of vulnerability of a single building, synthesised by a hybrid index.

Unlike from level 1, which is considered suitable for any type of structure, level 2 follows different methods according to whether the building is made of masonry (Benedetti et al., 1984a) or reinforced concrete respectively (CNR-GNDT, 1993).

The vulnerability index for masonry buildings is obtained from the sum of eleven parameters. Each parameter defines a particular factor which is considered decisive for the seismic performance. For each factor, the different situations which can arise in reality, are grouped into four classes. The first one, taken as reference, collects all the situations which may be considered as substantially conforming to the seismic codes. The other situations are arranged in an increasing scale of vulnerability, with corresponding scores. The scores of each factor, weighted in relation to the importance assigned to each class, are added together so that the total represents the vulnerability index for a given building (Benedetti et al.,1984a).

The capacity of the structure to resist an earthquake is defined by a special parameter, named *conventional resistance,* which is a function of the shear stress τ_k of the material. According to this criterion, collapse can only be caused when the shear strength is exceeded, while failure due to bending is completely disregarded.

The GNDT vulnerability index relating to a single building or a class of buildings, is also used for developing damage scenarios, using a tri-linear earthquake-damage relation introduced in §1.3.1, calibrated on just one test site (Guagenti et al., 1989). Further statistical calibrations of the GNDT vulnerability index were also carried out by Braga et al. (1987). GNDT level 2 has been used for several applications, one of the first being that carried out by Beconcini et.al in 1984, in a small town of central Italy (Castelnuovo in Garfagnana). The

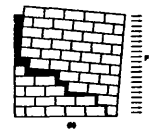

results of this application are particularly remarkable because they demonstrate that the criterion used by GNDT level 2 to assign scores based on conformity with seismic codes is not completely reliable. As a matter of fact, even new buildings, designed in accordance with the seismic regulations, show damage as heavy as the historic ones.

In the following years, the GNDT method was applied in the city of Catania, Sicily (Benedetti et al.,1988a, CNR-GNDT, 1999). In this case the data on building heights and construction periods used in the analysis have been either collected from field investigations, or from a database provided by ISTAT[1]. After assigning a range of likely values to the construction period data set, the final results indicated lower and upper boundaries for the vulnerability index of each building. The results show that the variable having most influence on the seismic performance is the construction period. Finally, damage scenarios have been produced for different earthquake severity through the vulnerability functions commonly used by GNDT.

An alternative attempt to create a comprehensive method to assess the vulnerability of buildings was carried out by ATC (ATC-14, 1985) . The novelty of this method lies in the fact that the risk of loss of human life is associated with the collapse of structural elements. Even in an embryonic form, this work is particularly valid as it identifies the most vulnerable structural features which play a central role in the seismic performance of 15 building types. For buildings showing particular deficiencies from a structural point of view, additional analyses are required and special tools are required such as equivalent lateral force or a more accurate dynamic analysis.

This same approach has also been pursued in a study carried out by the FEMA (FEMA 178, 1992), later developed into a more sophisticated procedure, FEMA 310 (1998). A double level of inspection and screening of the building is required. In the first phase the building has to undergo a global screening; if this is not successful, a structural analysis is required, using a displacement-based procedure (FEMA 273, 1997).

Nevertheless procedures such as ATC-14, FEMA 178, FEMA 310, FEMA 273, have the disadvantage that the information required is very detailed, even to the extent of carrying out destructive investigations on samples, and hence cannot be used for extensive applications.

Finally, some conclusions can be drawn on methods based on score assignments:

[1] Italian Research Institute providing data census and statistics elaborations.

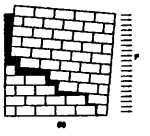

- One positive aspect is that no pre-defined classes or building types are used and the analysis is carried out by examining the individual building;
- A consequence of the previous point is that it becomes possible to "update" the building configuration, following modification or upgrading which can occur during its lifetime (Lang K., 2002);
- The amount of data collection required is usually time consuming, although the description of structural elements is very general and can be considered suitable for any location.
- There is some attempt to evaluate the structural performance, even though it is marginal. This means that only certain parameters of the amount of data required in the survey are used for structural evaluations.
- The final vulnerability index, calculated as the sum of different scores, is not related to physical entities, but mainly based on qualitative parameters.

1.4.4 Methods based on structural analysis

The methods introduced in §1.4.2 and §1.4.3, show approaches for assessing vulnerability, mostly based on qualitative considerations rather than on structural criteria. Their weak point is the uncertainty resulting from the subjective components as well as the very general description of those factors defining the seismic performance of buildings. Consequently, the measure of seismic vulnerability is not correlated to physical entities and hence the results from different methods are scarcely comparable with each other.

When vulnerability assessment is aimed at providing strategies to reduce seismic risk as well as for seismic upgrading, the evaluation of the structural performance becomes a basic requirement.

A complete evaluation of how buildings perform during earthquakes, would require the calculation of its dynamic response and the estimation of the consequent damage when the buildings are subjected to different intensities (Augusti et al., 2001).

This means that the seismic action should be modelled by a time history or frequency of vibration and the response of the building, defined by considering its own natural frequency of vibration, energy dissipation and deformation capacity.

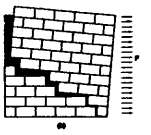

One interesting application to the field of seismic vulnerability is that conducted by Porter et al. (2001). The work, defined by an assembly-based vulnerability (ABV), aims to assess the level of vulnerability of single buildings by analysing their structural response when subjected to ground motion time history. The response is applied to fragility functions in order to simulate damage to each structural and non structural element in the building, and to its contents. Probabilistic construction cost estimation and scheduling are used to estimate repair costs and loss-of-use duration as random variables. The method is applied to steel office building.

In order to reduce the computational efforts static analyses are often used instead of dynamic analyses, while the building performance is commonly defined by linear elastic stiffness.

These methods, due to the reduced computational efforts as compared to dynamic analysis, can be applied to any type of structure and are considered generally suitable, although they provide poor models for the behaviour of masonry structures.

Among these, the work carried out in France (Thibault et al., 1994, 1995) aimed at vulnerability assessments at urban scale deserves to be mentioned. The method concentrates on an urban block, which represents the elementary core for structural analysis. This is described through the geometry of buildings included in the block, also defining the possible interaction between them. The seismic vulnerability, which refers to every homogeneous building-chain, is defined by means of the simple addition of parameters computed separately for each building.

The approach has been applied in a district of Nice, composed by 680 buildings grouped into 109 blocks, with a total height varying from 4 to 7 storeys. In the blocks examined, 7 structural types have been identified, although general and poorly effective. The constructive variety of buildings has then been reduced to 7 types of plan distribution and 2 types of structural frames. The seismic vulnerability analysis has been carried out for three levels of peak ground acceleration, in terms of equivalent static loads, and it has been applied to 4 different buildings heights. Three ranges have been considered for defining the structural behaviour of the buildings: the elastic range, the range lying between the elastic and plastic limits, and the plastic phase. While the first range corresponds to a safety area, the second, localised around the yield point, corresponds to the beginning of cracking. The last range

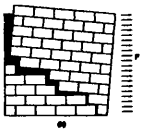

corresponds to collapse. Bending and shearing failure modes are examined separately, and shear failure is assumed to be more brittle and less stable than bending.

This assumption, derived from the behaviour of r.c. structures, represents the basic limit of this approach, which hence should be considered as poor model of masonry buildings.

A rather recent procedure is HAZUS, a method aimed at risk assessment, developed in 1997 and updated in 1999 (Hazus, 1999). In this case, the seismic action is modelled by spectral displacements and spectral accelerations. However, the software still relies on expert opinions for estimating the state of damage that would result from a given spectral displacement and acceleration. 36 building types are considered and for each building type qualitative descriptions of structural damage are provided. Similarly to the GNDT method, the vulnerability of the building is evaluated on the basis of its level of conformity to the seismic codes. Four possible seismic design levels are considered: high-code, moderate-code, low-code and pre-code, the latter referring to buildings without any seismic design, which hence should include masonry structures. Parameters defining the building capacity, typical drift ratios and final spectral displacements at the threshold of the different structural damage states are given for each building type and design level.

More sophisticated structural analyses are developed by ATC-40, and by FEMA 273, introduced in §1.4.3. These approaches are both based on non-linear static procedures, according to which the building model directly incorporates the non-linear force-deformation characteristics of its individual components and elements due to inelastic material response. The feature shared by all is that the nonlinear force-deformation characteristic of the building is represented by a pushover curve, i.e. a curve of base shear vs. top displacement, obtained by subjecting the building model to monotonically increasing lateral forces or increasing displacements, distributed over the height of the building corresponding to the first mode of vibration, until the building collapses. The maximum displacements likely to be experienced during a given earthquake are determined using either highly damped or inelastic response spectra.

The limit of approaches such as Hazus, ATC-40, FEMA 273, is that the same analytical approach is adopted for all building types, including masonry, and the structural performance of these is calculated through analytical procedures mainly developed for modern buildings.

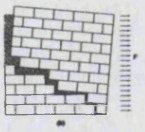

No particular effort is proposed for adapting the analysis criteria to historic masonry buildings.

A recent work carried out by Calvi (1999) has attempted to evaluate the seismic vulnerability of a buildings by analysing of probability to overcoming given limit states of the structure when subjected to a displacement response spectrum. The work is based on the formulation of the displacement capacity of different buildings as a function of relevant limit states, to be compared with displacement demands computed by entering appropriate displacement spectra with equivalent vibration periods. This method yields interesting results, particularly in the case of r.c. structures, while in the case of masonry buildings the results achieved are based on tests of clay brick buildings, while the extension to other masonry materials is arbitrary, and hence unsuitable for all types of masonry fabrics. The method has been recently applied to the city of Catania, (CNR-GNDT, 1999). In this case, the attempt to apply this procedure to an extensive sample of buildings, on the basis of very limited data (age of construction, number of storeys, construction material), leads to poorly reliable results in terms of the probability of occurrence of each limit state. Figure 1- 3 shows the comparison between damage scenarios obtained from the GNDT level 2 method and Calvi's displacement limit states. As can be observed, the two scenarios are not comparable, mainly because they refer to different damage rates, but also because they are obtained by methods unsuitable for historic centres.

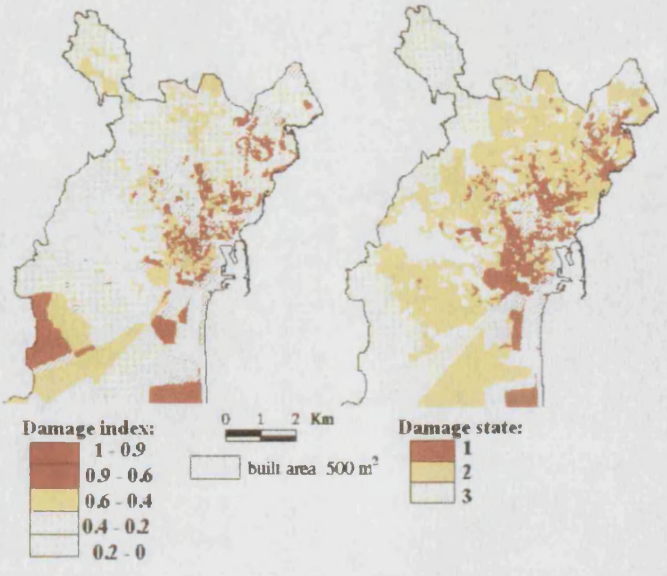

Figure 1- 3 – Damage scenarios of Catania: Maps of predicted damage to residential buildings. Left, predicted by GNDT level 2, right, predicted by the displacement limit state approach (CNR-GNDT, 1999).

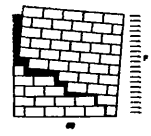

In conclusion, some considerations can be outlined concerning the evaluation of seismic vulnerability based on structural analysis :

- A great amount of detailed data is required for dynamic analysis, and the results obtained should be considered valid for individual buildings but unsuitable to be extended to building classes;
- In the case of masonry buildings, the use of pre-defined structural classes is unreliable, as each building, particularly when historical, is characterised by its own history, often resulting from a composite mixture of added or substituted structural elements, strongly interacting (Augusti et al., 2001);
- Detailed structural analyses of masonry buildings should take into consideration the non linearity of masonry. This would require experimental data which is not always available. These properties change from one masonry type to another.
- Forecasting the structural behaviour of historic buildings, because of the several variables and uncertainties inherent to the problem, would require great amount of data. Consequently, it happens that very often their structural performance is analysed "by analytical criteria specifically developed for modern buildings in most cases inadequate" (Augusti et al., 2001).
- A consequence of the previous points is that historic masonry structures require appropriate analytical tools sufficiently simplified to guarantee an adequate level of reliability in the description of their structural performance which can thus be applied more quickly to vulnerability evaluations.

1.4.5 Methods based on limit state analysis

The necessity of carrying out sufficiently extensive vulnerability assessments without foregoing a correct understanding of the structural performance of buildings, has led to the development over the last 15 years of a specific research field, focusing on the behaviour of masonry structures in historic centres.

A very effective approach, consists of the identification of feasible collapse mechanisms and by the calculation of their associated failure load factors using limit state theory. Unlike other structures, the behaviour of un-reinforced masonry buildings is characterised by the fact

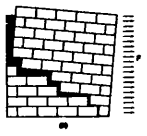

that the collapse occurs because of the onset of failure mechanisms more often bending than shear (Baggio et al., 1990). This approach to masonry structures derives directly from the assumptions made during the 18th century, before the development of the elastic theory, according to which masonry buildings were studied as mechanisms of rigid bodies (Mascheroni, 1785).

The limit state theory applied to masonry structures was first formulated by Heyman (1966), who describes the masonry structure as realised by rigid bodies with mono-lateral constraints, excluding the possibility of sliding along joints. The influence of friction on the bearing capacity of masonry structures was later introduced by Livesley (1978).

The application of limit state analysis to a given building, requires the preliminary formulation of all possible failure mechanisms, followed by identification of the one associated with the minimum load factor. This objective can be achieved by undertaking two possible approaches: static and kinematic. The former one allows the assessment of the ultimate load factor in terms of horizontal static action proportional to vertical loads producing the collapse around pre-defined hinges. The ultimate load factor is represented in this case by the greatest value of the horizontal force assuring the global equilibrium. The kinematic approach enables the ultimate load factor, relatively to some pre defined failure mechanisms to be calculated, according to which the global work of all forces acting in the system has to be 0.

According to this criterion, the failure mechanisms can be ranked according to their associated load factors, and among these the one with the minimum load factor, is the most likely to occur.

The basic assumptions of limit state analysis applied to vulnerability evaluations are:

- Dead load and horizontal equivalent force are applied at the centre of gravity of the wall under consideration, and are expressed as a function of the gravity constant;
- The failure mechanisms are defined as systems of rigid bodies articulated by constraints which can also simulate the role exerted by strengthening devices ;
- Displacements at failure are considered too small to affect the initial geometry significantly;
- The masonry is assumed to have zero tensile strength, but very high compressive strength;

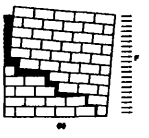

- Failure occurs slowly and in equilibrium so that a work balance between the work done by external load and that used internally is maintained.

Previous research on the vulnerability of masonry buildings carried out by Sinha (1978), Spence et al. (1992a) and by Giuffre' et al. (1993), has underlined the validity of this theory in this particular research field.

One of the first operative tools based on limit state theory aimed at seismic vulnerability assessments of masonry buildings, was developed by Bernardini (1986, 1987, 1989). This method arises from the need to set up a powerful tool for assessing the seismic vulnerability of small and regular sized masonry buildings. This method, later implemented in a numerical procedure known as VULNUS, is suitable for rather small samples of buildings. The survey proposed is very detailed, and aims to collect geometrical and structural data to assess the mechanical model of the building, based on a simplified numerical analysis.

Nevertheless, the range of collapse mechanisms, calculated by lower bound approach, is rather poor, and their occurrence in a multi storey building, is considered only in pre-defined storeys. The final level of vulnerability produced by VULNUS is a function of three different indices. The first two are the load factors, which refer respectively to in-plane and out-of-plane performance, while the third one refers to the level of information uncertainty, based on the fuzzy set theory, providing formal rules for treating data characterised by uncertainty (Bernardini et al., 1992, 1999).

This method is particularly valid as it represents one of the first "operative tools", for the vulnerability assessment of masonry buildings, providing the damage forecast in terms of the likelihood of failure mechanisms occurring. At the same time, the weak point is undoubtedly the extreme structural regularity of buildings required for the analysis, which is a condition very difficult to find within a historic centre. Moreover, the information required is very detailed so that the number of buildings which can be investigated by a single operator in one day is rather small.

VULNUS has recently been applied on 135 buildings in the historic centre of Catania (CNR-GNDT, 1999). After preliminary grouping of the buildings into the three MSK classes, the results have been compared with the vulnerability predictions obtained by DPM method. However, the results of this comparison suggest great caution, most of all because the DPMs are those calibrated for the Irpinia earthquake, and also because in order to make the

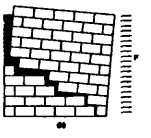

correlation possible, it has been necessary to convert the PGA into macro seismic intensities (Guagenti et al., 1989). Moreover, the data conversion from VULNUS data into MSK classes, has caused great loss of information, as the 135 buildings, surveyed in detail by VULNUS, have been compressed into just 3 MSK classes A, B, C.

In 1995 a study was carried out into the seismic vulnerability and associated risk of residential buildings in Rome (Colozza et al.1995). The work is particularly valid as it represents an attempt to calibrate the vulnerability through a new expert-probability-mechanical approach. The work is developed by first identifying 12 residential structural types representative of the historic centre of Rome. The description of each building type is sufficiently accurate to enable their structural layout to be understood satisfactorily. Each type is qualified by means of its structural components and associated average dimensions.

Similarly to other procedures, masonry fabric are still described by pre defined classes (brickwork, limestone and so on). For each building class a range of 10 mutually exclusive failure mechanisms is considered, which can occur involving variable number of storeys. The range includes not only in- and out-of-plane failure mechanisms, but also those occurring because the material resistance is exceeded. For every structural type, each failure mechanism and the probability of occurrence for a given earthquake is calculated. Finally, the global likelihood of occurrence of any mechanism for any structural type at any storey and any earthquake severity is computed. The results of this application are remarkable, and also show a certain dependence of failure mechanisms on the position of building within the block. In the range considered, the overturning of facades insufficiently anchored to orthogonal walls is the most likely to occur. In-plane failures are more approximately treated, by simply considering the shear strength τ_k of the masonry being exceeded.

In the same year a new methodology was presented, at the Seismic Engineering Congress in Siena (D'Ayala, Spence, 1995). The method was developed specifically for extensive analyses, based on speedy investigation and analysis while including a mechanical interpretation of the seismic behaviour of masonry buildings.

It was applied for the first time in a district of the historic centre of Lisbon as part of the TOSQA project (D'Ayala, Spence, 1996, 1997), and later developed following the 1997 Italian earthquake (Spence et al, 1998a,b, 1999, D'Ayala et al.1998).

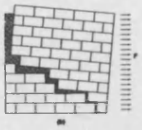

The approach is based on an original analysis of the structural characteristics of buildings: the site inspection is quick, and based on the collection of information all referring to the external features of buildings, without requiring an internal survey.

The information needed for the analysis is therefore limited to only those factors playing an important role in seismic performance. Very simple data like block shape, position of the building within the block, number of free walls, number of floors and so on, can give precious indications about the intrinsic level of vulnerability of structures, even in terms of feasible mechanisms. The vulnerability analysis is carried out by means of a range of failure mechanisms (Figure 1- 4), and the final indices produced represent the minimum and maximum equivalent shear capacity for each wall of the building.

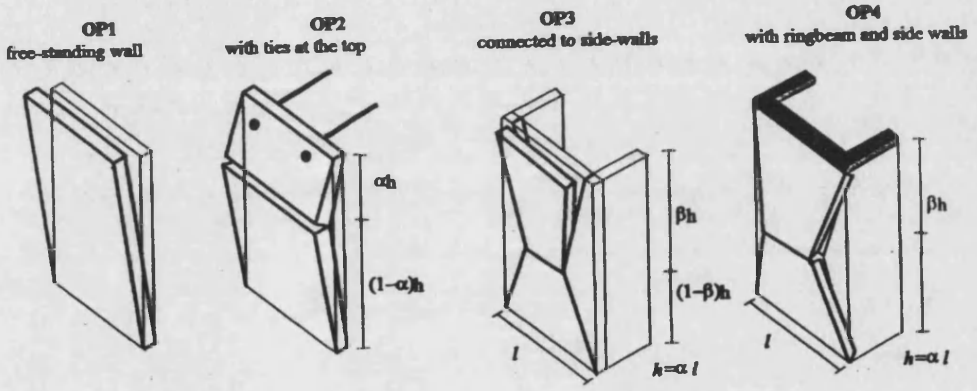

Figure 1- 4 – Failure mechanisms considered by the TOSQA project in the historic centre of Lisbon (D'Ayala et al, 1996) .

The method was later upgraded in order to include a wider range of mechanisms and also to suit different building types, such as ordinary buildings and churches (D'Ayala, 1998, 1999).

As for other procedures, the limit of this method, suitable for quite extensive samples as well as for any location, is the generalisation of the constructive techniques, particularly concerning masonry fabrics. However a simplified attempt to examine the different qualities of masonry fabric is made by reducing the wall thickness by pre defined percentages.

A parallel work, developed in 1994 (Doglioni et al., 1994) focusing on the vulnerability of churches, is based on a similar mechanical approach. The vulnerability is defined by means of a wide range of critical failure mechanisms which can occur involving different portions of the church, named *macro-elements*. Each mechanism, identified through a wide

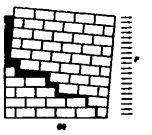

photographic review of damaged churches (Doglioni et al., 1994), has been analytically formulated according to the limit state analysis (Lagomarsino et al, 1997, 1998). The novelty of the work lies in the fact that the survey phase is organised in order to recognise and associate the damage pattern observed to a specific failure mechanism within a pre defined range, leading to useful correlations between observed and forecast damage. The approach has been recently upgraded by Augusti et al. (2001), who have attempted to formulate the probability of collapse and damage of each macroelement.

To sum up, some conclusions about methods based on limit state analysis can be outlined:

- The use of limit states and failure mechanisms for the vulnerability assessment of masonry buildings represents a simplified and reliable tool for modelling their seismic performance;
- The simplified structural analysis required enables extensive applications to be carried out on an urban scale, without foregoing a correct understanding of the mechanical performance of buildings. This intent can be pursued by reducing the data to those strictly necessary for the analysis to be conducted.
- The weak point of most methods so far described is that the formulation of failure mechanisms and their occurrence likelihood is not influenced by the mechanical quality of masonry, but only by the strength of the material, and by the general classes (such as brickwork, rubble and so on), unsuitable for a correct understanding of their mechanical behaviour.

1.4.6 Approaches taking into account the mechanical qualities of the masonry

The evaluation of the mechanical characteristics of masonry is a wide and complex topic, because of the extreme variety of masonry types as well as the marked non-linearity of their behaviour.

These features make such evaluation rather difficult to model, particularly when aimed at seismic vulnerability assessments, which require simplified yet at the same time reliable analysis criteria. Most procedures so far described analyse masonry according to criteria

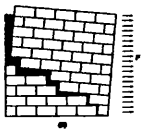

imported from other structural types, or in other cases by considering it as an homogeneous material, the behaviour of which is essentially described by its shear strength.

This last approach basically derives from early studies and experimental tests carried out in the 80's, aimed at testing the ultimate strength of biaxial masonry panels subjected to seismic actions, (Mann et al., 1982, Page, 1981, 1982, 1983), as well as on models at reduced scales (Samarasinghe et al., 1980). These tests also enabled early analytical formulations for experimentally observed damage failure to be devised (Ganz, 1989, Hamid et al., 1981, Mann et al., 1982, Turnsek et al., 1979, Benedetti et al. 1984b, Anthoine, 1991).

Among the methods analysing masonry as homogenous material, several applications can be mentioned also supported by laboratory tests, including those by Gambarotta et al. (1994), Chiostrini (1994), Kuobaa et al. (1994).

A very powerful analytical tool often applied to masonry, is Finite Elements (F.E.) analysis. In some cases F.E. are also used for vulnerability assessments, although their application is rather time consuming and hence the number of buildings which can be assessed is rather small.

F.E. have been applied in a recent work by Casolo et al. (2000) aimed at the seismic vulnerability evaluation of churches. The objective of the work is interesting, as it attempts to identify the most critical failure mechanisms common to some types of churches by means of a preliminary F.E analysis. However, the assumptions made are unsuitable for masonry structures, as the material model used is assumed to be homogeneous and isotropic (Casolo et al., 2000).

Some authors have pointed out that the hypothesis of "material" continuity, sensibly changes the real physical nature of masonry and hence can lead to errors in interpreting its mechanical performance and the associated failure mechanisms. The strong non-linearity and the intrinsic anisotropy of masonry, highlight the poor reliability of these mechanical models (Giuffrè, et al. 1989, 1994).

A research field known as the homogenisation technique (De Buhan et al., 1997) attempts to overcome these limits, while remaining in the hypothesis of material continuity. This technique, implemented within the framework of yield theory, enables the construction of a macroscopic strength criterion for masonry described as a regular assembly of bricks separated by joint interfaces. Making use of the kinematic definition of such a criterion, the

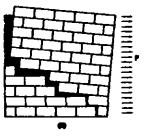

yield stress domain in the space of stresses is explicitly determined in the case of infinitely resistant bricks. The value of this method is that the model takes into account some important features of masonry, such as the anisotropic characteristics due to the orientation of bedding surfaces, as well as the elements geometry and friction along joints. (Buhan, et al. 1997).

Procedures based on limit states analysis and failure mechanisms clearly go beyond the concept of "continuum material". However, the validity of approaches based on the formulation of kinematic chains and failure mechanisms is strictly linked to the possibility of considering the masonry wall as a rigid monolithic body, where cracks can occur without failure of the material.

The observation of damage produced by catastrophic events, carried out by Tomazevic et al. (1989), demonstrates of how different masonry assemblies can deeply influence the crack pattern as well as the associated failure mechanisms. The work carried out by the same authors, outlines the most common damage patterns leading to the conclusion that the structural layout of the masonry exerts a crucial role in defining the mode of damage. The work also underlines that the fabric quality is particularly relevant at a wall intersection, and documentary evidence from different earthquakes testifies that the lack of connections can lead to the separation of peripheral walls (Tomazevic et al.,1989). Research and experimental tests carried out by the same authors also provide evidence of this (Tomazevic et al., 1982, 1999).

Studies and experimental tests aimed at defining the mechanical behaviour of masonry, carried out by Giuffrè et al. (1989, Baggio, et al., 1990, Ceradini, 1992, Giuffrè, 1994), have confirmed that the performance of walls during earthquakes is influenced by the quality of the structural assembly characterising the masonry fabric. The approach starts from the assumption that the *opus quadratum* is the best prototype of masonry to form a perfect connection throughout the wall thickness. Its principal mechanical characteristic, due to the extreme geometric regularity, is its monolithic behaviour which is obtained by a perfect connection and staggering between elements alternatively placed along and through the wall, respectively named *diatons* (headers) and *orthostats* (stretchers), (Figure 1- 5, above). The great potential of the opus quadratum becomes even more clear, when comparing it to a masonry fabric without headers. In this case the wall can be considered as made up of two different leaves with independent behaviour (Figure 1- 5, below) (Giuffrè, 1989).

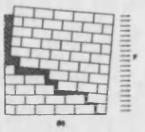

Thanks to the geometric regularity of this ideal model, it is possible to formulate its mechanical behaviour, and to compare it with the experimental results.

The model analyses the masonry stone by stone, assuming that its own weight is uniformly distributed along the layer surface. The contact surface between the stones is characterised by a mono lateral bond. The in-plane behaviour of such an ideal model is characterised by a shear strength along bedding surfaces, which the masonry is able to develop thanks to the presence of friction. The out-of-plane behaviour is basically governed by the quality of the structural assembly, i.e. the number and position of the headers .

This formulation was later implemented in a computer program, which has enabled the development of several numerical simulations (Baggio et al., 1993).

Experimental tests carried out on brickwork panels, show good correlation with the numerical results obtained from the same samples (Ceradini, 1992, Giuffrè, 1994). These have shown that, by reducing the number of headers and keeping the shape of the panels constant, the load factors tend to decrease almost linearly (Figure 1- 6).

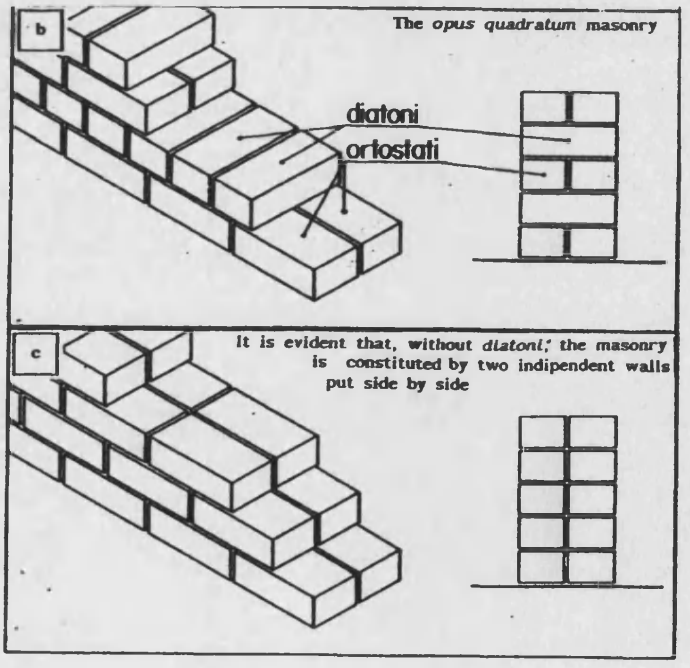

Figure 1- 5 – Geometric layout of the opus quadratum (above). Masonry fabric made without diatons (headers) (below). (Giuffrè, 1989)

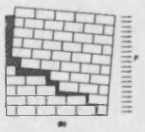

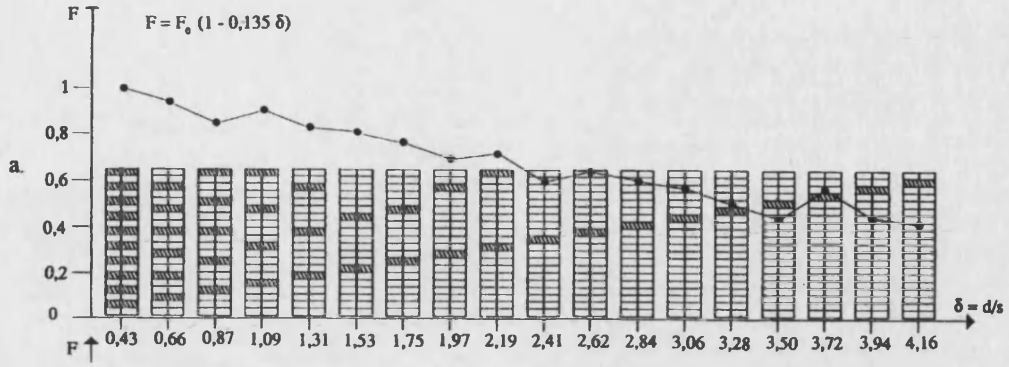

Figure 1- 6 - Diagram of the horizontal load factors for different masonry panels characterised by a decreasing number of headers (Ceradini, 1992).

According to this model, it is also possible to formulate the maximum shear strength exerted at connections, when horizontal loads are acting.

Further research into the topic has developed simplified out-of-plane failure mechanisms that take into account the connections with transverse walls (Spence, 1992a, Giuffrè, 1993). In more recent works carried out by De Felice (1999, De Felice et al.1998, 1999, 2000), different classes of mechanisms are compared, including: the overturning of an external building wall due to either vertical cracks at abutments or a diagonal crack on transverse walls; the overturning of a facade portion of triangular shape. These studies are remarkable in that they present a correlation between the results achieved by the analytical formulations of the failure mechanisms considered and those obtained by a discrete elements program (Udec). Despite the schematic nature of the failure mechanisms, the results obtained seem to catch the fundamental aspects of the problem, giving an adequate, realistic prediction of the strength of different walls having different shapes and masonry layout (De Felice et al., 1999). Some of the most interesting results achieved, underline the role exerted by effective connections between the buildings front and transversal walls, which can turn the failure mechanism of facade overturning into a mechanism involving portions of side walls. On the other hand, the effectiveness of connections is strictly linked to the quality of masonry, which is parametrically analysed by increasing the slenderness of its elements. The analysis has indicated a decreasing level of the seismic resistance with decreasing element size (in relation to the panel thickness) and decreasing quality of the masonry fabrics.

In conclusion, the results achieved by this research field, underline the importance of the masonry layout in defining the mechanical performance.

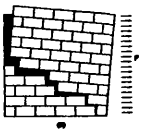

The opus quadratum ideal model can represent an effective tool for analysing the mechanical quality and performance of the ordinary masonry fabrics in historic centres. According to Giuffrè's approach, the quality of different types of masonry assembly can be assessed by comparing their structural layout with the ideal model of opus quadratum. Following this criterion, the closer the layout to an *opus quadratum*, the better the mechanical quality of the masonry fabric examined.

This assumption leads to the conclusion that the mechanical performance of historic buildings cannot be generalised and considered universally valid, as commonly occurs in several vulnerability assessment methods, since such performance strictly depend on the local craftsmanship, which should be analysed in detail in order to identify generalised structural features which can produce critical failure mechanisms (Giuffrè, 1993).

Despite its highly valuable results, a basic aspect limiting the suitability of this method for vulnerability evaluations, is that it can be considered valid only within the historic centre surveyed, and hence the results are scarcely comparable.

Moreover, the structural types together with the associated failure mechanisms, are those resulting from the original layout of the building, and hence do not take into account the retrofit interventions implemented after their construction.

Several studies and experimental tests carried out on masonry structures have shown that different retrofitting interventions can deeply influence the damage mode during seismic events. Recent research and laboratory tests on reduced scale carried out by Tomazevic (1993, 1996), demonstrate the different performances shown by buildings subjected to mortar grouting, replacement of wooden floors with r.c. slabs, insertion of metal ties. It is also worth noting the tests carried out on 14 models by Benedetti et al. (1998,b). Two particular systems have been tested: connection along vertical edges between orthogonal walls and the connection of slabs or wooden floors to walls.

Another remarkable study in this same research field is the work carried out by Binda et al. (1997,1999) who focuses on the performance of masonry fabrics by analysing their material properties as well as their internal assembly, in order to devise appropriate structural criteria for improving their performance. This approach has been more recently converted into a "multilevel approach" for assessing the vulnerability of ordinary buildings, where failure mechanisms due to previous repair intervention are examined.

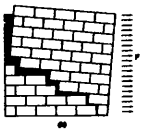

Finally, some conclusions can be drawn on the criteria of taking into account the mechanical performance of masonry:

- The analysis of masonry as homogeneous material notably changes the physical nature of the problem leading to under estimation of the mechanical performance of masonry and its associated failure mechanisms;
- Structural damage due to different earthquakes highlights how the quality of masonry assembly exerts a crucial role in defining the damage mode, particularly at wall connections;
- The opus quadratum model, according to Giuffrè's approach (1989), is able to offer a simplified yet at the same time realistic analysis of the masonry;
- Thanks to this ideal model the mechanical quality of masonry of ordinary fabrics can be evaluated, by comparing these with the ideal prototype;
- The opus quadratum also allows connections between orthogonal walls to be modelled, as well as the horizontal strength exerted during seismic events;
- The reliability of failure mechanisms is strictly linked to the possibility of considering the masonry wall as a rigid monolithic body, where cracks can occur without failure of the material;
- The range of failure mechanisms should also take into account those produced by previous retrofit interventions.

1.5 Statement of the objectives of the research work

The critical discussion of the literature available carried out in the previous sections, enables some conclusions to be drawn and the general objectives of the method presented in this work to be outlined.

The procedures so far used are often unreliable in defining seismic vulnerability, particularly of historic buildings.

Methods based on expert opinions and score assignments are very subjective and time consuming, so the use of structural analysis seems to be the most appropriate way to yield to obtain more reliable results.

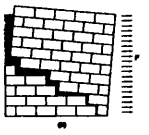

Among the analytical methods reviewed, the limit state analysis, based on the identification of failure mechanisms, can be defined as a simplified, but sufficiently appropriate tool for modelling the seismic performance of historic buildings. This analytical tool also allows rather extensive applications at urban scale to be carried out, without foregoing a correct understanding of the mechanical performance of buildings.

Among the available methods, the one used by D'Ayala and Spence (1995, 1996) is taken as the reference point for the final objectives, scale of assessments and analytical tool applied.

On the other hand, there is a general tendency in this research field, to neglect the fabric layout of masonry, considered incompatible with the extensive scale of vulnerability assessments. However, specific studies and experimental tests have underlined the influence of this structural feature in defining the likelihood of failure mechanisms, so that neglecting it can yield unreliable results.

Among the methods available focusing on this topic, the mechanical model of *opus quadratum* (Giuffrè, 1989), has been recognised as a simplified and yet realistic tool for the analysis of the masonry assembly. The model has been so far applied to the detailed analysis of single buildings, while no effort has been made so far to adapt this method to statistical purposes.

These observations highlight the final objective of the present work, that is, to devise a criterion for assessing the seismic vulnerability of historic buildings, from a statistical point of view, by means of a sufficiently wide range of common failure mechanisms whose likelihood has to be governed by an analytical formulation of individual masonry assembly, developed from *the opus quadratum* model.

The following presents a review of different damage patterns and associated failure mechanisms caused by different earthquakes (GNDT 1998, Tampone 1999), which is taken as an operative tool for developing the new method.

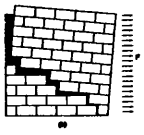

1.6 Identification of failure mechanisms for masonry buildings

The observation of damage produced by catastrophic events show that among the failure mechanisms which can be triggered in occasion of an earthquake, some of them are rather common to all historic centres in seismic prone areas, while others strictly depend on local constructive peculiarities and hence cannot be generalised (Bernardini 1986, Giuffrè et al. 1993, 1999, Lagomarsino et al. 1997, D'Ayala et al. 1995, GNDT 1998, Tampone 1999).

By reviewing the huge variety of earthquake damage so far documented by the literature available on the topic, it is possible to outline some frequent failure mechanisms, the onset of which is influenced by the structural peculiarities or deficiencies of buildings involved. The review has been carried out also by taking into account either the results of the investigation carried out in Nocera Umbra following the 1997 Italian earthquake, which are presented in Chapter 4, and those obtained in occasion of a further inspection performed after the earthquake in San Giuliano (Molise, Italy) in 2002. The failure mechanism reviewed involve predominantly building fronts, with the consequent possible participation of side walls and internal structures, such as internal party walls, horizontal structures and roofs.

Among all the damage modes which can be triggered in occasion of an earthquake, those associated with the overturning of external walls are very likely to occur, especially in those buildings where no strengthening device are present. As stressed by several authors, such as Tomazevic (1989), Giuffrè (1993), De Felice (1999), the onset of these failure mechanisms is usually influenced by the quality of lateral connections with orthogonal walls.

The overturning of the whole building façade, which can also involve side walls are very common (Table 1-1, a,b,c). Partial failures of corners or central/lateral portions of the facade, are also widely documented by the literature available (Tomazevic 1989, Giuffrè et al. 1993, 1999, Lagomarsino et al. 1997, GNDT 1998, Tampone 1999) (Table 1, d,e,f). D'Ayala et al (1996) suggest a particular crack pattern associated with the overturning of a central wall portion defined by two lateral inclined cracks (Figure 1-4, type OP3). Failure mechanisms due to overturning can occur in many other ways, like involving smaller portions of the building facade walled up in latter periods and badly connected to the original fabric, as type (g) of Table1-1.

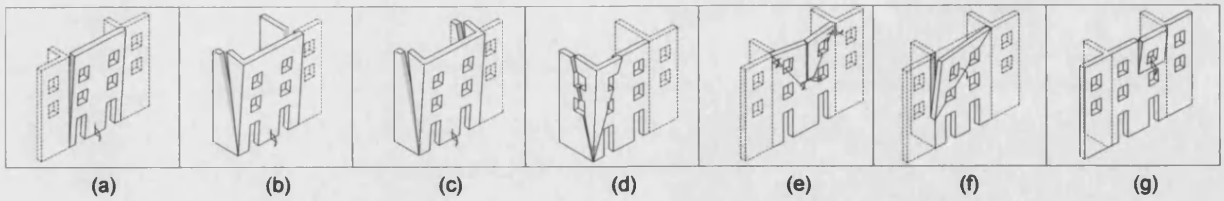

Table 1- 1 – Out of plane failure mechanisms

One more typical damage is that produced by the presence of openings. Several earthquake evidences show that when openings are too wide or even arranged according to particular layouts their presence can produce an increase in the seismic vulnerability. Notwithstanding a complete review of all possible openings layouts is not affordable, some authors have attempted to outline the more common crack patterns and associated failure mechanisms influenced by this feature. Giuffrè et al. (1993, 1999) have provided a detailed review of failure modes influenced by openings, although his research is limited to the case study of two Italian towns, such as Siracusa and Palermo. Laboratory tests carried out by Ceradini (1993) and Tomazevic (1989), have proved how the presence of openings can influence the crack pattern of masonry buildings. It is very common to observe, in buildings characterised by a massive presence of openings on the external walls, that overturning mechanisms, can be influenced by the position of openings such to affect the portion of wall involved in the failure. The flexional failure of a wall portion included by two vertical columns of openings is a typical example of how the overall overturning of the building front can occur in a different way in presence of this particular opening layout (Table 1-2,a). Further failure mechanisms can be also associated with this same layout, as the outwards bending of the wall, shown in Table 2 (b,c). One more common damage mode is the outwards displacement of the top horizontal string of wall, above the highest row of windows (Table 1-2,d).

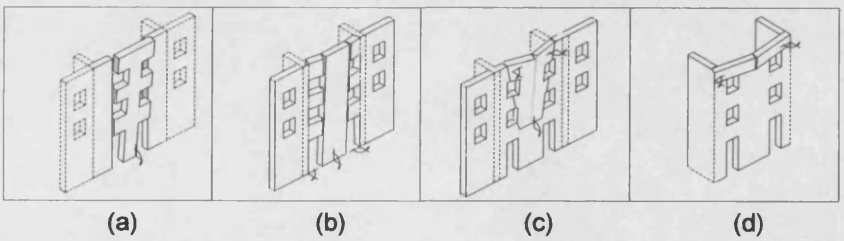

Table 1- 2 – Failure mechanisms influenced by openings layout

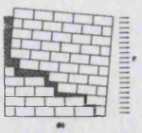

The role performed during earthquakes by different kinds of strengthening devices has been experimented in several laboratory tests as the ones carried out by Tomazevic in 1993. These tests give evidence of how the presence of strengthening devices, like ring beams or ties, can modify the structural performance of the building, producing failure mechanisms involving higher amount of energy to be triggered. One typical failure mechanism is the collapse by shear, or the flexional failure according to a vertical arch behaviour (Table 1-3,a,b). Dina D'Ayala et al. also take in exam failure mechanism OP4 of Figure 1-4 , which differs from the previous one for the presence of inclined cracks along the building wall. However observation from different earthquakes also testifies that some other common strengthening devices, as the replacement of old timber structures with r.c. ones, like slabs, can produce hammering effects, even with adjacent buildings (Table 1-3,c,d).

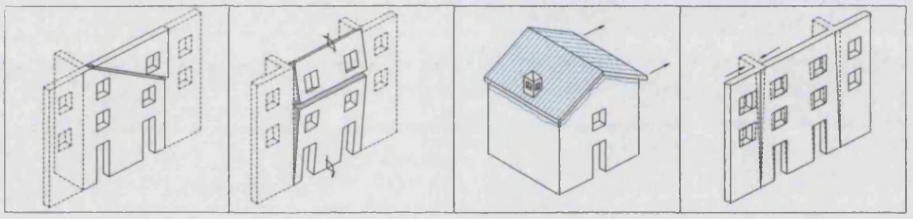

Table 1- 3 – Failure mechanisms influenced by strengthening devices

Finally, very common is the damage caused by the collapse of additional elements, like chimney flues, gable ends, attics, additional storeys or additional structures, which can seriously jeopardise people and structures lying below (Table 1-4,a,b,c,d). The failure of these elements usually occurs according to overturning mechanisms.

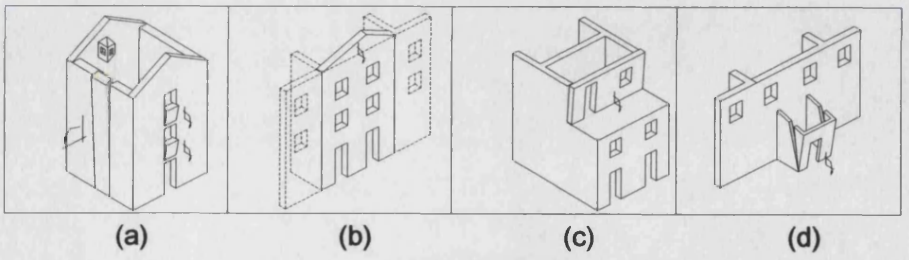

Table 1- 4 – Failure mechanisms involving additional elements

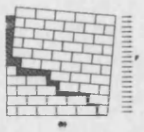

In the following a selection of the most common failure mechanisms so far observed in historic buildings is analysed in detail and these are taken as an operative tool for the new method.

1.6.1 Failure mechanisms depending on the quality of lateral connections

Of the failure mechanisms which can be triggered when an earthquake occurs, the overturning of the façade wall is undoubtedly one of the most common and it is mainly governed by the level of connection of the façade to the orthogonal walls.

The lack of connection at a wall intersection is typical of buildings of historic centres, where the diachronic process of filling up urban spaces has caused a non-uniform quality of construction.

So, while in adjacent buildings built around in the same period, walls are connected to each other (Figure 1- 7, type A), no or weak connections are present between the fronts and the lateral walls when the building construction period dates back to a period later than the building/s beside it. This condition historically has led to building up just the front and back walls, using the walls already existing, between which the building is located, as support for the horizontal and roof structures (Figure 1- 7, type C).

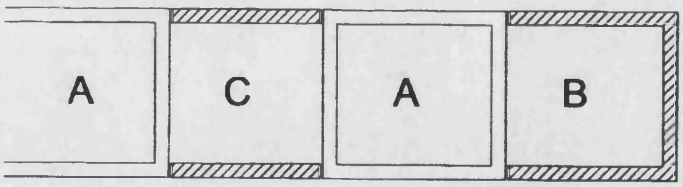

Figure 1- 7 – Diachronic construction process of buildings in historic centres (Giuffrè, 1993)

Figure 1- 8 (b) shows an example of orthogonal walls badly connected to each other. It is evident how the total lack of bonds has caused the interface between the two walls to widen during an earthquake.

(a) (b)

Figure 1- 8 – Example of two orthogonal walls without connections (Cifo, Italy, 1997)
(a) Global view – (b) Particular

Evidence from different earthquakes has shown that the absence or presence of lateral connections considerably changes the damage pattern and the associated failure mechanisms: in the former case the façade overturns without involving lateral walls (A, Figure 1- 9), while in the latter case the participation of party walls can be observed (B2, Figure 1- 10). These two failure mechanisms are characterised by different crack patterns, respectively vertical in the first case, inclined in the second. The B2 mechanism can also occur in external walls where the connections, originally missing, have been realised by metallic ties.

A combination of the two mechanisms (B1, Figure 1- 11), can be devised in buildings with non uniform lateral connections, such as type B of Figure 1- 7. In this case the crack pattern is characterised by vertical and oblique cracks at wall extremities.

The lack of connections can also produce partial failures, such as overturning corners as well as portions of facade (respectively Figure 1- 12, Figure 1- 13).

Corner failures can occur on those buildings placed at block extremities, such as B of Figure 1- 7. Evidence from different earthquakes shows that cracks are inclined on both walls, as sketched in Figure 1- 12, but their pattern can be influenced by openings very close to the corner, as shown in the pictures of Figure 1- 12.

A portion of facade (D) usually collapses when the building front is anchored to backwalls only on one side. In this case the free side can overturn around a diagonal line, as in Figure 1- 13.

A further failure mechanism influenced by the presence of lateral connections, is mechanism (G), which involves a central portion of the facade, identified by two inclined cracks (Figure 1- 14). The mechanism occurs due to horizontal arch behaviour which develops within the wall thickness, causing the wall to bend outwards.

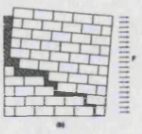

A	 (a)	 (b)	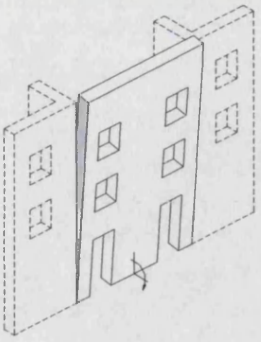 *Figure 1- 9 – Failure mechanism A: overturning of external wall (a, b) Umbria-Marche, Italy, 1997 (Tampone, 1999)*
B2	 (a)	 (b)	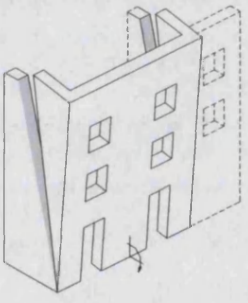 *Figure 1- 10 – Failure mechanism B2: overturning with participation of both orthogonal walls. (a,b)Umbria-Marche Italy,1997 (GNDT 1998, Tampone, 1999)*
B1	 (a)	 (b)	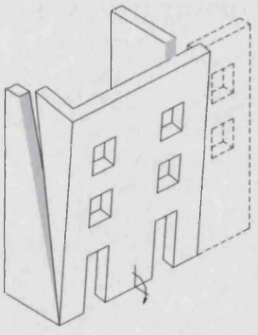 *Figure 1- 11 – Failure mechanism B1: overturning of external wall with participation of one side wall (a) Molise (Italy), 2002; (b) Umbria-Marche, Italy,1997 (Tampone, 1999)*

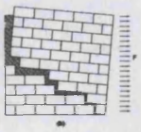

C

(a)

(b)

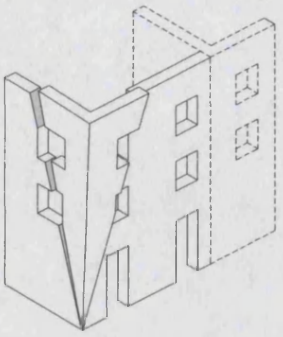

Figure 1- 12 – Failure mechanism C – corner overturning
(a, b) Umbria-Marche, Italy, 1997 (Tampone, 1999).

D

(a)

(b)

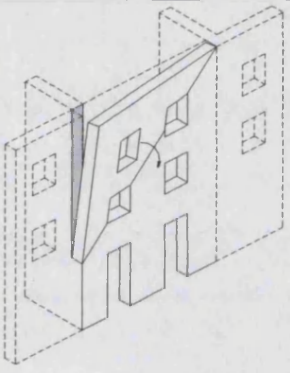

Figure 1- 13 – Failure mechanism D: overturning of a triangular portion.
(a, b) Umbria-Marche, Italy, 1997 (GNDT 1998, Tampone, 1999).

G

(a)

(b)

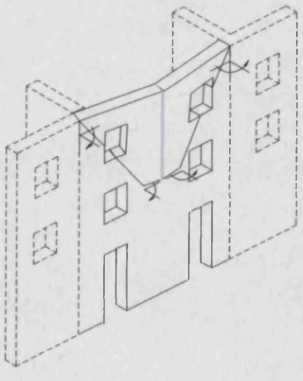

Figure 1- 14 – Failure Mechanism G: horizontal arch effect.
(a) Molise (Italy), 2002; (b)Umbria Marche (Italy), 1997 (Tampone, 1999).

1.6.2 Failure mechanisms depending on openings layout

Earthquake damage has highlighted that openings which are either too wide or placed too close to the external wall edges represent intrinsically weak points during earthquakes. In such cases, even when lateral connections anchor the building front to the back walls, detachment of the façade can occur along the openings, particularly when these are vertically aligned (E, Figure 1- 15).

When the openings are too close to the roof, the collapse can occur by a horizontal upper spandrel bending outwards, behaving like a horizontal arch (Gs, Figure 1- 16).

E

(a)

(b)

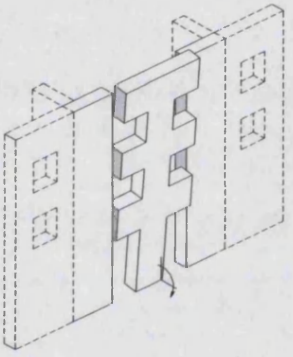

Figure 1- 15 – Failure mechanism E: collapse of a central vertical portion of wall
(a,b) Umbria-Marche, Italy, 1997.

Gs

(a)

(b)

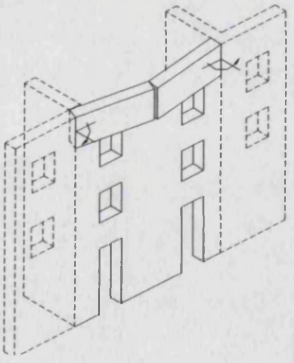

Figure 1- 16 – Failure mechanism Gs: arch effect on a top horizontal strip.
(a,b) Umbria-Marche, Italy, 1997.

1.6.3 Failure mechanisms depending on strengthening devices

The presence of strengthening devices due to retrofit interventions can substantially modify the structural behaviour of buildings during an earthquake, transforming failure mechanisms such as type A into others requiring a higher amount of energy to be triggered.

Evidence from earthquake damage shows that when the vertical span left between two reinforcements is too wide, the building can collapse according to mechanism (F), sketched in Figure 1- 17.

When the layout of strengthening devices is such as to prevent flexional failures, the building can still collapse due to a shear failure (H), shown in Figure 1- 18. The typical crack pattern associated with this damage is diagonal, which can also be symmetrical for seismic waves acting in opposite directions.

F

(a)

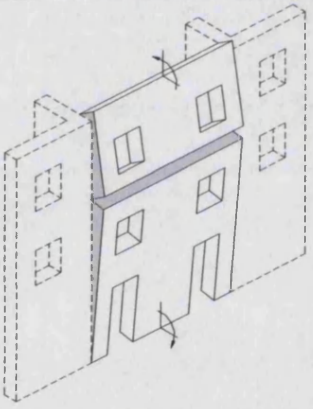

Figure 1- 17 – Failure mechanism F: vertical arch.
(a) Umbria-Marche, Italy, 1997.

H

(a)

(b)

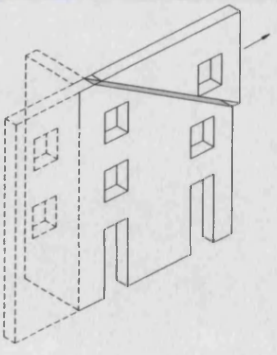

Figure 1- 18 – Failure mechanism H: shear effect
(a) Molise, Italy, 2002; (b) Umbria Marche, Italy, 1997.

1.6.4 Failures of further elements

Vertical additions and gable ends can be considered among the most vulnerable elements to suffer high damage in the event of an earthquake.

The overturning of the external wall of the vertical addition is usually due to the fact that this additional storey is commonly associated with a reduction of the wall thickness as well as the absence of lateral connections (I, Figure 1- 19).

Gable overturning (L, Figure 1- 20) more typical for churches than for ordinary houses, becomes particularly dangerous when the gable ends support the weight of the roof beams. In this case its collapse also involves the roof structure.

I

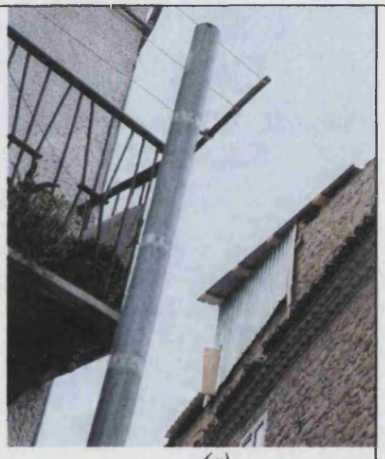

(a)

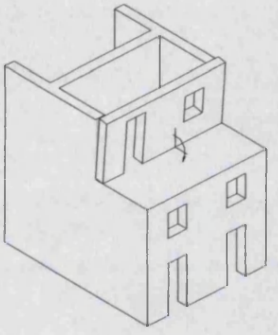

Figure 1- 19 – Failure mechanism I : overturning of vertical addition (a) Molise, Italy, 2002

L

(a)

(b)

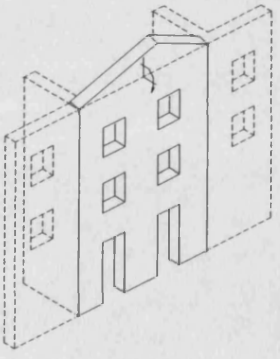

Figure 1- 20 – Failure mechanism L: overturning of Gable (a,b), Umbria-Marche, Italy, 1997 (Tampone, 1999)

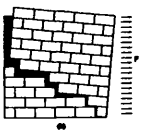

1.7 Conclusions

This Chapter has outlined an introduction to the research topic. After a brief introduction to some general concepts about seismic risk and vulnerability as well as definitions of damage and earthquake, a review on the available literature has been presented, in §1.4.

This is entirely devoted to an overview of the methods available for the evaluation of existing buildings, ranging from those based on expert opinions and observed vulnerability through methods based on score assignments, to methods using structural approaches. Finally an overview on procedures more strictly focusing on the mechanical behaviour of masonry has been outlined.

The critical discussion of the literature review, in §1.5, enables some conclusions and general objectives of the new method to be drawn, which are summarised in the following:

- Methods based on observed vulnerability and experts opinion are mostly based on the definition of building types and classes, suitable for any location worldwide, and hence highly arbitrary and scarcely reliable;
- Methods based on scores assignment are usually time consuming, although the description of structural elements is very general and can be considered suitable for any location. Moreover, the final vulnerability indices, calculated as the sum of different scores, are not related to physical entities, but mainly based on qualitative parameters. The structural analysis is hence outlined as the most appropriate tool for approaching the problem.
- Forecasting the structural behaviour of historic buildings, because of the several variables and uncertainties inherent to the problem, would require great amount of data, not always available. Moreover, very detailed analysis to singular buildings are scarcely suitable for extensive applications, aimed at vulnerability assessments. For this reason sufficiently simplified tools are required in order to guarantee an adequate level of reliability in the evaluation of their structural performance which can thus be applied more quickly to vulnerability evaluations.
- Limit state analysis and failure mechanisms are recognised as the most appropriate analytical tools for approaching the problem. A complementary analytical model, focusing on the mechanical behaviour of masonry, is assumed as the starting point for developing the new method.

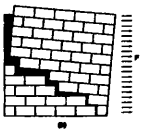

Finally, in §1.6, field observation of different earthquake damage, treated as experimental evidence, enable the most common failure mechanisms to be identified, and these are assumed as operative tool of the new method.

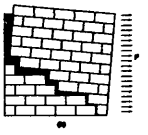

CHAPTER 2
MECHANICAL FRAMEWORK

2.1 Introduction

This Chapter is dedicated to the formulation of the theoretical basis of the method FaMIVE.

The procedure is aimed specifically at analysing historic masonry buildings on an urban scale, and is characterised by a particular effort to interpret their structural performance in a simplified and reliable way.

The analytical approach pursued for describing the structural performance of buildings subjected to earthquakes is represented by the theory of limit states and failure mechanisms, introduced in section §1.4.5.

A mechanical model formulated on purpose allows examination of the frictional behaviour of the masonry, described as an ideal dry ashlars fabric, composed of stone blocks all made of the same size and material.

This model serves as the basis to analyse in-plane overturning and sliding of isolated walls with and without live loads applied, using a limit-state approach to derive the ultimate load factors. At the end of this section, a parametric analysis is performed.

On the basis of this mechanical model, the out-of-plane failure mechanisms identified in §1.6 are then systematically formulated and presented.

The failure mechanisms developed through the limit state analysis are defined by systems of three-dimensional walls assemblies, and the out-of-plane behaviour of each wall is highly influenced by the type and strength of connection with the other masonry walls.

At the end of each analytical formulation, some parametric analyses are presented for a better understanding of the existing field of each failure mode, and also to find out which parameters are the most influent.

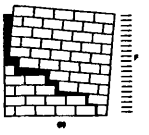

2.2 Formulation of a mechanical model for ashlars masonry: geometric characteristics of the fabric and Total Shear Strength.

Stone blocks of regular dimensions and nearly dressed, set in very thin mortar joints or in dry contact, represent the best possible layout of stones to ensure structural integrity within a masonry wall. Typical examples of such masonry are the Roman *opus quadratum* or the ashlars stonework of Gothic cathedrals. The Latin name refers to its morphology, characterized by overlapping square stones, with or without thin bedding mortar. This kind of masonry, known in ancient times as *opus isodomum*, is accurately described by Vitruvius Pollione, in "*De Architectura*" (I century B.C.) (Morgan, 1960). This construction technique is still in use in many European countries and constitutes the masonry fabric of most buildings in historic centres.

The mechanical features common to this construction system, introduced in §1.4.6, are characterised by a structural integrity of the wall which relies upon a regular staggering of blocks of subsequent courses as well as on the regular presence of blocks laid out orthogonally to the face of the wall, in order to connect the various leaves of the wall together (Giuffrè 1989). Section §1.4.6 has introduced the studies and experimental tests carried out so far, providing clear evidence of the function exerted by *diatones* (headers) in ensuring the monolithic behaviour of the wall and to improve its out-of-plane resistance, while successive courses of *ortostates* (stretchers) are staggered to improve the in-plane behaviour of the wall (Ceradini 1992, Figure1.6).

These results, analytically formulated in occasion of further development of the research (Giuffrè, 1989,1991; De Felice et al., 1998, 1999, 2000), represent an important starting point for formulating and calibrating the frictional model, introduced in the following sections.

2.2.1 Description of the geometric model

In order to examine the frictional behaviour of a wall, a simple geometric model is taken into consideration.

It is assumed that the masonry is entirely made up of regular square blocks, of geometric dimensions $\ell x h x b$ (Figure 2- 1), placed with their longer side parallel to the wall length . If a

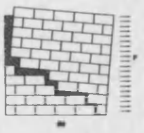

constant staggering length s between overlapping stones is considered to be equal to half the length of the block, the masonry assumes the configuration of Figure 2- 2.

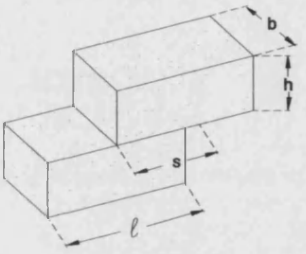

Figure 2- 1 -Geometric characteristics of the stone block

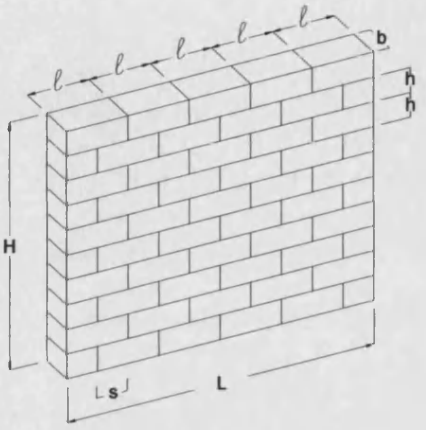

Figure 2- 2 – Masonry wall model

The weight w of a generic block is given by:

$$w = \ell \cdot h \cdot b \cdot \gamma \qquad (2\text{-}1)$$

where γ is the specific gravity of the stone.

2.2.2 Formulation of the Total Shear Strength of opus quadratum masonry along a vertical crack line

It is assumed that the block is subjected to: its own weight, external actions and friction between contact surfaces, according to the Coulomb's friction theory (Heyman, 1972), while no cohesion is assumed against vertical loads which tend to detach overlapping layers. This assumption is equivalent to consider a no–tension model, except from the tensile strength exerted by friction, acting along bedding surfaces. Experimental tests carried out since '70-'80 on brickwork samples (Ganze et al.1989, Mann et al.1982, Schneider et al., 1978, Dialer 1991) have proved that the mechanical performance of such a material is characterized by a very high anisotropy, so that the direction of bedding surfaces and element shapes plays a central role in defining the type of failure. Such experiments, further developed by other authors as Ceradini (1992), have stressed that failure in most of cases occurs by applying horizontal loads exceeding the friction coefficient, such to produce cracks along the joints without crashing of elements, while failure due to the overcoming of material strength (σ,τ)

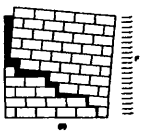

occurs for much higher applied loads. The theory of plasticity formulated by Heyman (1966) and later by Livesley (1978) basically relies on this mechanical behavior which qualifies masonry: tensile strength negligible, Coulomb's friction acting along bedding surfaces, compressive strength infinite. This approach allows adequate level of structural safety also to be guaranteed.

The mechanical behavior of the opus quadratum model has been formulated on these assumptions.

With reference to Figure 2- 3 and Figure 2- 4, the shear strength acting along a vertical crack line, can be formulated as follows (Giuffrè, 1989, 1991).

If n is the total number of layers in a given wall of total height H, F the horizontal force distributed along the height, the maximum shear strength C_i which can be developed by a generic layer i, is:

$$C_i = (h_i \cdot s \cdot b \cdot \gamma) \cdot f \tag{2-2}$$

where h_i is the height of the wall above level i, and f the friction coefficient.

The value of C_i, calculated at each interface between courses, is hence a stepwise function of h_i and of the weight of wall above the course considered.

The *Total Shear Strength* (C_{tot}) which a wall of given height and number of courses can develop is given by:

$$C_{tot} = \sum_{i=1}^{n} C_i = \sum_{i=1}^{n} (h_i \cdot s \cdot b \cdot \gamma) \cdot f \tag{2-3}$$

Equation (2-3) assumes that the block dimensions and their overlapping lengths are constant at least within a course. The equation shows that the shear strength associated with each layer depends on the length of overlap between stones, and this in turn depends on the dimensions of the stones.

Figure 2- 5 shows the variation of the ratio of total shear strength C_{tot} to total weight W in a wall, for different ratios of block height to wall height (h/H), and overlapping lengths to wall length (s/L) for a constant value of the friction coefficient. It can be observed that the greater the ratio of block height to wall height, the lower the value of C_{tot}/W_{tot}, so that increasing the number of courses and reducing the number of blocks in each course increases the total shear strength of the wall.

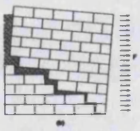

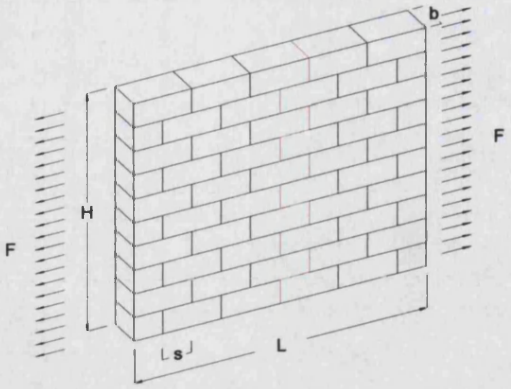

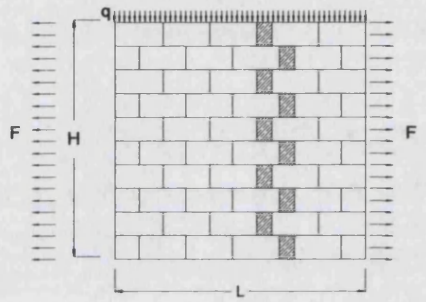

Figure 2- 3 – Identification of vertical crack line

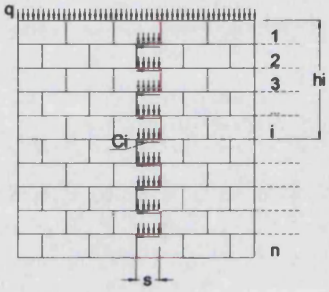

Figure 2- 4 – Identifications of acting forces

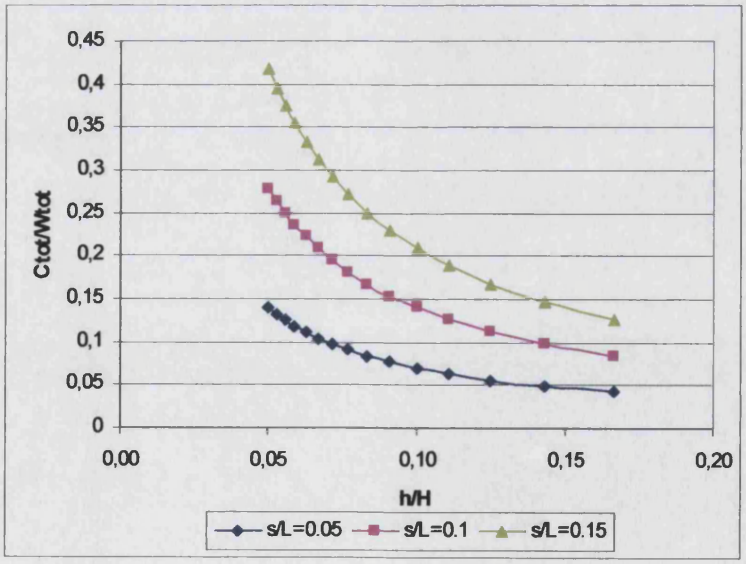

Figure 2- 5 - Normalised curves for Total Shear Strength C_{tot}

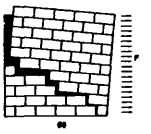

2.2.3 Formulation of the Total Shear Strength of opus quadratum masonry along a diagonal crack line.

The variation with height of the total shear strength implies that the occurrence of vertical cracks in reality are unlikely, while the application of a uniformly distributed horizontal force F along a wall of height H and length L, will result in a diagonal crack line, assumed to originate the lower right vertex of the panel, and identified by a generic angle α_c which it forms with the vertical axis. For a monolithic panel (Figure 2- 6), the friction resistance acts along the surface of the sloping crack line and can be defined as:

$$C_{tot(\alpha c)} = W_{tot(\alpha c)} \cdot \sin\alpha_c \cdot f \cdot \gamma = \frac{(H \cdot \sin\alpha_c)^2}{2\cos\alpha_c} \cdot f \cdot \gamma \qquad (2\text{-}4)$$

where $W_{tot(\alpha c)}$ is the weight of the wall portion identified by the angle α_c, for a unit thickness. $C_{tot(\alpha c)}$ is a monotonically increasing function of α_c.

If the same wall is formed of stone blocks (Figure 2- 7), with reference to the block dimensions previously introduced:

$$\alpha_b = \arctan\frac{s}{h}; \qquad \alpha_p = \arctan\frac{L}{H} \qquad (2\text{-}5)$$

The function of the Total Shear Strength $C_{tot(\alpha c)}$ developed along a generic angle α_c is strictly dependent on the value of the these two angles representing the stone overlap ratio (α_b) and the panel geometry (α_p) respectively.

The $C_{tot(\alpha c)}$ function can be described according to the following conditions :

if $\alpha_p < \alpha_b$

for $\alpha_c < \alpha_b$ $$\Rightarrow C_{tot(\alpha c)} = \frac{1}{2} \cdot \frac{s}{h} \cdot f \cdot H^2 \cdot b \cdot \gamma \qquad (2\text{-}6)$$

for $\alpha_p \le \alpha_c < \alpha_b$ $$\Rightarrow C_{tot(\alpha c)} = \left[\frac{1}{2} \cdot \frac{s}{h} \cdot \frac{L}{\tan^2\alpha_c} + \left(\frac{L}{\tan\alpha_p} - \frac{L}{\tan\alpha_c}\right) \cdot L\right] \cdot f \cdot b \cdot \gamma \qquad (2\text{-}7)$$

for $\alpha_c \ge \alpha_b$ $$\Rightarrow C_{tot(\alpha c)} = \left[\frac{1}{2} \cdot \frac{L^2}{\tan\alpha_c} + \left(\frac{L}{\tan\alpha_p} - \frac{L}{\tan\alpha_c}\right) \cdot L\right] \cdot f \cdot b \cdot \gamma \qquad (2\text{-}8)$$

if $\alpha_p > \alpha_b$

for $\alpha_c < \alpha_b$ $$\Rightarrow C_{tot(\alpha c)} = \frac{1}{2} \cdot \frac{s}{h} \cdot f \cdot H^2 \cdot b \cdot \gamma \qquad (2\text{-}9)$$

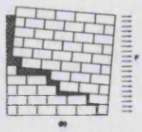

$$\text{for } \alpha_b \le \alpha_c < \alpha_p \quad \Rightarrow C_{tot(\alpha c)} = \frac{1}{2} \cdot \tan\alpha_c \cdot f \cdot H^2 \cdot b \cdot \gamma \tag{2-10}$$

$$\text{for } \alpha_c \ge \alpha_p \quad \Rightarrow C_{tot(\alpha c)} = \left[\frac{1}{2} \cdot \frac{L^2}{\tan\alpha_c} + \left(\frac{L}{\tan\alpha_p} - \frac{L}{\tan\alpha_c} \right) \cdot L \right] \cdot f \cdot b \cdot \gamma \tag{2-11}$$

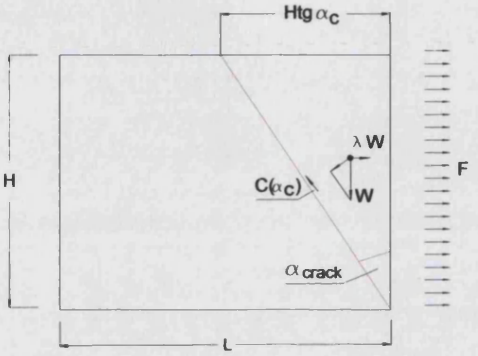

Figure 2- 6 – Monolithic wall with oblique crack.

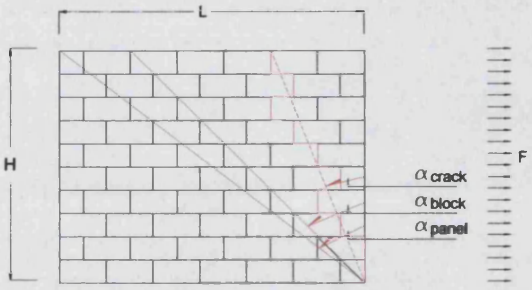

Figure 2- 7- Stone block wall with oblique crack.

To sum up, equations (2-6) to (2-11) of the Total Shear Strength can be synthesised in the following 4 ranges:

$$\text{for } \alpha_c < \min(\alpha_p, \alpha_b) \quad \Rightarrow C_{tot(\alpha c)} = \frac{1}{2} \cdot \frac{s}{h} \cdot f \cdot H^2 \cdot b \cdot \gamma \tag{2-12}$$

$$\text{for } \alpha_p \le \alpha_c < \alpha_b \quad \Rightarrow C_{tot(\alpha c)} = \left[\frac{1}{2} \cdot \frac{s}{h} \cdot \frac{L}{\tan^2\alpha_c} + \left(\frac{L}{\tan\alpha_p} - \frac{L}{\tan\alpha_c} \right) \cdot L \right] \cdot f \cdot b \cdot \gamma \tag{2-13}$$

$$\text{for } \alpha_b \le \alpha_c < \alpha_p \quad \Rightarrow C_{tot(\alpha c)} = \frac{1}{2} \cdot \tan\alpha_c \cdot f \cdot H^2 \cdot b \cdot \gamma \tag{2-14}$$

$$\text{for } \alpha_c \ge \max(\alpha_p, \alpha_b) \quad \Rightarrow C_{tot(\alpha c)} = \left[\frac{1}{2} \cdot \frac{L^2}{\tan\alpha_c} + \left(\frac{L}{\tan\alpha_p} - \frac{L}{\tan\alpha_c} \right) \cdot L \right] \cdot f \cdot b \cdot \gamma \tag{2-15}$$

It can be observed that equation (2-12) is a function of the geometry of the wall and of the stagger ratio, while it is independent of the crack angle. This means that for $\alpha_c < \min(\alpha_p, \alpha_b)$, $C_{tot(\alpha c)}$ is constant and equivalent to that portion of a triangular wall identified by the angle α_b, and the total height of the panel (H). For increasing crack angles, the pattern of the function changes according to the shape of the wall in relation to the block ratios. If the block ratio is greater than that of the wall ($\alpha_b > \alpha_p$), the value of $C_{tot(\alpha c)}$ is expressed by equation (2-

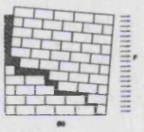

13), which is function of α_c, α_b, α_p. On the other hand, if $\alpha_p > \alpha_b$, the total shear strength becomes independent of the block shape ratios (equation 2-14). Finally, for crack angles greater than the max(α_b,α_p), $C_{tot\ \alpha c)}$ is still a function of α_p and α_c, while it is independent of α_b. In Figure 2- 8 the ratio $C_{tot(\alpha c)}$ to the total weight W_{tot} of a panel of dimensions H, L is plotted for two different L/H ratios and two different ratios of s/h, so as to include all the cases described by equations (2-12)-(2-14). The curves obtained are also compared with the curves of a monolithic wall with same geometry H,L.

One can observe that the values of $C_{tot(\alpha c)}/ W_{tot}$ are always greater for the opus quadratum than for the monolithic panel, showing that while the latter can be safely assumed as lower bound it underestimates the wall capacity. All 4 curves relating to opus quadratum panels begin with a constant value, according to equation (2-12). For panels with $s/h = L/H$ the initial value is constant up to $tan(\alpha_c) = s/h$ and then increases. For values of $L/H < s/h$, C_{tot} / W_{tot} is constant up to $tan(\alpha_c) = L/H$ and then decreases down to a minimum for $s/h = tan(\alpha_c)$ for which Equation (2-12) reduces to Equation (2-13). These are also the intersection points of curves with equal panel ratio and different block ratios. The value of α_c for which the minimum ratio C_{tot} / W_{tot} is obtained is independent of the geometric ratio L/H. (D'Ayala, Speranza, 2003).

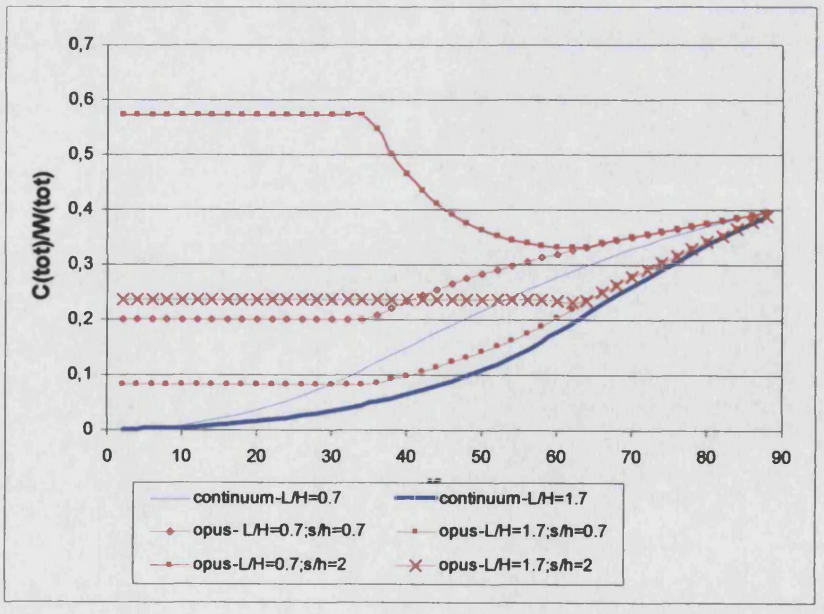

Figure 2- 8 - Total Shear Strength in monolithic and opus quadratum walls for different ratios H/L and s/h=0.7 (f=0.4).

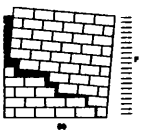

2.3 Introduction to failure mechanisms formulation

2.3.1 Introduction to formulation

The material model introduced in §2.2.2 and §2.2.3 is applied in the following paragraphs to calculate in-plane and out of plane mechanisms and the associated load factors of a generic masonry building wall.

The failure mechanisms are analytically developed on the basis of the limit state analysis, and are aimed at evaluating the corresponding critical accelerations.

The failure mechanisms are calculated by applying to the centre of mass of each element horizontal static action expressed as a percentage of the load itself, by means of a load factor λ. This factor is described by the ratio a/g, that is between the lateral acceleration a and the gravitational acceleration g.

Therefore, in formulating the mechanisms, the lowest value of the load factor λ_c able to maintain a limit equilibrium configuration corresponds to the maximum capacity of the wall to resist the earthquake. However, the load factor λ_c thus defined expresses a result which is conservative with respect to the real factor of failure under dynamic conditions.

To sum up, the assumptions on which this approach is based are the following:

- Dead load and horizontal equivalent force are applied at the centre of gravity of the building wall under consideration, and are expressed as a function of the gravity constant;
- The masonry walls are simulated as a system of rigid bodies, articulated by hinges, whose geometry is defined by the failure mechanism;
- The masonry is simulated by a discontinuum with friction;
- The strengthening devices of masonry walls are simulated using specific constraint conditions;
- Foundations and soil characteristics are disregarded.

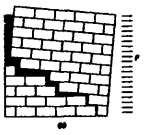

2.3.2 Geometric characteristics and parameters of the structure

A preliminary step for the analytical formulation of the failure modes of a generic external wall of a building requires the introduction of its generalised geometric characteristics together with the assumptions made to simplify the model.

With reference to Figure 2- 9, the generic wall is characterised by:

- Global geometric characteristics defined by total height H and total length L;
- Number of storeys N; this number refers just to the levels above ground and does not include basements, which are not considered.
- The assumption that all storeys have the same height H/N;
- The assumption that the wall thickness decreases by a constant amount at each floor from the top to the ground floor;
- A percentage of openings per storey Opi calculated on the basis of the number of openings per storey, and assuming average opening dimensions (l_oxh_o). This variable also takes into account the presence of chimney flues inserted within the wall thickness.
- Type of masonry defined by stagger ratio s/h length and thickness respectively ℓ and b. It is also assumed that just one masonry type can be associated with each wall.

On the basis of these assumptions, the weight of a generic storey can be calculated as:

$$W_i = \frac{H}{N} \cdot L \cdot T_i \cdot \left[\frac{100 - Op_i}{100}\right] \cdot \gamma \qquad (2\text{-}16)$$

where the thickness T_i at an intermediate storey i,, is given by:

$$T_i = T_b - i \cdot \frac{T_b - T_u}{(N-1)} \qquad \text{for } i\text{=1, N-1;} \qquad (2\text{-}17)$$

where

T_b is the thickness at the bottom of the wall;

T_u is the thickness at the top of the wall;

The total weight W_{tot} of the façade can therefore be formulated according to the following expression:

$$W_{tot} = \sum_{i=1}^{N} W_i \qquad (2\text{-}18)$$

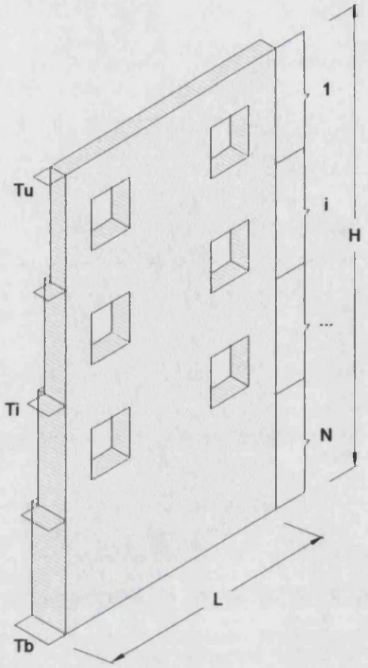

Figure 2- 9 – Geometric characteristics of the building wall

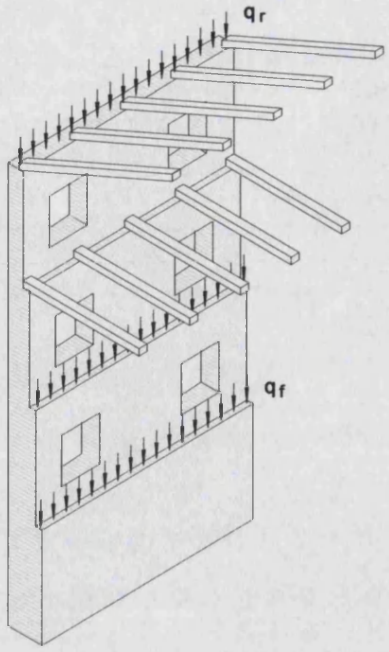

Figure 2- 10– Weight of horizontal structures and roof spread along the wall façade.

Moreover, the building wall is subjected to the action of vertically distributed loads, q_r and q_f, due to the presence of the roof on the top and intermediate floors (Figure 2- 10).

When taking into account the presence of floors and roof, the total weight of the façade simply becomes:

$$W_{tot} = \sum_{i=1}^{N} W_i + \left[q_f \cdot (N-1) + q_r\right] \cdot L \tag{2-19}$$

The roof and floors distributed on walls orthogonal to the façade are given by:

q_{fs} the weight per unit length of horizontal structures acting on orthogonal walls;

q_{rs} the weight per unit length of the roof acting on orthogonal walls.

Finally, in order to model the rest of the building, the following parameters are considered:

- Effectiveness of connection between façade wall and orthogonal edge walls. This characteristic is governed by the parameter ε which represents the number of edge party walls orthogonal to the façade under examination. This variable is 0 in the absence of any connections. It is 1 or 2 respectively in the case that one or both the edge connections are effective;
- Number of internal bearing walls orthogonal to the façade (β). This parameter refers only to those internal bearing walls well connected to the façade;

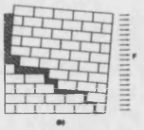

This structural feature, together with the previous one, expresses the level of bonding between the wall in question and the rest of the structure, expressed by the Total Shear Strength developed at each wall connection.

- Distance between openings and vertical edges of the facade (side piers) determined by parameter η. The width of the side pier is assumed to be regular when greater than the average opening width. The variable η reports the presence of irregular piers on the two façade extremities. The variable is set to 2 when all the side piers are regular on both the façade edges. It is set to 1 when the piers are regular on one side and at least one is irregular on the opposite side. Its value is 0 when at least one pier is irregular on both the edges of the façade.

2.4 Formulation of in-plane mechanisms (H)

The total shear strength acting along the horizontal layers of ashlars masonry, introduced at § 2.2, enables the formulation of two in plane mechanisms which a wall can be subjected to in the presence of a seismic action: *sliding* and *overturning*.

Both mechanisms are described by a diagonal crack, inclined at a variable angle α_c, which divides the wall into two portions. It is assumed that the lower-left-hand portion does not participate in the mechanisms. The equilibrium at incipient failure of the upper portion, which can be assumed triangular, trapezoidal or rectangular in shape, will be expressed in relation to the two possible mechanisms represented in Figure 2- 11 (a,b).

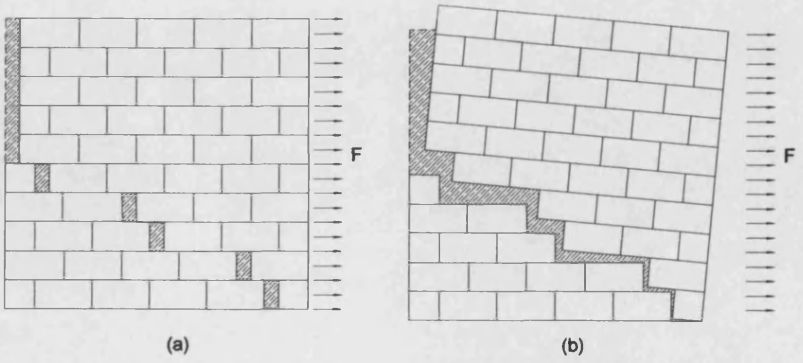

Figure 2- 11 -The two mechanisms considered : (a) sliding and (b) overturning.

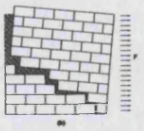

The mechanisms are first developed considering a single storey wall, of overall dimensions L,H, as shown in Figure 2- 12.

The weight $W_{tot}(\alpha_c)$ of the portion defined by the angle α_c can be divided into two sub-portions W_1 and W_2 as follows:

When

$$\alpha_c \leq \alpha_p \Rightarrow W_{tot(\alpha c)} = W_1 = \frac{H^2 \cdot \tan\alpha}{2} \cdot T \cdot \gamma \cdot \tag{2-20}$$

When

$$\alpha_c > \alpha_p \Rightarrow W_1 = \frac{L^2}{2 \cdot \tan\alpha} \cdot T \cdot \gamma \; ; \; W_2 = L \cdot \left(H - \frac{L}{\tan\alpha} \right) \cdot T \cdot \gamma$$

$$\Rightarrow W_{tot(\alpha c)} = W_1 + W_2 \tag{2-21}$$

where T is the wall thickness.

When considering the overturning mechanism, it is assumed that the total shear strength is able to develop only for crack angles smaller than α_b. This assumption is due to the fact that, for angles greater than α_b, the masonry fabric can no longer exert a restraining action against the physical detachment between the upper overturning body and the inactive portion of wall. Figure 2- 11b shows how the friction action along the layers can no longer influence the overturning of the wall portion.

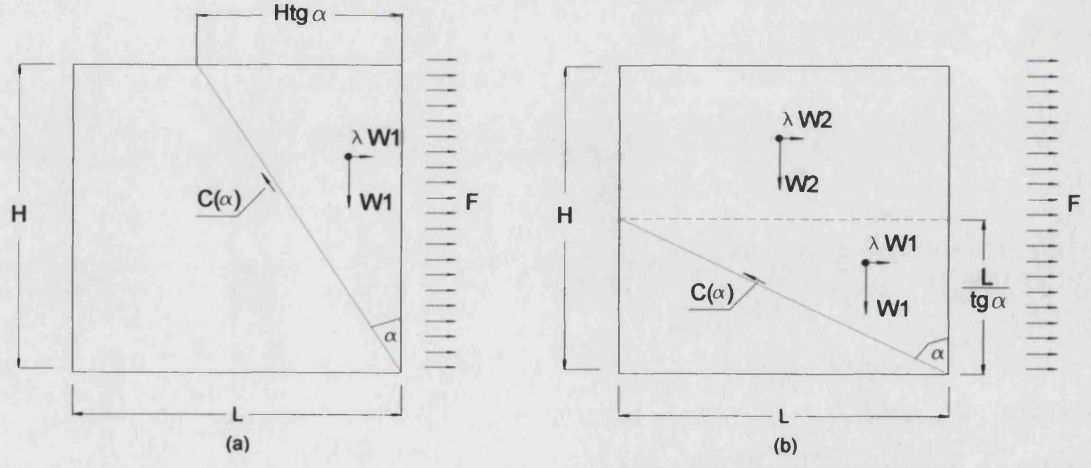

Figure 2- 12 -Sub-division of total weight W for: (a): $\alpha_c \leq \alpha_p$; (b): $\alpha_c > \alpha_p$

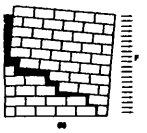

Moreover, the friction acting along vertical joints has been disregarded. The reason of this neglect is that the friction which would be developed along vertical joints, during the rotation of the right-hand wall portion, is not a Columbian friction, as not produced by lateral loads, but simply generated by the contact between two adjacent surfaces in a relative movement. Its formulation in analytical terms is hence rather difficult, and would require experimental data in order to be modelled in the appropriate way. However its neglect leads to results in favour of the structural safety.

Therefore the formulation of the critical load factor relative to the overturning mechanism is governed by :

$$\text{For } \alpha_c \le \alpha_b \Rightarrow \lambda_O = \frac{W_1 \cdot dx_1 + W_2 \cdot \frac{L}{2} + C_{tot(\alpha c)} \cdot dy_1}{2 \cdot W_1 \cdot dy_1 + \frac{W_2}{2} \cdot \left(H + \frac{L}{\tan \alpha} \right)} \tag{2-22}$$

$$\text{For } \alpha_c > \alpha_b \Rightarrow \lambda_O = \frac{W_1 \cdot dx_1 + W_2 \cdot \frac{L}{2}}{2 \cdot W_1 \cdot dy_1 + \frac{W_2}{2} \cdot \left(H + \frac{L}{\tan \alpha} \right)} \tag{2-23}$$

where:

$C_{tot(\alpha c)}$ is the Total Shear Strength previously introduced at (2-12)-(2-15), developed over the wall thickness T. Moreover, it is assumed that the $C_{tot(\alpha c)}$ resultant is acting at 1/3 of the vertical component of the crack line.

Furthermore:

for

$$\alpha_c \le \alpha_p \Rightarrow \quad dx_1 = \frac{H \cdot \tan \alpha}{3}; \qquad dy_1 = \frac{H}{3}; \tag{2-24}$$

for

$$\alpha_c > \alpha_p \Rightarrow \quad dx_1 = \frac{L}{3}; \qquad dy_1 = \frac{L}{3 \cdot \tan \alpha} \tag{2-25}$$

The sliding mechanism is governed by:

$$\lambda_S = \frac{C_{tot(\alpha c)}}{W_{tot(\alpha c)}} \tag{2-26}$$

This equation is only valid for $\alpha_c \le \alpha_b$, since beyond this limit $\lambda_S = f$.

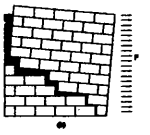

From equations (2-22; 2-23) and (2-26), if $\lambda_c = a/g$ is the collapse load factor, three domains of existence for the solution, depending on the ratio λ_o/λ_s can be identified:

$$\mathcal{D}_1=[\lambda < (\lambda_O \cup \lambda_S)] \quad \Rightarrow \text{safe configuration} \tag{2-27}$$

$$\mathcal{D}_2=\left[\frac{\lambda_O}{\lambda_S}<1\right] \quad \Rightarrow \text{overturning failures} \tag{2-28}$$

$$\mathcal{D}_3=\left[\frac{\lambda_O}{\lambda_S}>1\right] \quad \Rightarrow \text{sliding failures} \tag{2-29}$$

Among the possible values of α_c and λ_c, the limit state configuration is the one for which $\lambda_{min}=\min(\lambda_o,\lambda_s)$. This will identify which portion of wall fails and type of failure at the same time.

For slender panels with ratio $L/H < 1$ and $s/h > 1$, the failure occurs through overturning, with $\alpha_c=\alpha_b$ (Figure 2- 13). The load factor decreases with increasing in slenderness. However if $s/h > 1$ and also $L/H > f$, failure might occur by sliding even in panels with a slenderness ratio greater than 1. For a given angle of friction and geometric ratio of the panel, the staggering will affect the extension of the safe area in Figure 2- 13. For geometric ratios of the panel $L/H > 1$, failure occurs through sliding, according to the Coulomb criterion, if the ratio $s/h > f$, and $\lambda_{min}=f$, with a crack inclined at any angle ranging between $\alpha_c = \alpha_b$ and the horizontal, otherwise failure occurs by overturning a portion identified by an angle $\alpha_c < \alpha_b$ and a load factor $s/h < \lambda_{min} < f$ (Figure 2- 14).

The role exerted by staggering ratios becomes clearer in Figure 2- 15, which compares the load factor curves for different ratios s/h, having assumed L/H=0.4 and $f = 0.3$.

It can be noted how for increasing values of s/h, the load factor of the wall tends to increase up to the upper boundary, represented by the friction coefficient value. For ratios s/h≤1, the failure occurs through overturning, with load factors smaller than the friction coefficient, and failure cracks inclined at the critical angle α_b.

This means that for increasing values of s/h, the load factor also tends to increase. For $s/h = 2L/H$ the minimum load factor is only slightly smaller than the friction coefficient, while the crack angles for sliding and overturning coincide so that either can take place. Finally, for ratios $s/h > 1$ the failure is always sliding, the load factor is equal to the friction coefficient, while the crack angle will be inclined at any angle between the critic angle and the horizontal.

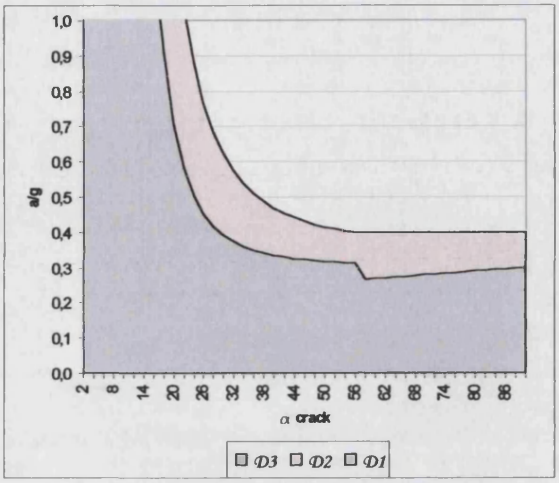

Figure 2- 13 – Functions of λo ,and λs for L/H=0.35;f=04; s/h=1.5.

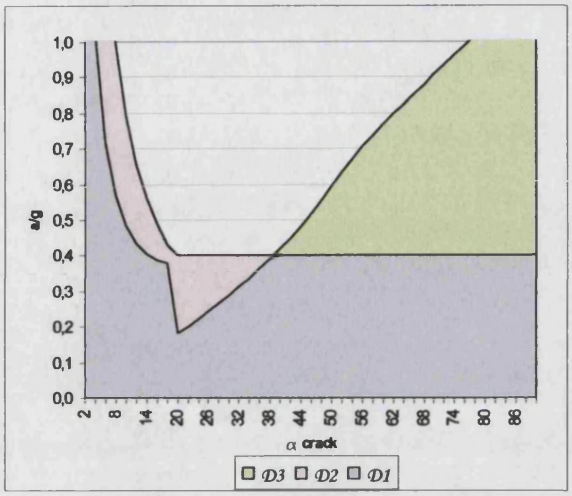

Figure 2- 14– Functions of λ ,and λs for L/H=1.2; f=0.4;s/h=0.35

Figure 2- 16 generalises the previous results, by varying s/h and L/H, keeping the friction coefficient constant. It can be observed that as the slenderness of the panel increases, the influence of the ratio s/h is negligible. On the contrary, for increasing ratios L/H, the load factor also increases following a more and more linear pattern up to s/h=L/H. Beyond this value, the curve tends to an asymptotic value λ_{min}= L/H for s/h= ∞ (monolithic case).

The role exerted by the friction coefficient, which usually undergoes notable variation according to to the masonry type, is outlined in Figure 2- 17.

The diagram shows the pattern of the load factor curves in a wall with L/H=0.7, s/h=0.5, and values of *f*. As can be observed, the curves with *f* greater than 0.2 have the same minimum, corresponding to overturning failure at a crack angle coinciding with α_b.

In conclusion, the friction coefficient influences the load factor in the same way as the staggering ratios s/h. Nevertheless, while, it is not possible to change the value of *f*, which depends on the level of smoothness of the sliding surfaces, in a wall of given L/H ratio, the final load factor can be modified by increasing or reducing the geometric layout of the fabric (s/h).

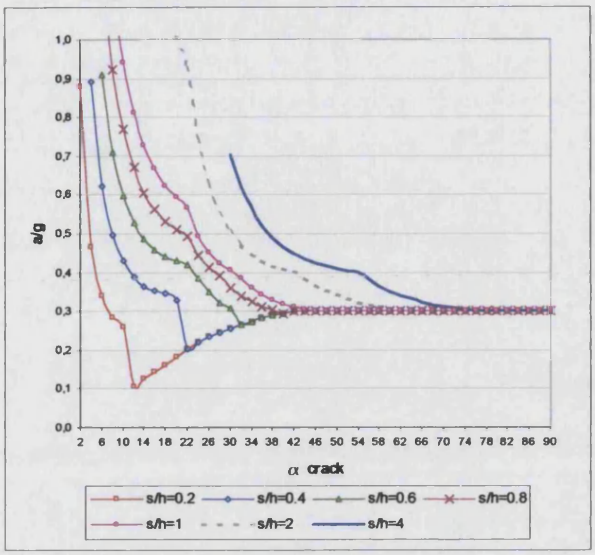

Figure 2- 15 – Functions of λ_c for L/H=0.4; f=0.3, for different ratios s/h.

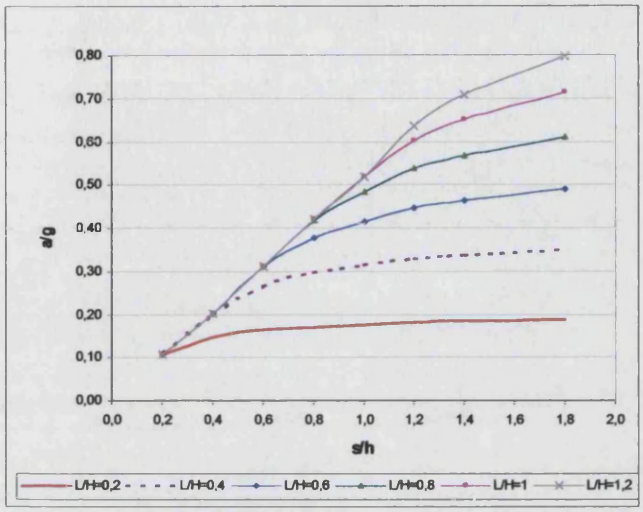

Figure 2- 16 - Variation of λc in function of s/h for different ratios L/H (f=0.3).

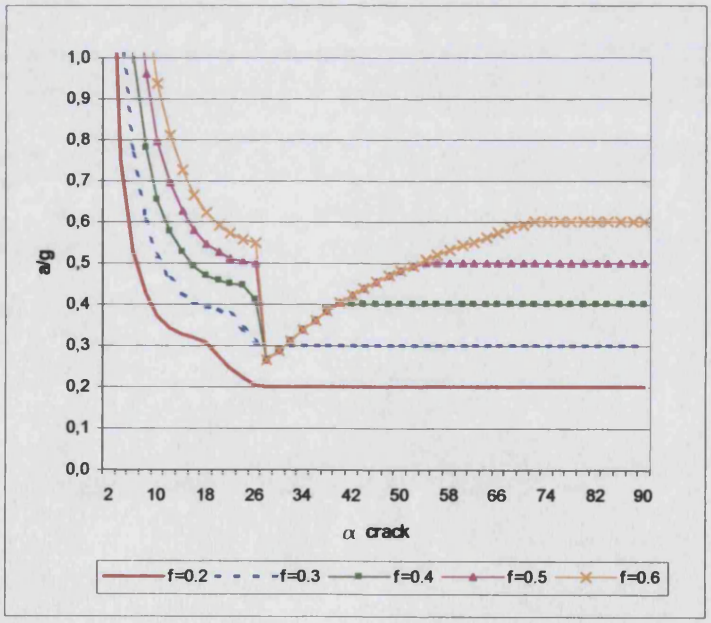

Figure 2- 17 - Functions of λ_c for L/H=0.7; s/h=0.5, for different friction coefficients.

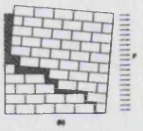

2.4.1 In plane mechanisms for a multi storey wall

In the case of a multi-storey wall, the formulations obtained at §2.4 for a single storey can easily be adapted, once the following assumptions have been introduced:

- Besides the collapse of the entire wall, a multi-storeys façade can also collapse partially involving only few storeys. The wall portion involved in the collapse can include a variable number of storeys from the top downwards. This means that failures involving only the central storeys will not be considered. According to this assumption, cracks will always reach the top of the wall, although they could start at any lower storey (Figure 2-18).
- Average thickness Tm of the wall between its base and top (Tb and Tu);
- Absence of openings on the facade surface;

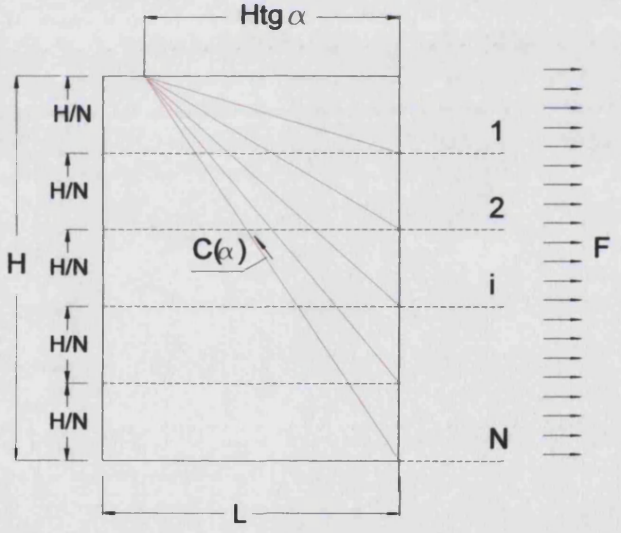

Figure 2- 18 – Multi storey wall – partial collapses

Equations (2-22),(2-23) and (2-26), relative to the overturning and sliding load factors (λ_o, λ_s) for a single storey of total height H, can be applied to a multi storey wall by substituting H with the variable H_i, defined as:

$$H_i = i \cdot \frac{H}{N} \qquad (2\text{-}30)$$

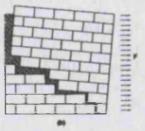

where N is the number of storeys considered. In the same equations, the value of $C_{tot(\alpha)}$, also depends on the variable height H_i.

Figure 2- 19 shows the load factor patterns for a multi storey wall and different ratios L/H. It is possible to observe that for multi storey walls characterised by rather small global ratios L/H, the load factor always coincides with the slender geometric proportions among all the possible ratios L/H_i, and hence coincides with the entire façade. On the other hand, for increasing L/H ratios, the curves become flatter up to the ratio L/H=0.8, so the collapse could occur indifferently at any storey of the wall under examination.

The evaluation of load factors at intermediate storeys is required when for one or more storeys at the bottom of the building, or at intermediate heights, the mechanism cannot be triggered because of specific conditions, for example the presence of strengthening devices.

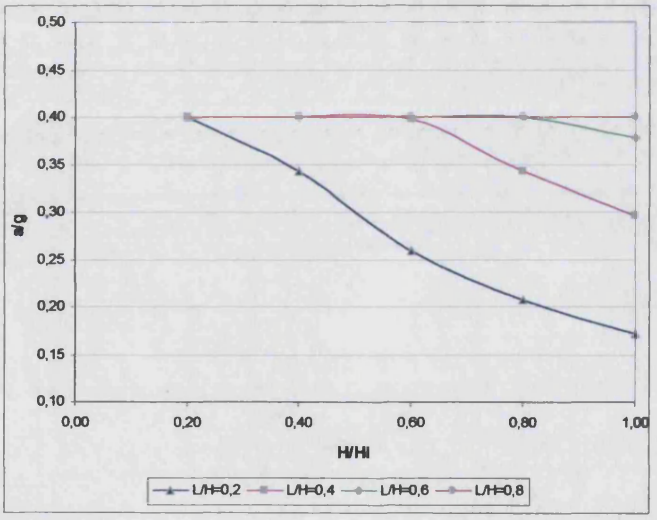

Figure 2- 19– Load factor pattern in a 5 storeys building (s/h=0.8;f=0.4).

2.4.2 In plane mechanisms in presence of loads horizontally distributed

The presence of horizontally distributed loads is a very common situation when considering the same panel previously examined as one of the building partitions. In this case the horizontally distributed loads simulate the action exerted by the roof and intermediate horizontal structures.

With reference to Figure 2- 20, representing a panel of overall dimensions L,H and number of storeys N, a uniformly distributed vertical load on top of the wall q_r, will be

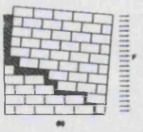

considered. Similarly, uniformly distributed vertical loads q_f will be considered on each of the N-1 levels (Figure 2- 20).

The weight of roof on the wall portion identified by the crack angle α_c is:

$$Q_r = q_r \cdot 3 \cdot dx_1 ; \tag{2-31}$$

where dx_1 has been previously introduced (see equations 2-24 and 2-25).

The total weight of the horizontal structures is:

$$Q_f = q_f \cdot \sum_{i=1}^{N-1} \ell_i ; \tag{2-32}$$

where ℓ_i is the segment length of each floor, given by the variable α_c.

It has been assumed that in the case of a single storey building Q_f=0.

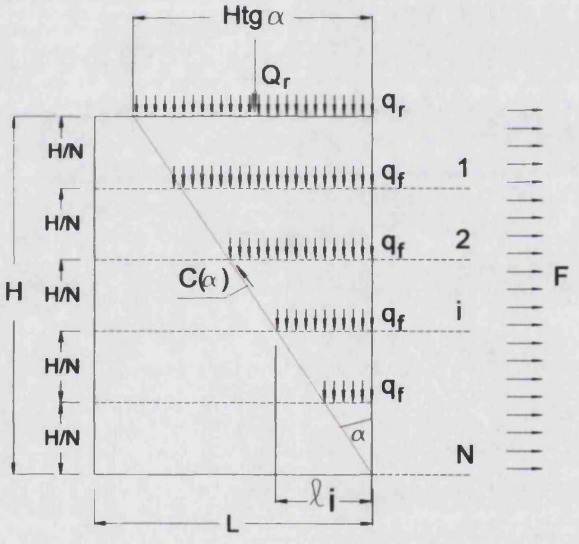

Figure 2- 20 - Uniformly distributed vertical loads of roofs and floors in a wall with N storeys.

Moreover, it has been assumed that, beside the vertical load action, these structural elements can also develop a restraining action exerted by friction acting at wall supports. This assumption has been made by considering all these structural elements as simply supported by walls, without any anchor device which would prevent friction developing. However, while this assumption is sufficiently realistic for wooden structures, it becomes less appropriate for other kinds of structures, such as r.c. slabs which are necessarily anchored to the walls.

The frictional effect of the roof (C_{qr}) and floors (C_{qf}) is given by:

$$C_{qr} = Q_r \cdot f ; \tag{2-33}$$

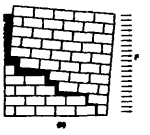

$$C_{qf} = Q_f \cdot f ; \tag{2-34}$$

Hence, the expressions for the overturning and sliding mechanisms introduced in (2-22), (2-23) and (2-26) become:

For $\alpha_c \leq \alpha_b$:

$$\lambda_O = \frac{W_1 \cdot dx_1 + W_2 \cdot \frac{L}{2} + C_{tot(\alpha)} \cdot dy_1 + dx_1 \cdot \left(\frac{3}{2} Q_r + Q_f\right) + H \cdot \left(C_{qr} + \frac{2}{3} C_{qf}\right)}{2 \cdot W_1 \cdot dy_1 + \frac{W_2}{2} \cdot \left(H + \frac{L}{tg\alpha}\right) + H \cdot \left(Q_r + \frac{2}{3} Q_f\right)} \tag{2-35}$$

for $\alpha_c > \alpha_b$:

$$\lambda_O = \frac{W_1 \cdot dx_1 + W_2 \cdot \frac{L}{2} + dx_1 \cdot \left(\frac{3}{2} Q_r + Q_f\right) + H \cdot \left(C_{qr} + \frac{2}{3} C_{qf}\right)}{2 \cdot W_1 \cdot dy_1 + \frac{W_2}{2} \cdot \left(H + \frac{L}{tg\alpha}\right) + H \cdot \left(Q_r + \frac{2}{3} Q_f\right)} \tag{2-36}$$

$$\lambda_S = \frac{C_{tot(\alpha)} + C_{qr} + C_{qf}}{W_1 + W_2 + Q_r + Q_f} \tag{2-37}$$

Note that in equation (2-35) the weight of roof Q_r has been considered as acting in the middle of the segment H tgα. Moreover, the increase of the total shear strength due to the weights of roofs and horizontal structures has been disregarded.

Figure 2- 21 and Figure 2- 22 compare the functions of λ_c for walls with the same parameters as those in Figure 2- 13, Figure 2- 14, in presence and absence of uniformly distributed loads Q_r and Q_f, acting on 5 storey walls. As can be observed, the presence of Q produces a considerable increase in λ_c in both cases, rising from λ_c=0.26 to λ_c=0.4 in the first case, and from λ_c=0.18 to λ_c=0.4 in the second case. However Figure 2- 21 and Figure 2- 22, are purely indicative, as increasing the number of floors actually increases the load factors.

These results are generalised in Figure 2- 23, which outlines the effect produced by increasing the distributed loads for the same wall characterised by different s/h ratios. The increase in distributed loads (Q_{tot}) leads an increase in the final load factor. However, this increase is more significant for small s/h ratios, while for progressively higher s/h values each curve tends to become flat when associated with higher friction coefficient. To sum up, it can be concluded that the presence of horizontally distributed loads produces an improvement in the mechanical performance of the panel in relation to in-plane failures, but only for a rather small staggering ratio, always lower than 1.

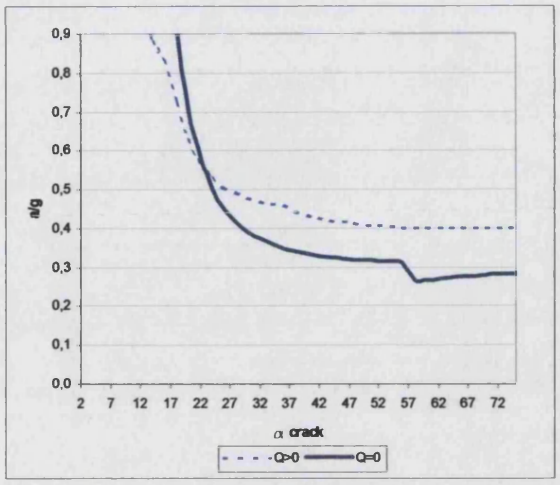

Figure 2- 21 - Functions of λo ,and λs for L/H=0.35;f=0.4;s/h=1,5,N=5, in presence and absence of Q_r ,Q_f (Q_r=4KN/m; Q_f=3KN/m)

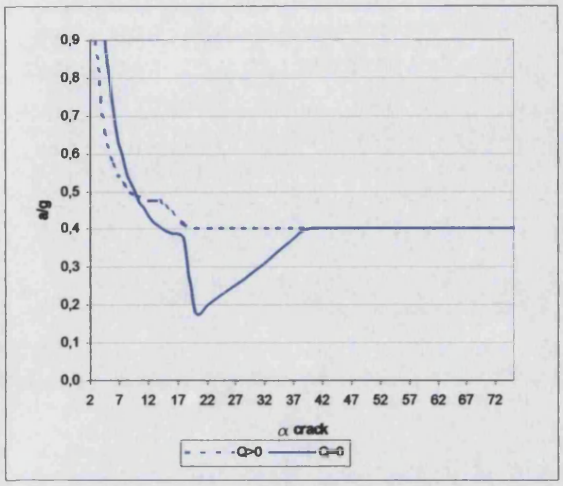

Figure 2- 22 - Functions of λo ,and λs for L/H=1.2;f=0.4;s/h=0.35, N=5 in presence and absence of Qr ,Qf (Q_r=4KN/m; Q_f=3KN/m)

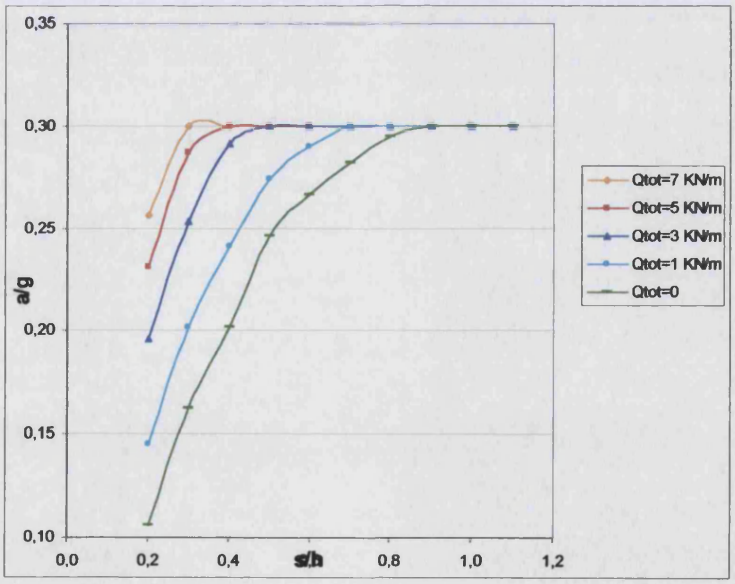

Figure 2- 23 – Patterns of λc as function of s/h, for different values of Q_{tot} (Q_r+Q_β), for L/H=0.4;f=0.3.

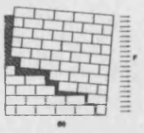

2.5 Formulation of out-of-plane mechanisms

This section contains the formulation of 8 out-of-plane collapse mechanisms of outer walls, as previously identified in §1.6 of Chapter 1. It also considers the occurrence of local collapse of vertical additions or gable ends.

The formulation of out-of-plane mechanisms is developed by taking into account, when required by the model, the restraining action developed at connections between the façade and the party walls according to the mechanical model described in §2.2.

2.5.1 Overturning of façade and of facade with side walls (A,B1,B2)

The failure mechanisms presented in this paragraph are all characterised by the overturning of the façade wall, and differ from each other in the position of the cracks, as shown in Figure 2- 24.

Type A refers to overturning of the façade without the participation of the party walls, because no connection is present at the edges of the wall, or when such connection is rather poor due to the geometric dimensions of the connecting elements. Mechanisms B1 and B2 will occur instead of mechanism type A when the level of connection is sufficient to involve either one or both party walls in overturning the façade wall. These mechanisms develop through the occurrence of a diagonal crack along the party wall and a horizontal hinge on the façade.

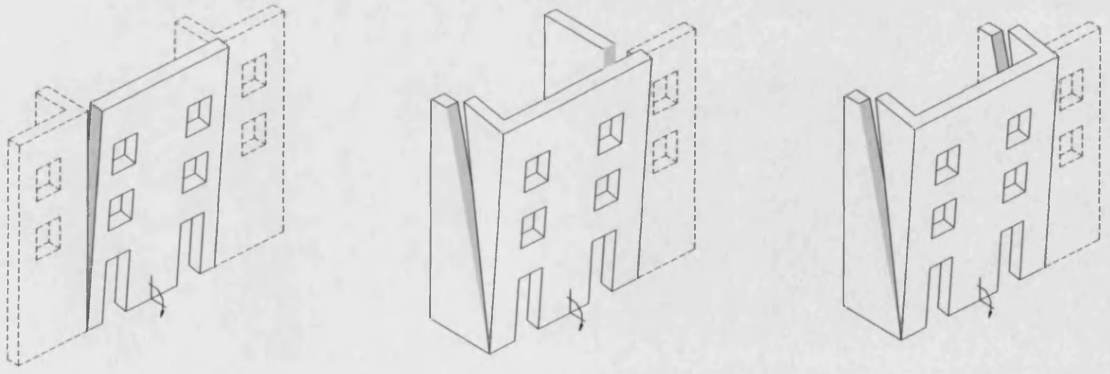

(A) (B1) (B2)

Figure 2- 24 – (A) Façade Overturning; (B1) Façade Overturning with one lateral wing; (B2) Façade Overturning with two lateral wings.

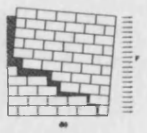

The position of the crack angles in both mechanisms B1 and B2 is optimised by means of the in-plane formulations in §2.4.

Moreover, it is assumed that all the mechanisms could occur partially as well as by involving the whole façade. Their analytical formulation is developed in a general form, suitable for any of the N storeys of the building, with the horizontal hinges forming at any storey level.

Figure 2- 25 shows the geometric parameters and the centre of mass of vertical and horizontal loads, acting in failure type A.

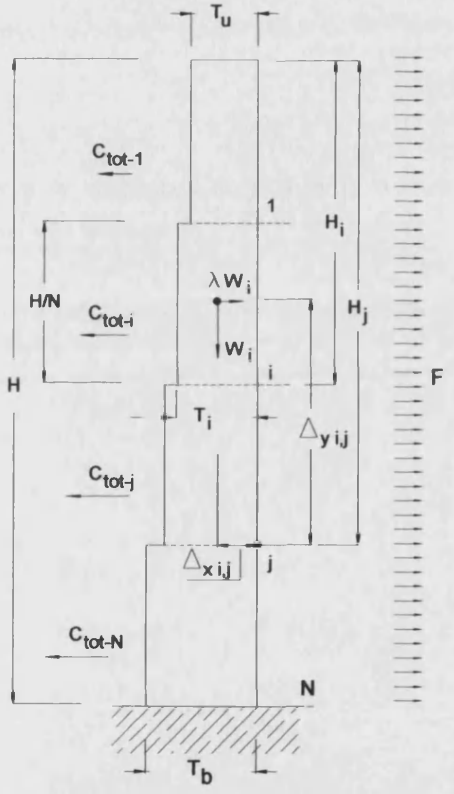

Figure 2- 25 – Free standing wall: geometric parameters, and acting loads.

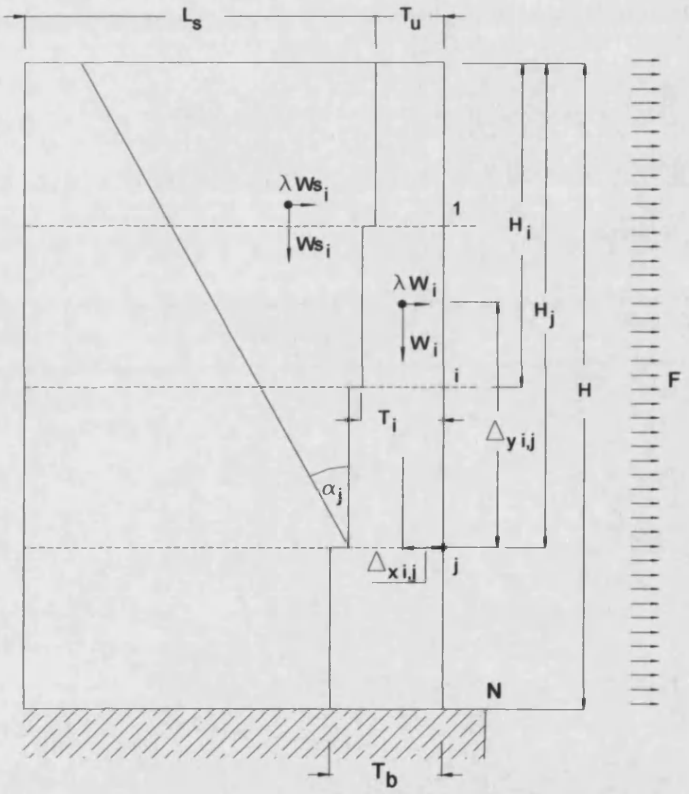

Figure 2- 26 – Wall and party walls overturning: geometric parameters, and acting loads

The equilibrium to rotation of a generic storey *i* around a generic hinge *j*, placed at a lower storey (*j*> *i*), yields the net moment:

$$M_{i,j} = W_i \cdot \Delta x_{i,j} - \lambda \cdot W_i \cdot \Delta y_{i,j} \tag{2-38}$$

where the vertical and horizontal lever arms $\Delta x_{i,j}$ and $\Delta y_{i,j}$ are governed by:

$$\Delta x_{i,j} = \frac{T_i}{2}; \qquad \Delta y_{i,j} = H_j - \left(H_i - \frac{H}{2N} \right); \tag{2-39}$$

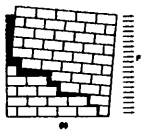

For case (A), the sum of the bending moments regarding all the storeys above level j, in relation to a given hinge j, is the following:

$$\sum_{i=1}^{j} M_{i,j} = \sum_{i=1}^{j} \left(W_j \cdot \Delta x_{i,j}\right) - \sum_{i=1}^{j} \left(\lambda \cdot W_i \cdot \Delta y_{i,j}\right) \tag{2-40}$$

The seismic factor λ for mechanism A relative to a generic hinge j (with $1 \leq j \leq N$) placed along the height H of the building is:

$$\lambda_{(0),j} = \frac{\sum_{i=1}^{j} \left(W_i \cdot \Delta x_{i,j}\right)}{\sum_{i=1}^{j} \left(W_i \cdot \Delta y_{i,j}\right)} \tag{2-41}$$

Expression (2-40) does not consider any restraining force exerted at the façade connections. Hence, formulation (2-40) is suitable for a building wall where the connections at the edges of which, are insufficient or totally missing.

However, when the edge connections are effective, the total shear strength C_{tot} along the vertical edges, has to be taken into account. In this case the load factor becomes:

$$\lambda_{(0),j} = \frac{\left[\sum_{i=1}^{j} \left(W_i \cdot \Delta x_{i,j}\right)\right] + (\varepsilon + \beta) \cdot \left(C_{tot-j} \cdot \frac{H_j}{3}\right)}{\sum_{i=1}^{j} \left(W_i \cdot \Delta y_{i,j}\right)} \tag{2-42}$$

where

ε is the number of edge party walls considered orthogonal to the façade under examination, introduced at §2.3.2.

β is the number of internal bearing walls orthogonal to the façade, and effectively anchored to it, as described at §2.3.2.

C_{tot-j} is the total shear strength developed along a vertical crack of height H_j, as formulated in (2-2) and (2-3), applied at 1/3 of the height H_j. This formulation is applied to all $(\varepsilon+\beta)$ orthogonal walls considered, characterised by sufficient connections with the front wall.

In the cases of failure modes B1 and B2, it is assumed that at least one edge connection, between the façade and orthogonal walls is sufficient to involve the lateral wings in the overturning. The crack angle α_c in both mechanisms B1 and B2 is optimised by means of the in plane formulation discussed in §2.4.

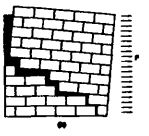

However, as in this case the walls subjected to the in-plane actions are those placed behind the façade and connected at its edges, the load factor expressions (2-22),(2-23) and (2-26) refer to the perpendicular walls, and not to the main façade.

On the basis of the in-plane approach developed in §2.4, it is therefore possible to determine the critic angle α_c, which represents the slope of the crack along the side walls. The calculation can be performed for any storey of the building, considering progressive values of H_i as increasing from the top.

Once the limit angle α_c has been optimised at any storey *i*, it is possible to proceed to the calculation of mechanism B1 and B2 (Figure 2- 26).

The load factor λ, expressed in relation to hinge j, is governed by:

$$\lambda_{(\alpha),j} = \frac{\left[\sum_{i=1}^{j}\left(W_i \cdot \Delta x_{i,j}\right)\right] + (\varepsilon+\beta)\cdot Ws_{(\alpha j)}\left(\frac{1}{3}H_j \cdot \tan\alpha_j + T_i\right)}{\left[\sum_{i=1}^{j}\left(W_i \cdot \Delta y_{i,j}\right)\right] + (\varepsilon+\beta)\cdot Ws_{(\alpha j)} \cdot \frac{2}{3}H_j} \qquad (2\text{-}43)$$

for ε =1,2 respectively for failure mechanisms B1 and B2, where:

$Ws_{(\alpha j)}$ is the weight of the side wall portion identified by angle α_j. It has been assumed that $Ws_{(\alpha j)}$ and the relative crack angle α_j are the same for all orthogonal walls participating in the failure mechanism. This assumption is equivalent to considering all the orthogonal walls as having the same fabric layout (s/h) as well as the same overall geometric parameters (L/H).

As can be noted, equation (2-43) does not consider the variable $C_{tot(\alpha j)}$, relative to the total shear strength along the crack line inclined at α_j, since the variable has already been taken into account when optimising the crack angle according to equations (2-22, 2-23) and (2-26). This is equivalent to assuming that the overturning failure sets in only once the inclined cracks have cut the party walls.

When roof and floors vertical loads are acting, as shown in Figure 2- 27 and Figure 2-28, equations (2-42) and (2-43) become:

$$\lambda_{(0),j} = \frac{\left[\sum_{i=1}^{j}\left(W_i \cdot \Delta x_{i,j}\right)\right] + (\varepsilon+\beta)\cdot\left(C_{tot-j}\cdot\frac{H_j}{3}\right) + Q_r\left(\frac{T_u}{2} + f\cdot j\frac{H}{N}\right) + \sum_{i=1}^{j}Q_f\cdot\left(dx_j + f\cdot\frac{H}{N}(j-i)\right)}{\sum_{i=1}^{j}\left(W_i\cdot\Delta y_{i,j}\right) + Q_r\cdot j\frac{H}{N} + \sum_{i=1}^{j}Q_f\cdot\frac{H}{N}(j-i)} \qquad (2\text{-}44)$$

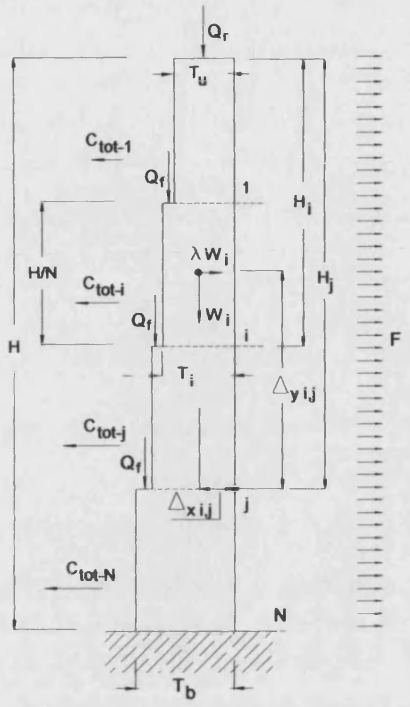

Figure 2- 27- Free standing wall with vertical loads applied

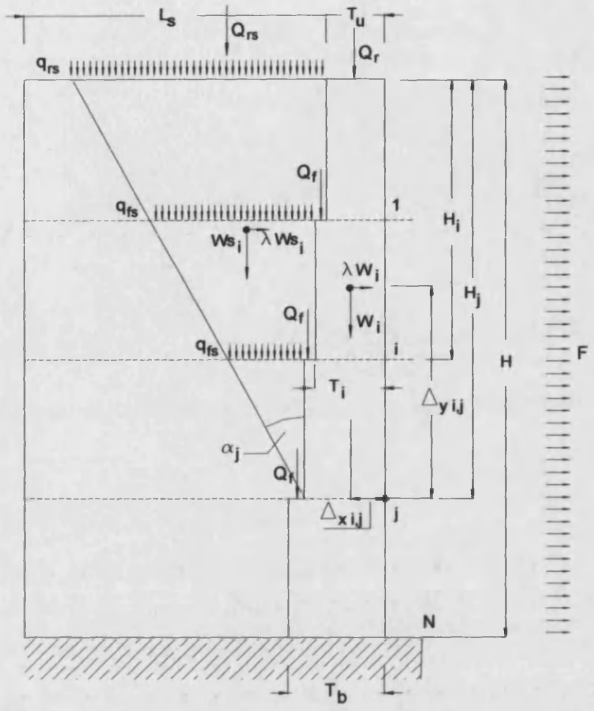

Figure 2- 28 - Overturning with side walls, with vertical loads applied

$$\lambda_{(\alpha),j} = \frac{[\sum_{i=1}^{j}(W_i \cdot \Delta x_{i,j})] + (\varepsilon+\beta)\cdot Ws_{(\alpha j)}\left(\frac{1}{3}H_j \cdot \tan\alpha_j + T_i\right) + Q_r\left(\frac{T_u}{2} + f \cdot j\frac{H}{N}\right) + \sum_{i=1}^{j} Q_f \cdot \left(dx_j + f \cdot \frac{H}{N}(j-i)\right)}{[\sum_{i=1}^{j}(W_i \cdot \Delta y_{i,j})] + (\varepsilon+\beta)\cdot Ws_{(\alpha j)} \cdot \frac{2}{3}H_j + Q_r \cdot j\frac{H}{N} + \sum_{i=1}^{j} Q_f \cdot \frac{H}{N}(j-i)} \quad (2\text{-}45)$$

for ε =1,2 respectively for failure mechanisms B1 and B2, where the lever arm dx_j is:

$$dx_j = T_i - \frac{(T_b - T_u)}{2\cdot(N-1)} \quad (2\text{-}46)$$

and $Ws_{(aj)}$ is the weight of the portion of side wall identified by angle α_j, including the weight of the roof and horizontal structures, as formulated in (2-31) and (2-32). In this case, the centre of masses of the roof and floors is assumed to coincide with that of the wall portion.

The three failure mechanisms A, B1 and B2 are compared in Figure 2- 29, Figure 2- 30, where the associated load factors for a 5-storey wall are plotted against the slenderness (Hi/Ti) relative to increasing wall portions, with the number of storeys progressing from 1 to 5 (entire wall height). The wall thickness has been kept constant for all storeys, so the slenderness ratios from the bottom storeys upwards increases linearly. Each curve of the

following diagrams is then characterised by 5 load factors, the first 4 of which concern partial collapses, with the number of storeys involved increasing to the right, while the 5th represents the collapse of the entire facade.

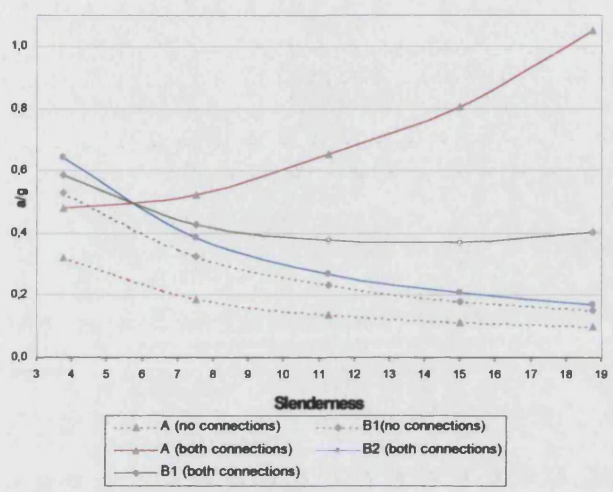

Figure 2- 29 –Comparison of the 3 failure modes in presence and absence of edge connections.

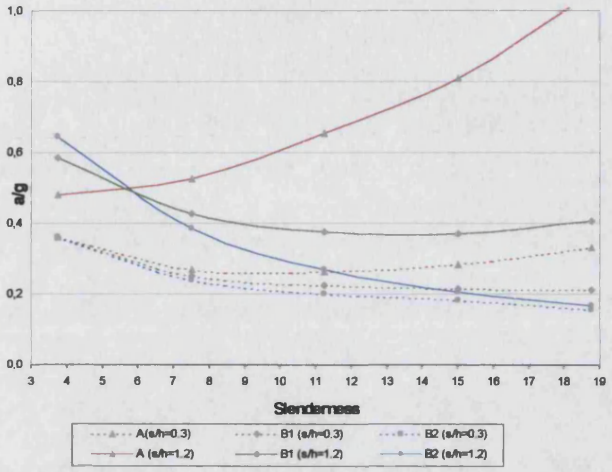

Figure 2- 30 – Load factors patterns for different values of masonry stagger ratios s/h (H/L=3;f=0,4;th=0.8;Ls=4; s/h=1.2)

Figure 2- 29 outlines the role exerted by edge connections on the 3 failure modes under examination. One can observe how the load factors associated with each failure mode are ranked in relation to this structural feature. Figure 2- 30 compares the failure mechanisms by considering two very different values of s/h (0.3 and 1.2) in order to outline the role exerted by this parameter in defining the probability of collapse and the number of storeys most likely involved.

It is important to note how the simple overturning mechanism (A) proves to be the one most influenced by the presence of connections: while in the absence of edge connections the collapse is more likely to involve the whole façade rather than just a part of it, when edge connections are present, the most critical storey becomes the topmost. This behaviour is clearly understandable by considering that, while in the first condition the only variable affecting the load factor is the façade slenderness, in the second case the total shear strength $C_{tot(j)}$, placed at numerator of (2-42), produces a radical change in the curve pattern. This change is due to the fact that $C_{tot(j)}$ increases linearly downwards with façade height more quickly than the slenderness ratio. However, as outlined in §2.2.2, the increased ratio of the

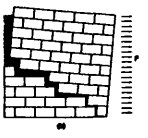

total shear strength $C_{tot(j)}$ is governed by the stagger ratio s/h. The diagram of Figure 2- 30 shows that, even in the presence of edge connections, when the stagger ratio is smaller than that one considered in Figure 2- 29, the critical storey becomes an intermediate one. In conclusion, for failure type A, while in the absence of edge connections the whole façade is always involved in the mechanism, in the presence of connections the failure strictly depends upon the stagger ratio s/h. For increasing s/h ratios, the façade load factor will also increase, while the number of storeys involved gets gradually smaller.

Similar behaviour is illustrated in the two diagrams for failure type B1. In this case too, the presence of edge connections leads to greater values of the load factor, while the critical number of storeys tends to decrease. However, this mechanism is less influenced by connections than failure mechanism A. As a matter of fact, in this case only one vertical edge is considered, while on the other edge the crack is inclined along the orthogonal wall. Similarly, the increase in the stagger ratio produces an improvement in the seismic behaviour, in terms of load factors and number of storeys involved.

However, failure type B2 is not influenced by vertical connections since this mechanism is characterised by all cracks inclined along the party walls.

Similarly to failure modes A and B1, an increase in the stagger ratio s/h produces a general improvement in the seismic performance, as the load factors also increase. However, the number of storeys involved does not change as the minimum load factor always corresponds to the entire façade height.

2.5.2 Corner failure (C)

As shown in Figure 2- 31, this mechanism is characterised by the overturning of a corner around a hinge placed at the basement of the building or at any upper storey, in the case of partial collapses involving a smaller number of storeys. The assumptions on which this failure mode is based, are:

- Constant thickness T_i (i.e. thickness of the façade at the bottom of the i-th storey from top), along the corner involving i storeys of the facade, for both orthogonal walls (Figure 2- 32);
- Rotation of corner around the hinge A_i, point of intersection of the orthogonal walls;

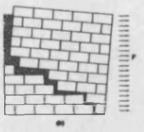

Crack angles α_{fi} and α_{si}, respectively on the façade and orthogonal wall, result from the optimisation process of the in-plane behaviour (§2.4). As for failure modes B1 and B2, it is assumed that the overturning failure can onset only once the cracks have cut both orthogonal walls;

A consequence of the previous point is that no restraining action due to the total shear strength of the masonry is considered along the cracks, since this was previously taken into account in the crack angle optimisation process (2-22, 2-23) and (2-26).

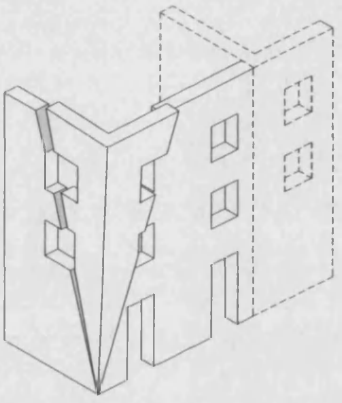

Figure 2- 31 – Corner failure (c)

Having identified the crack angles, α_{fi} and α_{si} at any storey i, it is possible to proceed with the calculation of the mechanism, whose geometric parameters are shown in Figure 2-32.

The net equilibrium of a generic corner at level i, around hinge A_i, is:

$$\lambda \cdot \left(W_{fi} + W_{ci}\right) \cdot \frac{2}{3} \cdot i\frac{H}{N} = W_{fi} \cdot d_{fi} + W_i \cdot d_{si} \tag{2-47}$$

Therefore the load factor is:

$$\lambda \cdot = \frac{W_{fi} \cdot d_{fi} + W_i \cdot d_{si}}{\left(W_{fi} + W_{ci}\right) \cdot \frac{2}{3} \cdot i\frac{H}{N}} \tag{2-48}$$

where:

W_{fi} is the weight of a portion of facade, identified by crack angle α_{fi}, with origin at A_i. W_{fi} also includes the weight of the roof and horizontal structures Q_f and Q_r, as formulated in (2-31) and (2-32).

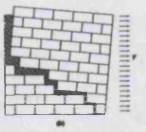

W_{si} is the weight of the side wall portion, identified by crack angle α_{si}, with origin at A_i. W_{si} also includes the weight of the roof and horizontal structures Q_{fs} and Q_{rs}, as formulated in (2-31) and (2-32).

d_{fi} is the lever arm of W_{fi};

d_{si} is the lever arm of W_{si};

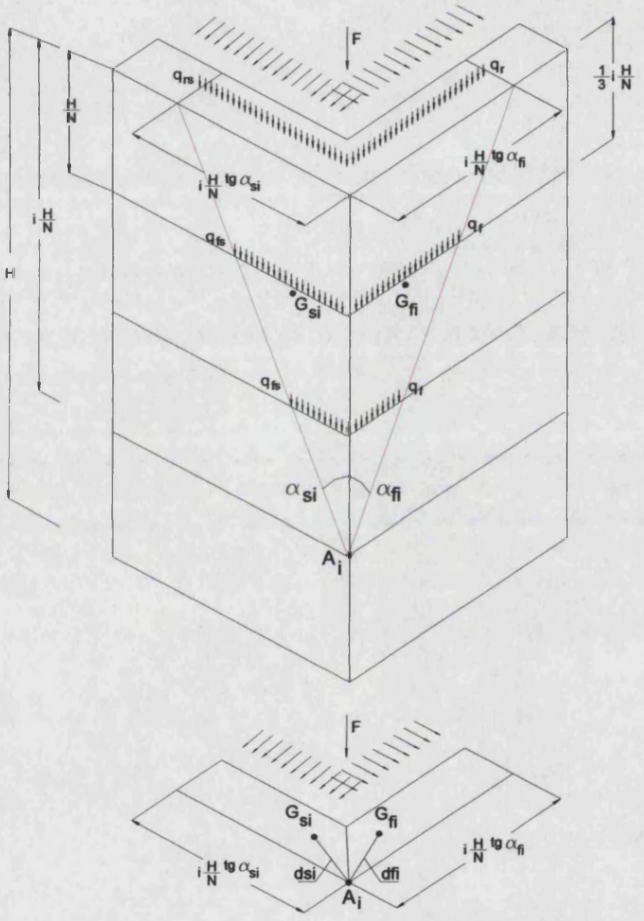

Figure 2- 32 – Geometric parameters characterising the corner failure

The lever arms d_{fi} and d_{si} are obtained by considering that the centres of mass G_{fi} and G_{si} of W_{fi} and W_{si} respectively, are assumed to coincide with those of the 2 triangles, as shown in Figure 2- 32.

$$d_{fi} = \sqrt{\left(\frac{1}{3} \cdot i \frac{H}{N} \cdot tg\alpha_{fi}\right)^2 + \left(\frac{T_i}{2}\right)^2}\ ; \qquad d_{si} = \sqrt{\left(\frac{1}{3} \cdot i \frac{H}{N} \cdot tg\alpha_{si}\right)^2 + \left(\frac{T_i}{2}\right)^2} \tag{2-49}$$

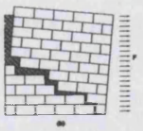

The pattern of the load factor λ is outlined in Figure 2- 33, as a function of the façade slenderness H/Ti, for a given value of the friction coefficient f.

The diagram shows how for very low values of the stagger ratios (from 0.4 to 1.6), the collapse of the corner involves the entire façade. It can be observed that increasing s/h ratios give rise to increasing load factors, showing an improvement of the seismic performance. For s/h ratios greater than 1.6, the curves pattern changes, showing the same minimum load factor on the upper storeys for any value of s/h.

This behaviour is in agreement with that described for failure mode A outlined in Figure 2- 30.

Similarly to failure mechanisms A, B1, B2, the friction coefficient influences mechanism C in same way as s/h, so that for increasing values of f, the set of curves moves upwards, showing an improvement in the seismic performance.

In conclusion, for mechanism C, the likelihood of occurrence as well as the number of storeys involved, is deeply influenced by the masonry fabric, and hence by the s/h ratio, so that the smaller the overlapping length between the stones, the greater the associated load factor of the façade as well as the number of storeys involved.

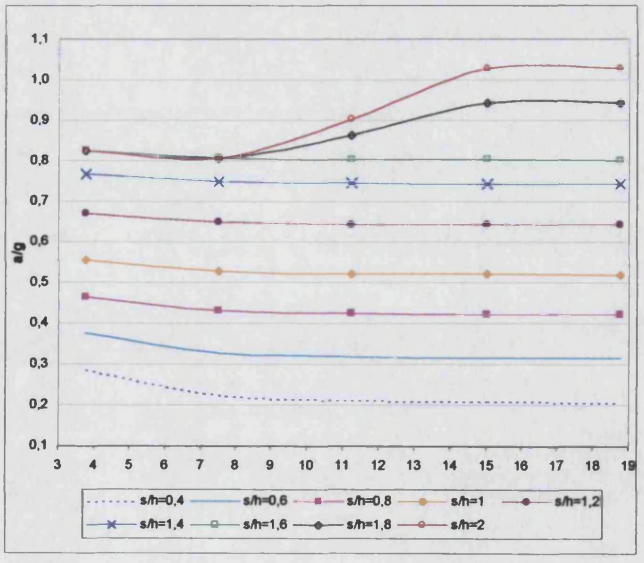

Figure 2- 33 – Load factor patterns for different slenderness (H/Ti) and slenderness ratios (s/h) (H/N=3;f=0.4;Lb=4) .

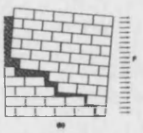

2.5.3 Partial overturning (D)

This mechanism, shown in Figure 2- 34, has been developed in a general form, in order to involve a variable number of storeys *i*. The assumptions made are:

- Inclination of the crack line is defined by the diagonal through *i* storeys and is not influenced by the opening layout;
- Average thickness T_{mi}, between thickness at the top (T_u) and at level *i* (T_i);
- Torsional friction resistance along the inclined crack line is not considered.

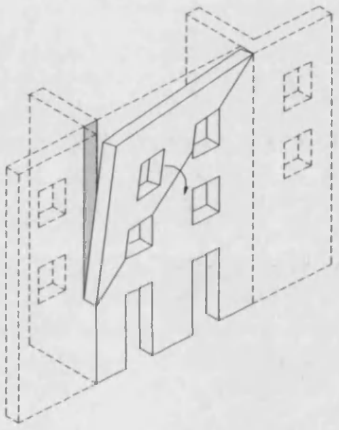

Figure 2- 34 – Partial overturning (D)

Figure 2- 35 (a,b) shows the geometric parameters involved.

The mechanism can be formulated by expressing the equilibrium of a triangular portion of *i* storeys from the top around the cylindrical hinge x_i (Figure 2- 35, a,b).

The equilibrium around x_i is:

$$\lambda \cdot \cos\alpha_i \cdot \left(W_i \cdot \Delta y_i + Q_r \cdot \frac{H_i}{2} + Q_{fi} \cdot \Delta y_i \right) =$$

$$\cos\alpha_i \cdot \left(\frac{H_i}{3} \cdot \left(C_{tot-i} + C_{tot-\beta i} \right) + \Delta z_i \cdot \left(W_i + Q_r + Q_{fi} \right) + f \cdot H_i \cdot \left(\frac{Q_r}{2} + Q_{fi} \cdot \frac{2}{3} \right) \right) \quad (2\text{-}50)$$

where:

W_i is the weight of the triangular portion in question of thickness T_{mi};

Q_r is the total weight of the roof along L;

Q_{fi} is the total weight of horizontal structures acting on the triangular portion delimited by α_i;

C_{tot-i} is the total shear strength developed along the vertical edge of height H_i, as formulated in (2) and (3), applied at 1/3 of the height H_i ;

$C_{tot-\beta i}$ is the resultant total shear strength developed along the β internal bearing walls of segment lengths included by angle α_i, as formulated in (2-2) and (2-3), applied at 1/3 of the height H_i ;

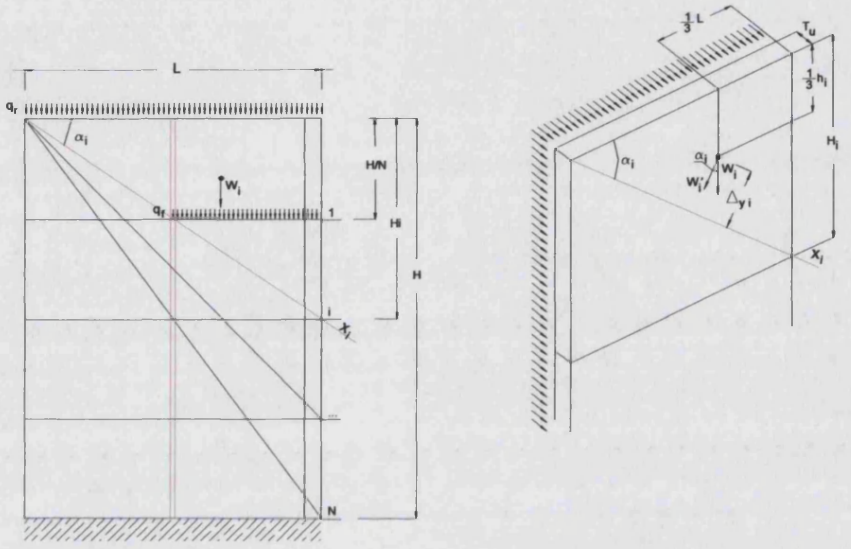

(a) (b)

Figure 2- 35 – Geometric parameters involved in the mechanism

The total weight of horizontal structures Q_f is:

$$Q_f = q_f \cdot \sum_{1}^{i} \ell_i \qquad (2\text{-}51)$$

where ℓ_i is the segment length of each floor, identified by the angle α_i, as introduced at (2-32). It is assumed that in the case of a single storey, Q_f=0.

Equation (2-50) also considers the restraining actions developed by roof and horizontal structures due to the friction effect.

The lever arms Δ_{zi} and Δ_{yi} are governed by:

$$\Delta z_i = \frac{T_{mi}}{2}; \qquad \Delta y_i = \frac{2}{3} \cdot H_i; \qquad (2\text{-}52)$$

Finally, the load factor is:

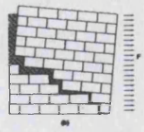

$$\lambda = \frac{\left(\frac{H_i}{3}\cdot\left(C_{tot-i}+C_{tot-\beta i}\right)+\Delta z_i\cdot\left(W_i+Q_r+Q_{fi}\right)+f\cdot H_i\cdot\left(\frac{Q_r}{2}+Q_{fi}\cdot\frac{2}{3}\right)\right)}{\left(W_i\cdot\Delta y_i+Q_r\cdot\frac{H_i}{2}+Q_{fi}\cdot\Delta_{y_i}\right)} \qquad (2\text{-}53)$$

The behaviour of this failure mechanism is highlighted in Figure 2- 36, obtained by plotting the load factors as a function of the slenderness ratio Hi/Ti.

The diagram outlines the role exerted by the stagger ratio s/h, shown to be equivalent to that observed for mechanism A (Figure 2- 37). For increasing values of the s/h ratio, the function tends to shift upwards with increasing steepness, outlining the onset of the mechanism for fewer and fewer storeys: for s/h = 0.3, the mechanism involves 3 storeys, while for s/h=2 just the top storey fails.

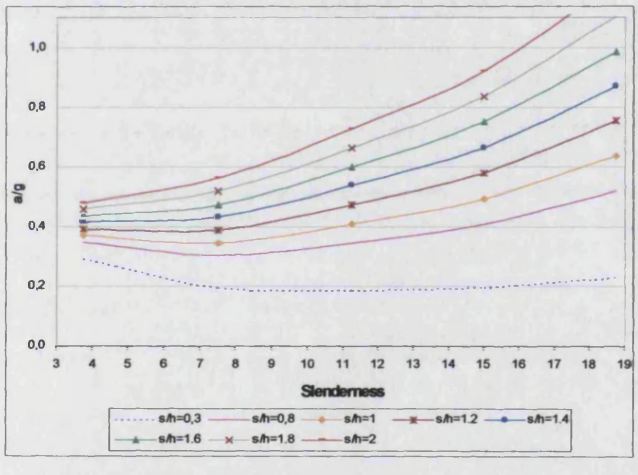

Figure 2- 36 – Load factor curves as a function of the slenderness, for different values of the stagger ratio s/h, in presence of lateral connection (H/L=5; Tb=0.8).

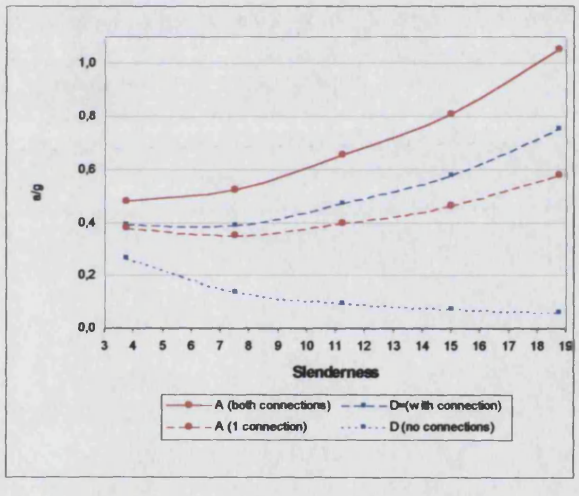

Figure 2- 37 – Comparison between failure mechanisms D and A (with and without connections) (H/L=5; Tb=0.8, s/h=1.2)

Figure 2- 37 mechanism compares D and A taking into account the level of connection at the edges. It can be observed how the edge connections influence their ranking as well as the number of storeys involved. If the wall is strongly anchored to party walls (ε=2), mechanism D is more likely to occur than A, and just the two top storeys would fail. When the connections are asymmetrical, the onset of mechanism D on the side where the connection is missing can be seen to become the most probable. This means that D is still the most vulnerable and in this case the entire façade is involved in the mechanism.

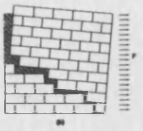

2.5.4 Partial overturning influenced by opening layout (E)

When the opening layout is characterised by two columns of windows vertically aligned, the façade can collapse according to the failure mode sketched in Figure 2- 38.

The collapse can also occur partially, involving a variable number of storeys *i*, which overturn around a cylindrical hinge placed at the bottom of level *i*.

It is assumed that the portion of façade involved is conditioned by the width of the side piers, which define the distance between the column of the openings and the closest vertical edge. Therefore if the windows are aligned vertically and the width of the side pier is greater than the width of the window and if the edge connection is active, the vertical crack can occur within the façade itself, on one or both sides of the façade.

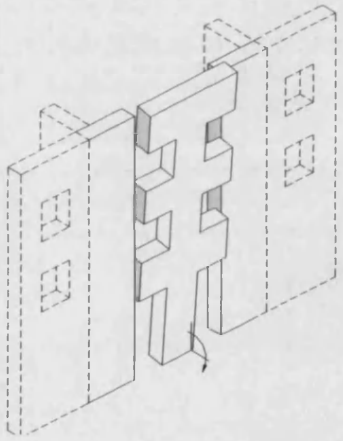

Figure 2- 38 – Partial overturning conditioned by opening layout

In order to define different failure modes, the width of side piers is considered *regular* when greater than the window width. This geometrical feature is governed by the variable η, introduced in §2.3.2.

Three different failure mechanisms, depending on the width of side piers, can be identified and these are sketched in Figure 2- 39 (a,b,c). When the openings are sufficiently distant from both vertical edges of the façade (η=2), the failure occurs according to Figure 2- 39 (a). In this case both cracks are internal to the façade and run along the external alignments of the two window columns. When one of the two piers is not regular, the crack moves along the external edge of the window column (Figure 2- 39, b).

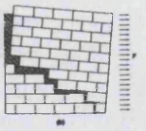

Finally, when the openings are very close to both façade edges (η=0), as shown in Figure 2- 39 (c), it is reasonable to suppose that the cracks appear directly at façade edges ($L_{var} \equiv L$). Figure 2- 40 summarises all the geometric parameters defining this failure mechanism.

The analytical formulation of this mechanism can be directly derived from the one obtained for simple façade overturning (A) (2-44).

The equilibrium to rotation of a generic storey *i* around a generic hinge *j*, placed at a lower storey ($j>i$) yields to equation of the load factor, valid for any value of η:

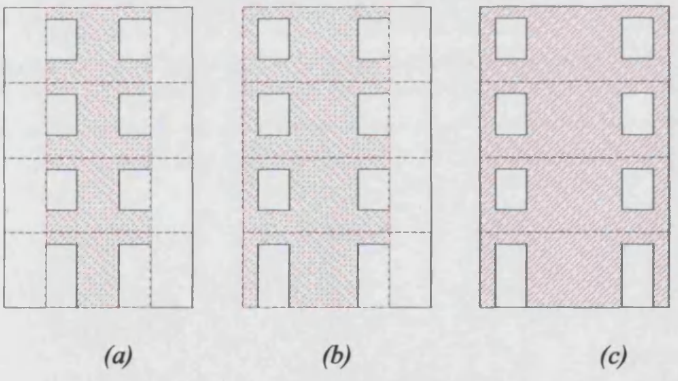

Figure 2- 39 – Portions of façade involved in the collapse in relation to the spandrel length

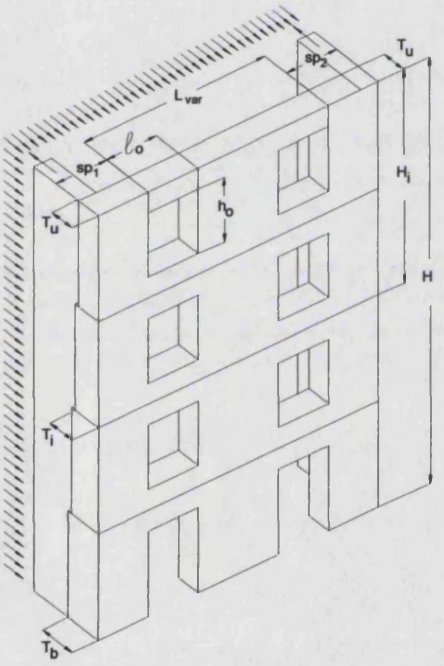

Figure 2- 40 – Geometric parameters involved

$$\lambda_{(0),j} = \frac{[\sum_{i=1}^{j}(W_i \cdot \Delta x_{i,j})] + C_{tot-j} \cdot \left[\left(\beta \cdot \frac{H_j}{3}\right) + \frac{(n_{\varepsilon,\eta} + \eta) \cdot (H_j - j \cdot h_{op})}{3}\right]}{\sum_{i=1}^{j}(W_i \cdot \Delta y_{i,j}) + (q_r \cdot L_{var}) \cdot j\frac{H}{N} + \sum_{i=1}^{j}(q_f \cdot L_{var})\frac{H}{N}(j-i)} +$$

$$+ \frac{(q_r \cdot L_{var}) \cdot \left(\frac{T_u}{2} + f \cdot j\frac{H}{N}\right) + \sum_{i=1}^{j}(q_f \cdot L_{var}) \cdot \left(dx_j + f \cdot \frac{H}{N}(j-i)\right)}{\sum_{i=1}^{j}(W_i \cdot \Delta y_{i,j}) + (q_r \cdot L_{var}) \cdot j\frac{H}{N} + \sum_{i=1}^{j}(q_f \cdot L_{var})\frac{H}{N}(j-i)} \qquad (2\text{-}54)$$

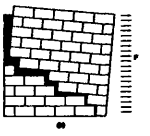

where $n_{(\varepsilon,\eta)}$ is a finite number depending on ε and η, related to the effectiveness of the connections between the façade portion involved in the failure and the edge orthogonal walls. Its value is governed by the following conditions:

for $\eta=2 \Rightarrow n_{(\varepsilon,\eta)}=0$

for $\eta<2 \Rightarrow n_{(\varepsilon,\eta)}=(\varepsilon-\eta)$

$n_{(\varepsilon,\eta)}$ is assumed to be 0 in all cases where $(\varepsilon-\eta)<0$.

In the same equation, W_i represents the weight of the façade involved in the mechanism of variable length L_{var}. The other symbols have been previously defined.

As can be observed, the main difference between equation (2-44) obtained for mechanism A and equation (2-54) relative to failure type E, consists in the total shear strength C_{tot}.

In the presence of openings, the C_{tot} distribution has been simplified by considering a continuous distribution along the height $(H_i-j\cdot h_{op})$ in place of a discontinuous function interrupted over the opening heights.

Figure 2- 41 compares the load factor patterns for failure mode (E) relative to a façade characterised by the same opening layout but different side piers.

When both edge connections are missing ($\varepsilon=0$) which means that the façade is a free standing wall, mechanism (A) becomes the most critical failure and its curve is coincident with that of E with both lateral piers irregular ($\eta=0$). Lateral piers either asymmetrical ($\eta=1$), or both regular ($\eta=2$), are associated with higher load factors. Moreover, it can be observed the coincidence between the curves ($\varepsilon=0$; $\eta=2$) and ($\varepsilon=2$; $\eta=2$) due to the fact that when $\eta=2$, the load factor is not influenced by the effectiveness of lateral connections, because in both these cases the vertical cracks are internal to the façade.

When the connections of the façade to the orthogonal walls are both effective ($\varepsilon=2$), it can be observed that the three E curves for the three different opening layouts ($\eta=0$, $\eta=1$, $\eta=2$) are rather close to each other, their slight differences just depending upon the different masses involved in the mechanism. However, it is evident that in this case mechanism E is much more likely than A, and the storeys involved, whatever the lateral pier, are the two at the top.

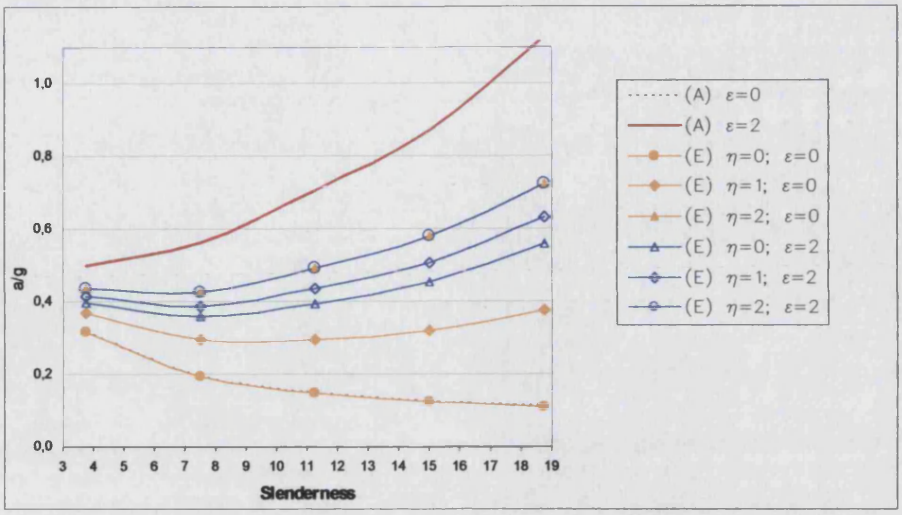

Figure 2- 41 – Load Factor patterns for (E) for the same opening layout and different edge spandrels, in the presence and absence of connections with orthogonal walls. Comparison with failure type A. (H/L=5; Tb=0.8;s/h=1.2)

2.6 Out of plane mechanisms based on the "arch effect"

2.6.1 Out of plane mechanism based on vertical arch effect (F)

As introduced in §1.6, this failure mechanism onsets when the presence of strengthening devices cause vertical strips of the façade to tend to deflect outwards, being restrained at the top and bottom (Figure 2- 42). The analytical model simulates the presence of strengthening devices by identifying two cylindrical horizontal hinges placed at variable height along the façade of the building. As the cylindrical hinges simulate the restraining action exerted by strengthening devices, it is assumed that the two extreme hinges are positioned at floors and roof levels only (D'Ayala, Speranza, 2003). When the mechanism is triggered, a third central hinge forms along the façade, whose position is marked by a horizontal crack, at an intermediate position between the two edge hinges.

The mechanical model is formulated in a general form, assuming that the two edge hinges are located at any level along the total height H of the façade.

Moreover, a linear variation in the thickness of the façade from the bottom to the top has also be assumed.

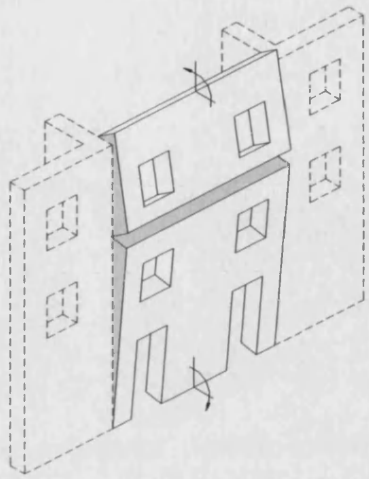

Figure 2- 42– Vertical strip arch failure (F)

Figure 2- 43 describes the geometric parameters involved. The total height H of the façade is split into three portions, respectively:

H_u is the wall portion above the upper hinge *i*, simulated by a vertical load Q_u acting on the portion beneath ;

H_{var} is the wall height directly involved in the mechanism. It is identified by the position of the extreme edges *i* and *j*.

H_b is the wall portion placed below the lowest hinge *j*. It does not take part to the failure.

The third hinge k is placed in a variable position along H_{var}. The hinge k divides the height H_{var} in two sub-portions, H_1 and H_2 .

H_1 and H_2 can also be expressed as a function of H_{var} as follows:

$$H_1 = \frac{H_{var}}{\nu} \; ; \qquad H_2 = H_{var} \cdot \frac{(\nu - 1)}{\nu} \; ; \tag{2-55}$$

where ν is a variable governing the position of intermediate hinge *k*.

The static system will be solved by means of the Virtual Works Principle, according to the formulation previously developed by Tocci et al. (1995), by expressing the work produced by every single force acting in the system.

As highlighted in Figure 2- 44, the two portions 1 and 2 rotate respectively around the centres Ω_1 and Ω_2, which represent the instantaneous rotation centres of the system.

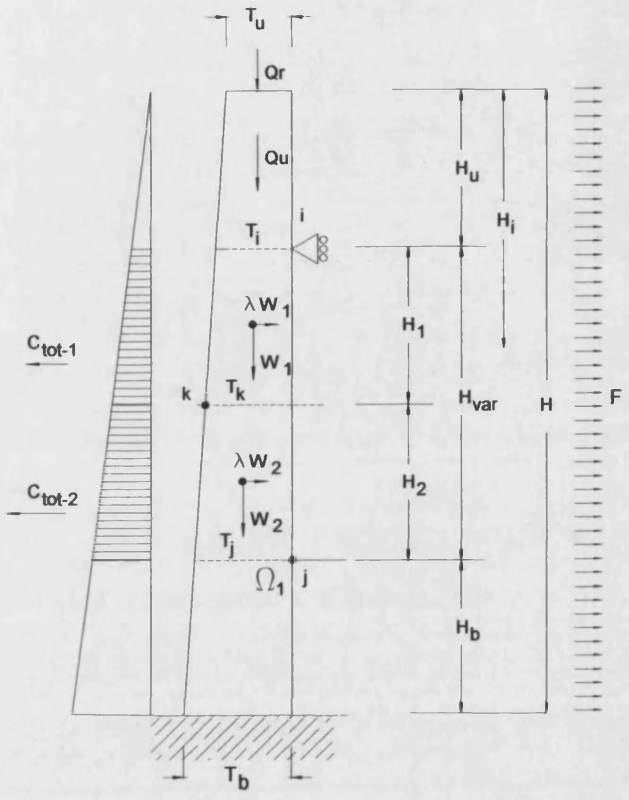

Figure 2- 43– Geometric parameters influencing the model

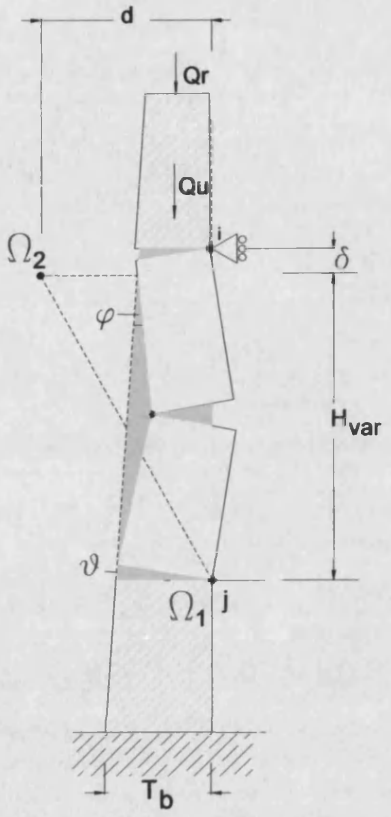

Figure 2- 44– Centres of instantaneous rotation of the model

The rotation angle φ of portion 2 around Ω_2, can be expressed as a function of θ, which represents the rotation angle of portion 1 around Ω_1:

$$\varphi = \vartheta \cdot \frac{H_2}{H_1} = \vartheta \cdot (\nu - 1) \tag{2-56}$$

To sum up, the forces acting in the system are:

W_1 and W_2 Weights of portions 1 and 2, respectively;

λW_1 and λW_2 Horizontal forces of portion 1 and 2 developed by seismic action;

Q_u Vertical load above the wall portions 1 and 2.

Q_r Roof weight on the whole façade of length L;

Q_{fi} Floors weights on the whole façade of length L;

$f \cdot Q_{fi}$ Restraining action exerted by floors through friction;

$\lambda \cdot Q_{fi}$ Horizontal forces produced on Q_{fi} by the seismic action;

$C_{tot(1)}$ Restraining action exerted by edge and internal orthogonal walls along H_1;

$C_{tot(2)}$ Restraining action exerted by edge and internal orthogonal walls along H_2;

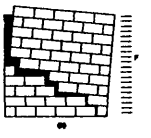

The weights W_1 and W_2, relative to portion 1 and 2, are:

$$W_1 = \left[\left(\frac{T_i + T_k}{2}\right)\cdot\frac{H_{var}}{\nu}\right]\cdot L\cdot\gamma; \qquad W_2 = \left[\left(\frac{T_k + T_j}{2}\right)\cdot H_{var}\cdot\frac{(\nu-1)}{\nu}\right]\cdot L\cdot\gamma \tag{2-57}$$

where T_i, T_k, T_j, are respectively the wall thickness at the levels of hinges i,k,j.

The relative displacement of the forces W_1 and W_2 and λW_1 and λW_2 are:

$$\delta W_1 y = (d - X_1)\cdot\varphi = (d - X_1)\cdot\vartheta(\nu-1); \tag{2-58}$$

where

$$d = \frac{T_i\cdot H_{var}}{H_2} = \frac{T_i\cdot\nu}{(\nu-1)} \tag{2-59}$$

$$\delta W_2 y = X_2\cdot\vartheta; \tag{2-60}$$

$$\delta\lambda W_1 x = (H_{var} - Y_1)\cdot\varphi = (H_{var} - Y_1)\cdot\vartheta\cdot(\nu-1); \tag{2-61}$$

$$\delta\lambda W_2 x = Y_2\cdot\vartheta; \tag{2-62}$$

where X_1, Y_1, X_2, Y_2, are the coordinates with origin at hinge j, expressing the position of the centres of mass of W_1 and W_2.

The vertical load Q_u is:

$$Q_u = (T_u + T_i)\cdot H_u\cdot\gamma\cdot L \tag{2-63}$$

Moreover, the vertical loads Q_u and Q_r can be added, as follows:

$$Q_{tot} = Q_u + Q_r \tag{2-64}$$

and the relative displacement of Q_{tot} is:

$$\delta Q_{tot} y = \left(d - \frac{T_u}{2}\right)\cdot\varphi = \left(d - \frac{T_u}{2}\right)\cdot\vartheta\cdot(\nu-1) \tag{2-65}$$

in which Q_{tot} is assumed to act at the midpoint of the top thickness T_u.

The displacements of Q_{fi} $f\cdot Q_{fi}$, and $\lambda\cdot Q_{fi}$ are governed by:

For $H_u \le H_i \le (H_u + H_1)$:

$$\delta Q_f y = \left(d - \frac{T_u}{2}\right)\cdot\varphi = \left(d - \frac{T_u}{2}\right)\cdot\vartheta\cdot(\nu-1) \tag{2-66}$$

$$\delta Q_f x = H_i\cdot\varphi = H_i\cdot\vartheta\cdot(\nu-1) \tag{2-67}$$

For $(H_u + H_1) < H_i \le (H - H_b)$:

$$\delta Q_f y = \frac{T_u}{2}\cdot\vartheta \tag{2-68}$$

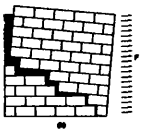

$$\delta Q_f x = \left(H_{var} + H_u - H_i\right) \cdot \vartheta \tag{2-69}$$

In these cases too Q_f is assumed to act at the midpoint of the top thickness T_u.

The restraining actions $C_{tot(1)}$ and $C_{tot(2)}$ are:

$$C_{tot(1)} = C_{tot(k)} - C_{tot(i)}; \tag{2-70}$$

$$C_{tot(2)} = C_{tot(j)} - C_{tot(k)} \tag{2-71}$$

where, $C_{tot(i)}$, $C_{tot(k)}$, $C_{tot(j)}$ are the cumulative restraining action of the wall under examination respectively, at levels *i*, *k* and *j*, according to the frictional model formulated in §2.2.

The displacements of $C_{tot(1)}$ and $C_{tot(2)}$, are:

$$\delta C_{tot(1)} x = \frac{2}{3} H_1 \cdot \varphi = \frac{2}{3} \cdot (\nu - 1) \cdot \frac{H_{var}}{\nu} \tag{2-72}$$

$$\delta C_{tot(2)} x = \frac{1}{3} \cdot H_2 \cdot \vartheta = \frac{1}{3} \cdot (\nu - 1) \cdot \frac{H_{var}}{\nu} = \frac{1}{2} \delta C_{tot(1)} x \tag{2-73}$$

Finally, the total work is:

$$\begin{aligned} &(\lambda W_1 \cdot \delta W_1 x) + (\lambda W_2 \cdot \delta W_2 x) + (Q_{fi} \cdot \delta Q_{fi} x) = \\ &= (W_1 \cdot \delta W_1 y) + (W_2 \cdot \delta W_2 y) + (Q_{tot} \cdot \delta Q_{tot} y) + (Q_{fi} \cdot \delta Q_{fi} y) + (f \cdot Q_{fi} \cdot \delta Q_{fi} x) + (C_{tot(1)} + \frac{1}{2} C_{tot(2)}) \cdot \delta C_{tot(1)} x \end{aligned} \tag{2-74}$$

Hence, the load factor λ, is:

$$\lambda = \frac{(W_1 \cdot \delta W_1 y) + (W_2 \cdot \delta W_2 y) + (Q_{tot} \cdot \delta Q_{tot} y) + (Q_{fi} \cdot \delta Q_{fi} y) + (f \cdot Q_{fi} \cdot \delta Q_{fi} x) + (C_{tot(1)} + \frac{1}{2} C_{tot(2)}) \cdot \delta C_{tot(1)} x}{(W_1 \cdot \delta W_1 x) + (W_2 \cdot \delta W_2 x) + (Q_{fi} \cdot \delta Q_{fi} x)} \tag{2-75}$$

The value of the load factor λ depends upon the parameter ν, influencing the position of the intermediate hinge k. This means that the horizontal intermediate crack along the façade will occur at the level giving the minimum value of λ.

By comparing the load factor functions drawn as a function of ν in the presence and absence of a vertical load Q (Figure 2- 45), it is possible to observe that while for Q=0 the function has no minimum, for Q>0 the minimum occurs at an intermediate position along the height H_v.

This leads to the conclusion that, when no vertical load is present, the crack occurs just below hinge i, whereas when Q is present, its position will move downwards along H_v.

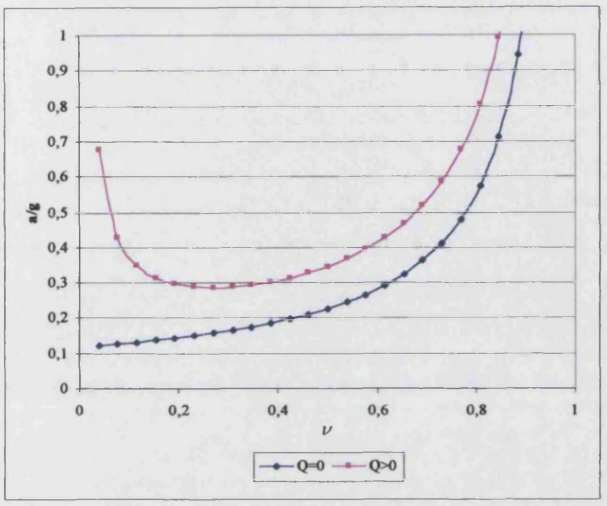

Figure 2- 45 – Load factor patterns as a function of the variable v, governing the position of the intermediate hinge k. (H=15, L=5; Tb=0.8;s/h=0.3)

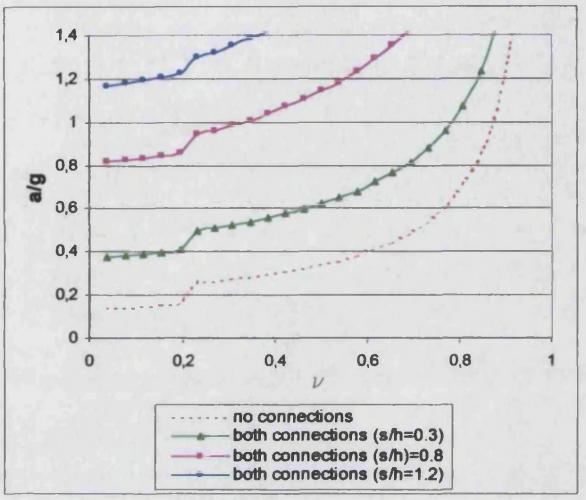

Figure 2- 46 – Position of hinge and minimum load factor for different level of connections and stagger ratios (H=15, L=5; Tb=0.8)

The role exerted by the lateral connections as well as by stagger ratios s/h is outlined in Figure 2- 46. The presence of the restraining action developed at wall edges by the total shear strength produces an improvement in the seismic performance, which gradually increases as s/h increases. It can be observed that the curves become gradually higher for increasing s/h ratios, while the lowest load factor curve corresponds to the case of total absence of lateral connections. Since the diagram of Figure 2- 46 is plotted for Q=0, the critical hinge is always placed just below the top horizontal hinge.

The presence of lateral connections as well as the increase in stagger ratios s/h, produces a similar effect on the load factors when Q>0. In this case, higher load factors are associated to increasing values of s/h, while the critical hinge is always placed at an intermediate height of the wall, as in Figure 2- 45 for Q>0.

2.6.2 Horizontal strip arch failure (G,Gs)

This mechanism is characterised by a central trapezoidal portion which, under the effect of the seismic action, tends to shift outwards as shown in Figure 2- 47a,b. In order to onset, the mechanism requires the formation of one cylindrical hinge (C) along the vertical

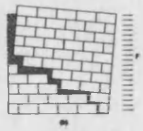

symmetry axis of the façade and two horizontal sliding rollers (A,B) placed at the bottom of the portion of wall in question, at the level of the horizontal crack line .

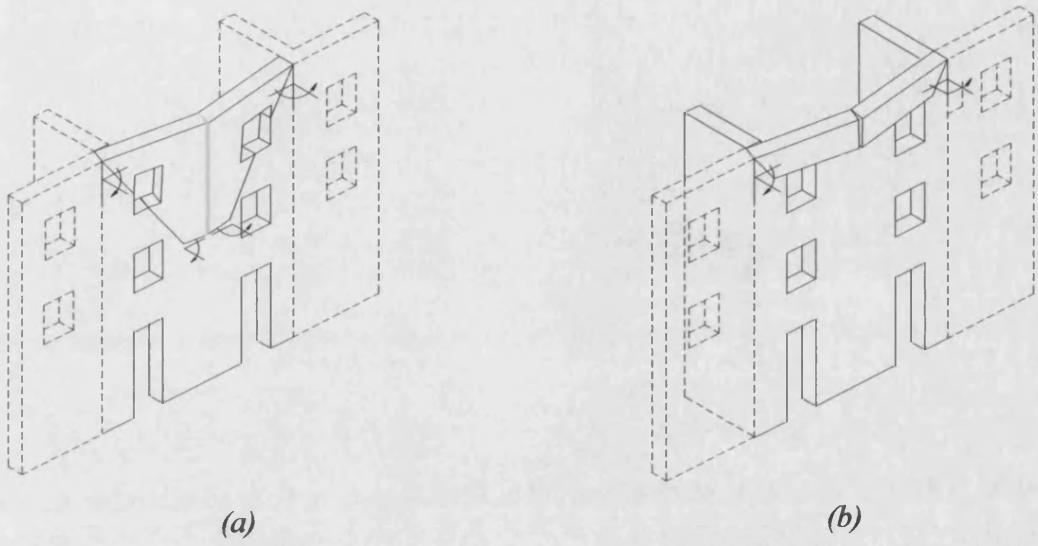

Figure 2- 47- Horizontal strip arch failure (a - failure mechanism G; b – failure mechanism Gs)

The failure is characterised by the central trapezoidal portion which is split into equal sub-portions, which, under the effect of the seismic action, tend to be displaced outwards from the façade plane rotating around the instantaneous centres of rotation Ω_1 and Ω_2 (Figure 2-48). Because of the outward displacement of the central hinge, edges A and B are also forced to move along the horizontal. In order to be triggered, the mechanism must satisfy the condition according to which the resistance to the outward displacement, developed by the edges of the façade, is overcome. This resistance has been assumed as the force required to trigger the sliding of the triangular edges along the bottom horizontal layer (Figure 2- 48).

The mechanism has been formulated in general form, valid for for a variable angle α and for a variable height Hi of the wall which fails, according to the portions involved by the two failure mechanisms of Figure 2- 47 (a,b).

The assumptions at the basis of the analytical formulation are:

- Constant wall thickness T_u, along the variable height H_i.
- Horizontal floor actions are disregarded;
- Torsion friction is disregarded;

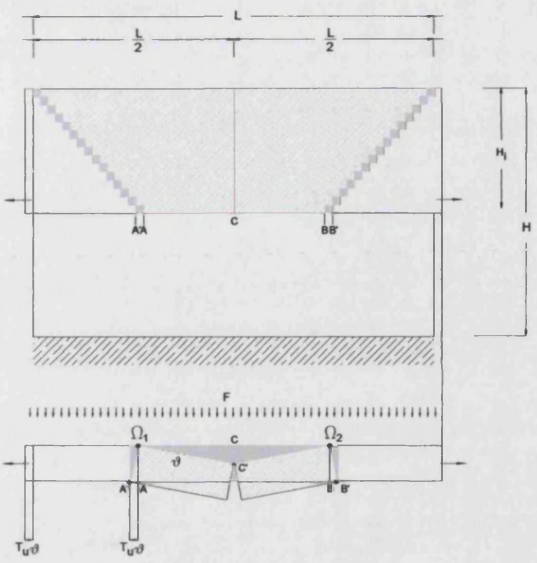

Figure 2- 48 –Displacements and centres of instantaneous rotation.

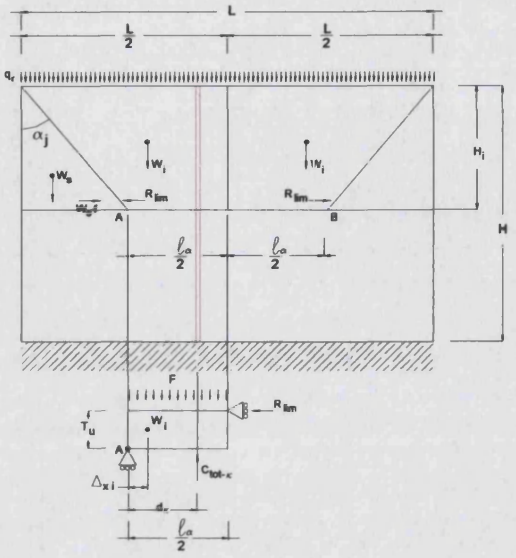

Figure 2- 49 – Geometric parameters involved.

Figure 2- 49 illustrates the mechanical and geometrical parameters involved. The formulation of the mechanism consists of expressing the equilibrium of the generic horizontal strip of trapezoidal shape, height H_i, and top and bottom lengths L and ℓ_α respectively. The system can be analysed through the horizontal cross section of the façade, at the level of the bottom length. Moreover, because of the symmetry of the system, it is possible to reduce the system to one half, and express the equilibrium of this sub-portion around hinge A (Figure 2-49, bottom).

A horizontal thrust R, is assumed to act on the inside of the façade, with vertical lever arm T_u .

The failure can occur only when the horizontal thrust reaches the frictional resistance R_{lim} developed by the lateral triangular edge.

Therefore, the limiting horizontal thrust R_{lim}, is:

$$R_{\lim} = (W_{s,i} \cdot f) + C_{tot(\alpha,i)} \qquad (2\text{-}76)$$

where:

$W_{(\alpha,i)}$ is the weight of the lateral triangular portion;

$C_{tot(\alpha,i)}$ is the total shear strength developed along the crack line from the top to H_i.

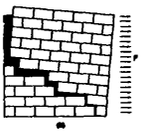

The net moment equilibrium around hinge A is governed by:

$$\lambda\left(W_i + q_r \cdot \frac{L}{2}\right) \cdot \Delta x_i - \left((H_i \cdot T_u \cdot \gamma) + q_r\right) \cdot \frac{\ell_\alpha^{\,2}}{8} \cdot f - \sum_{k=1}^{\beta/2} C_{tot(k)} \cdot d_k - R_{\lim} \cdot T_u = 0 \qquad (2\text{-}77)$$

in which the variable length ℓ_α is a function of angle α:

$$\ell_\alpha = L - 2 \cdot tg\alpha \cdot H_i; \qquad (2\text{-}78)$$

the weight W_i is:

$$W_i = \left(L + \ell_a\right) \cdot \frac{H_i}{4} \cdot T_u \cdot \gamma; \qquad (2\text{-}79)$$

and Δ_{xi} is the horizontal lever arm of W_i. Equation (2-77) is valid only for $\Delta_{xi} > 0$.

In the overall equilibrium has also taken into account the restraining action exerted by the internal bearing walls $C_{tot(\beta)}$.The contribution of party walls is expressed as the sum of the moments developed by the β/2 internal walls, hence placed at one half of the façade length. It is assumed that d_k must always be smaller than $\frac{\ell_a}{2}$.

Finally, the load factor of the façade, for a variable angle α and height H_i of the collapse portion, is given by:

$$\lambda_{\alpha,hi} = \frac{\left[(H_i \cdot T_u \cdot \gamma) + q_r\right] \cdot \frac{\ell_\alpha^{\,2}}{8} \cdot f + \sum_{k=1}^{\beta/2} C_{tot(k)} \cdot d_k + R_{\lim} \cdot T_u}{\left(W_i + q_r \cdot \frac{L}{2}\right) \cdot \Delta x_i} \qquad (2\text{-}80)$$

Among the possible values of α and height H_i, the limit state configuration is that for which $\lambda_{min}=\min(\lambda_{\alpha,Hi})$. This will identify which wall portion fails and the value of the angle of the lateral crack.

Figure 2- 50 shows the load factor patterns as a function of α, for different L/H ratios, in relation to a façade with no internal bearing walls (β=0), or distributed vertical load (q_r=0).

As it can be observed, the function λ is strictly dependent upon the ratio L/H. In particular, for increasing values of L/H the load factor decreases. Moreover, the greater the L/H ratio, the higher the crack angle associated with the failure. The functions show a minimum for ratios less than 1.33, while beyond this value they do not admit minimum.

The influence of the stagger ratios together with the presence of internal bearing walls is outlined in Figure 2- 51. As it can be observed, in the absence of internal bearing walls, the

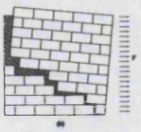

increase in the stagger ratio produces an improvement in the seismic performance only for L/H ratios less than 1. Beyond this limit, the two curves coincide.

When an internal bearing wall is present, an increase in the stagger ratios from 0.3 to 1.2 produces a uniform improvement in the seismic performance for any value of L/H.

In conclusion, as the number of internal bearing walls increases, the increase in the stagger ratios s/h becomes more and more effective, and hence the overall seismic performance against this failure mode improves.

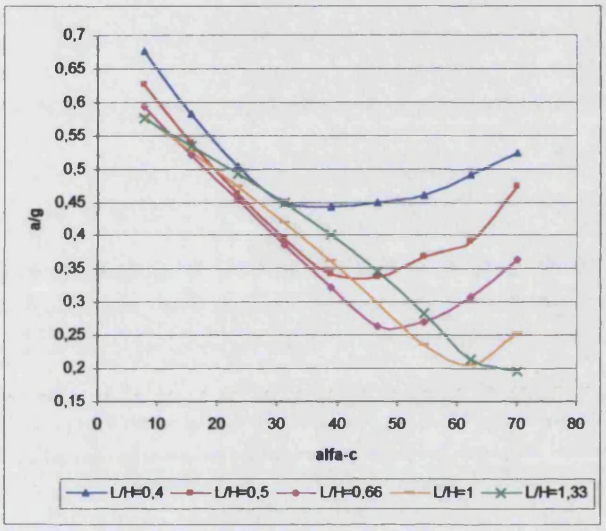

Figure 2- 50 – Load factor patterns as a function of α, for different ratios L/H (Tu=0.8,s/h=1.2, β=0;f=0.4)

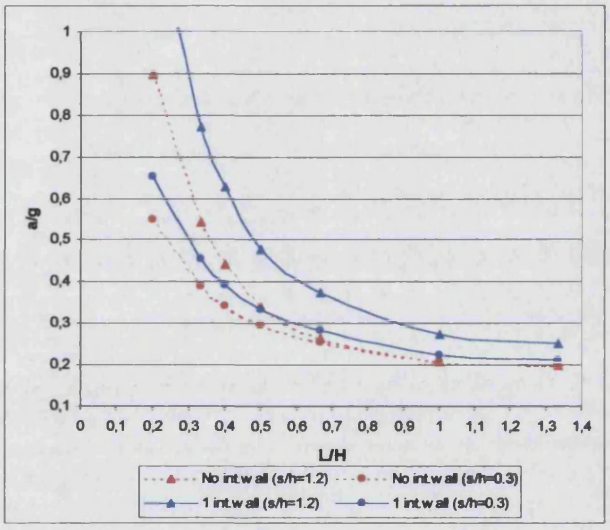

Figure 2- 51 – Load factors patterns as function of L/H, for different stagger ratios s/h, in presence and absence of 1 internal bearing wall.

2.6.3 Vertical addition and gable overturning (I,L)

These mechanisms are associated with the presence of structural features particularly vulnerable to seismic action.

Vertical additions, when built up after the original building construction, are often associated with a notable reduction in thickness and a lack of effective connection between orthogonal walls. In such cases, a very typical failure is the simple overturning of its façade (Figure 2- 52, a).

One most vulnerable elements, is the gable end at the top of the building façades. If the connections to the rear structures are weak and the geometric proportions are too slender, this element can undergo the failure mode sketched in Figure 2- 52, b.

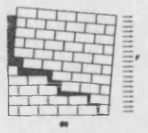

However, both mechanisms, if triggered, can produce partial collapses, which do not affect the stability of the entire building structure, but which may jeopardise human life.

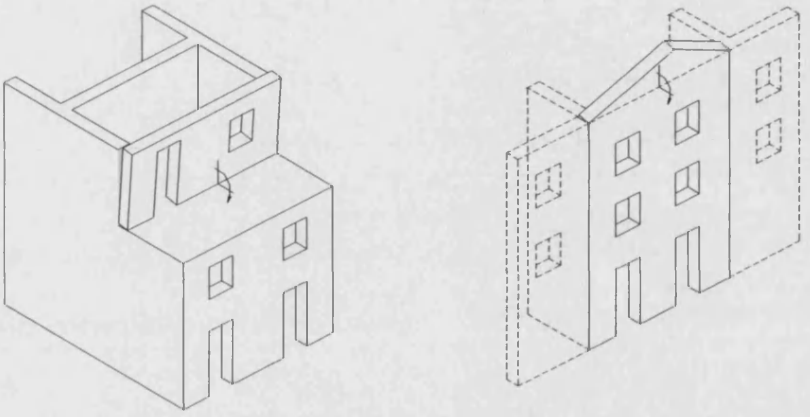

(a) *(b)*

Figure 2- 52 – Vertical addition and gable overturning

From a mechanical point of view, the two mechanisms are equivalent because they are characterised by the simple overturning of a geometric element around a cylindrical hinge placed at its base. As well as their own weight and the lateral seismic action, a further load taken into account in the analytical formulation is the action of the roof, assumed to be horizontally distributed along the top surfaces.

Figure 2- 53 and Figure 2- 54 outline the geometric parameters required for the analytical formulation of the two failure modes.

The load factor relative to the overturning of the vertical addition is simply governed by:

$$\lambda_v = \frac{\frac{T_v}{2}\cdot(W_v + Q_r) + (Q_r \cdot f \cdot H_v)}{H_v \cdot \left(\frac{W_v}{2} + Q_r\right)} \qquad (2\text{-}81)$$

where W_v, H_v and T_v, are respectively the weight, total height and thickness of the vertical addition. Q_r is the resultant of the horizontally distributed load along the building length L:

$$Q_r = L \cdot q_r \qquad (2\text{-}82)$$

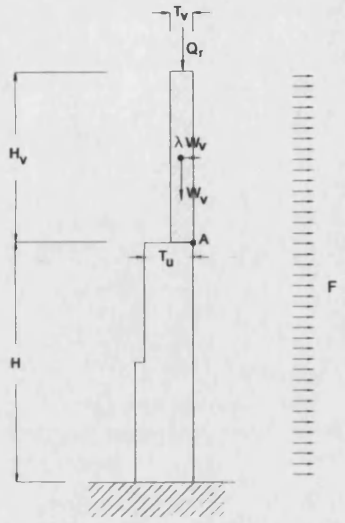

Figure 2- 53– Vertical addition – Geometric parameters involved in the problem

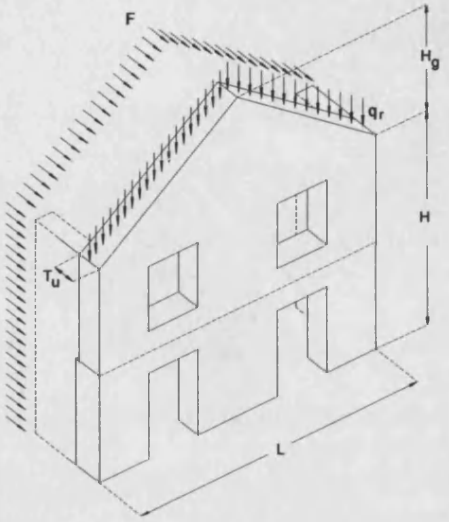

Figure 2- 54 - Gable overturning - Geometric parameters involved.

The load factor relative to the gable overturning is:

$$\lambda_v = \frac{\frac{T_u}{2}\cdot\left(W_g + Q_r\right) + \left(Q_r \cdot f \cdot \frac{H_g}{2}\right)}{\frac{H_g}{3}\cdot\left(W_g + Q_r\right)} \tag{2-83}$$

where W_g and H_g are respectively the weight and total height of the gable. The gable thickness is assumed to be equal to the thickness T_u at the top of the building.

Q_r is the resultant of the horizontally distributed load along the two gable pitches inclined at angle α_g :

$$Q_r = 2\cdot\left(\frac{H_g}{\sin\alpha_g}\right)\cdot q_r \tag{2-84}$$

The only constraining action considered in equations (2-81) and (2-83) is the one exerted by roof weight because of the friction effect.

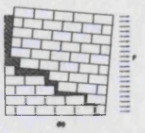

2.7 Comparative analysis

A comparison of the mechanisms formulated in the previous sections helps to clarify their behaviour and to find out which variables are most significant in relation to the overall equilibrium of the building façade.

The following parametric analysis refers to a sample building facade, characterised by 5 storeys, façade length and height of 5 and 15m respectively, depth of party walls 4m, constant thickness 0.8m; no internal bearing walls; intermediate stagger ratio of the masonry s/h=1.2, and friction coefficient 0.4 .

The role exerted by the lateral connections to the orthogonal walls is highlighted in Figure 2- 55 and Figure 2- 56, relative to the presence or absence respectively of both edge connections. In general, it can be observed that the presence of connections produces an improvement in the load factors for all failure types, except for those (B2,C,H) which are not influenced by this variable. In this case, failure E also proves not to be influenced by lateral connections, because of the opening layout chosen (η=2).

While in absence of lateral connections the façade load factor is 0.062, and the associated failure mechanism is D, when the connections are effective, the value increases up to 0.176, with associated failure mode B2.

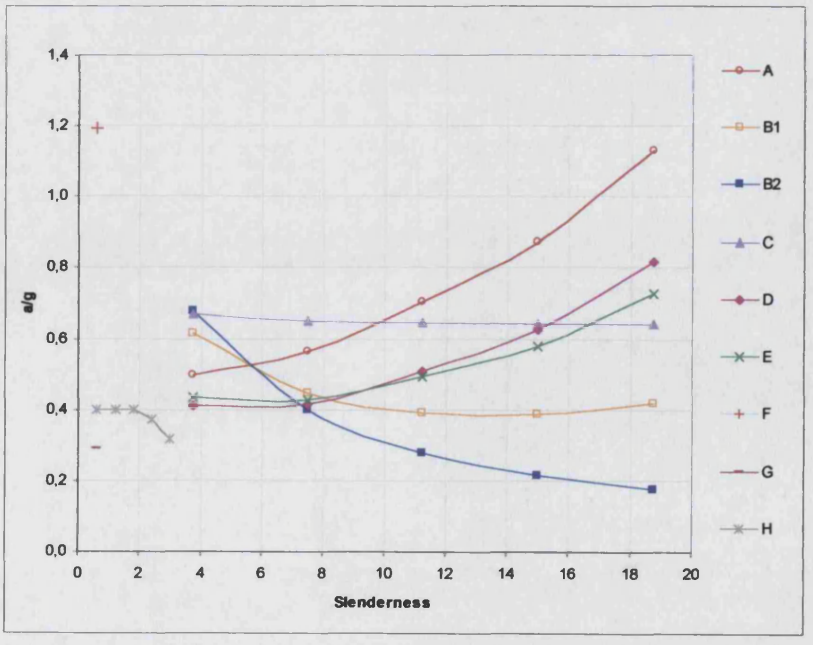

Figure 2- 55 – Load factor values as a function of the slenderness ratio in a - storeys façade in the presence of both lateral connections (L/H=3;Tb=0.8; f=0.4; s/h=1.2;ε=2;η=2).

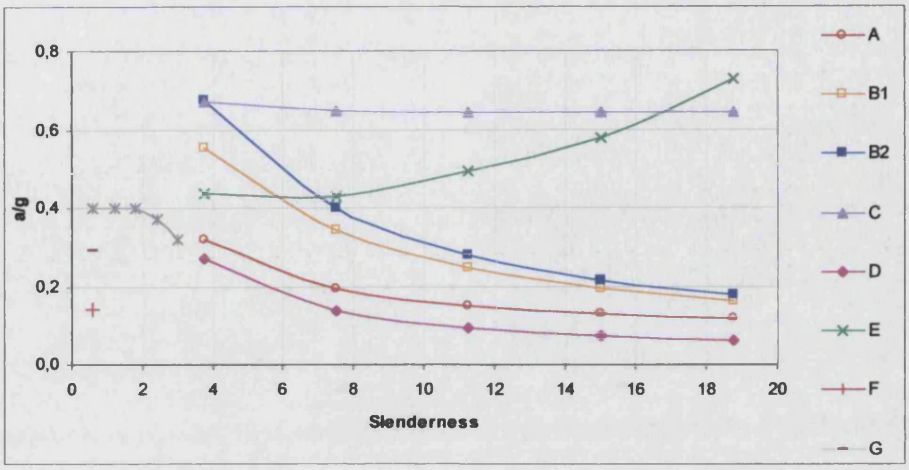

Figure 2- 56 - Load factor values in function of the slenderness ratio in a 5 storeys façade in absence of lateral connections (L/H=3;Tb=0.8; f=0.4; s/h=1.2;ε=0;η=2).

Figure 2- 57 illustrates the role exerted by the masonry stagger ratio.

This structural feature represents a crucial parameter as it yields the definition of the frictional resistance along masonry layers. It influences all the mechanisms analysed, though to varying extents.

The failure modes most influenced by the s/h ratio are the vertical "arch effect" F, the corner C, with load factors increasing according to a steep linear seen to be pattern.

For all the other failure mechanisms an increase in the stagger ratio produces a general increase in the associated load factors.

Finally, Figure 2-58 highlights the role of a horizontal load simulating the roof and the floors action (Q). The mechanisms are affected by this variable rather uniformly.

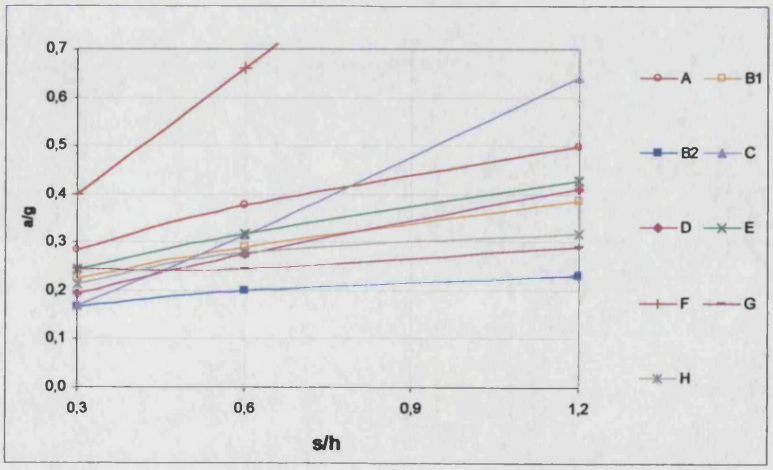

Figure 2- 57 - Load factors curves in function of the staggering ratio s/h.

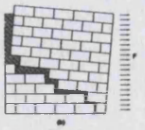

It can be observed how the presence of quite small vertical loads, compared with the weight of the total façade, produces an improvement in the seismic behaviour of these mechanisms, since for increasing values of Q, the load factors also increase. An exception is failure mechanism G, for which the associated load factors decrease with increasing values of Q. In conclusion, the presence of Q worsens the overall seismic behaviour for failure G, while an appreciable improvement is observed in all the other failure types.

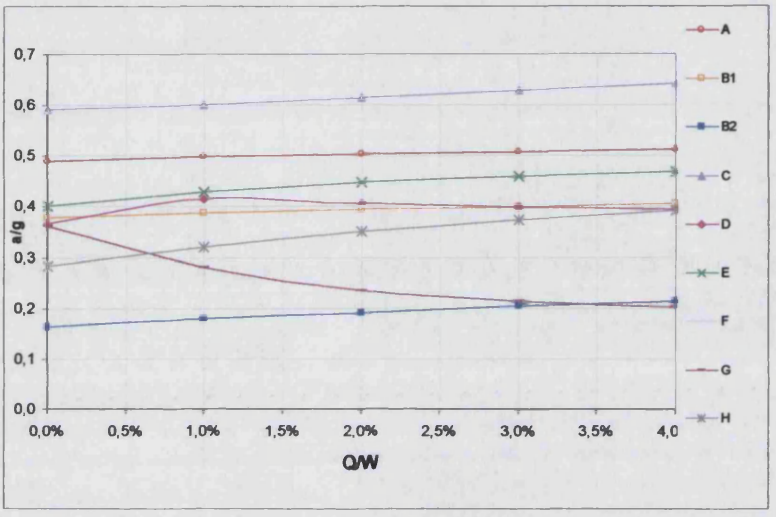

Figure 2- 58- Load factors curves plotted against the horizontal distributed load (Qr=Qf=Q) normalised with respect to the total weight of the façade W.

2.8 Conclusions

This Chapter has presented the mechanical formulation of the failure mechanisms identified in §1.4.5. The first part of the Chapter was dedicated to the development of a frictional model for regular ashlars masonry, able to express the total shear strength acting at connections between orthogonal walls, as well as along variably inclined crack lines, dividing the wall into two portions. Thanks to this preliminary general model, the formulation of the individual failure mechanisms identified in §1.6 has been introduced. Each failure mechanism has also been critically discussed through some parametric analysis which enabled the role exerted by the most significant structural features influencing the mechanism under examination to be highlighted. Finally, comparative analyses have led to understanding the way in to which the mechanisms behave and are ranked in relation to significant structural features.

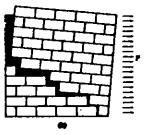

CHAPTER 3
DEVELOPMENT OF THE METHOD

3.1 Introduction

This Chapter presents the development of the FaMIVE method and its implementation as a spreadsheet based computer program.

After a brief introduction to the general framework of the procedure, the Chapter describes and critically discusses the data inspection criteria.

This phase enables all the structural parameters involved in the analysis to be introduced, and to be discussed in relation to the way they are processed for the evaluation of the seismic vulnerability. A special section is dedicated to the criteria used to examine the reliability of information which allows the method to be used at different levels of detail.

3.2 The FaMIVE framework

The salient steps qualifying the FaMIVE procedure can be described as follows:

Survey In this phase the operator is required to collect information about the building front under examination. The survey pursues a double purpose: collect preliminary general information concerning the most representative structural types of the urban centre in question, together with specific information about the geometry, structural features, decay and damage of each façade;

Calculation Once the 1st step is completed, the failure mechanisms can be calculated according to the formulations introduced in Chapter 2. Load factors are calculated for each failure mechanism, at every storey of the façade under examination;

Screening The results (obtained in the 2nd step) are then screened in relation to features such as connections with transverse walls, or strengthening devices surveyed in the building concerned. This can lead to the total or

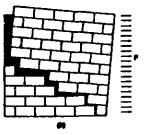

partial exclusion of some failure mechanisms, depending on the boundary constraint pattern. Feasible mechanisms are identified through a set of decision-criteria introduced and discussed at §3.4.3. and §3.4.4.

Results of Calculation After checking the feasibility of all failure mechanisms, these are ranked according to their associated load factors. The smallest of them, defined critical load factor (μ), represents the ultimate capacity of the façade under examination to resist an earthquake. The value of μ is strictly related to the failure mechanism expected and to the extent of the building involved in the mechanism.

Vulnerability The seismic vulnerability is defined by two indices: the structural and the failure extent index. A qualitative criterion is proposed for combining the two indices and for providing a final assessment of vulnerability.

Reliability A criterion for weighing the reliability of the information recorded in the survey allows lower and upper boundaries of the final vulnerability to be defined.

Figure 3- 1 shows the structure of the FaMIVE computer program, and its capabilities in terms of input data checks and interface with the operator.

Once the survey is completed, the data are checked in order to highlight wrong or incompatible information. The check is carried out by a systematic check of all the data introduced by the operator. If this is not successful, the wrong data, listed in a "error check list", have to be corrected. Once successfully checked, the data are stored in a database, where they can also be retrieved and modified for further calculations.

After these preliminary operations, the calculation program (2^{nd} step) can be run. This is composed of 4 different sub-routines, which calculate individual or sets of failure mechanisms, as shown in Figure 3- 1. Then, having screened the feasible failure mechanisms by means of specifically developed decision-criteria, the critical load factor (μ) is calculated and the final vulnerability defined. Finally, the results are stored in a database.

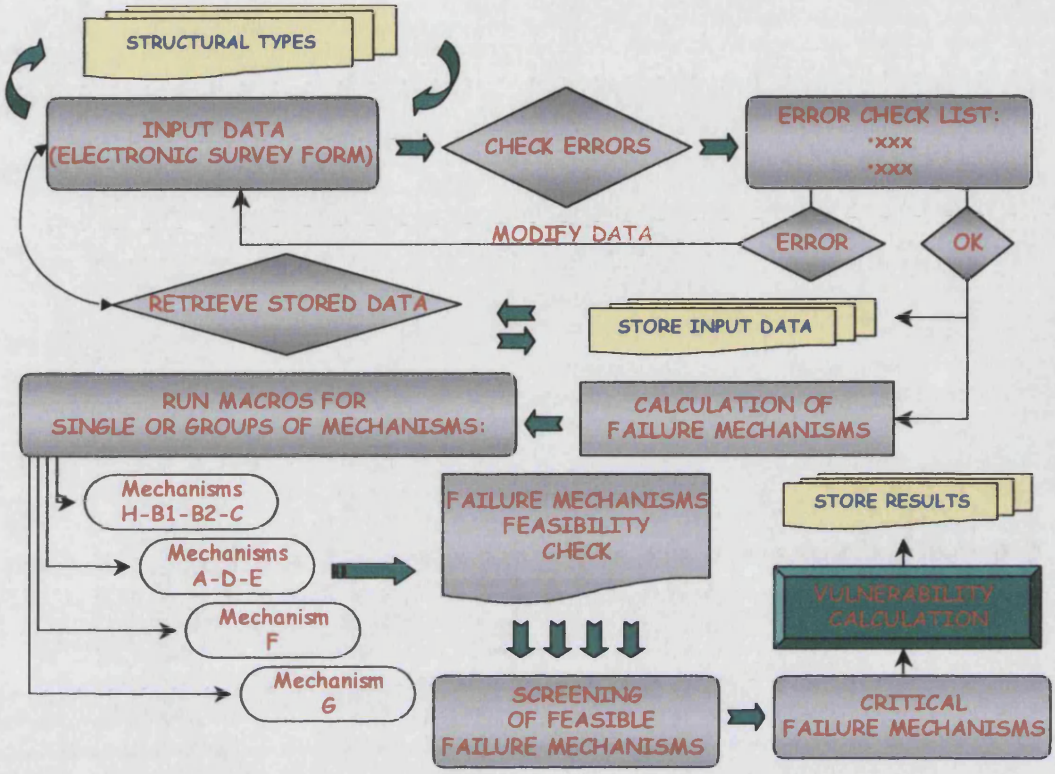

Figure 3- 1– Bar chart showing the framework of the FaMIVE computer program

3.3 Survey method

The methodological approach pursued for the survey basically derives from that developed by Cobourn in 1984. Unlike other investigation criteria (Braga, 1984; ATC-13, 1985; Benedetti, 1984, FEMA 154, and 155, 1988), critically discussed at §1.4, this method aimed to record elementary enquiries, from the urban position of the block to the construction features, in order to achieve an overall organic understanding of the structural behaviour of the building. The novelty of the inspection process was also that the damage was described not only in terms of severity but by the type of damage involved. Following this approach, further investigation forms were later developed such as the one by D'Ayala et al. (1996), and more recently by Okada et al. (2000) which propose an interesting criterion, focused on Japanese building types, to help investigators classify damaged buildings in structural terms.

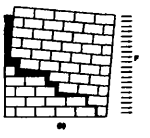

Despite the benefits deriving from an inspection process based on structural approaches, this type of investigation undoubtedly shows some limits in its applicability.

The level of knowledge and experience needed to carry out this kind of survey, especially in post-earthquake situations, requires the presence of a specialised technician, while inexperienced operators, often working in emergency situations, cannot be regarded as suitable.

The FaMIVE survey method presented is characterised by the following objectives:

- Reduction of the amount of data needed to that strictly necessary to qualify the seismic performance of buildings and consequent attempt to reduce data collection time;
- Description of the structural layout of the building by means of local construction types. These have to be surveyed in a preliminary stage of the survey.
- Damage description in terms of feasible failure mechanisms, as well as damage level and crack pattern.

Sections §3.3.1 and §3.3.2 are dedicated to the description of the survey form, which is the operative tool of the method.

3.3.1 Presentation of the survey form: geometrical and structural description

The form is composed of 7 sections, 6 of which are dedicated to the description of geometric and constructive characteristics of the wall under examination, while the 7th concerns the damage survey and association of failure mechanisms (Figure 3- 2; Figure 3- 7). The latter is required only in post earthquake situations.

The form can be used both in the case of detailed surveys, when all the measurements required can be provided by the operator, and in the case of qualitative inspections only, when the measurements are simply estimated. A special field at the end of each section, requiring the average level of reliability of the information provided, is used to weigh the data to be processed to evaluate the vulnerability.

The building where the wall to be surveyed is located, is identified by a number, assigned by the surveyor, and by its cadastre unit. It is a fundamental requirement that the building

must be an independent unit under a structural point of view. How the building is used and its estimated percentage of use must also be known.

The topographic description of the building is completed in section1, using data on the position of the building within the urban context.

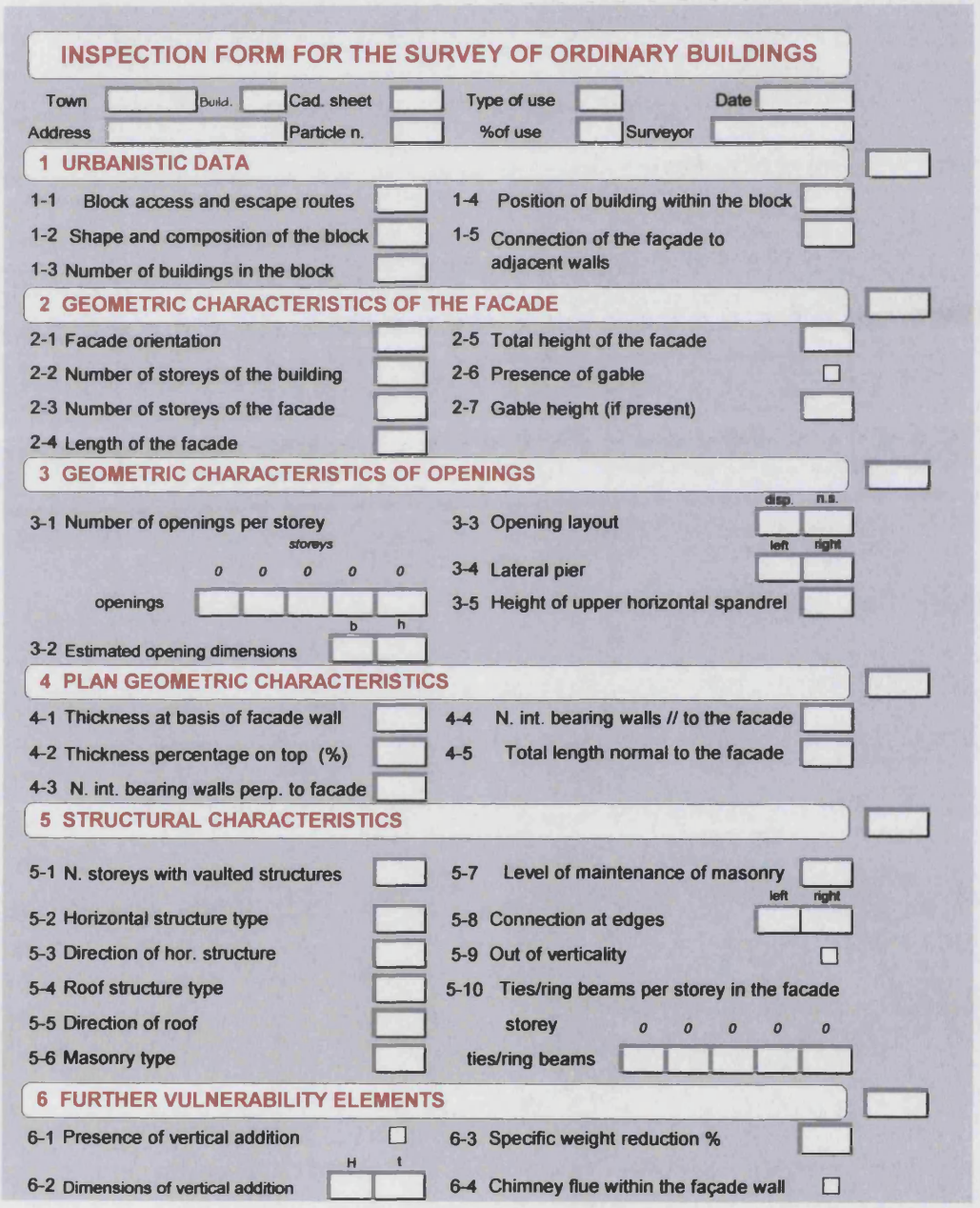

Figure 3- 2 – Survey form: description of geometric and structural features (sections 1-6)

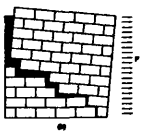

Entries from (1-1) to (1-4) require a description of the urban context surrounding the building, while field (1-5) specifically refer to the façade under observation.

Fields (1-4) and (1-5) require respectively *Position of the building within the block* and *Connection of the façade to adjacent walls.* These features exert a direct influence on the feasibility of some failure mechanisms.

The position of the building within the block, is described by 5 possible topographic arrangements, sketched in Figure 3- 3, describing the most common situations relating the building to the urban context.

A further element is required specifically for the external wall under examination, provided by the boundary conditions in terms of the number of free corners according to Figure 3- 4.

This information has to be congruent with data field (1-4), so that if, for example, the building is isolated, the wall in question cannot be in any of the situations shown in Figure 3-4, (c),(d),(e). Specific conditions assumed for the feasibility of each failure mechanism in relation to fields (1-4) and (1-5) are introduced at §3.4.3.

The geometric survey of the façade is provided in Section 2, together with the facade orientation (2-1). Number of storeys of the building (2-2) and of the façade (2-3), total length (2-4) and height (2-5) define its global geometry, while fields (2-6) and (2-7) identify the presence of and describe gable ends. A sketch of the façade elevation and a plan of it can also be added in a special section.

An entire section (3) is devoted to the describing the layout of openings. This feature is analysed in only a few methods. Giuffre' et al. have identified and analytically developed several failure mechanisms which occurred in the historic centre of Siracusa and Palermo (Italy), due to particular opening layouts (1993, 1999). Furthermore structural analysis and experimental tests have confirmed that openings deeply influence the crack pattern and can lead to the development of particular failure mechanisms (Ceradini 1993, D'Ayala et al. 1995, CNR-GNDT.-2000).

Field (3-1) requires the number of openings per storey, while the average dimensions of windows are required in the following field.

The opening layout, recorded in (3-3), is described by the range shown in Figure 3- 5, which outlines the most typical arrangements characterising historic buildings.

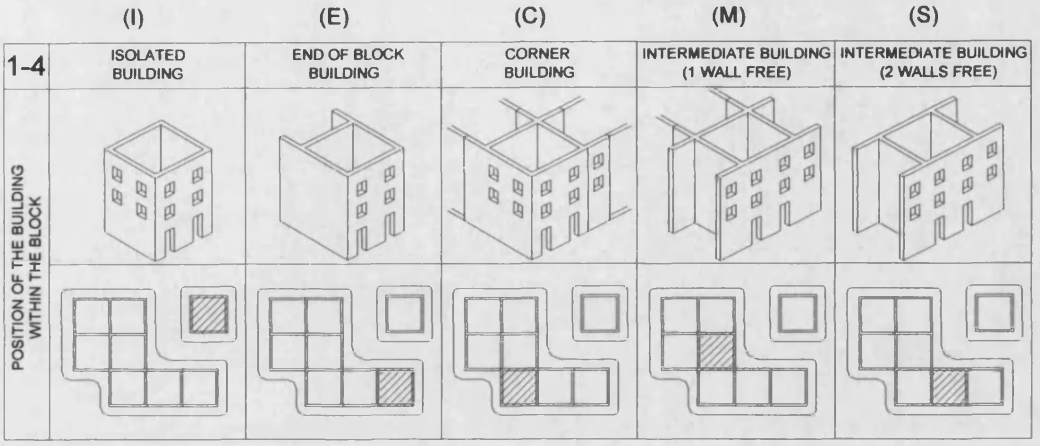

Figure 3- 3 – Position of the building within the block

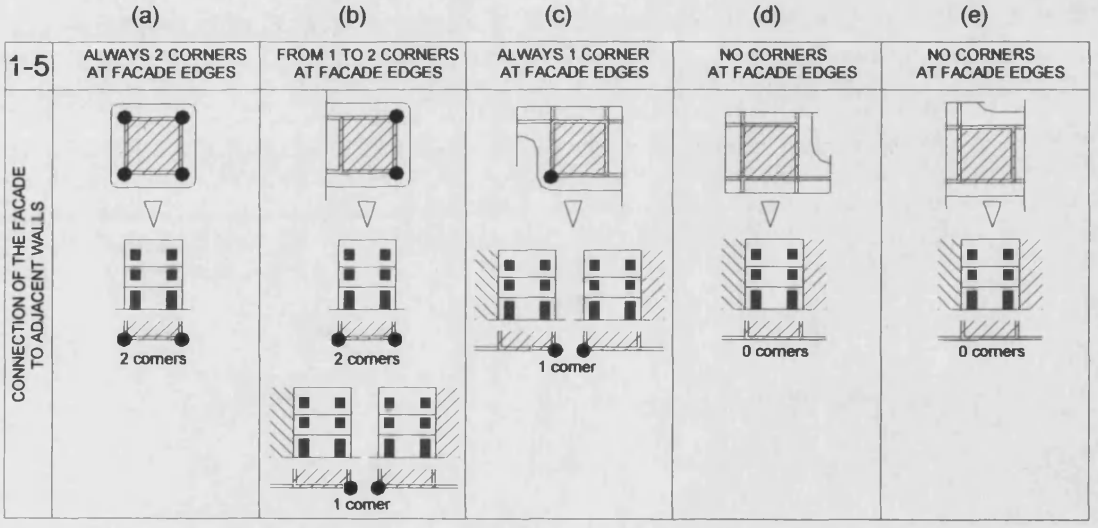

Figure 3- 4 – Connection of the façade to adjacent walls

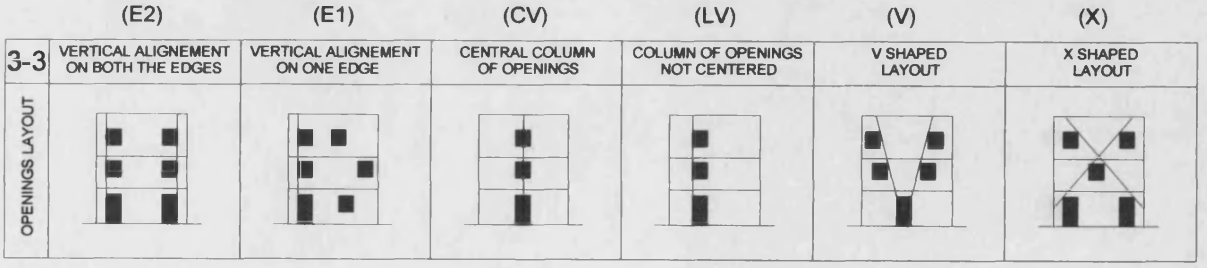

Figure 3- 5 – Field 3-3- Openings layout

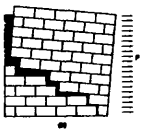

The number of consequent storeys (starting from the top) influenced by the chosen layout must also be recorded in the adjacent box. The way in which this feature can influence the feasibility of failure mechanisms is discussed in §3.4.3.

The width of lateral piers must be entered in field 3-4. As introduced at §2.3.2, these are defined by the distance between the closest opening along the building height, and the lateral edge of the façade. As in the approach pursued by Bernardini (1986), the later piers are assumed to be regular when greater than the average opening width and are required for both wall edges.

Finally, in (3-5) the height of the upper horizontal spandrel refers to the height of the horizontal strip between the highest windows and the top of the wall.

The geometric features of the building plan are surveyed in Section 4. Information required includes the wall thickness at the base (4-1) and top (4-2); number of internal bearing walls perpendicular (4-3) and parallel to the façade (4-4); and total length normal to the façade.

When the survey is carried out only from the street, or even using photographic material, information on the interior can be obtained from cadastre plans, or ground floor plans, associating a low level of reliability to these data.

Section 5 deals with the structural characteristics of the façade. Horizontal structures (5-2) and the roof (5-4) as well as masonry types (5-6) are described by matching each of these structural elements to specific types, which can be surveyed by the operator in a preliminary stage of the inspection, aimed at recognising the common structural layouts of floors and roof structures, as well as of masonry fabrics within the urban centre. If the wall is plastered, or the fabric layout is not applicable, the surveyor can attribute the same type as that identified in other buildings with similar features, assigning a low vulnerability to this information.

The operator is required to match each building to a given type chosen from those surveyed. When no preliminary survey is carried out, the operator can choose the most suitable structural types from an on-line database, consisting of types defined in previous field investigations.

This is a crucial step in the process of investigation, as it enables each external wall of a building to be associated with a set of information concerning the interior, which otherwise would go unobserved. However, this association necessarily implies a margin of uncertainty,

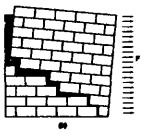

as indicated by the reliability level.

A similar approach has recently been undertaken by EERI (2001), which carried out an extensive survey in seismically prone areas of the world aimed at recognising and qualifying the most common housing construction types from a structural point of view. The work is particularly valid, as it enables the structural layout of buildings, their peculiarities and deficiencies, to be described concisely and effectively, and then compared using the EMS 98 classes.

Further parameters qualifying the structural performance of the wall are the direction of horizontal and roof structures (5-3, 5-5).

The description of the masonry layout (5-6) is completed by specifying its maintenance level (5-7). This information is used for decreasing the mechanical quality of the masonry under examination, when its level of decay is considered particularly relevant.

Special criteria governing the relation between maintenance level and masonry fabric are discussed in §3.4.1.

The connection at wall edges (5-8), introduced at §1.6 and 2.3.2, refers to the level of bond between the façade and the side walls. As outlined in the review on damage effects (§1.6), as well as by the analytical developments of the failure mechanisms (Chapter 2), this structural feature greatly affects the mechanical performance of the building. Consequently, particular attention has to be paid by the surveyor to checking the wall extremities. The best way to do this is to observe the presence of vertical cracks at wall edges, brought to light during previous earthquakes. When no recent earthquake has occurred, and hence no damage can be observed, this information can be achieved by examining cadastre maps from different periods, in order to compare the age of construction of the building under examination with those adjacent to it, according to the criterion outlined in §1.6 (Figure 1-7).

Field (5-9) identifies whether the façade is out of plumb. A criterion for taking in exam this feature by reducing the mechanical capability of the wall is assumed, and this is introduced in §3.4.1.

Field (5-10) collects information on the strengthening devices on the façade, which have to be recorded at every storey. The strengthening devices are described not only by the number of items surveyed, but also by their layout over the facade. Six different layouts are considered for each storey, as sketched in Figure 3- 6.

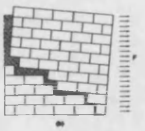

The strengthening layout of each single storey is described by the number and position of anchors and ring beams surveyed over its surface. The anchors are linked to the presence of metallic (or wooden) ties orthogonal to the façade. The A3 layout applies to those situations with a number of anchors equal to or greater than 3.

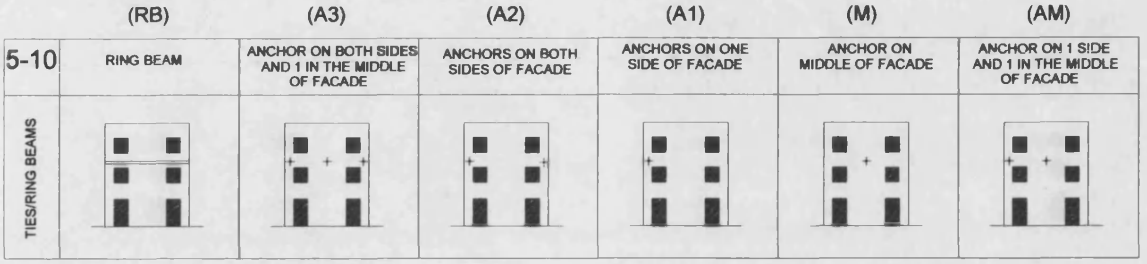

Figure 3- 6 – Field 5-10 – Strengthening devices

The criterion as to whether the layout of strengthening device can prevent the entire or partial onset of the failure mechanisms identified in §1.6 is presented in §3.4.3.

Finally, the presence of vaulted structures is recorded. Although the method does not take into account this information, it is required in order to enable further upgrading of its capability.

Section 6 collects data about the vulnerability of further elements, including additional storeys (6-1), erected in a later stage of construction. As introduced in §1.6, this element is very often associated to a considerable reduction in the wall thickness, which becomes very vulnerable to the seismic action. When a vertical addition is present, the surveyor is required to express the length and height of its façade, and to estimate the reduction in mass density if the construction material of this storey is different from that employed in the building façade. Field (6-4) records the presence of chimney flues within the façade wall. This feature, quite common in the historic buildings, can represent a further weakness of the wall. The criterion according to which these elements are processed is discussed in §3.4.1.

3.3.2 Presentation of the survey form: damage inspection

The damage Section (7th) (Figure 3-7) pursues a double purpose: identification of failure mechanisms which have occurred (field 7-1) and description of the crack pattern (field 7-2).

The mechanism is required to be identified only when the severity of damage is sufficient to allow a collapse pattern, whether incipient or fully developed, to be recognised.

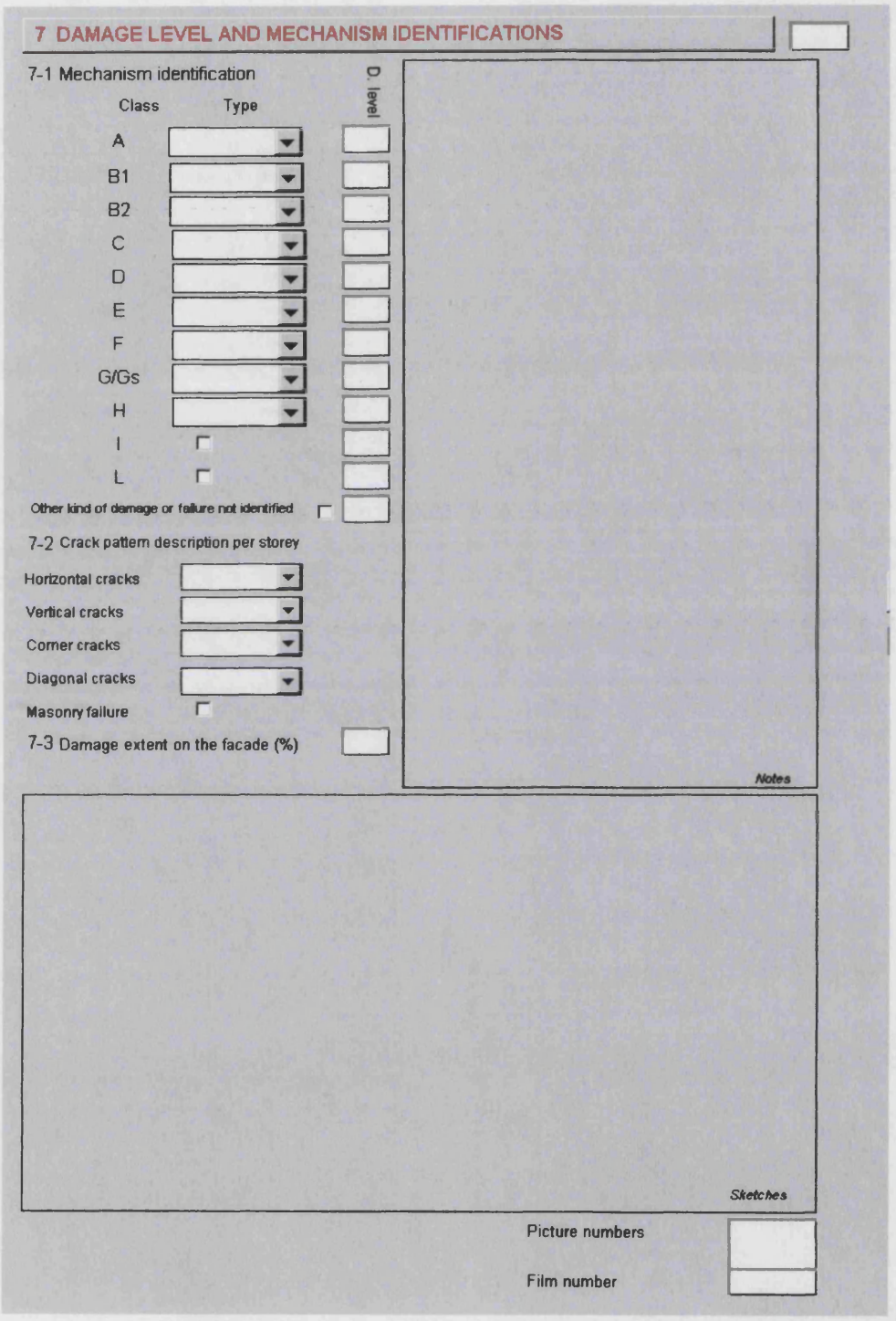

Figure 3- 7 - Survey form: damage description (Section 7)

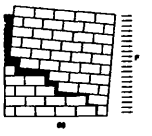

Field (7-1) requires the portion of façade affected and the relevant damage level to be recorded for each failure mechanism identified. The damage extent can be indicated by 3 different descriptions (collapse of top storey; partial collapse, total collapse). The damage level is described by a 6-points scale of the EMS'98 (Grunthal, 1998), ranging from D0 (no damage) to D5 (total failure), and has to be recorded in the adjacent box.

When the failure mechanism is not immediately recognisable, or the damage level seems too slight for a reliable opinion to be expressed, the surveyor is required just to tick a box at the bottom of section (7-1), and only to express the overall damage level.

The description of the crack pattern at field (7-2) requires the operator to choose from a pre-defined range the crack pattern which best fits the damage under examination, and also to express the extent of the façade affected. A special field allows the damage suffered by masonry fabric characterised by the local expulsion of elements (stones/bricks) to be described.

The description of the crack pattern, possibly accompanied by a sketch drawn by the surveyor, enables the damage interpretation and the association of failure mechanism to be postponed to a later phase.

Finally, field (7-3) records the damage extent as indicated by the percentage of the wall surface damaged.

3.3.3 Structural types

Some structural characteristics of the building, such as roof and floor types, as well as masonry fabrics of the façade, need a preliminary survey and data storage.

The structural types have to represent a sufficient range of the craftsmanship present in the urban centre under examination, to enable the operator, during the survey, to match to each façade to its proper structural types, as required by Section 5 of the inspection form.

This criterion leads to a notable reduction in the data collection time for each façade, because the matching process certainly requires less time than investigating the same structural characteristics in every building.

Floor and roof structure types are stored together in a database, and are distinguished by special labels (such as A, B) which refer to general structural features, such as "wooden

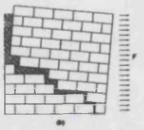

structures", "steel structures" and so on. These structures are described by the horizontally distributed weight (KN/m), acting along the façade under examination, and orthogonal walls.

Figure 3- 8 shows the storage criterion assumed for masonry fabrics. Each type is identified by a label and possibly by a title identifying macro-types such as "ashlars masonry", "rubble" and so on. In order to better describe the fabric layout, a short description can be added at field (M-8).

	MASONRY FABRICS							
	Title	.....	.....	.....	.....			
	TYPOLOGY	A1	A2	B1	B2	C1	C2	D1	D2
M-1	Elements dimensions (m) (bxh)	....	....	....	....	....	....	....	....
M-2	Overlapping length	.....	.....	.....	.....	.....	.....	.....	.....
M-3	Masonry fabric	.....	.....	.....	.....	.....	.....	.....	.....
M-4	Level of connection in the thickness	.....	.....	.....	.....	.....	.....	.....	.....
M-5	Level of cohesion of the fabric	.....	.....	.....	.....	.....	.....	.....	.....
M-6	Specific weight	.....	.....	.....	.....	.....	.....	.....	.....
M-7	Friction coefficient	.....	.....	.....	.....	.....	.....	.....	.....
M-8	Description	.....	.....	.....	.....	.....	.....	.....	.....

Figure 3- 8 – Storage table for structural typologies: masonry fabrics

Data fields (M-1) and (M-2) refer to the geometric average characteristics of fabric elements, indicated by length, height and overlapping lengths, as previously defined at §2.2.1, and sketched in Figure 3- 9.

This information can be obtained by a simple observation of the external surface of the masonry, having removed a small portion of plaster, if present.

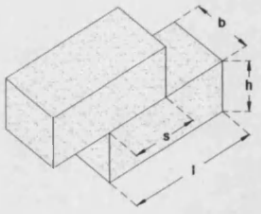

Figure 3- 9 – Geometric characteristics of the fabric

Field (M-3) provides a description of the fabric through its thickness, for which a specific expertise is needed. This type of information can be collected in several ways such as by observing a collapsed portion of masonry, by carrying out instrumental investigations, e.g. endoscopies aimed at analysing the internal wall composition, or by accurate inspection of the external and internal leaves and by induction of the total thickness.

The fabric is assumed to be described by the range of 5 types sketched in Figure 3- 10.

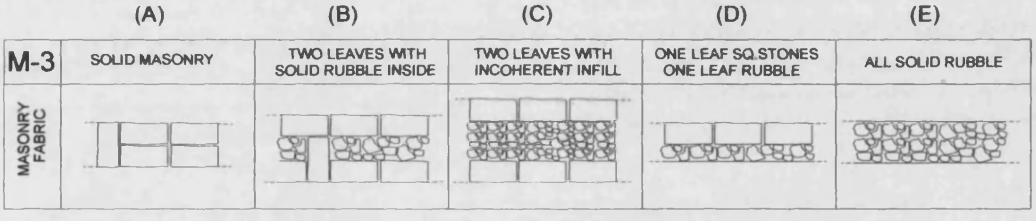

Figure 3- 10 – Field M-3: Masonry fabric

The 5 types are ranked according to the carving of the masonry, and hence range in order from the most regular, composed of solid elements having regular size, to the most irregular, made of rubble. The identification of the carving level of the fabric allows identification of the effective sliding surface through the wall thickness and hence the expression of the total shear strength which each fabric type can develop. The method uses this information to convert the ideal model of "*opus quadratum*" and its associated total shear strength (§2.1), to ordinary fabric layouts, according to the criterion introduced at §3.4.2.

Fields (M-4) and (M-5) refer respectively to the level of connection in the thickness and to the level of cohesion of the fabric. The former defines the level of bond through the thickness due to the fabric layout, and is influenced by the shape and position of elements along and through the wall. The operator is required to express an overall judgement by simply considering the connection as either "sufficient" or "insufficient".

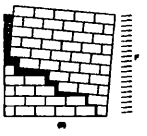

The level of cohesion refers to the quantity, quality and state of conservation of mortars employed. In this case too the operator is required to express a subjective judgement by considering the cohesion as either "sufficient" or "insufficient".

The two fields (M-4) and (M-5) are used to define the level of integrity of the wall and hence its ability to collapse according to given failure mechanisms. When the level of integrity is considered insufficient, the failure mechanisms cannot be triggered and the most probable collapse is the local failure of masonry, as by expulsion of material. The conditions on which this behaviour is assumed to be based are discussed at §3.4.3.

Finally, fields (M-6) and (M-7) provide the mass density and the friction coefficient which can be derived from specific literature on the topic or by experimental tests on masonry samples.

3.4 From input data to calculation of the critical load factor

Once the survey phase has been carried out, the data collected are used for the calculation of failure mechanisms.

Each mechanism is calculated according to the formulations described in Chapter 2. The relationship between the input data and the variables involved in the calculation is illustrated in Figure 3-11 and Figure 3- 12 and discussed in the following paragraphs.

3.4.1 Thickness reduction and weights calculation

Figure 3-11 shows the logic pattern followed to calculate the thickness reduction and the weight Wi of each storey *i* of the façade considered; as well as the weights W_g and W_v relating to gable ends and vertical additions, respectively.

In the bar chart, the interrelations between different variables are represented by black dots at intersections of segments belonging to each variable. All the variables shown in the figure have been introduced in §2.3.2.

First, in order to take into account the maintenance level of the masonry (5-7) and lack of verticality (5-9), the actual wall thickness recorded in the survey (T_{bI}) is reduced by a given percentage, as to obtain the theoretical thickness T_b. The percentage reduction applied by (5-7) and (5-9), respectively $\%tr_1$ and $\%tr_2$, are governed by the following criteria.

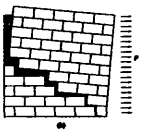

The maintenance level of the masonry (5-7) can be considered by the operator as good (G), medium (M), bad (B), or not applicable (na). Each of these choices corresponds to the following values:

(G) ⇒ $\%tr_1=0$

(M) ⇒ $\%tr_1=0.1$

(B) ⇒ $\%tr_1=0.25$

(na) ⇒ $\%tr_1=0.1$

When the facade is judged to be out-of-vertical ("True"), the variable ($\%tr_2$) assumes the following possible values depending on the number of storeys N of the facade. It is assumed that the facade being out-of-vertical can affect its structural performance, only if N is greater than or equal to 2, as follows:

"True" ⇒ For N≥2 ⇒ $\%tr_2=0.3$

For N<2 ⇒ $\%tr_2=0$

"False" ⇒ $\%tr_2=0$

The reduced value of the thickness at base T_b, is then:

$$T_b = T_{b1} \cdot [1 - \%tr_1 - \%tr_2] \tag{3-1}$$

Once the thickness has been reduced the weights can be calculated. For the calculation of the the weight of the façade, defined by equation (2-16), the percentage of openings per storey, Op_i, which is defined by the number and average size of windows as well as by chimney flues (field 6-4) within the wall thickness, is also considered.

The chimney flues are assumed as a fixed percentage ($\%tr_5$) added to the percentage of facade openings (Op_1), as follows:

$$Op_i = Op_1 + \%tr_5 = \frac{(n_{oi}) \cdot (l_o \cdot h_o)}{(H_i \cdot L)} + (\%tr_5) \tag{3-2}$$

where ($\%tr_5$) is assumed to be equal to 0.1 when the chimney flue is present; 0 when it is absent. All the other variables are the same introduced in §2.3.2.

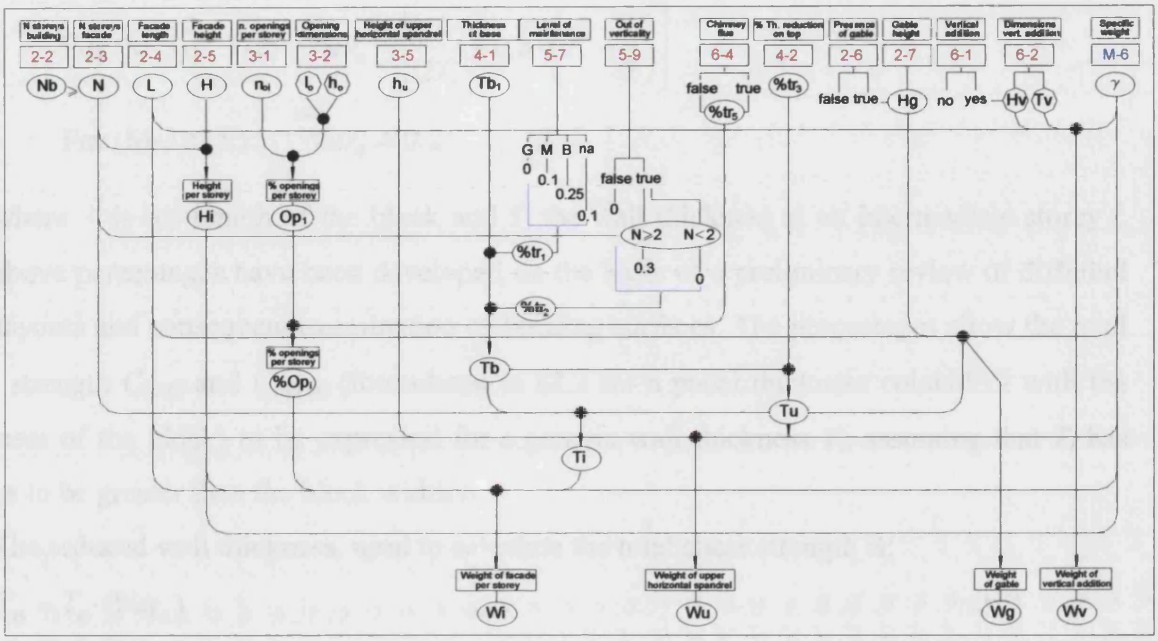

Figure 3- 11 – Bar chart showing calculation of the weights starting from survey input data

3.4.2 Calculation of the total shear strength

As outlined in §2.2, the failure mechanisms strictly depend on the frictional behaviour of the masonry which has been analytically formulated for an ideal prototype of ashlars masonry to express the restraining action exerted between orthogonal walls or along inclined crack lines.

A criterion is then proposed for adapting the layout of the ideal model to any of the samples previously shown. Such criterion is based on a progressive reduction of the sliding surface from the best prototype of masonry, i.e. type A of Figure 3- 10, to the worst, characterised by all rubble (type E). The reduction in the contact surface applied to each of the 5 types is:

$$\text{For (M-3)=(A)} \Rightarrow \quad \%tr_4 = 1$$

$$\text{For (M-3)=(B)} \Rightarrow \quad \%tr_4 = \left[\frac{\ell}{T_i} + \frac{1}{3}\cdot\frac{(T_i - \ell)}{T_i}\right]$$

$$\text{For (M-3)=(C)} \Rightarrow \quad \%tr_4 = \left[\frac{\ell}{T_i}\right]$$

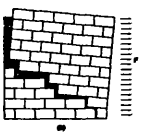

For (M-3)=(D)⇒ $\%tr_4 = \left[\frac{\ell}{2T_i} + 0.5 \cdot \left(T_i - \frac{\ell}{2}\right)\right]$

For (M-3)=(E)⇒ $\%tr_4 = 0.2$

where ℓ is the length of the block and T_i the wall thickness at an intermediate storey *i*. The above percentages have been developed on the basis of a preliminary review of different wall layouts and consequent examination of bedding surfaces. The percentages allow the total shear strength $C_{tot(i)}$ and $C_{tot(\alpha i)}$ (formulated in §2.2 for a panel thickness coincident with the thickness of the block) to be expressed for a generic wall thickness T_i, assuming that T_i has always to be greater than the block width *b*.

The reduced wall thickness, used to calculate the total shear strength is:

$$T_{ri} = T_i \cdot (\%tr_4) \qquad (3\text{-}3)$$

After formulating the total shear strength $C_{tot(i)}$ and $C_{tot(\alpha i)}$ over a reduced wall thickness T_{ri}, it is possible to calculate the restraining actions due to connections with orthogonal walls which the building wall is subjected to.

These are defined by a special field (5-8) of the survey form, according to which the operator is required to express a qualitative judgment on the level of connection at lateral edges (good/bad). This information sets the value of the variable ε, introduced in §2.3.2, defined according to the following criterion:

- Both connections of Good level ⇒ ε=2
- Both connections of Bad level ⇒ ε=0
- One connection of good level and the other of bad level ⇒ ε=1

Moreover, the number of connections with internal walls, specified at field 4.3 of the survey form, defines the variable β (§2.3.2).

Having calculated the restraining actions exerted by lateral and internal walls, the load factors of each failure mechanism at every storey of the façade examined, can be calculated.

Figure 3- 12 shows a bar chart displaying the logic pattern for calculating $C_{tot(i)}$ along a vertical crack line and the failure mechanisms depending on it, such as A,D,E,F.

The logic pattern followed to calculate failure mechanisms influenced by both $C_{tot(i)}$ and $C_{tot(\alpha i)}$ (B1,B2,C,G, Gs,H) is shown in Figure 3- 13. This bar chart also outlines the process

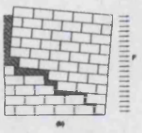

used to calculate the total shear strength along party walls $C_{tot(as\text{-}i)}$, obtained by substituting the geometric features of the party walls in the analytical formulation of $C_{tot(ai)}$ (§2.2.3).

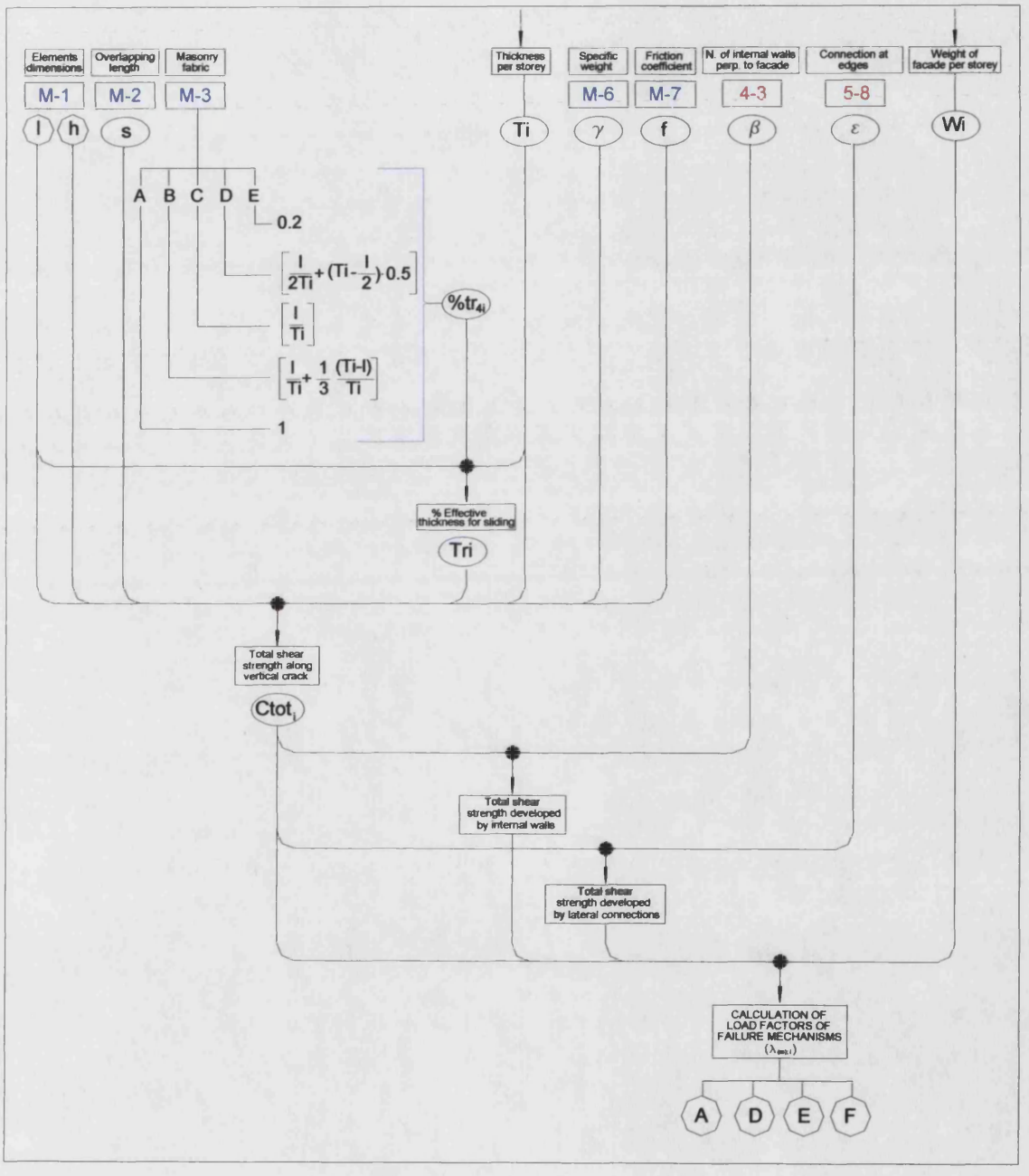

Figure 3- 12 –Bar chart showing the calculation of the total shear strength along vertical cracks and associated failure mechanisms

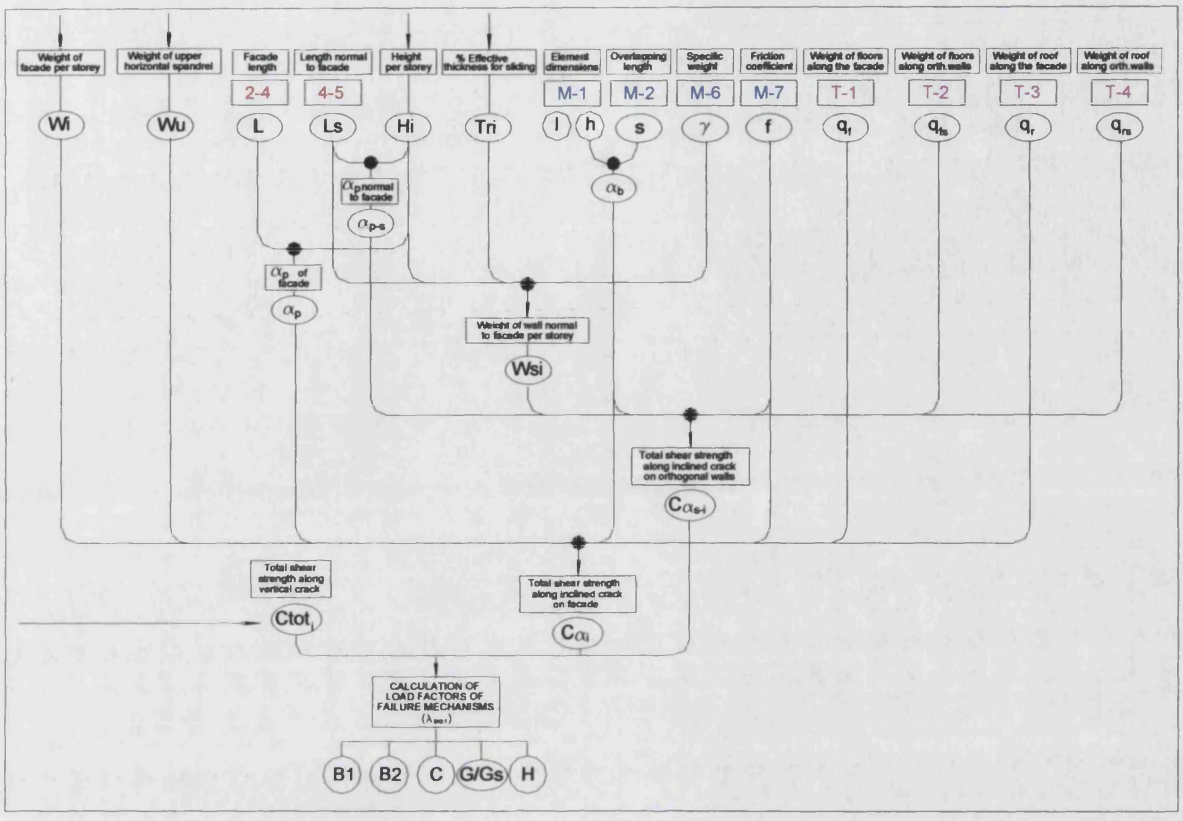

Figure 3- 13 - Bar chart showing the calculation of the total shear strength along inclined cracks

3.4.3 Conditions governing the feasibility of failure mechanisms

As introduced in §3.3.1, some fields of the inspection form are used to assess the feasibility of failure mechanisms in relation to specific features.

The bar chart in Figure 3-1 shows that, having calculated each failure mechanism, a further check has to be carried out, in order to find out which damage mode has to be excluded from the final calculation of the critical load factor (μ) or which can onset only partially.

This screening phase is carried out by means of decision criteria, mainly based on the fields introduced in §3.3.1: *Position of the Building within the block* (1-4), *Opening layout* (3-3), *Connection at edges* (5-8), and *Strengthening devices* (5-10). Table 3-1 summarises the conditions governing the feasibility of each failure mechanism. The symbol Y/N is associated to those failure mechanisms whose partial onset could involve a variable number of storeys.

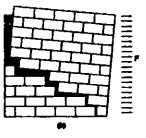

The table shows that the most influential fields are (5-8) and (5-10), while the others have a lesser impact.

It has been assumed that field (1-4) can influence failure mechanisms as C and G only. This choice has been made by checking the compatibility between the position of the building and the failure mechanisms which the building could develop.

When the building is located in a middle position within the block of houses, with one or two sides free (Figure 3- 3, M,S), the corner failure (C) and the horizontal arch failure (G) cannot be triggered, because the lateral restraints exerted by the adjacent buildings would impede any lateral displacement. The formulation of these failure mechanisms, introduced in §2.5.2, are in fact based on the overturning/sliding of the façade extremities.

Failure mechanism H has been assumed to be compatible with all the building positions of Figure 3- 3, including the internal ones (M,S), because the in-plane displacements produced are very small or infinitesimal. Finally, all the others failure mechanisms are considered compatible with the building positions of Figure 3- 3.

Field (3-3) can only affect failure mechanism E. This is not admitted when the openings layout is of type (CV) and (LV) (Figure 3- 5), characterised by single columns of openings. Although these layouts are not associated to any mechanism so far, they are required in the survey so as to be taken into account in further development of the method.

Failure mode (E) is admitted for layouts E1, V, and X, though only on the top storey, as these layouts are characterised by the presence of at least 2 openings at this level.

It is also assumed that the connection layout (field 5-8) can influence the feasibility of damage modes. This assumption arises from the mechanical behaviour observed in Chapter 2. A clear example emerges from the comparison between failure mechanism A and D, in Figure 2-37. The diagram shows that mechanism D is always the more vulnerable, for any type of connection, while mechanism A could never onset. This performance of D, which can be partially attributed to the torsional friction resistance neglected along the inclined crack, causes the feasibility occurrence of A and D to be associated to two different connection layouts, becoming mutually exclusive. Hence, it is assumed that A is computed when both connections are missing, D being computed when only 1 side is anchored to the orthogonal wall. In this case the portion of wall involved in the mechanism is always the one with no connection. In this case failure mode B1 is also admitted, which hence is associated with

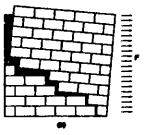

asymmetrical connection. When both connections are present, failure modes as B2, C and E are computed. The last two are also admitted when just 1 bond is present. Finally, it is assumed that failure mechanism F can be triggered only when both lateral connections are missing.

The presence of strengthening devices (field 5-10) influences the feasibility of all the failure mechanisms considered by the method. Table 3-1 shows that failure mechanisms from (A) to (L) can be triggered in the total absence of strengthening devices, unlike from the (F) which requires their presence to onset.

As can be observed, the same screening criterion has been assumed for failure modes from (A) to (B1): any type of strengthening device from ring beam to metallic ties however placed at whatever storey, can prevent this storey and the ones below from being involved in the mechanism. To give an example, if a ring beam is placed on the top of a 5-storey building, none of these three mechanisms could occur, whereas if the ring beam is placed between the fourth and fifth storey, the load factors of (A), (B1), (B2) relative to the top storey are computed for the final evaluation of the critical load factor (μ).

In the case of partial failure mechanisms such as (C), (D),(E),(G), the feasibility conditions are diversified, but always based on the assumption that if a strengthening device can impede the collapse of the storey where the device is applied, it produces the same effect on all the storeys below the one considered.

It has been considered that in presence of strengthening devices distributed asymmetrically, (A1,M,AM of Figure 3- 6) mechanism (C) can always be triggered, because these are implicitly considered on the opposite side of the corner which collapses. Otherwise, this can be prevented by reinforcement devices like (RB,A3,A2).

Failure mechanism (D) is characterised by more restrictive conditions, because this is admitted only in presence of a lateral metallic tie (A1), which is implicitly considered as placed on the opposite side of the portion which fails.

(E) and (G) behave in the same way, because they can be prevented by strengthening layouts (like RB, A3, M, AM) able to restrain the central portion of the façade.

The in-plane failure mode (H) can be impeded only by ring beams, while metallic ties are considered ineffective for preventing the displacements caused by H.

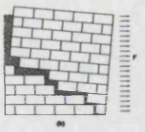

FAILURE MECHANISM		1-4 POSITION OF THE BUILDING WITHIN THE BLOCK					2-6 GABLE		3-3 OPENINGS LAYOUT							5-8 CONNECTIONS			5-10 STRENGTHENING DEVICES							6-1 V. ADDIT.	
		I	E	C	M	S	YES	NO	E2	E1	CV	LV	V	X	0	0	1	2	0	RB	A3	A2	A1	M	AM	YES	NO
	A	☑	☑	☑	☑	☑	☑	☑	☑	☑	☑	☑	☑	☑	☑	☑	⊘	⊘	☑	☑⊘	☑⊘	☑⊘	☑⊘	☑⊘	☑⊘	☑	☑
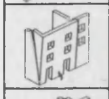	B1	☑	☑	☑	☑	☑	☑	☑	☑	☑	☑	☑	☑	☑	☑	⊘	☑	⊘	☑	☑⊘	☑⊘	☑⊘	☑⊘	☑⊘	☑⊘	☑	☑
	B2	☑	☑	☑	☑	☑	☑	☑	☑	☑	☑	☑	☑	☑	☑	⊘	⊘	☑	☑	☑⊘	☑⊘	☑⊘	☑⊘	☑⊘	☑⊘	☑	☑
	C	☑	☑	☑	⊘	⊘	☑	☑	☑	☑	☑	☑	☑	☑	☑	⊘	☑	☑	☑	☑⊘	☑⊘	☑⊘	☑	☑	☑	☑	☑
	D	☑	☑	☑	☑	☑	☑	☑	☑	☑	☑	☑	☑	☑	☑	⊘	☑	⊘	☑	☑⊘	☑⊘	☑⊘	☑	☑⊘	☑⊘	☑	☑
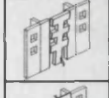	E	☑	☑	☑	☑	☑	☑	☑	☑⊘	☑⊘	⊘	⊘	☑⊘	☑⊘	☑⊘	⊘	☑	☑	☑	☑⊘	☑⊘	☑	☑	☑⊘	☑⊘	☑	☑
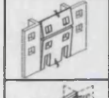	F	☑	☑	☑	☑	☑	☑	☑	☑	☑	☑	☑	☑	☑	☑	☑	⊘	⊘	⊘	☑	☑	☑	☑	☑	☑	☑	☑
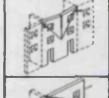	G	☑	☑	☑	⊘	⊘	☑	☑	☑	☑	☑	☑	☑	☑	☑				☑	☑⊘	☑⊘	☑	☑	☑⊘	☑⊘	☑	☑
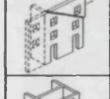	H	☑	☑	☑	☑	☑	☑	☑	☑	☑	☑	☑	☑	☑	☑				☑	☑⊘	☑	☑	☑	☑	☑	☑	☑
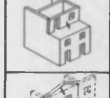	I	☑	☑	☑	☑	☑	⊘	☑	☑	☑	☑	☑	☑	☑	☑				☑	☑	☑	☑	☑	☑	☑	☑	⊘
	L	☑	☑	☑	☑	☑	☑	⊘	☑	☑	☑	☑	☑	☑	☑				☑	⊘	☑	☑	☑	☑	☑	⊘	☑

YES ☑ NO ⊘ Y/N ☑⊘

Table 3- 1 – Conditions governing failure mechanism feasibility

Finally, while for the collapse of vertical addition (I) none of the considered strengthening layouts considered is effective (because all are placed on the building façade), the overturning of gable ends (L) can be impeded by a ring beam at the top.

3.4.4 Conditions governing the failure of masonry

The review of the literature available on the topic presented in §1.4.6, has outlined that the basic assumption by which masonry structures can be analysed according to failure mechanisms is strictly linked to the possibility of considering the masonry fabric as a

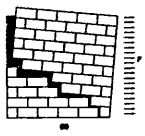

monolithic body, where a crack can occur without failure of the material (Giuffre' .1989, Baggio et al., 1990, Spence 1992a, Ceradini 1992, Giuffre' et al. 1994).

Fields (M-4) and (M-5) of the survey form developed for masonry (§3.3.3) aim to check the "level connection" and "cohesion" through the thickness of each masonry type, which the operator is required to express as a qualitative judgment.

It is assumed that when at least one of these two features is considered structurally insufficient to assure an adequate level of integrity within the fabric, the feasibility of any rigid mechanism is considered highly improbable, with more likely failure of masonry occurring through expulsion of elements (bricks, stones).

3.4.5 Conditions governing associated collapses of roofs and horizontal structures

The conditions assumed for the collapse feasibility of horizontal structures and roofs are drawn up in Table 3-2.

These conditions have been based on the results achieved by recent research carried out in Italy by SSN (Di Pasquale, et al., 1999), aimed at assessing the statistical distribution of damage among different structural elements in masonry buildings damaged by different earthquakes. The results achieved suggest a direct correlation between the out-of-plane displacements of walls and the damage occurring in horizontal structures and roof. Damage distributions for roof and floors as a function of the damage to vertical structures are provided for different structural types.

The results give rise to the assumption according to which the collapse of roof and internal floors is associated with the onset of out-of-plane failure mechanisms involving the façade, such as A,B1,B2 and E. However, no distinction is provided among different structural types.

The results achieved by the research carried out by SSN do not take into account the influence of beam direction in defining the damage extent. However, other research and methods developed have highlighted the influence of this feature (Bernardini, 1986, Giuffrè, 1993), so that the extent of the damage to these structures is considered to be dependent on their orientation.

When the orientation is parallel to the wall under examination, and hence the distributed weight is supported by party walls, the collapse of either roofs or floors is assumed to occur

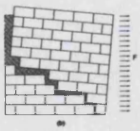

partially. When the beam direction is orthogonal to the facade, and hence the weight of roof/floors is borne by the wall under examination, a total collapse of these structural elements is associated.

In the case of partial failure modes like (C) and (D), it is assumed that, while the former causes a partial involvement of floors and roof regardless of the beam direction, the latter involves the whole roof only.

Mechanism (F) is characterised by the collapse of horizontal structures of the storeys involved, while it is assumed that the failure of the roof cannot onset, because of the presence of restraints at the top of the wall.

It is also assumed that the failure of floors is impeded when mechanism G is triggered, since this failure mechanism is associated with the top storey only, while the extent of the roof failure is influenced by the beam direction. A final assumption is that no damage to the roof or horizontal structures is produced by the onset of failure mechanism (H).

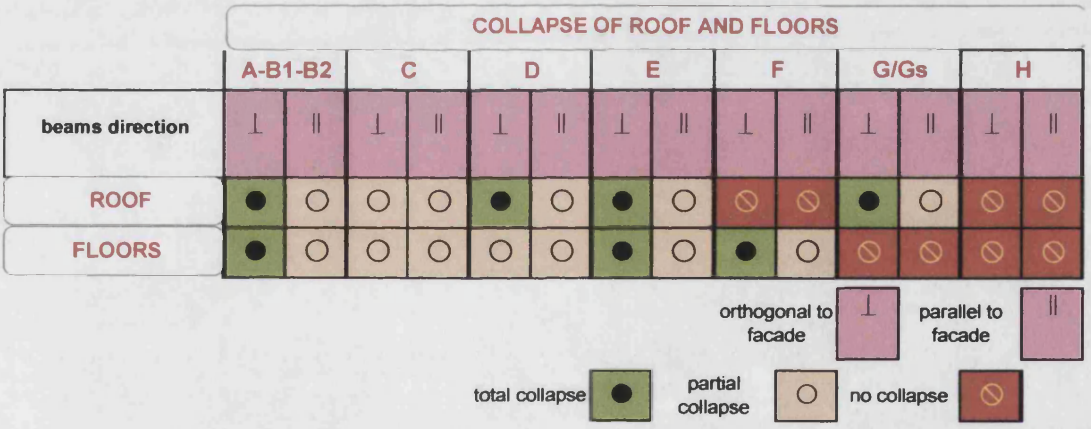

Table 3-2 –Conditions governing the collapse of roof and horizontal structures

3.4.6 Calculation of the critical load factor

The decision criteria introduced in Table 3-1 enable the feasibility of each failure mechanism to be defined, while the respective load factors are obtained from the formulations presented in Chapter 2.

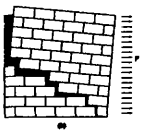

Table 3-3 shows the process of the screening load factors, and the consequent calculation of the critical load factor (μ) of the wall under examination, taken as the minimum load factor of those resulting from the screening process.

The critical load factor (μ) borne by the façade is:

$$\mu = \min(\lambda_{(m,i)}) \tag{3-4}$$

where $\lambda_{(m,i)}$, is the load factor relative to the given failure mechanism at i-th storey of the façade.

The third column of the Table shows the list of the load factors computed at every storey, for every failure mechanism.

The following column shows the load factors resulting from the screening process. The smallest of them is assumed to be the critical load factor of the wall in question. As evidenced by the bar chart, all the failure mechanisms except G,Gs, I and L, can involve a variable number of storeys.

The number of storeys involved by mechanism F is obtained by first optimising the most critical couple of strengthening devices associated with the lowest load factor, along the wall height. Failure mechanism G is computed on the top storey only. In place of G, when openings are present on this storey, failure Gs is computed by involving the horizontal strip above openings. Mechanisms I and L are associated with specific structural elements.

The final results of the calculation process are then:

- Critical load factor (μ);
- failure mechanism associated with the critical load factor (μ);
- number of storeys involved in the collapse (j);

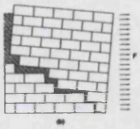

FAILURE MECHANISMS	STOREYS	LOAD FACTORS ($\lambda_{(m);i}$)	FEASIBILITY CHECK	CRITICAL LOAD FACTOR CALCULATION
A	N	$\lambda_{(A)\,N}$		$\mu = \min(\lambda_{(m);i})$
	N-1	$\lambda_{(A)\,N-1}$		
	...	$\lambda_{(A)\,...}$		
	1	$\lambda_{(A)\,1}$		
B1	N	$\lambda_{(B1)\,N}$		
	N-1	$\lambda_{(B1)\,N-1}$		
	...	$\lambda_{(B1)\,...}$		
	1	$\lambda_{(B1)\,1}$		
B2	N	$\lambda_{(B2)\,N}$		
	N-1	$\lambda_{(B2)\,N-1}$		
	...	$\lambda_{(B2)\,...}$		
	1	$\lambda_{(B2)\,1}$		
C	N	$\lambda_{(A)\,N}$		
	N-1	$\lambda_{(C)\,N-1}$		
	...	$\lambda_{(C)\,...}$		
	1	$\lambda_{(C)\,1}$		
D	N	$\lambda_{(D)\,N}$		
	N-1	$\lambda_{(D)\,N-1}$		
	...	$\lambda_{(D)\,...}$		
	1	$\lambda_{(D)\,1}$		
E	N	$\lambda_{(E)\,N}$		
	N-1	$\lambda_{(E)\,N-1}$		
	...	$\lambda_{(E)\,...}$		
	1	$\lambda_{(E)\,1}$		
F	...	$\lambda_{(F)}$		
G/Gs	N	$\lambda_{(G/Gs)}$		
H	N	$\lambda_{(H)\,N}$		
	N-1	$\lambda_{(H)\,N-1}$		
	...	$\lambda_{(H)\,...}$		
	1	$\lambda_{(H)\,1}$		
I		$\lambda_{(I)}$		
L		$\lambda_{(L)}$		

Table 3-3 – Screening process for the calculation of the critical load factor (μ)

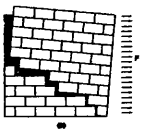

3.5 Parameters involved in the vulnerability assessment

The vulnerability assessment performed in methods aimed at predicting failure mechanisms introduced in §1.4.5 (Bernardini, 1984, Giuffrè, 1993, Doglioni, 1994, D'Ayala et al. 1995, 1996, Lagomarsino 1997) is mainly based on the evaluation of the ultimate load factor of the structure (μ).

However, it should be considered that buildings with an equal critical load factor μ, but different failure mechanism and number of associated storeys, should correspond to different vulnerability levels.

This leads to the conclusion that the ultimate value of μ alone cannot represent a sufficient criterion for expressing the seismic vulnerability.

The method proposed attempts to combine the performance of the structure against the earthquake, expressed by the critical load factor μ, with the number of storeys and type of failure mechanism associated with the value of μ, in order to achieve a more reliable evaluation of the seismic vulnerability.

The failure mechanisms considered in the analysis, differ from each other in terms of the damage which could develop, and the danger to people. By comparing mechanisms A and H, it can be noted that the former is considerably more dangerous than the latter, because the overturning of the façade, although just incipient, could cause the collapse of internal horizontal structures and roof. On the other hand, the onset of an in-plane failure such as H would leave the internal structures still standing.

Moreover, the number of storeys involved, which can also be expressed as a percentage of the wall surface, can provide a further indication about the level of safety of the building against the earthquake, and hence on its usability after the seismic event.

On the basis of this considerations, two indices can be defined:

- the *Structural* index;
- the *Failure extent* index;

These two indices, used for the final assessment of the seismic vulnerability of the wall, are introduced in the following.

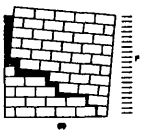

3.5.1 The Structural and the Failure extent index

The *structural index* (I_s) is simply defined as the inverse of μ. As with the index proposed by D'Ayala et al (1995, 1996), used to evaluate final vulnerability ranges, it refers to the capacity of the structure to resist the earthquake. As inverse of the minimum load factor, low values of I_s refer to good seismic performances and vice versa.

The *failure extent* index (I_f) is defined by the following features, all associated with the value of the critical load factor μ:

- number of storeys involved in the mechanism, expressed as percentage of wall surface ($\%F_w$);
- extent of failure of roof and/or horizontal structures ($\%F_{rf}$) ;
- type of failure mechanism weighted (by means of specific weights W_F) to take into account the severity of each failure mode in relation to the danger which could be caused to the building structure and to the people living within it.

The index is expressed as:

$$F_{ind} = (\%F_w + \%F_{rf}) \cdot W_F \tag{3-5}$$

where the percentage of wall surface involved in the mechanism, is:

$$\%F_w = \frac{j \cdot \frac{H}{N} \cdot L}{H \cdot L} = \frac{j}{N} \tag{3-6}$$

where j is the number of storeys involved in the mechanism, N, H, and L are respectively total number of storeys, total height and length of the façade, as introduced in §2.3.2.

The variable $\%F_{rf}$ of equation (3-5) is defined as:

$$\%F_{rf} = \%F_r + \%F_f \tag{3-7}$$

i.e. the sum of the two percentages relative to the collapse of horizontal structures ($\%F_r$) and roofs ($\%F_f$), depending on beam direction, wall surface percentage involved in the mechanism, and type of failure mechanism associated. Their values, calibrated on a rough estimation of the damage to roof and floors surveyed in Nocera Umbra (Italy) following the 1997 earthquake, are expressed as a percentage of the wall surface involved in the mechanism.

$\%F_r$ and $\%F_f$, stored in a special FaMIVE database, cover the following respective ranges:

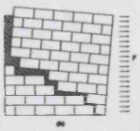

$$0 \le \%F_r \le 0.333 \quad (3\text{-}8)$$

$$0 \le \%F_f \le 0.24 \quad (3\text{-}9)$$

Hence, $\%F_{rf}$ ranges as follows:

$$0 \le \%F_{rf} \le 0.573 \quad (3\text{-}10)$$

Finally, in equation (3-5), W_F is the weight applied to each failure mechanism, depending on the severity of the mechanism in relation to the danger to structural safety and human life. This variable also takes into account the level of involvement of the wall in each failure mode, so that smaller weights are assumed for partial failures (like C,D,E,C) (Table 3-4).

	WEIGHT FOR INDIVIDUAL FAILURE MECHANISMS											
	A	B1	B2	C	D	E	F	G	Gs	H	I	L
Wf	1	1	1	0,5	0,5	0,6	0,8	0,7	0,5	0,5	0,3	0,3

Table 3- 4 Weights assumed for each failure mechanism

The highest weights are associated with those out of plane failure mechanisms involving the entire façade in different ways (A, B1, B2). A lower weight has been assigned to F, due to the reduced impact which this mechanism can produce on the whole structure, thanks to the presence of strengthening devices which impede global overturning. The in-plane mechanism (H) is characterised by half the weight of A-B2, because of its smaller severity in terms of danger. Finally, the collapse of additional structures is characterised by a low weight (0.3), as the risk associated is rather limited .

The variable W_F ranges as follows:

$$0.3 \le \%F_f \le 1 \quad (3\text{-}11)$$

Finally, the range of the failure extent index (I_f) is:

$$0 \le \%I_f \le 1.573 \quad (3\text{-}12)$$

The combination between the Structural and Failure Extent indices, which can also be normalised between 0 and 1, is able to describe the danger which the building under examination poses.

Once calculated, the two indices are processed according to the criterion described in the following.

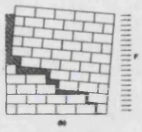

3.6 A criterion for the appraisal of information reliability

As introduced in §3.3.1, the method requires a reliability level of information to be assigned to each of the 7 sections of the survey form.

The information reliability is processed by means of the parameter R_L associated with decreasing scores for each level which the operator can express (High, Medium, Low).

It is also assumed that the information reliability is weighted in relation to the importance of the data contained in each section of the form, according to the following table:

Survey sections	1	2	3	4	5	6	7
R_{Wk}	0.4	1	0.8	1	1	0.7	1

Table 3- 5 – Weights relative to the inspection form sections

The weights R_{Wk} have been calibrated by considering that the most important sections are the 2nd ,4th ,5th and 7th, which all provide geometric and structural features of the façade together with the damage description. Lower weights are assigned to the remaining fields.

The total reliability of information (R_T) is defined as follows:

$$R_T = \sum_{k=1}^{7} R_{Lk} \cdot \sum_{k=1}^{7} R_{Wk} \tag{3-13}$$

where k is a variable ranging between 1 and 7 which identifies the section of the inspection form.

The upper and lower boundaries of R_T are defined as:

$$R_{T\min} = \sum_{k=1}^{7} R_{Wk} \cdot R_{L\min} \tag{3-14}$$

$$R_{T\max} = \sum_{k=1}^{7} R_{Wk} \cdot R_{L\max} \tag{3-15}$$

where R_{Lmin} and R_{Lmax} are the minimum and maximum reliability levels respectively.

Having divided the R_T existing field (R_{Tmax}- R_{Tmax}) into three equal ranges, a percentage coefficient (%R) is associated with each of them:

$$R_T \geq R_{T\min} + \frac{2}{3}\left(R_{T\max} - R_{T\min}\right) \Rightarrow \%R = 0.05 \tag{3-16}$$

$$R_{T\min} + \frac{1}{3}\left(R_{T\max} - R_{T\min}\right) \leq R_T < R_{T\min} + \frac{2}{3}\left(R_{T\max} - R_{T\min}\right) \Rightarrow \%R = 0.1 \tag{3-17}$$

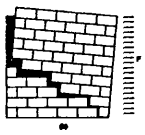

$$R_{T\min} \le R_T < R_{T\min} + \frac{1}{3}\left(R_{T\max} - R_{T\min}\right) \qquad \Rightarrow \%R = 0.15 \qquad (3\text{-}18)$$

A low percentage coefficient of 5% is associated with high reliability, exceeding the lower R_T boundary by 2/3. An intermediate percentage of 10% has been assigned to values of R_T ranging between 1/3 and 2/3 of R_{Tmin}. Finally, a high percentage coefficient of 15% has been associated with low values of the total reliability, not exceeding 1/3 of the R_{Tmin} value.

The percentage coefficients (%R) are used to define the upper and lower boundaries of the Structural and Failure extent indices, according to the following criterion:

$$\text{Lower Boundaries} \Rightarrow \quad I_{s(-)} = I_s \cdot (1 - \%R); \quad I_{f(-)} = I_f \cdot (1 - \%R) \qquad (3\text{-}19)$$

$$\text{Upper Boundaries} \Rightarrow \quad I_{s(+)} = I_s \cdot (1 + \%R); \quad I_{f(-)} = I_f \cdot (1 + \%R) \qquad (3\text{-}20)$$

A limit of this criterion is that it necessarily requires the reliability level to be expressed for all 7 sections of the inspection form. This means that in the total absence of damage, a level of reliability must nevertheless be associated with section (7). In this case it is assumed that a High level of reliability has to be assigned by the operator, leading to a consequent slight increase in the total reliability over the 6 sections.

3.7 Final vulnerability assessment

The seismic vulnerability of the wall under examination is taken to be defined by the two indices introduced in §3.5.1. According to their definition, the seismic vulnerability is considered as a function independent of the earthquake intensity and depending on:

- the ultimate capacity of a building to resist earthquakes (critical load factor μ),
- failure mechanism associated with the value of μ,;
- percentage of surface most likely to be involved, associated with the value of the critical load factor μ;

Consequently, this type of assessment cannot provide a measure of the most likely damage level to which the building would be subjected as the result of an earthquake of given severity.

However, it is assumed that the μ value, to which an incipient failure is associated, corresponds to a damage level D2 (from the 6-points scale of EMS '98). This enables a

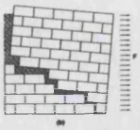

statistical correlation between observed and predicted damage to be carried out, as discussed in Chapter 5.

Although the two indices, when compared, are able to provide a measure of the seismic vulnerability, a criterion for converting them into a qualitative final assessment of the seismic vulnerability is proposed and shown in Table 3-6.

The Structural index, once normalised by assigning the reasonable value I_s=8 (corresponding to μ=0.125) to 1, has been divided into 4 ranges, while the Failure extent index, normalised to 1, has been divided into 3 ranges.

The result of this combination of the 7 ranges considered, leads to the definition of a Vulnerability Matrix which provides different levels of vulnerability, shown in Table 3-6 .

		Structural index			
		$I_s>1$	$1>=I_s>0.5$	$0.5>=I_s>0.3$	$0.3>=I_s>0$
Failure extent index	$I_f>1$	VERY HIGH	HIGH	MEDIUM	MEDIUM
	$1>=I_f=>0.5$	HIGH	MEDIUM	MEDIUM	LOW
	$0.5>I_f>0$	MEDIUM	MEDIUM	LOW	LOW

Table 3- 6 –Seismic vulnerability levels as a function of Structural and Failure extent indices.

Using the same Vulnerability Matrix it is also possible to identify the upper and lower vulnerability levels, taking into account the reliability of information, as described in §3.6.

The limit of this approach is that the definition of the Vulnerability level mainly relies on the value of the critical load factor μ, rather than on the combination between the two indices (I_s and I_f). The value of the Damage extent index is assumed to be that associated to the minimum μ. This can lead in some cases to setting a final vulnerability level which is not necessarily the highest associated with the wall under examination.

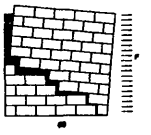

3.8 Conclusions

The Chapter has presented an overall description of the FaMIVE method, ranging from the investigation process to the final evaluation of the seismic vulnerability.

The description of the survey phase is carried out accurately, in order to introduce all the variables examined, and how they are processed.

The seismic vulnerability is defined as a function independent of the earthquake intensity which depends on two indices: the structural index and the damage extent index.

Finally, a criterion for combining the two above-mentioned indices into a qualitative assessment of the vulnerability is proposed. A special criterion developed to treat the reliability of information provided in the survey phase enables the upper and lower boundaries of the seismic vulnerability levels to be identified.

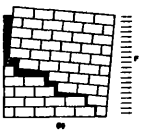

CHAPTER 4
APPLICATION OF THE SURVEY METHOD TO THE HISTORIC CENTRE OF NOCERA UMBRA, ITALY

4.1 Introduction

This Chapter presents an application of the survey method introduced in Chapter 3, to the historic centre of Nocera Umbra (Italy), which was hit by a long sequence of seismic shocks between September and October 1997.

This small hill-top town was first surveyed in order to analyse the effects of the severity of damage produced by the same seismic intensity on around 80 buildings characterised by similar constructive techniques but different strengthening devices. Moreover, the damage to each building was recorded in terms of damage levels using the EMS 92 scale (Spence et al. 1998a,b, 1999, D'Ayala 1999).

The application of FaMIVE in 1999 has been carried out over the same building stock, using some data about constructive features surveyed by Spence et al. A more accurate survey was carried out on two more blocks of houses in order to analyse local structural features and the strengthening devices of buildings in detail (D'Ayala et al.,1999, 2000).

In order to test the applicability of the new damage investigation criteria proposed in Chapter 3, based on failure mechanisms recognistion, the damage to buildings was recorded on a wider sample of 200 buildings.

The Chapter presents the urban layout of Nocera and its historical seismicity, then discusses the results obtained from the survey, in terms of structural features and damage surveyed. These are used to test the applicability of the investigation method proposed, particularly concerning the feasibility and reliability of the mechanism identification process. The set of data collected, together with those obtained in previous investigations, enables the calculation of the seismic vulnerability of the sample, which is presented and criticlly discussed in Chapter 5.

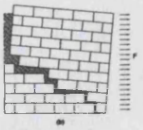

4.2 Introduction to the case study

4.2.1 Urban layout of Nocera Umbra

Nocera Umbra is located in central Italy (Figure 4- 1), on a narrow, elongated hilltop wedged between the Appenines mountains and the town of Assisi. Figure 4- 2 shows the region surrounding Nocera, together with a list of distances (Km) from some principal towns (Menichelli et al., 1995).

The geological situation is typical for a hill-mountain centre, with limestone foundation soils, which outcrops at the surface on the hill top but is covered by detritus material along the slopes. The south-west side of the hill is affected by a significant land slide, which has been under observation for several years. The 1997 earthquake has emphasised this phenomenon considered as an additional cause of damage surveyed in buildings located on this side of the hill (EERI 1997, Capotorti et al., 1997).

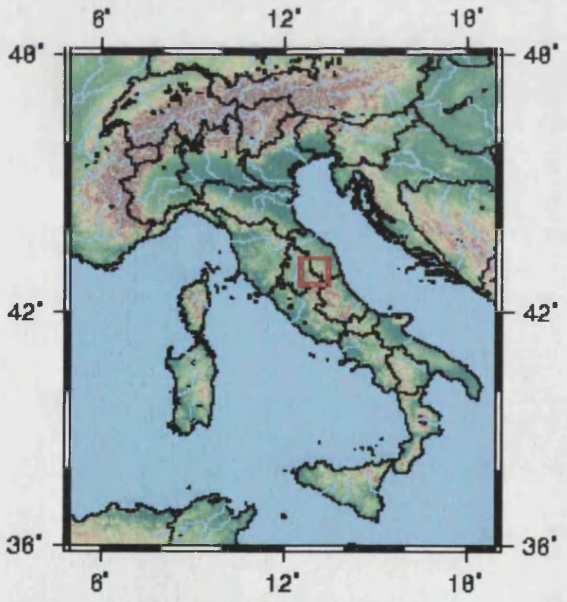

Figure 4- 1 – Location of Nocera Umbra on a map of Italy (ING, 1997)

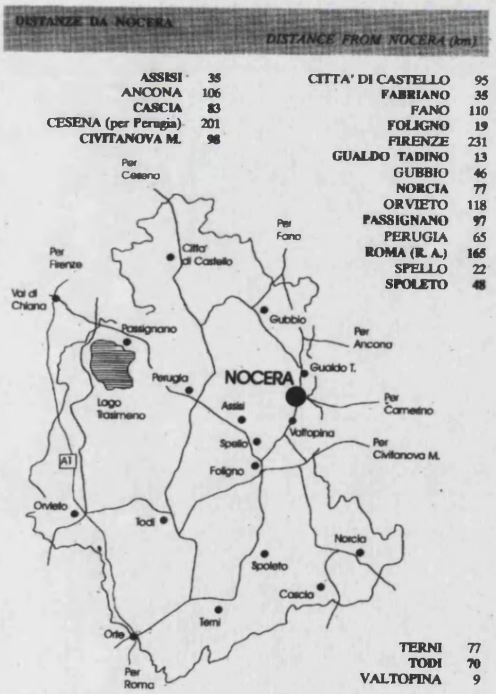

Figure 4- 2 Map of the region around Nocera with distances expressed in Km. (Menichelli et al.1995)

The historic centre, surrounded by city walls and characterised by around 220 buildings, is typical of a medieval town, with buildings arranged in long, parallel, almost concentric arrays (Figure 4- 3).

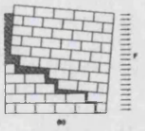

Later alterations, correlated to historic earthquakes which occurred in the 17th and 18th centuries, have modified the original urban layout to some extent. The recent growth of the town has occurred beyond the city walls, so that the original nucleus is relatively well preserved, with a considerable number of valuable heritage architecture. Houses are arranged in long terraced arrays, with common party walls and a variable number of storeys (2 –3 on the hill side, 4-5 on the valley side). A detailed description of the most representative building types is provided in §4.3.1.

Figure 4- 3 – Map of the historic centre of Nocera.
Items highlighted are monumental buildings such as Churches or Palaces.

4.2.2 Historic earthquake occurrence

The seismic activity of Nocera Umbra, catalogued in the National Seismic List as second class since 1981 (Postpischl D., 1986), shows a long history of significant though not catastrophic earthquakes, with events occurring in the region at regular intervals. The GNDT National Catalogue (GNDT, 1998), lists 22 events with epicentral intensities exceeding MCS=8 occurring in this region since 1277 A.D. A pattern of significant repeated shocks

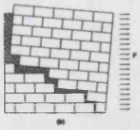

occurring over a period of weeks or months is clearly recognisable, as happened in the 1997 earthquake. Dates, magnitudes and epicentres of these are shown in Figure 4- 4 .

The Italian Catalogue of Historic Strong Earthquakes (ICHSE) from 461 B.C. to 1990, reports the 1279 and 1751 earthquakes as being among the strongest historically (Boschi et al.1997).

The former hit a wide portion of the central region of the peninsula; destruction and victims (about 1000 in the town of Camerino alone) were registered in many other centres, like Fabriano, Matelica, Foligno, Spello, Camerino, San Severino, Cingoli (all within a range of 100 Km). In Nocera it is documented that the old Monastery of the Cathedral was destroyed, together with the adjacent Curia buildings attached, and around half the buildings of the town collapsed causing the death of many people (Giovannini, 1998). The ICHSE assigns a magnitude of 6.4 to this earthquake of IX MCS intensity (Boschi et al.1997).

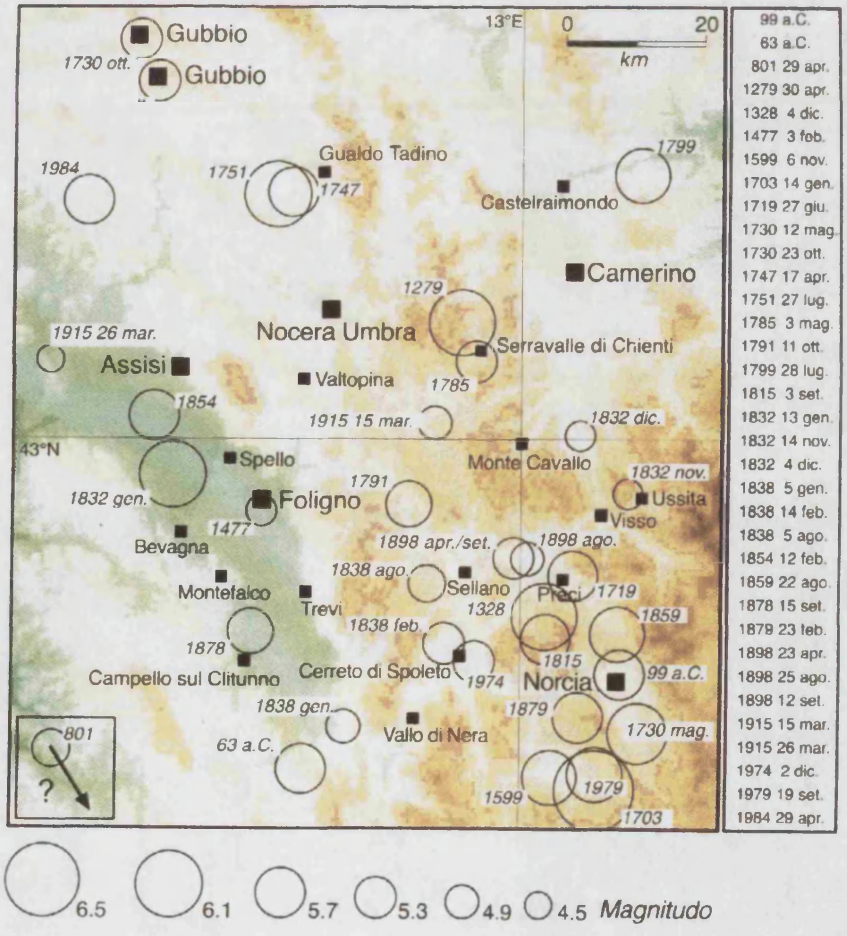

Figure 4- 4 Map of the historic earthquakes in the region around Nocera (ING, 1997)

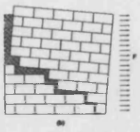

Following a series of small seismic shocks which began in 1742, on the 26th of July, 1751 intensity IX MCS was reached. This earthquake hit about 45 towns of the central Appennines region, and was followed by another long sequence of seismic events which ended on the 24th of September of the same year. The most damaged town was Gualdo Tadino, about 10 km from Nocera, where two thirds of the buildings were destroyed. Damage was also documented in Nocera: one arch of the Cathedral collapsed, followed by a partial failure of the roof. Cracks were also recorded in the Prior's Palace and in the Fortress, together with the collapse of the roof and most of the internal walls of the Seminar (Binia A. 1751, An., 1751). The Bishop's Palace suffered serious damage, and many cracks in private buildings are evidenced by several requests of help documented in the Diocesan Archive in Nocera (Borgia A, 1910). Further shocks occurred in 1752, without causing losses, probably as the tail of the strong event of 1751. In the buildings of the historic centre it is still possible to recognise signs of the repairs implemented following the 1751 earthquake, particularly on upper storeys, which were repaired with recycled materials or poor rubble masonry fabrics (Figure 4- 5).

Figure 4- 5 – Metallic anchor on a wall made up of poor material

Before the latest seismic shocks of 1997, a further seismic event of minor severity was recorded in 1979. This earthquake reached intensity VI MCS, and hit the Valnerina region particularly, also causing damage in Nocera (Camassi et al.1997, Calabrese 1990).

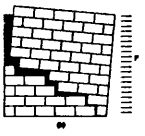

4.2.3 The 1997 earthquake

On the 26th of September 1997 a sequence of seismic shocks hit the region surrounding Nocera Umbra, Camerino and Colfiorito. The first two events, respectively at 2:33 and 11:40 hours, reached Magnitude 5.5 and 5.8, according to the assessments carried out by the Italian Institute of Geophysics in Rome. Many further shocks occurred over a period of 8 months, until April 1998. Among these, the strongest events were registered in Nocera Umbra and Colfiorito respectively on the 3rd and 7th of October, with magnitude of 5.1 and 5.3 M. A further shock on October 14th, with epicentre in Sellano, reached magnitude 5.5 M (Camassi et al, 1997, Decanini et al., 1997).

The macroseismic survey, carried out over the whole region, identified a maximum intensity for the first shock of VIII MCS, whereas the overall cumulative intensity was estimated of IX MCS. Figure 4- 6 shows the isoseismals relative to the shock of 26th of September. Dots with different colours indicate the intensity on the MCS scale relative to the towns involved (Camassi et al, 1997, Albini et al. 1997).

The seismic sequence was also monitored through a temporary network of recording stations, provided by the National Seismic Service, and the Italian National Institute of Geophysics, scattered over the epicentre area of the earthquakes. These stations enabled the waveforms of accelerations and hypo central locations to be recorded (Capotorti et al., 1997, Decanini et al., 1997).

The recordings obtained for Nocera Umbra, strongly influenced by the morphological features of the hill where the station was placed, show very high amplifications, with peak ground accelerations reaching 0.56g on the 26th of September. However, an analysis of the damage caused, suggests that these values, much higher than the other values recorded at other stations, were overestimated, leading to doubts as to their reliability. (Camassi, 1997; Capotorti, 1997).

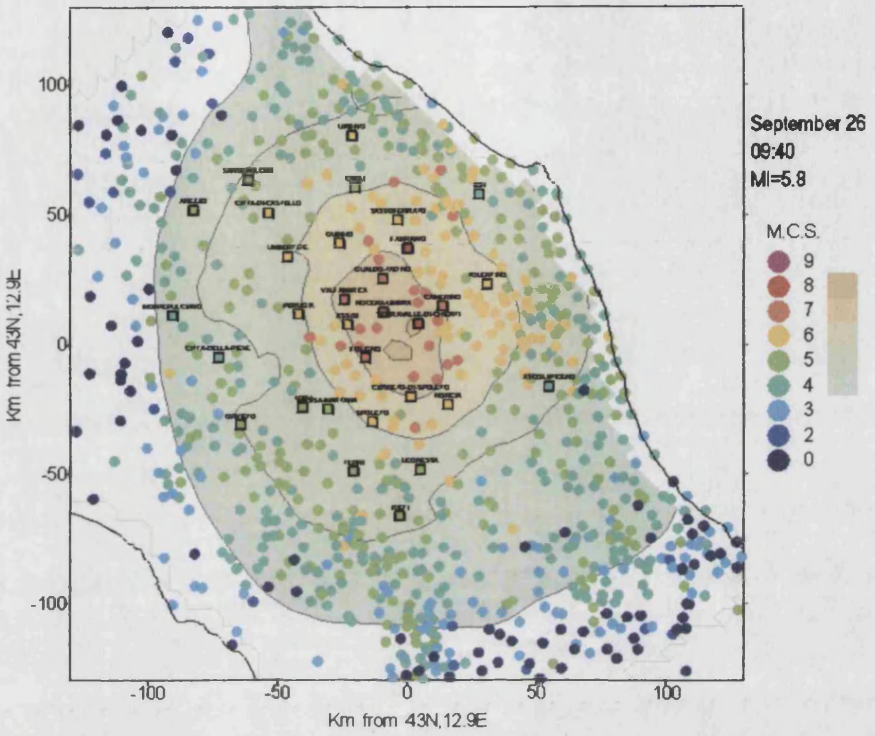

Figure 4- 6 – Macroseismic survey of the region hit by the earthquake (ING, 1997)

4.3 Results of the survey: description of structural features of buildings

During the spring of 1999 a survey was carried out on about 200 ordinary buildings, in order to test the applicability of a pilot version of the form introduced in §3.3, for what concerns the damage investigation process, based on failure mechanism identification. During this survey some of the main structural features of buildings were also recorded throughout a smaller sample of 80 buildings, previously surveyed by D'Ayala and Spence (Spence et al. 1998a,b, 1999). The missing information on some structural features of the sample was later provided using the set of information obtained by the same authors (Spence et al. 1998a,b, 1999), as well as using photographic documentation.

An accurate investigation was carried out on two more blocks of houses (around 20 buildings), in order to analyse in detail the common structural features (such as masonry fabric and roof/floor types), as required by section §3.3.3 (D'Ayala, Speranza, 2000, 2001).

The final database is then realised by around 200 buildings, 100 of which are completely described in terms of structural features (section 1-6 of the form shown in Figure 3-2) and damage (section 7 of the form, Figure 3-7), while the remainder buildings are described only

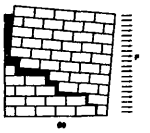

in terms of damage occurred. While a uniform low level of information reliability is associated to the former, (except from those buildings surveyed in detail), in the latter the reliability attributed to each single case has been recorded. This has enabled lower and upper bounds of the critical load factors and final vulnerability calsses to be defined in relation the quality of information, according to the criterion discussed in §3.6.

The following presents the results obtained from the survey in terms of structural features and damage caused and finally some conclusions are drawn about the applicability of the survey method proposed.

4.3.1 Architectural and structural layout of ordinary houses

An ordinary house in Nocera, shows an architectural layout which completely fits in with the natural features of the town, characterised by the presence of a marked slope. Most buildings can be dated back to the middle ages, though most of them underwent major alterations during the 17th and 18th centuries following severe earthquakes, and more recently in the last century.

The typical house is usually composed of one or two masonry cells, depending on the depth of the block, with the staircase, usually but not necessarily, running along the party walls (D'Ayala, Speranza, 2000, 2001).

A common feature of the ordinary houses is that they have frequently been modified over the years, with many combinations of older and newer constructions within the same building. It is very common to observe changes in the original plan distribution and to the constructive features, mainly due to the needs of the changes in lifestyle which have taken place in the last 20-30 years.

Figure 4- 7 and Figure 4- 8 show the construction layout of the two blocks of houses, representative examples of the types of masonry fabric, the internal layout and horizontal structures, surveyed in detail in 1998 (D'Ayala, Speranza, 2001). The figures also highlight the damage pattern.

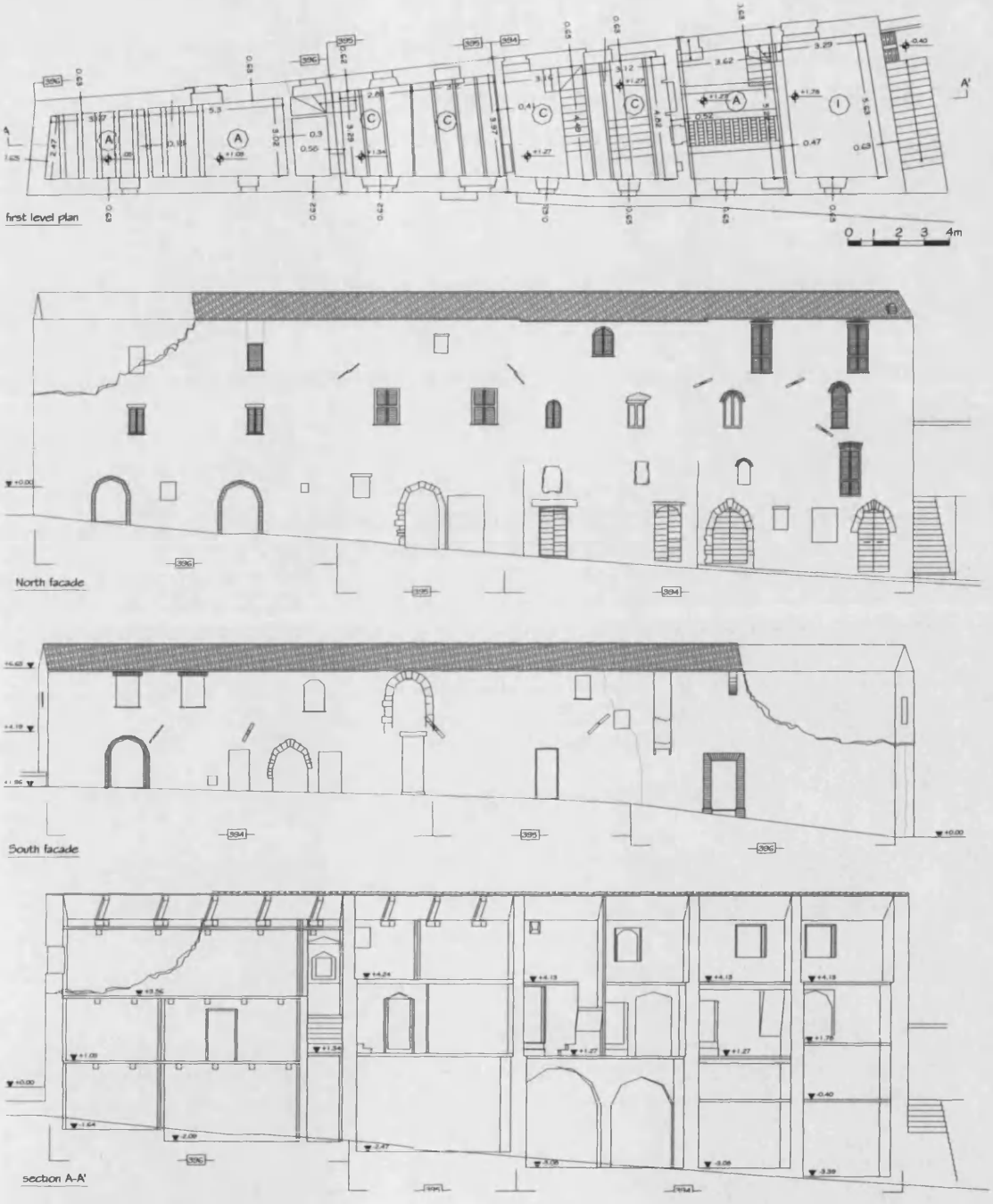

Figure 4- 7 – Units 394, 395, 396. Construction layout and damage pattern.

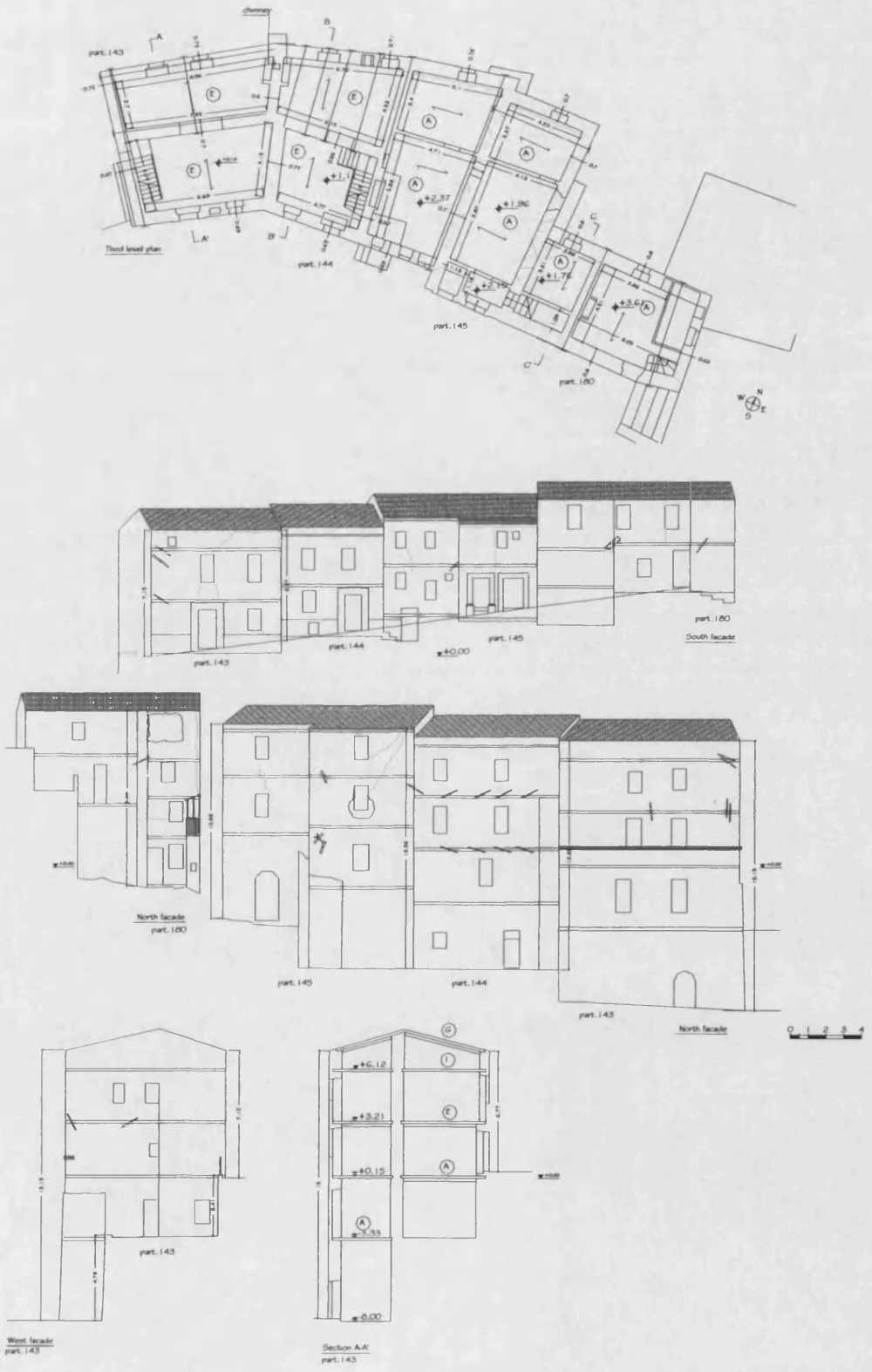

Figure 4- 8 - Units 143,144,145,180. Construction layout and damage pattern.

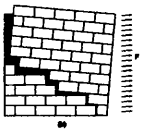

4.3.2 Masonry fabrics

The masonry work of ordinary buildings varies from well dressed stone ashlars with mortar joists of a few millimetres thickness to coarse rubble with poor mortar in thick joints. The connection through the wall depends on the wall thickness and on the dimensions of the element, generally very poor in the case of double- leaf walls, and rather good in solid ashlars masonry. In a few cases, the walls are made of brickwork with a medium-level connection through the wall thickness. Usually the beds are reasonably regular and horizontal, with staggering lengths variable in relation to the element's dimensions. Insertion of horizontal layers of brickwork, window surrounds in brickwork and stone lintels in local tuff stone are common. The quality of connections between orthogonal walls is usually good.

In total, 7 masonry types have been recognised within the historic centre of Nocera Umbra and then incorporated into the worksheet introduced in §3.3.3.

These have been surveyed in detail and classified as shown in Figure 4- 11. Once the 7 types had been grouped into 4 classes, each identified by a different label A,B,C,D, defined as: (A) roughly squared masonry, (B) mixture of ashlars and rubble masonry, (C) rubble, (D) brickwork.

The general characteristics of each type are briefly described in the following:

MASONRY TYPE A1: *Solid masonry made up of long shaped stones, roughly squared, and placed along horizontal layers. The connection through the thickness can be considered good.*

MASONRY TYPE A2: *Two leaves of dressed stones, roughly squared with some elements through the wall thickness. The infill between the two leaves is coherent, and the global connection in the thickness can be estimated as medium.*

MASONRY TYPE B1: *Mixed masonry limestone in long dressed elements, small squared stones and rubble. The fabric layout is characterised by alternate layers of long elements placed along the bedding surface (stretchers), and others placed through the wall thickness (headers). Rubble is often used to fill the gaps between the stones and for the infill, which is incoherent. The overall connection in the thickness can be assumed as weak.*

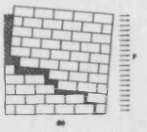

MASONRY TYPE C1: *Masonry mainly characterised by rubble, with layers nearly horizontal. The fabric layout is characterised by three/four layers of small stones, alternating with layers made up of higher elements. The cross section is made up of small pieces with a large quantity of weak mortar. The overall connection through the thickness can be assumed as weak.*

MASONRY TYPE C2: *Masonry characterised by rubble of small size with some bigger elements inserted. The tiny dimensions of fabric elements and the weak quality of mortar do not allow any connection through the thickness so that this masonry fabric can be considered of very poor quality.*

MASONRY TYPE D1: *Brickwork masonry arranged in horizontal layers without infill. The level of connection and cohesion of the fabric is good.*

MASONRY TYPE D2: *Brickwork masonry arranged in horizontal layers, with a poor connection through the thickness.*

Figure 4- 9 and Figure 4- 10 show an example of some fabrics A2, B1,C1 and C2 .

Figure 4- 9 Examples of fabric types A2 (left) and B1 (right)

Figure 4- 10 – Examples of fabric types C1 (left) and C2 (right)

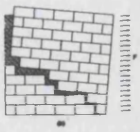

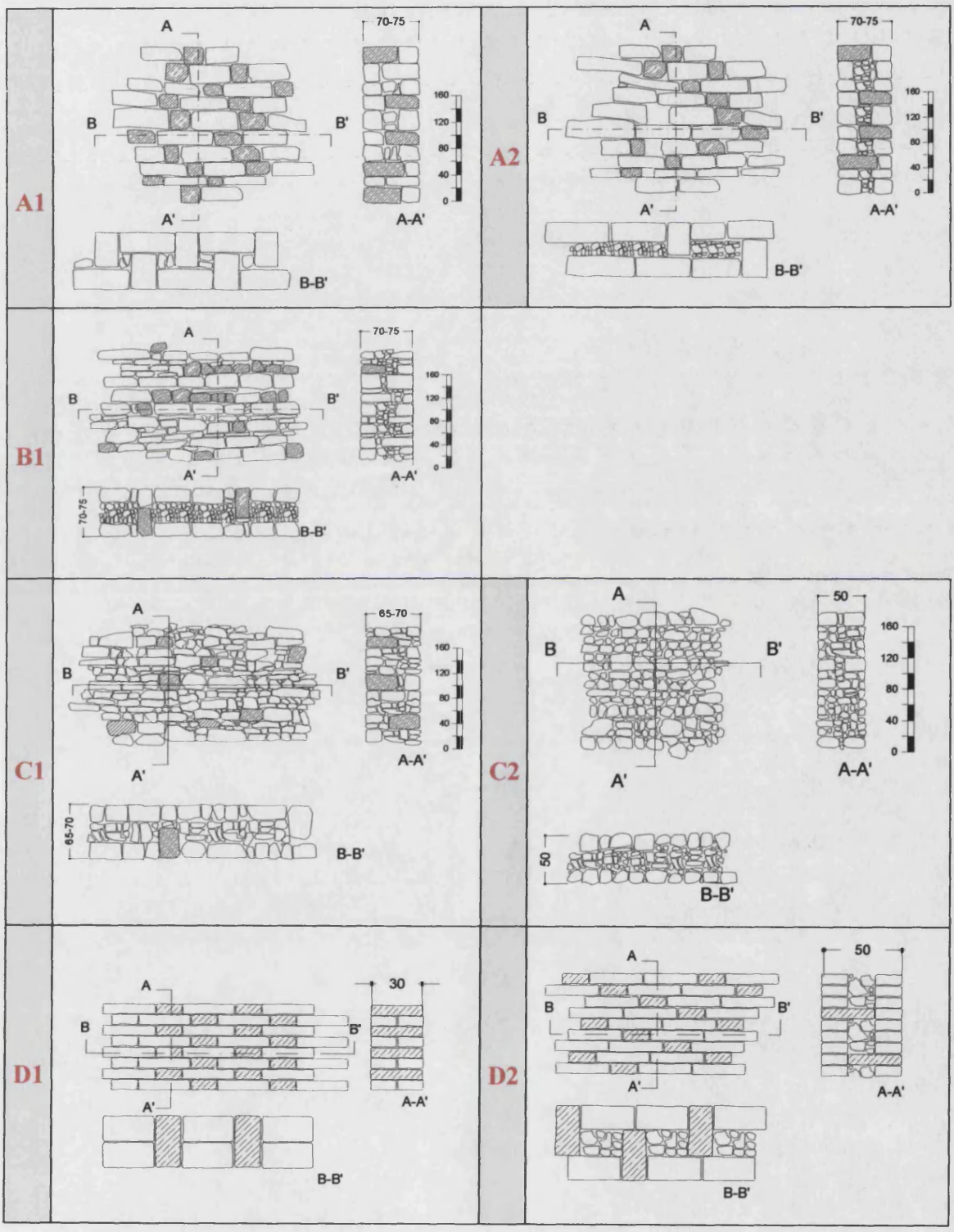

Figure 4- 11 – Masonry fabrics surveyed in Nocera Umbra.

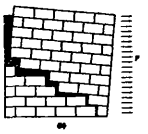

Table 4- 1 shows how the masonry types recorded are stored, according to the format introduced in §3.3.3.

The top quality attributed to class A, i.e. solid masonry, is demonstrated by rather high stagger ratios (>1 in both cases), obtained by dividing the overlapping length (field M-2, Figure 3-1) by the block height (field M-1 right box, Figure 3-1); as well as by high percentages of the effective sliding surfaces, (field M3, Figure 3-10). The levels of connection and cohesion through the wall thickness are assumed to be sufficient to guarantee the monolithic behaviour required of the masonry at §3.4.4.

The following types (B1, C1 and C2) are characterised by decreasing mechanical properties, according to which the level of integrity of the masonry, when subjected to a seismic action, cannot be assured, and hence the above mentioned types could most likely be characterised by failure of the masonry fabric, excluding the possibility of any failure mechanism developing. It is also assumed that these types are characterised by rather reduced effective sliding surfaces, classified in field M3 as C and E (Figure 3-10).

Finally, brickwork fabrics D1 and D2 are defined by very different mechanical features, although both are characterised by the same stagger ratio (2.66). While type D1 is associated with a solid fabric (A, field M-3), together with a sufficient level of bonding through the thickness, type D2 is assumed to be a poorer fabric, barely able to maintain its integrity within the thickness of the wall and hence associated with type B of field M-3. The comparison between these two masonry types highlights how fabric characterised by equal external fabric layouts, can show very different mechanical performance according to their internal composition.

These values have been estimated on the basis of the overall smoothness of the unit surfaces, assuming as basic reference point the values of the coefficients obtained from experimental tests carried out on brickworks (Mann et al., 1982, Schneider et al., 1978, Ceradini, 1992, 1993). Notwithstanding, the literature available on this topic shows a wide range of experimental data, including friction coefficients, on very regular dressed stone/brick fabrics, less work is present when dealing with irregular fabrics, also with mortar joints, because of the major difficulties of carrying out this type of tests. Among this, the recent work of Binda et al. (1999) providing detailed analysis of mechanical properties of different masonry samples, has been however useful in the process of friction coefficients

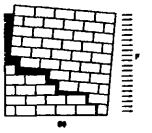

assignment, as it lead to a qualitative description of each bedding surfaces. One more reference was also the recent work of Baggio et. al (2000), which analyses a wide range of fabrics, and for each of them an index of the mechanical quality of masonry is provided (MQI). This index is obtained by comparing the mechanical behaviour of each fabric, with the opus quadratum one. The ratio between the two associated load factors (relative to out of plane and in plane actions) is assumed to be the MQI. These set of values have been useful for calibrating the friction coefficients of fabrics surveyed in Nocera.

In absence of appropriate experimental data, it is clear that this process implies a rather high level of uncertainty, so that the assignment of the friction coefficients could become arbitrary if carried out without sufficient accuracy, and hence could lead to unreliable evaluation of the Total Shear Strength introduced at §2.2 . Reliable values of friction coefficients could be achieved on by undertaking on purpose experimental tests, which could be carried out in a future development of the research.

The distribution of the masonry fabric surveyed overall in the building sample is shown in Figure 4- 12. The most common fabric is type B1 found in 40% of buildings inspected, followed by C1 and A2 found in 25% and 14% of buildings respectively. The latter occurs mainly in aristocratic residences than in ordinary houses. A1, C2 and D1 are present is small percentages, while brickwork masonry of the worst quality (type D2) has been found in 12.5% of buildings.

In conclusion the average masonry fabric of the buildings inspected can be considered medium-poor, and the rather low level of maintenance and high degree of alteration to walls makes their mechanical performance even worse.

		MASONRY FABRICS													
	Title	*Solid masonry*				*Mixed masonry*				*Rubble*				*Brickwork*			
	TYPE	A1		A2		B1		B2		C1		C2		D1		D2	
M-1	Elements dimensions (m) (bxh)	0,5	0,18	0,5	0,18	0,4	0,15			0,13	0,13	0,1	0,1	0,32	0,06	0,32	0,06
M-2	Overlapping length (m)	0,25		0,2		0,1				0,04		0,03		0,16		0,16	
M-3	Masonry fabric	A		B		C				E		E		A		B	
M-4	Level of connection in the thickness	SUFFICIENT		SUFFICIENT		INSUFFICIENT				INSUFFICIENT		INSUFFICIENT		SUFFICIENT		INSUFFICIENT	
M-5	Level of cohesion of the fabric	SUFFICIENT		SUFFICIENT		SUFFICIENT				INSUFFICIENT		INSUFFICIENT		SUFFICIENT		INSUFFICIENT	
M-6	Specific weight (KN/mc)	22		21		20				19		19		18		18	
M-7	Friction coefficient	0,45		0,4		0,35				0,3		0,3		0,4		0,4	
M-8	Description	Solid masonry realised by long shaped stones, roughly squared, and placed along		Masonry characterised by two leaves of squared stones, roughly squared with some		Mixed masonry of limestone long elements, small stones and rubble. The fabric layout is		....		Masonry characterised by rubble with layers nearly horizontal. Every three or four		Masonry characterised by rubble of small size with insertions of some bigger		Brickwork masonry organised in horizontal layers, with solid masonry in the thickness		Brickwork masonry organised in horizontal layers, with a weak connection in the	
	GENERAL CONDITIONS FOR LEVEL OF CONNECTION	—		—		Insufficient connection in the masonry		—		Insufficient connection in the masonry		Insufficient connection in the masonry		—		Insufficient connection in the masonry	

Table 4- 1– Format of masonry types surveyed

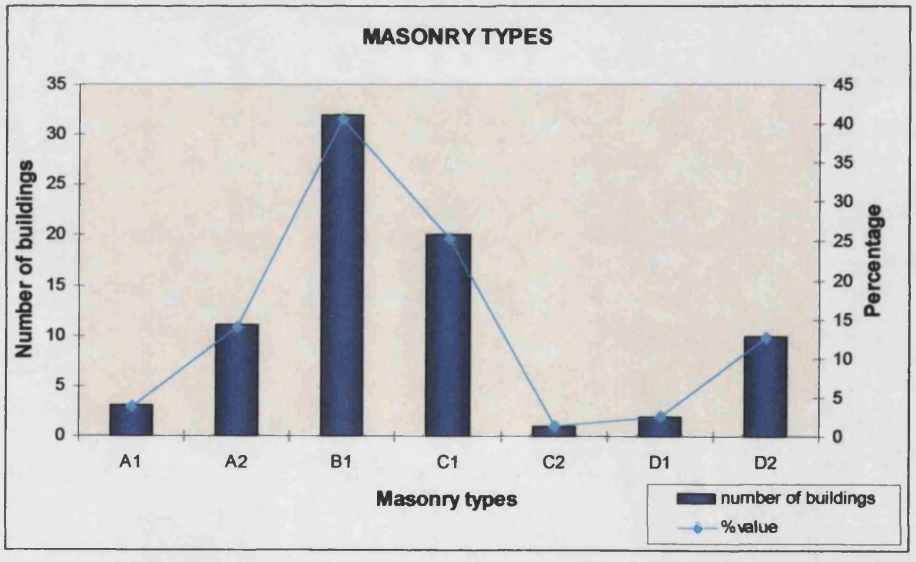

Figure 4- 12 – Distribution of masonry types in the sample surveyed

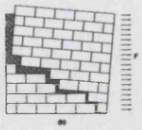

4.3.3 Horizontal structures and roofs

The horizontal structures, when original, are timber and are characterised by beams supporting span joists covered by tiles or planks. Sometimes the beams are placed on small masonry corbels in order to reduce their span. The beams are quite close to each other and are oriented along the shortest distance between the opposite walls. Roofs are usually double pitched and when original are in timber. Similarly to horizontal structures, the rafters support span purlins covered by boards and tiles.

During the last century floors and roof structures were strengthenend or totally replaced by precast concrete beams and lightweight tiles. In some cases original structures were replaced by r.c. slabs. A total of 4 types of floors and roofs have been identified in the historic centre of Nocera, as described in the following:

TYPE A: *Timber structures characterised by timber beams supporting secondary purlins covered by tiles or planks.*

TYPE B: *Timber structures of type A strengthened by metallic mesh within a thin concrete layer, placed over the tiles or planking level. Usually, but not necessarily, the mesh is anchored to the bearing walls.*

TYPE C: *Precast concrete joists and lightweight tiles. No device is usually employed to anchor the joist edges to the walls.*

TYPE D: *Reinforced concrete slabs.*

Figure 4- 13 and Figure 4- 14 show an example of structure types A,B and C.

Figure 4- 13 – Examples of horizontal structures of type A (left) and C (right) surveyed in Nocera

Figure 4- 14 – Examples of roof structures of types B (left) and C (right)

The structural types surveyed in Nocera have been stored according to the format presented in §3.3.3.

As illustrated in the chart of Figure 4- 15, the buildings surveyed in Nocera show a considerable level of alteration to traditional horizontal structures. Only 44.3% of buildings are still characterised by timber floors and roofs, while the remaining portion comprises buildings which have undergone either simple strengthenings to or replacements of the original structures. Commonly, but not always, the same structural system adopted for floors is also used on roofs, though combinations of the various structural systems can be found in the same building.

This is clearly outlined by the histogram below which shows that 13.9% of buildings characterised by both reinforced roofs and floors, whereas all the internal structures have been replaced by modern structural systems such as precast joists and lightweight tiles (i.e. type C, 8.9% of buildings), and r.c. slabs (type D, 21% of buildings), most common type of alteration. The remaining percentages refer to combinations between different structural types, as shown in Figure 4- 15 .

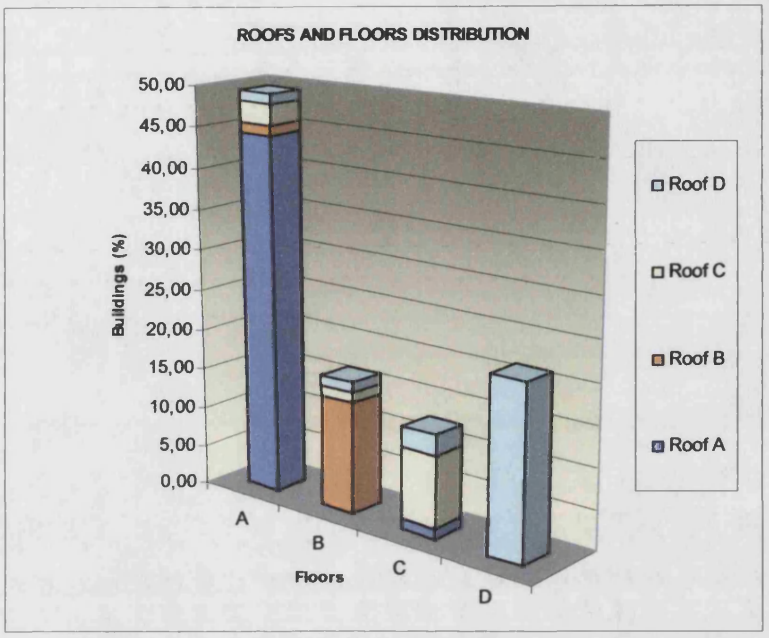

Figure 4- 15 – Distribution of roofs and horizontal structures in the building sample

The historic buildings of Nocera are also characterised by a wide use of strengthening devices, mostly implemented in the past.

Historically, the most common strengthening devices are metallic ties, strong quoins or masonry buttresses. In more recent times, the use of reinforced concrete ring beams, often associated with slabs, has partially replaced some of the traditional systems, so that, of these, only metallic ties are at present still used.

Figure 4- 16 shows the distribution of seismic strengthening devices, obtained from the first survey carried out following the 1997 earthquake by Spence et al., (1998a,b). Four types of seismic reinforcements are described: the first two refer to traditional systems, whereas the latter refers to seismic provisions suggested by the Italian code[1](Braga et al., 1997a).

[1] According to the Italian seismic code (D.M. 19/6/1984) improvement and upgrading refer to two different levels of strengthening devices. The first one concerns monumental listed structures (Churches, Palaces), as it aims to introduce a global improvement in the seismic behaviour in relation to preservation work. The second is to be applied to ordinary buildings which must reach an higher level of safety, by means of stronger and much more intrusive kind of strengthening provisions.

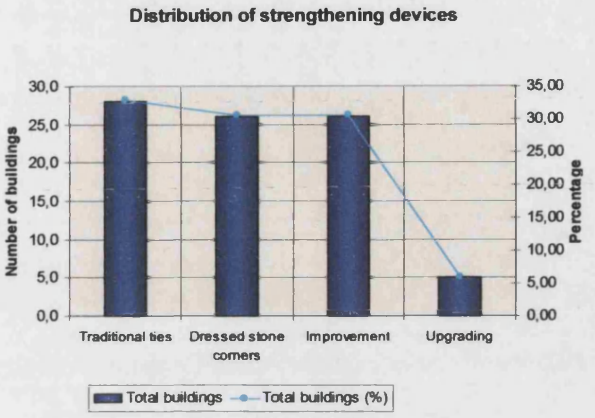

Figure 4- 16 – Distribution of strengthening devices in Nocera surveyed by Spence et al. (1998)

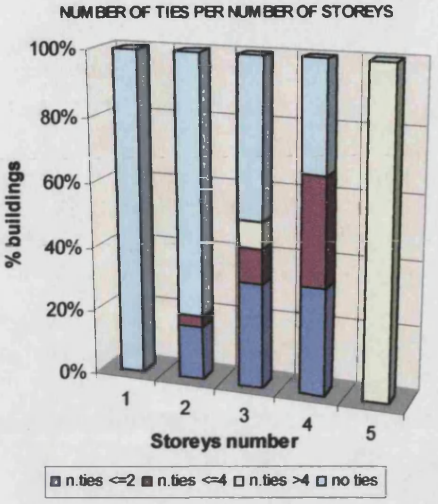

Figure 4- 17 – Distribution of number of ties per number of storeys of the building

Figure 4- 17 shows the results of the survey in terms of the occurrence of ties in relation to the number of storeys. One can observe how as the number of storeys increases from 1 to 5, the number of ties also increases, while at the same time the percentage of buildings without any ties tends to decrease to 0 for the maximum number of storeys (5).

Figure 4- 18 shows the combination between masonry types and strengthened buildings.

Three types of strengthening are considered: ties, ring beams, and a combination of the two. R.c. roofs are also considered because of their high incidence in the sample outlined by the chart of Figure 4- 15.

When first looking at the cumulative percentages, it can be observed that around 1/3 of the total buildings surveyed (35.4%) are not strengthened at all, while strengthened buildings (64.6%) are divided into: 29.1% with ties, 7.6% with ring beams, 1.3 % with both ties and ring beams, and 26.6% with concrete roofs. It is clear how metallic ties and concrete roof have the highest incidence in the sample, although the percentage of ring beams could be underestimated, because they could have passed unobserved in a street survey.

The histogram shows that buildings made up of masonry fabric of type B1, described in §4.3.2, are mostly strengthened by traditional ties (12.7% of total buildings), ring beams (6.3%), a combination of the two (ring beam and ties, 1.3%) and concrete roofs (8.9%).

As can be observed, all buildings constructed with better qualities of masonry fabrics, like A1 and D1 are characterised by concrete roofs, not associated with ring beams. Buildings

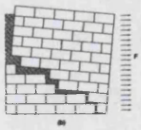

with masonry types like A2, C1 and D2 are mostly strengthened with traditional ties and concrete roofs. Brickwork buildings of type D1 prove not to be strengthened at all, though this result could be attributed to the small number of D1 fabrics observed in the sample.

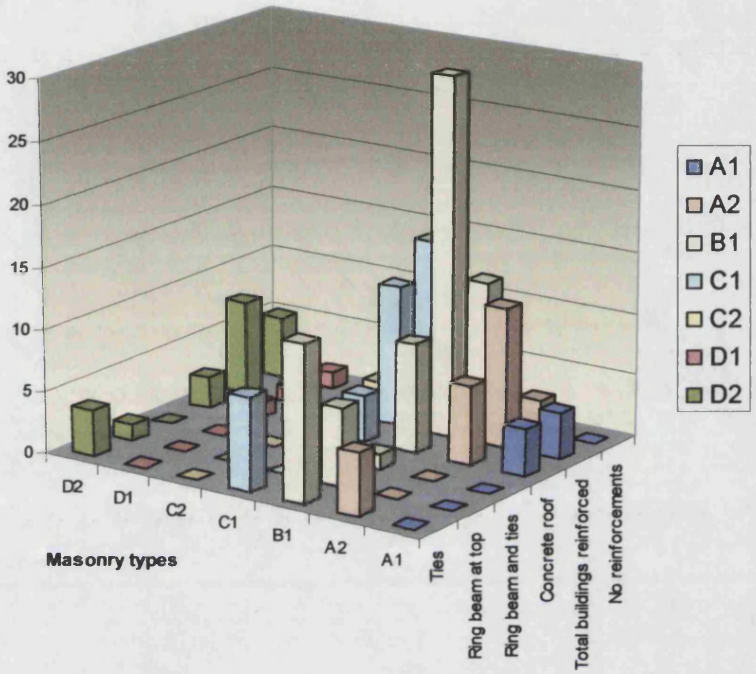

Figure 4- 18 – Distribution of strengthening devices and masonry fabrics in the building sample

4.4 Damage assessment in the historic centre of Nocera

4.4.1 Previous damage assessment

Following the earthquakes of September 1997, several investigations were carried out by emergency teams and research groups to assess the damage caused to masonry buildings (Baratta et al. 1997, Braga et al.1997b, EERI 1997, Mucciarelli et al.1997a,b, Sarà et al.1997, Spence et al. 1998a,b, 1999).

Most of the studies were aimed at assessing the damage in a qualitative way, by outlining the most frequent damage patterns surveyed, associated with the structural features of buildings, and sometimes by attempting identifying common vulnerability causes (Sarà et al., 1997, Baratta et al 1997).

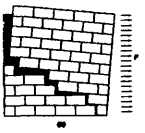

In other cases the damage was systematically assessed through damage levels, in order to correlate the severity of damage to the structural features of buildings and strengthening implemented (Spence et al. 1998a,b, 1999, D'Ayala 1999). In this case the damage level of each building was recorded using the 6-point scale of the EMS'92 (Grunthal, 1993), which refers to levels of physical damage and assigns a numeric value corresponding to the mean damage ratio to each level of damage. For masonry buildings the levels of damage are described as follows:

Damage level	*Mean damage ratio*	*Damage type*	*Description of physical extent*
D0	0.00	Undamaged	No visible
D1	0.05	Slight damage	Hairline cracks
D2	0.20	Moderate damage	Cracks 5-20 mm wide
D3	0.50	Heavy damage	Cracks>20 mm or heavy damage to structural walls
D4	0.90	Partial collapse	Collapse of individual wall or individual roof support
D5	1.00	Collapse	More than one wall collapsed or more than half of roof

Table 4- 2 – Definition of damage levels (after EMS '92) (Grunthal, 1993)

The damage distribution obtained in Nocera by D'Ayala and Spence, shown in Table 4-3 (Spence et al. 1998a,b, D'Ayala 1999), highlights an average level of 0.40, slightly lower than level D3 (0.5 being the numeric value associated with this level).

Town	*Intensity EMS**	*D0*	*D1*	*D2*	*D3*	*D4*	*D5*
Nocera Umbra	7-8	0.05	0.2	0.27	0.32	0.09	0.07

Table 4- 3- Damage distribution surveyed in Nocera (Spence et al., 1998)

*European Macroseismic Scale (Grunthal, 1993)

4.4.2 Damage assessment using the FaMIVE method

The damage was assessed in around 200 buildings, including those previously inspected by D'Ayala and Spence (Spence et al., 1998a,b, 1999, D'Ayala 1999) and was based on a pilot version of the form presented in Chapter 3. According to the data inspection process followed, the information referred to all the building walls (up to a maximum of 4), each wall being identified by its orientation (D'Ayala et al., 1999).

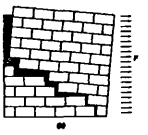

In order to maximise the quality of information, the survey method was later changed into the one introduced in §3.3, where the set of data required by the form refers to each wall of the building. In case of very extensive analysis the survey can be limited to the most vulnerable wall, which the surveyor is required to choose.

The pilot version of the form used for the damage inspection was also characterised by a wider range of failure mechanisms, including 25 failure modes, shown in Figure 4- 19. Figure 4- 20 shows the failure mechanisms analytically formulated in Chapter 2, considered by the FaMIVE method.

In order to allow correlations between predicted and observed damage, presented in Chapter 5, the failure mechanisms used for the damage inspection have been reassigned to those of Figure 4- 20. Besides the failure modes of the FaMIVE method, two more classes of failure mechanisms are defined (J and K), in order to include damage types at present not considered.

Class J include all those failure modes producing the collapse of extensions to the original structures, attics and chimneys, as well as wall portions not connected to the original masonry, such as chimney flues. Class K include in plane mechanisms due either to hammering effects between adjacent buildings or rigid slabs or roofs.

The results of reassignment, are the following:

Pilot survey form failure mechanisms		*FaMIVE failure mechanisms*
A_1	⇒	A
C_5	⇒	B_1
C_1	⇒	B_2
C_2	⇒	C
A_2	⇒	D
B_1, B_2	⇒	E
A_4, B_4, C_4	⇒	F
A_3, B_3, C_3, E_3	⇒	G/Gs
F_2	⇒	H
D_1	⇒	I
E_4	⇒	L

And the additional failure modes are:

E_1, E_2, D_2, D_3, D_4	⇒	J
F_1, F_3	⇒	K

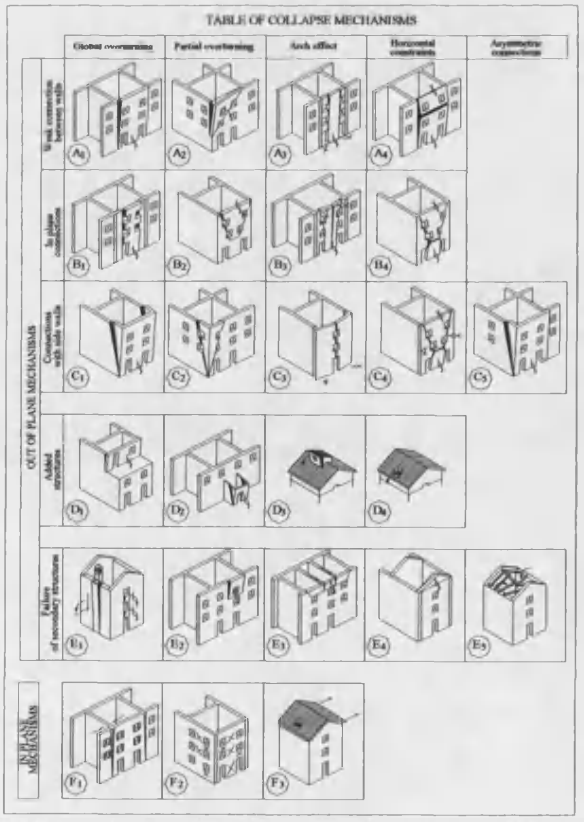

Figure 4- 19 – Pilot version of the form used for the failure mechanisms identification (D'Ayala, Speranza, 1999)

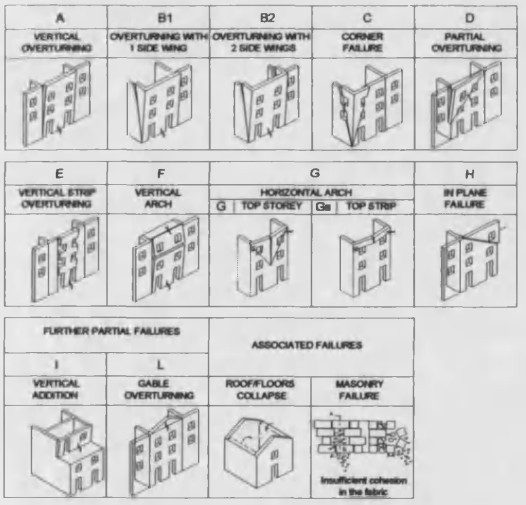

Figure 4- 20 – Table of failure mechanisms considered by FaMIVE

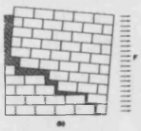

The distribution of observed failure mechanisms is shown in Figure 4-21. The percentages shown also include failure mechanisms developed partially, involving only few storeys of the walls inspected.

As can be noted, two mechanisms are prevalent, the corner failure C (17%) and the shear collapse H (17.78%). The collapse of wall portions or additional elements J also shows a high percentage of occurrence (16.30%). Rather high percentages are also reached by mechanisms A,B1,B2, with 11.11%,9.63%,5.93% respectively. Partial collapses such as D, E and G are present in small percentages which do not exceed 4%. It is also possible to note the presence of damage due to hammering structures (K, 6.67%), and the very small occurrence of collapse types F, I and L.

The cumulative results (Figure 4- 22) show that out-of-plane failure modes A, B1, B2, F, reach 28%, while higher percentages are obtained for partial collapses C, D, E, G (30%). However, this percentage is mainly attributed to the massive presence of corner failures observed. Finally, in plane failure mechanisms like H, K and collapses of additional elements (I,L) reach 24% and 18% respectively. This last percentage is coherent with reality, because it testifies the high level of alteration to the original structures.

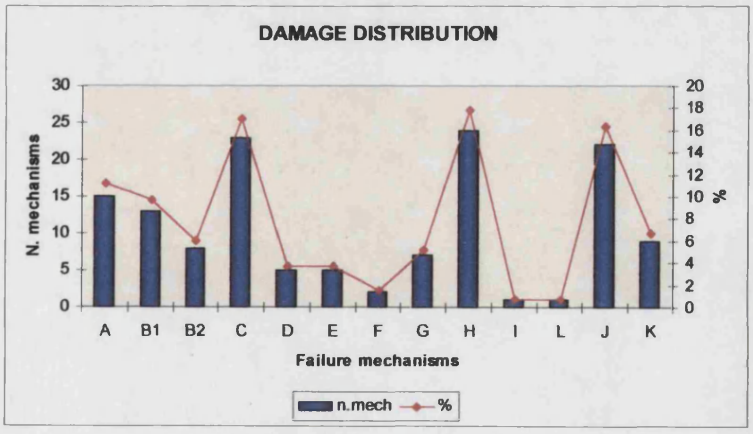

Figure 4- 21 – Failure mechanisms surveyed

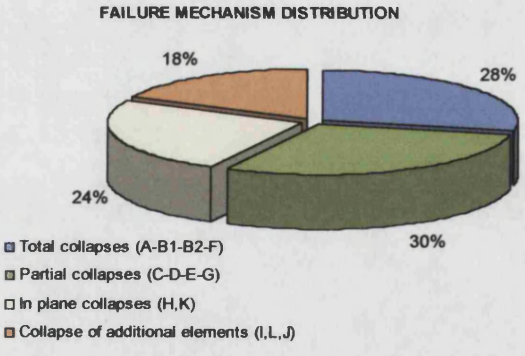

Figure 4- 22 – Failure mechanism distribution (cumulative results)

The cumulative results of Figure 4- 22 correlate fairly with those obtained by Sarà et al. (1997) on 78 buildings of 3 different towns hit by the same earthquakes (Nocera Umbra,

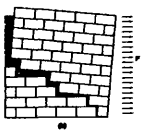

Foligno, Serravalle di Chienti). Although the damage investigated by these authors was mainly described through typical damage patterns, some very general classes of failure mechanisms are considered and on the basis of these some considerations can be expressed.

According to these authors, the damage due to out of plane performance of the wall amounts to 32.5% of buildings inspected, whereas the damage due to in-plane behaviour is attributed to 21%. The former value is associated with failure modes entirely affecting the walls, while partial failures, amounting to 33%, are described as "collapses of roof and of supporting structures". Besides the collapse of roof and floors, this failure mode would also seem to include collapses involving upper storeys of the walls, which can be associated with D, E G, Gs of the FaMIVE range. Finally, 13.5% of damage is classified by the same authors as "local damage due to singularities of different origin", and refers to the damage involving non structural elements, like chimney flues, balconies and so on. Although the vulnerable elements considered in this case are slightly different from those taken into examination by FaMIVE (vertical additions, gable ends), it is remarkable that the cumulative percentages associated with non structural features are rather close to each other (13.5% against 18% respectively).

The chart of Figure 4- 23 compares the damage levels with the failure mechanisms recognised in the same building in order to highlight the recognition feasibility of each failure mode. It can be observed that all identifications took place beyond the threshold represented by level D3, as slight damage (D1-D2) precluded clear recognition. The histogram also illustrates that among the three levels D3-D4-D5, most failure mechanisms were identified in the presence of modest damage (D3), which is associated with fully readable crack patterns. The presence of partial or full collapses which characterise damage levels D4-D5 in most cases made it difficult to interpret the failure mechanism which occurred. For this same reason the highest percentage of unidentified failure mechanisms is associated with damage level D4.

The chart also shows that buildings characterised by medium damage D3 (63.8% of the total sample), were mainly subjected to total and partial out-of-plane collapses (19.1% and 25.5% respectively), while a smaller portion was associated with in plane mechanisms (6.4%) and collapse of additional elements (4.3%). Finally, for the remaining percentage (8.5%) no mechanism was associated. Buildings with damage level D4 (31.9% of the total sample), were associated with total and partial out-of-plane collapses amounting to 19.2%, while half the

buildings which suffered damage D5 (4.3%) could be unequivocally associated with out-of-plane failure mechanisms.

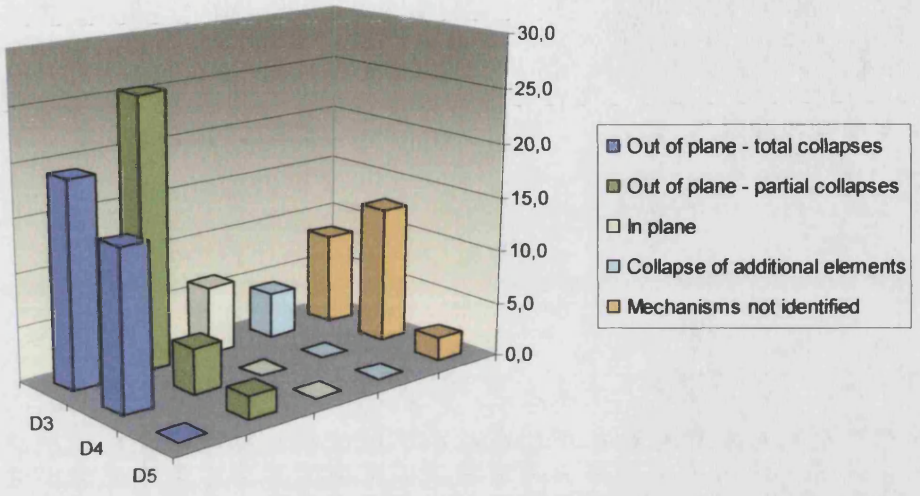

Figure 4- 23 – Damage levels and failure mechanisms

The results of the damage survey become more interesting when comparing the damage with the strengthening devices implemented (Figure 4-24), having considered, for each building, the mechanism which has developed the highest damage level. The chart shows that building unstrengthened (35.4% of total) were subject to consistently high damage (≥D3).

When looking at strengthened buildings and associated damage levels, the data would seem controversial, since the highest percentage for each type of reinforcement correspond to the highest damage too. The reason for this result is that the presence of strengthening devices does not exclude the possibility of partial collapses, confirming the assumption made in §3.4.3 according to which any type of strengthening device, however placed at whatever storey, can only prevent that storey and the ones below from being involved in the mechanism. A clarification of this result could be obtained only by analysing the strengthening device pattern of each building, at least in terms of the number of storeys restrained compared with the total façade. However this comparison is not possible since the available data were recorded in terms of total number of restraints, without specifying their pattern and the associated number of storeys restrained.

The correlation between failure modes and strengthening devices, shown in Figure 4- 25, shows that for buildings subjected to total and partial out-of-plane mechanisms (amounting to 66% of the total sample), half have no strengthening device (14.89%+10.64% for total and partial collapses respectively), while the remainder are mainly characterised by metallic ties and concrete roofs in the same percentage. The interpretation of these data is basically the same as for the previous data set (damage levels/strengthening devices), that is, the presence of a given strengthening device pattern on a wall does not exclude the possibility of partial failure mechanisms developing, involving the unrestrained storeys. The ambiguities of these results, due to the incompleteness of the original set, particularly stress the importance of describing the strengthening device pattern on the wall under examination, storey by storey, according to the criterion proposed in §3.3.

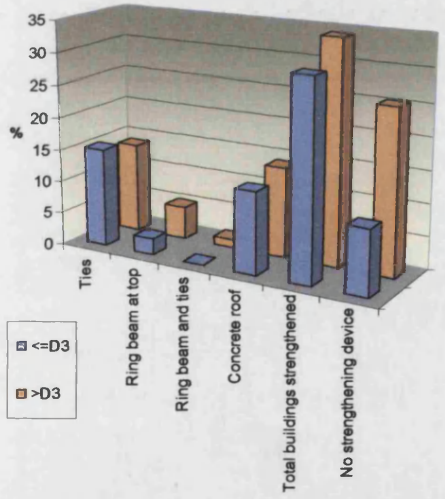

Figure 4- 24 – Damage levels and strengthening devices

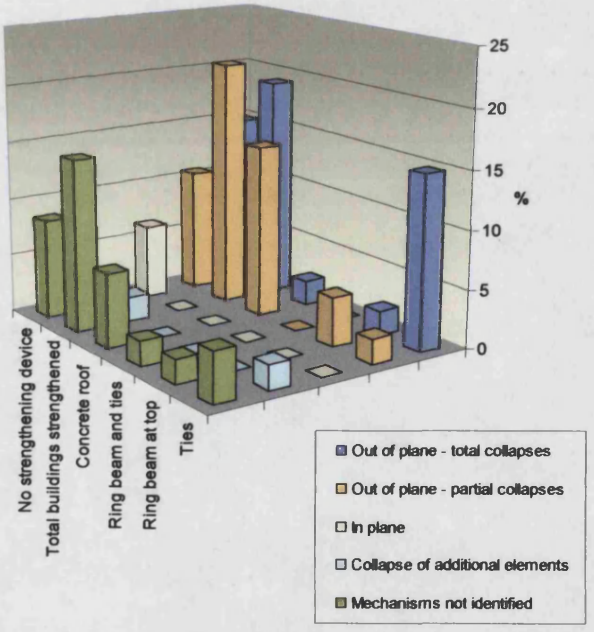

Figure 4- 25 – Failure mechanisms and strengthening devices

The relation between the damage level and masonry types is highlighted in Figure 4- 26. Despite the small size of the building samples, some interesting conclusions can be drawn, particularly for the most common masonry types surveyed in Nocera (such as A2, B1, C1, D2). Buildings with the best quality of masonry were subject to damage levels slightly lower than those with poor fabric layouts: type A2, which can be considered as the best prototype of

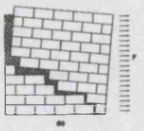

those considered, shows damage peak for level D2, unlike types B1, C1, D2, whose peak is closer to or even exceeds level D3.

The results also outline a notable increase in the damage level when passing from the first prototype (like A1, C1, D1) of each macro-class to the poorer type such as A2, C2, D2. This can be considered as a confirmation of the order in which the fabric layouts surveyed have been ranked in §3.3.3.

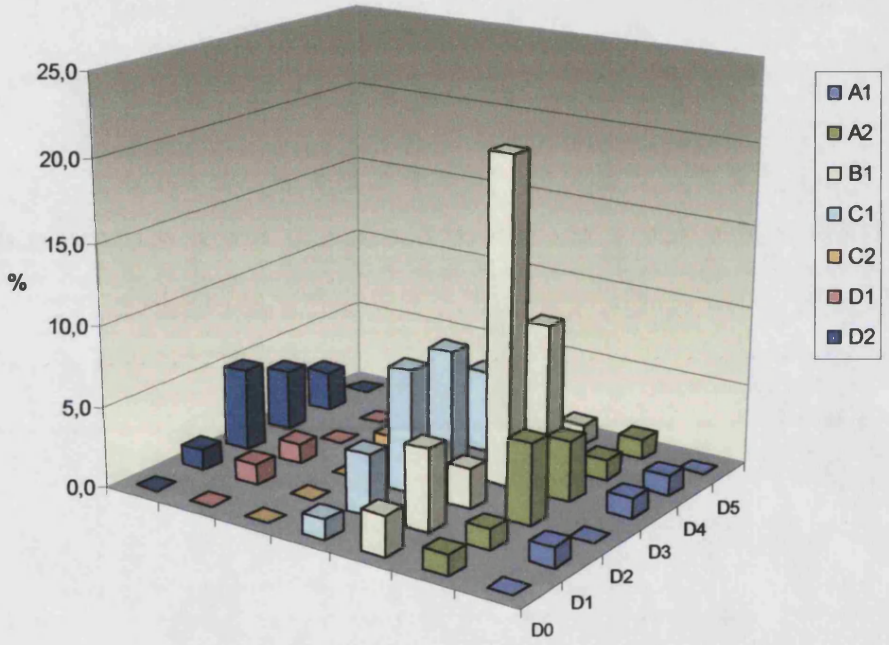

Figure 4- 26 – Damage levels and masonry types

This issue is particularly relevant in the charts of Figure 4- 27, which can be used to check the reliability of the criterion according to which the masonry types have been paired and then ranked. Notably, the second A and D classes show a general increase in the damage, passing from type 1 to type 2. This is also true for class C, as can be observed by comparing the average damage levels (0.4 and 0.5). However, while type C1 shows presence of all damage levels, type C2 is entirely characterised by a single damage level D3.

Finally, by comparing the stonework fabrics, i.e. A, B and C, a progressive worsening of the structural behaviour can be observed in terms of the average damage level registered.

When examining the results obtained in Figure 4- 26 and Figure 4- 27 it should be underlined that, although the mechanical quality of masonry plays a central role in the

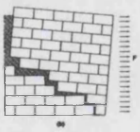

definition of the structural performance and of the associated damage level of buildings, the results obtained have also been influenced by the intrinsic structural peculiarities of each building. A more effective comparison of the mechanical performance of different masonry fabrics should be carried out by keeping the other structural features of the buildings constant.

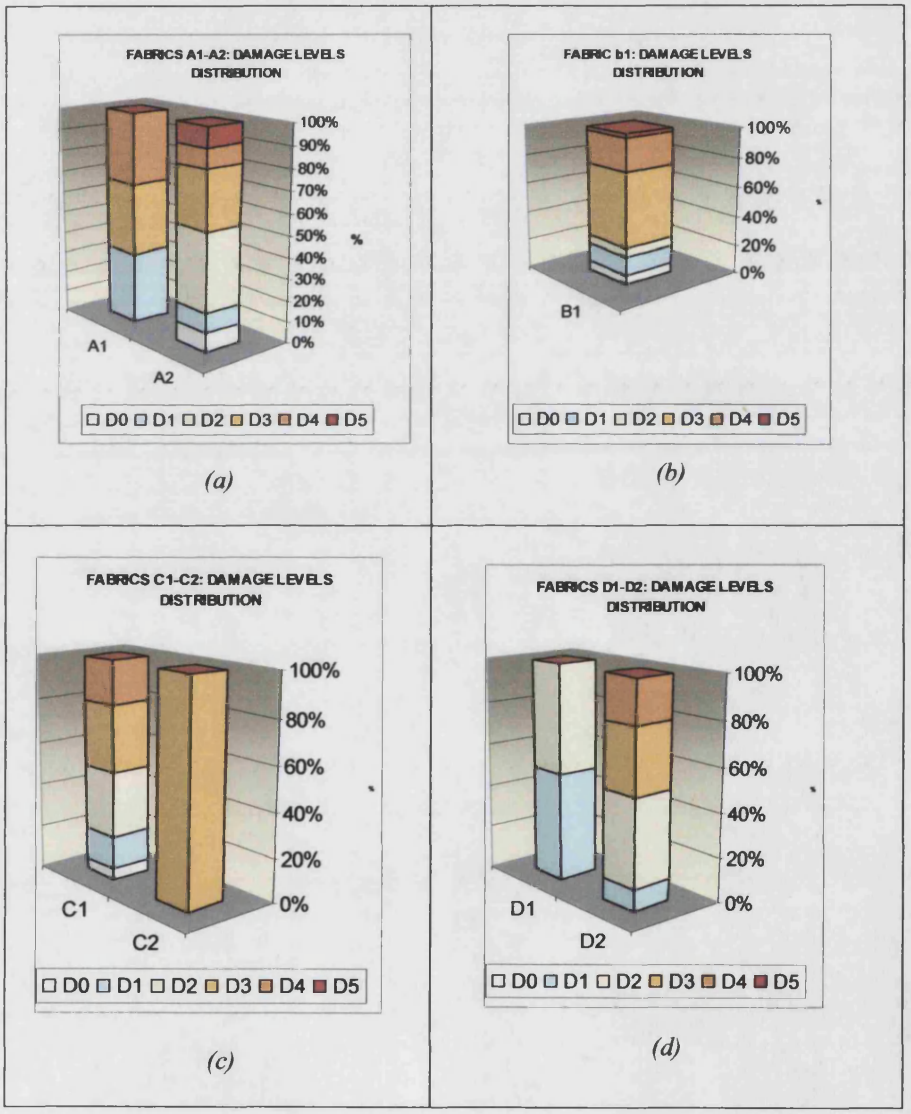

Figure 4- 27 – Damage level distribution for each type of masonry fabric

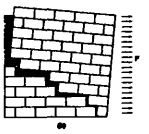

4.5 Critical discussion on the survey method

The results achieved in the previous sections enable some considerations to be drawn.

On the one hand, the incompleteness of some data items with respect to those required by the survey form of §3.3 highlights the ineffectiveness of information relating cumulatively to the whole façade rather than to individual storeys. This lack of completeness does not allow a full understanding of how the failure mechanisms surveyed occurred, since some failure modes could have a partial onset, involving only those storeys where no strengthening devices have been implemented. This leads to the conclusion that information can be better processed when recorded per storey as proposed in §3.3.

A more crucial issue characterising the survey procedure is that it operates through a range of failure mechanisms which the surveyor, when operating in a post earthquake situation, is required to recognize. The charts of Figure 4- 21 and Figure 4- 22, displaying the failure mechanism distribution obtained for Nocera Umbra, highlights a net prevalence of certain failure types, such as A, B1, B2, and a rather small percentage for mechanisms like F,D,G,I,L.

The reasons for this result can be attributed, on the one hand, to the local characteristics of buildings, so that in every historic centre some mechanisms are more frequent than others (A.Giuffrè, 1993). On the other hand, failure mechanisms undoubtedly exhibit different levels of recognition feasibility. For example, failure F can be recognised only if horizontal deformation along the wall is observed together with the presence of one horizontal and two vertical cracks at its extremities. In the event that the wall under observation is too high to allow an accurate inspection of the upper part, this particular mechanism can go unobserved, especially if the damage is also quite low.

The issue of the different level of recognition feasibility can also affect some structural characteristics or reinforcement types required by the survey form. A typical example is represented by ring beams, not always visible from the outside, especially when the wall under examination is particularly high. Sometimes concrete ring beams are placed in the internal face of the external wall. In this case only an accurate inspection could reveal their presence.

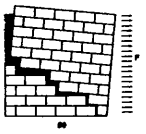

Moreover, when surveying the strengthening devices, their real effectiveness can never be assured. Metallic ties and ring beams may have lost their structural effectiveness for several reasons, or they may have been implemented incorrectly, thus compromising their effectiveness. A typical example is a concrete ring beam on top of the building, not connected to the walls where it is placed. In this case, its presence often causes a general worsening of the seismic performance of the building.

All these aspects can easily lead to under- or overestimating the structural performance of the building in question, and can also help to clarify some controversial results emerging from the survey, such as the ones of Figure 4- 24, comparing the strengthening devices implemented with the damage levels surveyed.

4.6 Conclusions

This Chapter was dedicated to the discussion of the results achieved by the inspection of the historic centre of Nocera Umbra, hit by an earthquake in 1997 and the applicability of the survey method introduced in Chapter 3.

Though some missing data do not allow further correlations, the results obtained are able to provide a satisfactory report of the main structural features of the sample under examination, by describing its general features, strengthening types, masonry fabrics and damage caused (damage levels and failure mechanisms identified).

To sum up, the following conclusion can be drawn:

- The buildings of the sample, having between 2 and 5 storeys, show a high level of alteration compared to the original structural types;
- Masonry fabrics, when original, are generally characterised by medium quality (type B1); reinforcements are widely used, the most common being metallic ties. The use of concrete roofs, to substitute the original timber structures, is very frequent and not always associated with the presence of ring beams;
- The average damage level is D3, and this level also represents the threshold beyond which also failure mechanism were identified during the survey;
- In the range of Figure 4- 20, the most common collapses are corner failures, in plane shear, and the collapse of additional elements (C , H, J respectively). When

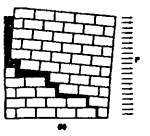

looking at the cumulative results, out-of-plane partial collapses (C, D, E, G) prove to be the more frequent than out-of-plane total collapses (A, B1, B2, F), in-plane failures (H, K), or additional wall portions (J).

Finally, in §4.5 a discussion on the applicability of the form has highlighted the importance of collecting the survey information for each individual storey of the building, as proposed in §3.3.3, while cumulative data relating to the whole façade make the results difficult to compare. Some considerations are finally drawn on the different level of recognition feasibility of the failure mechanisms.

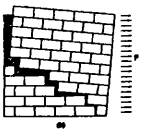

CHAPTER 5

SEISMIC VULNERABILITY ASSESSMENT: APPLICATION TO THE HISTORIC CENTRE OF NOCERA UMBRA

5.1 Introduction

This Chapter discusses the results obtained by an application of the FaMIVE vulnerability assessment method to the historic centre of Nocera Umbra.

The results, presented in terms of seismic vulnerability and failure mechanism identification, are also discussed first in relation to the structural features surveyed, (as described in Chapter 4), and then compared with the damage observed.

While the comparison between predicted and actual failure mechanisms can be easily made, the correlation with damage levels is more controversial.

Although a considerable amount of literature is available concerning the definition of damage classes and their relation to earthquake intensities, little work has been carried out trying to correlate damage levels, earthquake intensities and structural behaviour defined by failure mechanisms (see Chapter 1).

As introduced in §3.7, the vulnerability assessment provided by the method represents an intrinsic feature of the building, which is independent of the earthquake intensity and hence cannot provide a measure of the most likely damage level to which the building would be subjected as the result of an earthquake of given severity.

An attempt to devise a method of correlation between damage levels experienced by each building and predicted vulnerability is proposed and critically discussed in §5.3.1.

The correlation between actual and predicted failure mechanisms is discussed in §5.3.2 and in §5.4 some conclusions are drawn about the correlation results and the overall reliability of the method proposed.

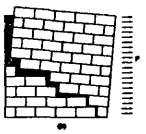

5.2 Critical load factors, failure mechanisms and seismic vulnerability in the sample surveyed

5.2.1 Critical load factor and failure mechanism distribution

Buildings and relative facades analysed with the FaMIVE method are those highlighted in red in Figure 4-3, showing a map of the historic centre of Nocera. Figure 5- 1 outlines the distribution of the critical load factors (μ) obtained for each building over the sample analysed. In order to make the map more readable, 4 μ ranges have been defined, with the upper range $\mu \geq 0.4$, corresponding to very good seismic performances.

An histogram of the results obtained is presented in Figure 5- 2. As can be observed, the histogram does not provide a typical normal distribution, which is usually assumed when statistical models such as PSI or DPMs are developed (Spence et al.1991, Whitman et al. 1973). This could be attributed to the small sample of buildings considered in the analysis (around 100), but more probably to the different approach pursued. The normal distribution assumed by the methods mentioned above relates to *observed damage*, and is calibrated on a large amount of data gathered from different earthquakes. As outlined in §1.4.2, atypical distributions or incomplete data are corrected or filled by statistical processes, such as binomial functions (Braga et al., 1982b). Unlike these approaches, the FaMIVE method is based on the *prediction* of the structural performance of the building under seismic action, which is independent of the observed damage and depends on several factors, mainly of a structural nature. This leads to the conclusion that the histogram of Figure 5- 2 should be seen as the result of the combination of the numerous parameters involved in the analysis interacting with each other, which does not necessarily imply that the critical load factor μ follows a normal pattern, as the "types" of failure will be different.

The histogram in Figure 5- 2 shows that almost 50% of the buildings in the sample have a critical load factor $\mu \leq 0.2$, and 66% ≤ 0.3. Consequently, 34% of buildings are characterised by a rather high $\mu > 0.3$.

To sum up, the critical load factor distribution, with an average value of 0.36, shows that only earthquakes of medium intensity are able to produce significant damage on the building sample under examination.

Figure 5- 1 – Distribution of critical load factors μ over the building stock

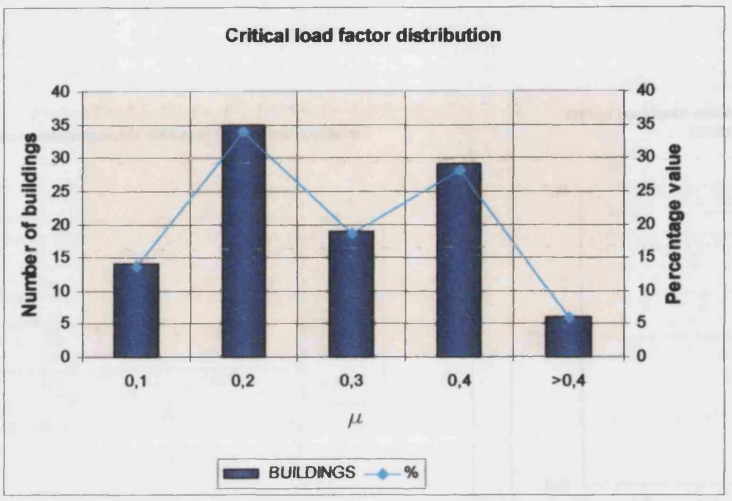

Figure 5- 2 – Critical load factor(μ) distribution in the sample surveyed

Figure 5- 3 and Figure 5- 4 show the distribution of the critical load factor and associated failure mechanism of each building. The charts are plotted against two slenderness ratios which qualify the mechanical performance of two groups of failure mechanisms: out-of-plane mechanisms such as A,B1-B2,C,D,E,F are mostly influenced by the ratio H/t (Figure 5- 3), whereas the H/L ratio exerts most influence on failure modes such as horizontal arch (G/Gs) and in-plane failure (H) (Figure 5- 4).

The critical load factors obtained can be observed to range between 0.04 to 0.45, while the ranges become smaller when associated with each failure mechanism. The chart also enables the failure mechanisms to be ranked according to upper and lower boundaries defined by relative minimum and maximum μ values. It is possible to observe how buildings with in-plane failure H are characterised by rather high load factors, which correspond mainly to the friction coefficients assigned to the relative masonry fabrics, as outlined in §4.3.2.

Figure 5- 5 shows in how many cases each failure mechanism considered is critical, i.e. the one with the minimum load factor (μ). One can observe that the most frequent failure mode is in-plane H (26.5%), followed by B1-B2 associated with 17.6% of buildings, D and E (16.6% each), and A (6.8%). Failure mechanisms such as C and F have both been associated with almost 2% of the total buildings, corresponding to just 2 buildings for each failure mode.

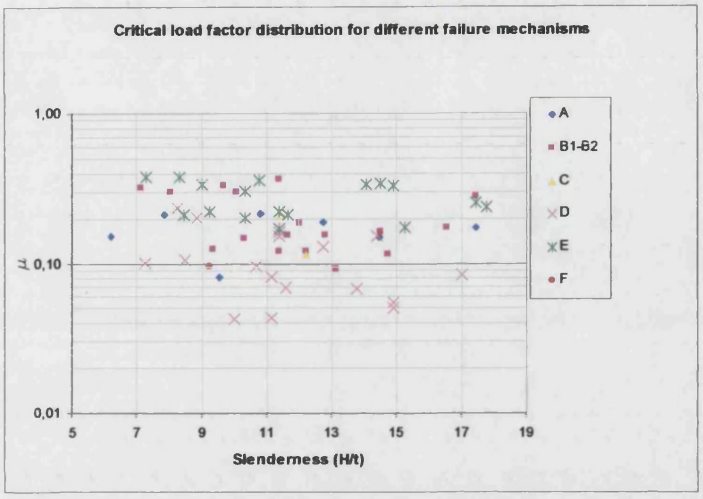

Figure 5- 3 – Critical load factor (μ) distribution for different failure mechanisms plotted against the slenderness H/t

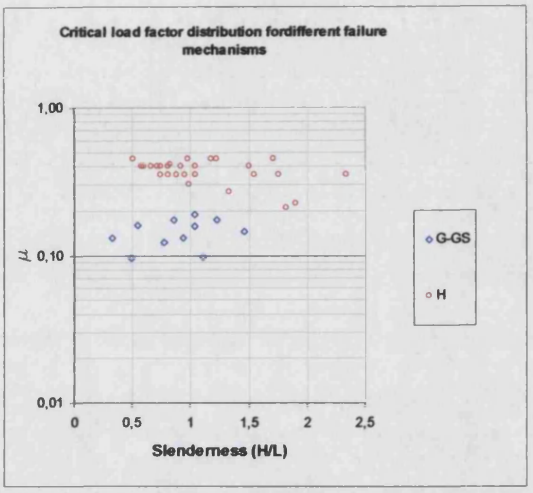

Figure 5- 4 – Critical load factor (μ) distribution for failure mechanisms G-GS and H, plotted against the slenderness H/L.

Figure 5- 6, shows a histogram displaying the average μ values for each failure mechanism, ranked upwards. The histogram indicates a certain correspondence between low μ values and partial failure modes (such as D,G,C), with μ ranging from 0.11 (D) to 0.16 (C). Failure mechanisms involving the whole façade/storeys such as A,B1-B2,E,H correspond to progressively higher μ values, ranging from 0.17 (A) to 0.37 (H).

However, the average values for failure mechanisms such as C and F cannot be considered fully reliable, due to the very small sample of buildings associated. In particular, the average value of 0.13 found for F depends on the peculiarities of the two buildings considered, both characterised by a total lack of lateral connections.

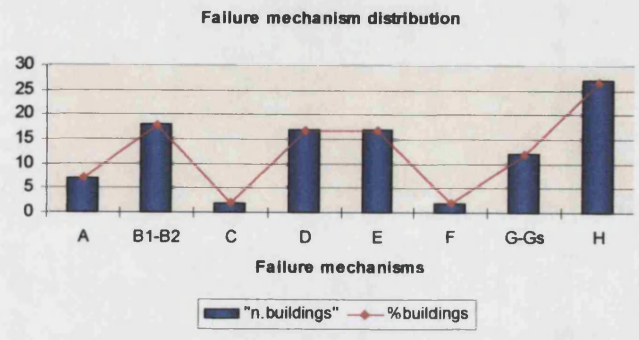

Figure 5- 5 – Failure mechanism distribution

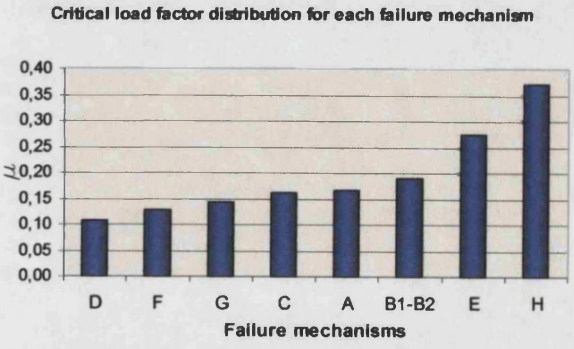

Figure 5- 6 – Average μ distribution for each failure mechanism

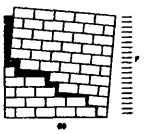

Diagrams of Figure 5- 7, Figure 5- 8, Figure 5- 10 highlight the role exerted by certain structural features in the seismic performance of the building stock surveyed.

The diagrams show the μ distribution, as a function of the slenderness ratios of the facades, respectively in relation to maintenance level, masonry fabrics and presence of connections between facade and orthogonal walls. This also enables the effectiveness of the relative variables processed by the method associated with these structural features to be tested.

Figure 5- 7 shows a fair correspondence between low levels of maintenance and low level of the seismic performance, i.e. low μ values, and vice versa as one would expect. Good maintenance levels associated with low μ values, are obtained in just a few buildings, and this apparently controversial result clearly depends on the further structural parameters involved in the analysis, which also exert a direct influence on the seismic performance of buildings.

Similarly, Figure 5- 8 shows the relation between critical load factors μ and the masonry fabric, highlighting the importance exerted by each masonry type in the definition of the ultimate load factor of the building. In the diagram of Figure 5- 9, the masonry types, introduced in §4.3, are ranked in relation to the relative average μ obtained.

The ranking can be seen to agree with the classification made in §4.3.2 defining the mechanical quality of each masonry layout, and thus represents a validation of the process followed in the mechanical definition of structural types. Masonry types A1/2 and D1 (ashlars and brickwork respectively) are the ones associated with the best structural performance (see Table 4-1), followed by types D2, B1, C1, C2, for which decreasing effective sliding surfaces (field M-3 of Table 4-1) as well as friction coefficients are assumed. The ranking shown in Figure 5- 9 is also validated by the survey results discussed in §4.4.2 and highlighted in Figure 4-26. Figure 5- 9 shows that buildings featuring good masonry types such as A1/2, D/1 are characterised by average μ values ranging from 0.41 (A1) to 0.27 (D1). Poorer fabric layouts (D2, B1, C1/2) show decreasing ultimate load factors down to a minimum of 0.12 obtained for type C2. However, average μ values obtained for types D1 and C2 are obtained on few buildings (2 and 3 respectively) so that the average value obtained has little meaning.

Considering Figure 5- 10, it can be observed that buildings with both connections are associated with rather high μ values, with average of 0.23. Buildings with 1 or no connection

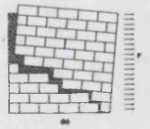

clearly show reduced structural performances, although higher μ values are obtained for buildings with no connection at all. This result, which could be considered controversial, can be attributed to the massive presence (in buildings with no connection) of strenghening devices which led to an improvement of the original structural performance and hence to higher load factors.

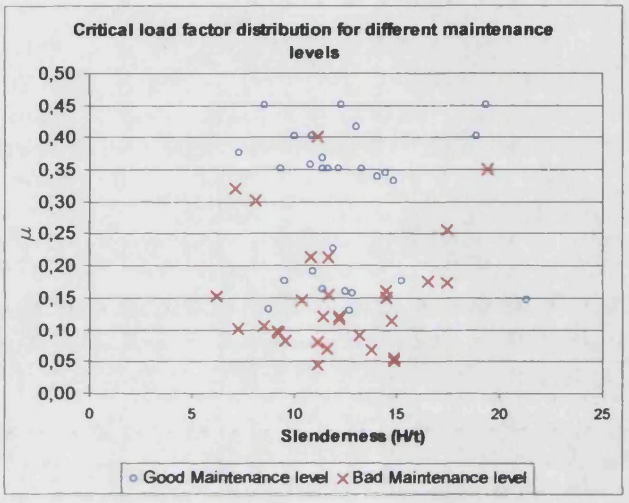

Figure 5- 7 – Critical load factor(μ) distribution for different maintenance levels

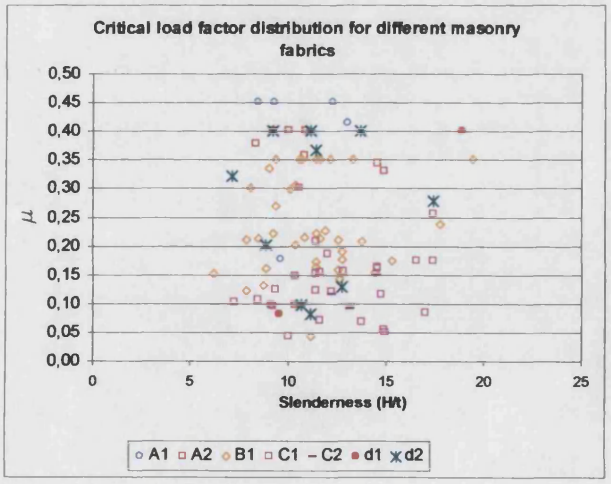

Figure 5- 8 – Critical load factor(μ) distribution for different masonry fabrics

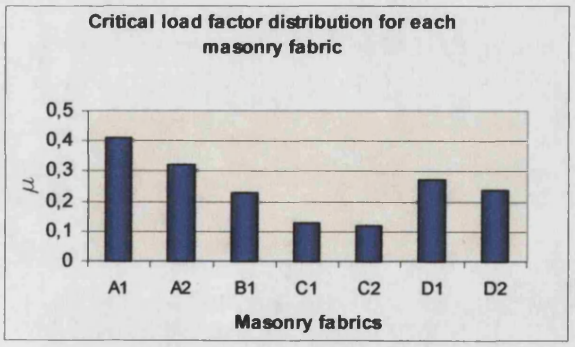

Figure 5- 9 – Average μ distribution for each masonry fabric

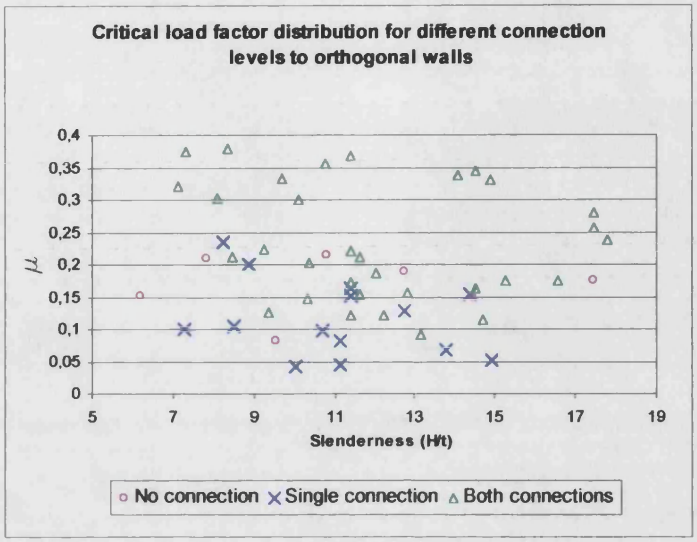

Figure 5- 10 – Critical load factor(μ) distribution for different levels of connection to orthogonal walls

5.2.2 Seismic vulnerability distribution

Figure 5- 11 (a) plots out the Failure Extent and Structural indices (I_f and I_s, §3.5.1) of the whole sample relative to lower boundaries, central values and upper boundaries respectively, obtained according to the criterion introduced in §3.6, relying on input data reliability. It is evident an increase in the values of indices when passing from lower to upper boundaries data set, which corresponds to an increase in vulnerability levels.

Figure 5- 11 (b) compares the distribution of the vulnerability classes percentages relative to the three data sets. As it can be noted, lower and upper boundaries percentages show a notable decrease/increase in vulnerability classes compared to the central values, particularly for Low and Very High Vulnerability classes which pass from 38% and 1.9% to 26% and 17.4% respectively. Medium classes are present averagely in the same percentage in the three distributions, while High vulnerability shows a light decrease when passing from lower bound to upper boundaries distribution, and this is mainly due to the fact that some buildings pass from High to Very High class. The notable difference between lower and upper boundaries depends on the Low level of reliability associated to all the input data of the sample, except from few buildings surveyed in detail to which a High vulnerability was assigned. The difference between the two boundaries would have been lighter in case of more

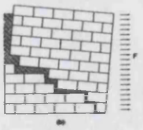

accurate surveys and hence quality of information. The central distribution, which is considered as main reference for further considerations and correlations, show 30% of buildings in the sample with Low Vulnerability, and 38.8%, 26.2% and 5% respectively in progressively higher classes.

Figure 5- 12 shows the distribution over the building stock of the central vulnerability classes obtained with the FaMIVE method. Despite the marginal role exerted by the urban position of the building in the vulnerability assessment process, a light increase of vulnerability levels in buildings placed at block edges than in those in intermediate positions can be observed.

Figure 5- 13 plots out the central Failure Extent and Structural indices of the whole sample against the relative vulnerability classes obtained following the criterion introduced at §3.7. The diagram emphasises the novelty of the procedure proposed for evaluating the vulnerability.

Unlike other procedures based on mechanical approaches (see Chapter 1), the vulnerability class is processed as the combination between the two parameters, which leads to identifying different ranges for the vulnerability classes outlined in Table 3-6. Exceeding a given threshold of I_f or I_s does not necessarily imply the passage from one class to another, but requires the index value to be combined with the ranges corresponding to the complementary index.

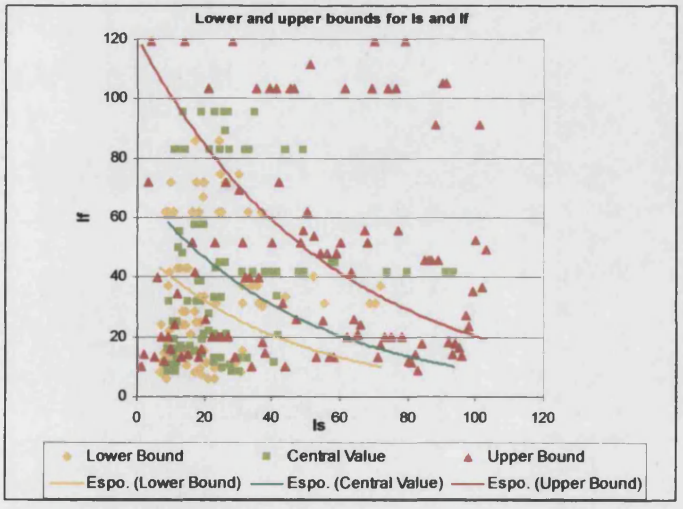

(a)

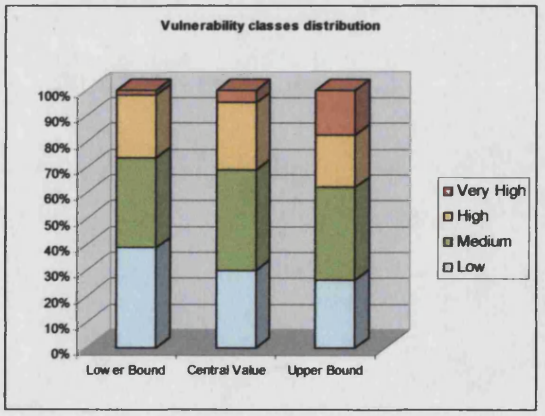

(b)

Figure 5- 11 –Lower, upper and central bounds results of: (a) - I_s and I_f distribution -(b) - vulnerability classes percentages;

Figure 5- 12 – Distribution of the seismic vulnerability classes over the building sample

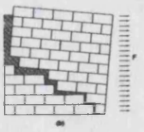

The diagram of Figure 5- 13 shows that buildings characterised by similar μ, i.e. the same Structural index, but different Failure extent indices are associated with different vulnerability classes. The diagram also enables the identification of the field of existence of each vulnerability class as a function of the two indices, although the building sample is too small to allow exploration of some empty areas of the diagram.

Holes in diagram, for I_s >45 and I_f <40, or I_s >20 and 80< I_f <50, could be filled by widening the building sample or by including data from different historic centres.

However, it should be considered that empty areas in the diagram could also be due to the fact that the two indices are not completely independent; they could also depend on the importance factor associated with failure mechanisms in Table 3-4. Such considerations could lead to the conclusion that buildings with high Structural index and low Failure extent index are unlikely to occur.

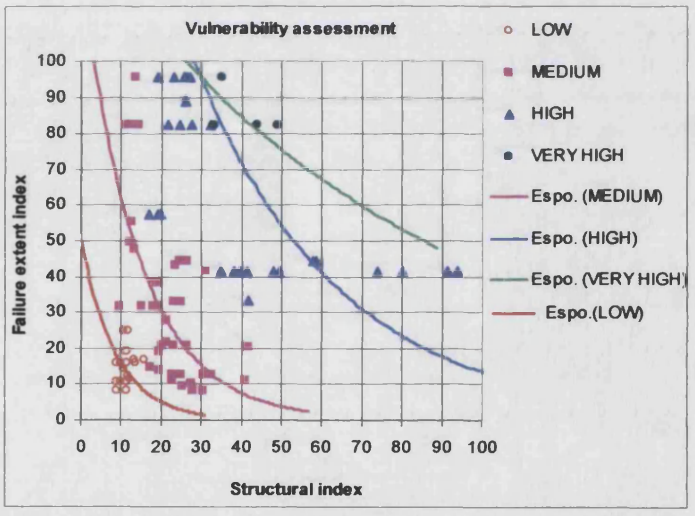

Figure 5- 13 – Vulnerability classes plotted against Failure Extent and Structural indices (normalised on 100)

Figure 5- 14 correlates the vulnerability class distribution with the strengthening devices of all the building stock. It can be noted that the presence of strengthening devices leads to a considerable decrease in the vulnerability if compared with the percentages obtained in their total absence. The cumulative histograms outline that, in the first case, 45.8% of buildings show Low vulnerability while 41.4% and 12.8% respectively show Medium and High. In the total absence of strenghening devices, the percentages become: 30.2% Medium, 54.6% High, 15.2% Very High, showing a notable increase in seismic vulnerability.

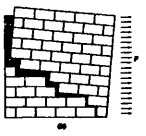

Analysing the effects produced by each strengthening type clearly outlines the effective role exerted by ring beams at the top and ring beams with ties, whereas the results for ties and concrete roofs are not so evident. In the first case, characterised by 27%, 56.8%, 16.1% for Low, Medium and High classes respectively, the apparently controversial results, are due to the fact that the histogram is related to cumulative percentages of buildings in which only some storeys could be anchored, leaving the remainder free, and hence vulnerable. As a matter of fact buildings restrained by ties at low storeys could be subjected to partial collapses at upper storeys, and hence their seismic vulnerability is not necessarily low.

The percentages shown in Figure 5- 14 for concrete roofs, similar to the survey percentages shown in §4.4.2, include buildings that could also be restrained by ties and ring beams.

The results show that 59% of buildings are associated with a Low vulnerability class, followed by 27.4% and 13.6% assigned to Medium and High classes respectively. This result correlates fairly well with the damage level distribution associated with buildings having similar features (Figure 4-24), according to which around one half of the buildings were subject to low damage (≤D3) and the remainder to damage >D3.

However, it should be considered that these results are conditioned by the possible presence of strengthening devices associated with the presence of concrete roofs.

When looking at buildings with concrete roof only, (although there are very few in the sample considered), the average vulnerability clearly increases: 75% of buildings are associated with Medium vulnerability and the remaining percentage with High.

One aspect to underline is that the results obtained are strongly conditioned by the assumption that the strengthening devices surveyed in the wall under examination are always effective, i.e. the ring beams are always anchored to masonry walls and ties never fail under tension nor the masonry around them in compression. However, it is reasonable to suppose that a certain percentage of strengthening devices could have lost their effectiveness and hence could not prevent some failure mechanisms occurring. This leads to possible limitation of the method, which may produce final vulnerability levels slightly lower than the actual values.

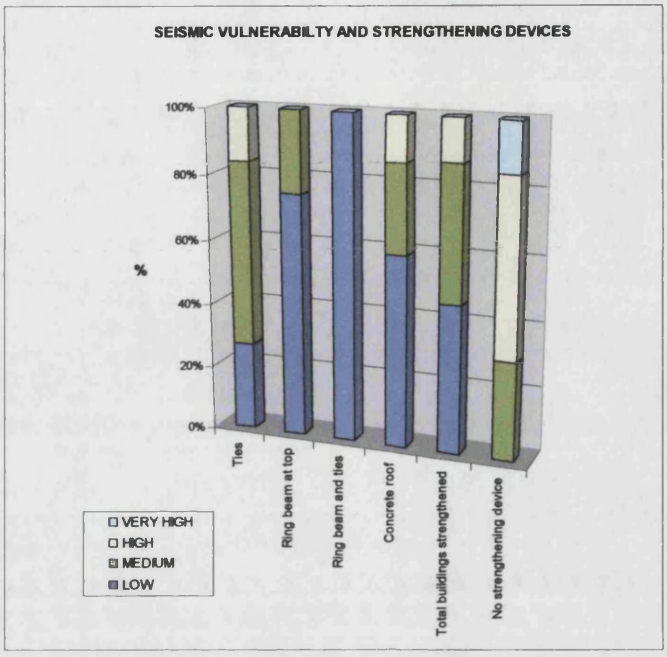

Figure 5- 14 – Vulnerability classes and strengthening devices in the sample under examination

5.3 Correlation between forecast and surveyed damage

The validation of the results can be carried out by measuring the correlation between the set of data on the damage investigated obtained from the survey, and the dataset of forecasts produced by FaMIVE.

While in the case of failure mechanisms a comparison between surveyed and predicted data is fairly straightforward, the major difficulty arises when dealing with damage levels. In the next section, the method adopted for correlating the damage levels with FaMIVE results will be critically discussed, followed by a discussion on the correlation between actual and forecast failure mechanisms.

5.3.1 Damage levels: a criterion for appraisal of correlation

As introduced in §3.7 the seismic vulnerability is defined as a function independent of the earthquake intensity but dependent upon the ultimate capacity of a building to resist earthquakes (μ), corresponding to a given failure mechanism and a percentage of façade most probably involved. The critical load factor μ value is assumed to correspond to a failure at an

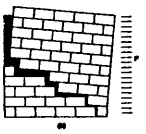

incipient stage associated with a moderate damage, represented by level D2 (from the 6-point scale of EMS '98). This is equivalent to assuming a certain ductility in the mechanical behaviour of masonry walls, which means that the failure mechanism will have to develop completely before producing a total collapse (by overturning or sliding).

Since the results produced by the method, (i.e. Structural and Failure Extent indices, defined in §3.5, producing the final Vulnerability levels) are independent of the earthquake severity, they are not able to forecast the damage pattern in terms of likelihood of damage level or damage scenarios. Consequently, an attempt to devise a proper criterion to establish a reliable correlation between surveyed and forecast damage is developed.

The literature available on the damage evaluation contains a large amount of work dealing with observed damage, whereas the approaches aimed at forecasting damage are much more heterogeneous (see Chapter 1). Moreover, not all the methods try to correlate damage levels, earthquake intensities and structural behaviour defined by failure mechanisms (Bernardini et al. 1986, 1999), (Spence et al., 1991, 1992a,b).

As underlined in Chapter 1, the correlation between damage and earthquake is basically a probabilistic problem, and damage can be predicted by setting up proper probability models (Bernardini A., 1986), or using large amounts of data from different earthquakes aimed at creating damage scenarios (Braga et al 1982, Cobourn et al., 1992, Dolce, 1996, 1997, 2000, Faccioli et al.1999).

When large amounts of data are not available, an alternative approach is based on the identification of deterministic fragility curves (earthquake severity/damage levels) which best match the structural features of the building types under examination. This method can be considered sufficiently reliable only when each building sample is described by appropriate functions, while the use of the same fragility curve for any location and structural type would yield unreliable results, as in the case of the Italian GNDT method (§1.4.3), based on a tri-linear fragility curve calibrated on a single building sample (Guagenti et al., 1989).

From a structural point of view, the damage level, is defined by EMS '98 (Table 4.2) as the response of a building in terms of relative displacements, when subjected to an earthquake of given severity.

However, as outlined in §1.4.4, the displacement capacity of masonry buildings is not easily formulated because several variables influence the structural behaviour. The method

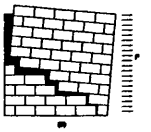

proposed by Calvi (1999) to formulate the displacement capacity of masonry buildings cannot be considered fully reliable as this is based on the formulation of the structural performance of r.c. structures, while the extension to masonry is rather arbitrary (§1.4.4).

Previous research on the same topic (Lewand et al., 1978, Powell et al.,1988), has proposed approaches based on deterministic functions, to define the prediction of the structural damage, in order to speed up vulnerability evaluations.

Particularly relevant in this context is the work of Powell et al. who propose a two criteria method: the first is based on the balance between a demand parameter of structures and their corresponding capacity, and the second on the degradation of structural parameters. For each criterion one or more damage parameters are processed, and from these a structural damage index is finally calculated. It is worth noticing that this index can also be related to the economic damage estimates. The method is interesting, as it attempts to devise simplified criteria to predict the structural damage without being based on processing data sets of previous damage. Its limitation is that it requires highly accurate evaluation of the structural parameter, and hence its suitability in extensive vulnerability investigations is limited.

This discussion leads to a better focus of the most appropriate way to correlate the observed and forecast damage:

- On the one hand, in the building sample under examination, the damage-related data involve a rather small set, and all associated with a given seismic severity. This would not allow any damage probability matrix to be created, since a large damage distribution from different earthquake intensities would be required.
- On the other hand, the theoretical model assumed for predicting the structural performance of masonry buildings introduced in Chapters 2 and 3 is not able to predict damage levels to which buildings would be subject under the effect of different earthquakes, as the seismic vulnerability is considered independent of earthquake intensity.

These considerations lead to the conclusion that the data set available can be processed to set up fragility curves correlating earthquake severity with damage levels. It is assumed that earthquake severity is measured in terms of Mean Acceleration, while the Peak Ground Acceleration recorded in Nocera cannot be considered reliable (Camassi, 1997, Capotorti, 1997), as introduced in §4.2.3.

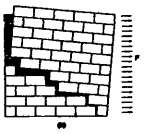

According to the assumptions made, a building with a given μ value, undergoes damage of level D2 when subjected to an earthquake of severity A/g =μ.

In other words the first point of the hypothetical fragility curve of a given building is represented by its μ value associated with damage level D2.

However, it could be argued that if the same building was subjected to stronger earthquakes (A/g >μ), it would probably be subjected to higher damage levels or it could pass from one critic mechanism to another.

Consequently, for earthquake severities progressively higher than A/g =μ, the crack pattern of the building would widen, until a total collapse corresponding to damage level D5, is reached. Conversely, earthquakes severities lower than μ would produce less damage on the building under examination.

The patterns of the vulnerability function before and after the point μ/D2 are unknown, and mainly depend upon the ductility of the building under examination.

Considering that the structural behaviour of masonry buildings is basically characterised by inelastic behaviour preceded by an initial short elastic phase, a first straight segment is assumed up to damage level D2, followed by a curvilinear pattern showing a rapid increase in damage for a rather small increase in earthquake severity.

The two patterns of the function are formulated as follows:

$$\text{(for } i \le \text{D2)} \quad A/g_i = \left(\frac{1}{2}\cdot(i-1)\cdot(2-\alpha)\cdot A/g_2\right) + \alpha \cdot A/g_2 \tag{5-1}$$

$$\text{(for } i > \text{D2)} \quad A/g_i = \frac{(A/g)_{(i-1)}\cdot i}{(i-1)}\cdot\beta \tag{5-2}$$

where:

- i is the damage level, represented by a discrete variable ranging from 0 to 5;
- A/g_i is the value of A/g required to produce damage of level i;
- A/g_2 is the value of A/g required to produce damage of level D2, and hence is equal to the μ value;
- α is a variable ranging from 1 to 2 governing the inclination of the diagram up to damage level D2;

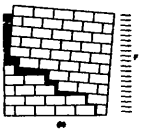

β is a variable ranging from 1 to 2 governing the inclination of each segment of the diagram from damage level D2 to D5;

The two variables, being unknown, have been identified by an optimisation process in order to maximise the correlation between the surveyed and forecast damage (Figure 5- 15). The process has led to a maximum correlation factor of 0.63, obtained for values of the two variables α and β, respectively 1.8 and 1.2.

The correlation has been carried out by considering an Mrsa (Mean Response Spectrum Acceleration) of 0.4, (as average of the 4 acceleration peaks registered before and after the peak ground acceleration), instead of the overestimated PGA registered on the 26th of September (0.56). The Mrsa has been calculated after a careful examination of the accelerograms, particularly that registered at 11:40 a.m, which has enabled the most significant peaks around the PGA value to be highlighted.

The diagram of Figure 5- 15 displays the distribution of damage levels for each building plotted against their calculated μ (green dots). This distribution is compared with that associating damage levels obtained from the fragility curves of Figure 5-16 with the same values of μ, relative to the building under examination (red dots).

The fragility curves obtained (Figure 5-16) for building types with different μ values show a first straight and very steep segment followed by a more gentle curve for damage levels greater than D2. As with the GNDT fragility curves (CNR-GNDT, 1993), the onset of damage is associated with $A/g > 0$, although in the case of GNDT the functions follow straight segments up to level D5.

The curves proposed also allow the creation of damage scenarios. Figure 5- 17 shows the cumulative results, expressed in building percentages, obtained for each damage level, in relation to different earthquake severities. This diagram offers a further opportunity for correlation, by comparing the actual damage level distribution caused by the 1997 earthquake with that forecast. The resulting correlation factor (0.68) can be considered fairly acceptable.

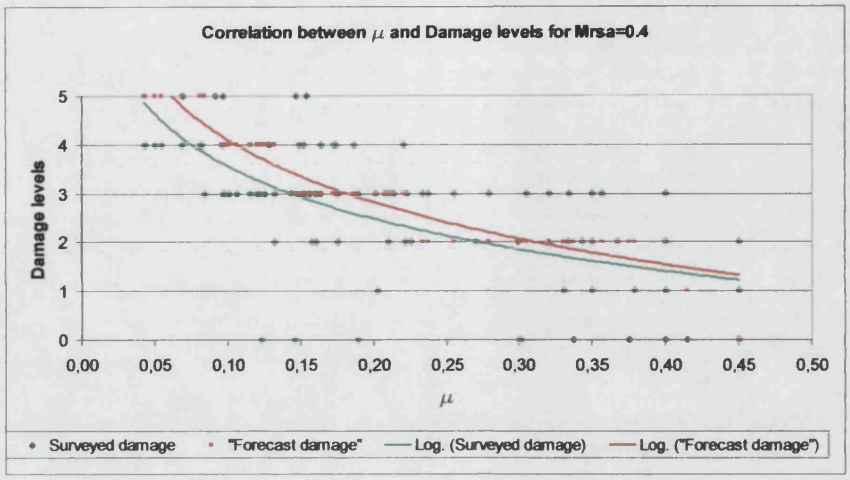

Figure 5- 15 – Correlation between μ and Damage levels surveyed and predicted

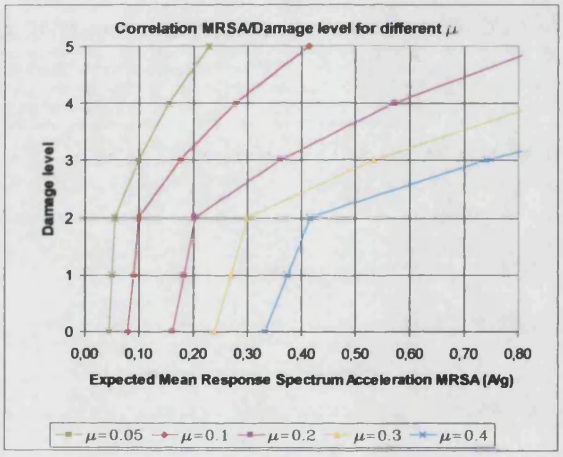

Figure 5- 16 – Fragility curves for different μ values

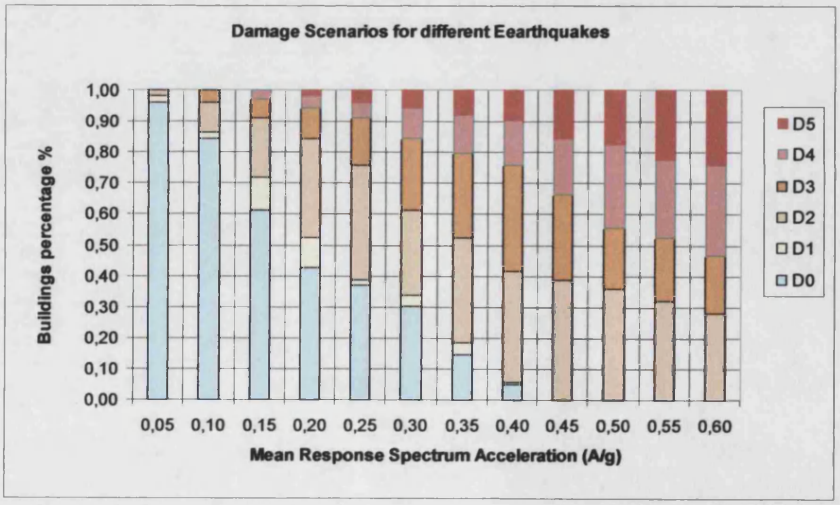

Figure 5- 17 – Damage scenarios for Nocera for different earthquakes

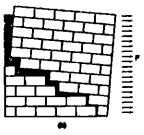

5.3.2 Correlation between failure mechanisms surveyed and forecast

The method proposed is further validated by comparing the results produced by FaMIVE in terms of failure mechanisms predicted with those recognised in the survey introduced in §4.4.2.

Figure 5- 18 displays the results side by side in terms of the cumulative percentages for each failure mechanism surveyed and predicted. As can be noted, the correspondence is rather good, particularly for global mechanisms (A, B1-B2), while for partial overturning mechanism, such as D, E and G the forecast percentages are considerably higher than those observed. These results clearly indicate the tendency of the procedure to favour some mechanisms to the detriment of others.

This issue leads directly to a re-examination and critical discussion of the process by which each failure mechanism is screened and the seismic vulnerability evaluated.

As described in §3.7, the final vulnerability class, obtained as a combination of the Structural and Damage Extent indices (§3.5), does not necessarily correspond to the highest vulnerability of the building, since it focuses on the lowest collapse load factor of the structure.

The Failure Extent index is involved in the vulnerability assessment only once the failure mechanism has already been screened, so that it is not totally independent of the other index.

In other words, the vulnerability resulting from this process tends to "privilege" failure mechanisms associated with very low μ, such as D, E, G and Gs, while failure mechanisms whose onset requires a higher amount of energy, such as F, B1 or B2, are less likely to occur.

Figure 5- 18 highlights the presence or absence of correlation, between the failure mechanism recognised and predicted for each building. The correlation between these two sets of data (0.76) is fairly acceptable.

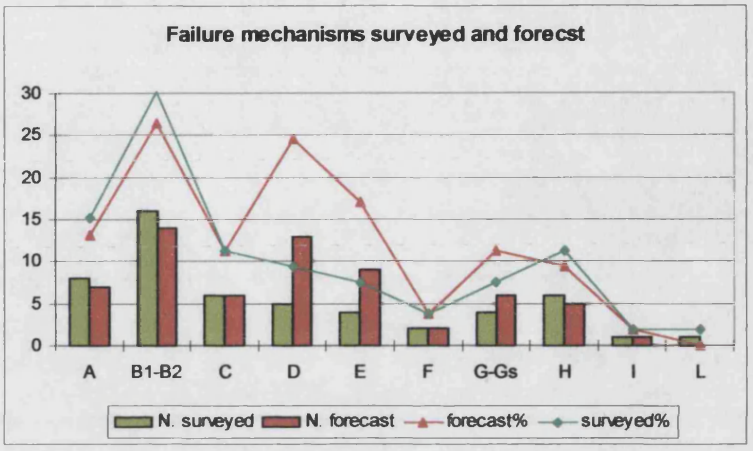

Figure 5- 18 – Comparison between failure mechanisms surveyed and forecast

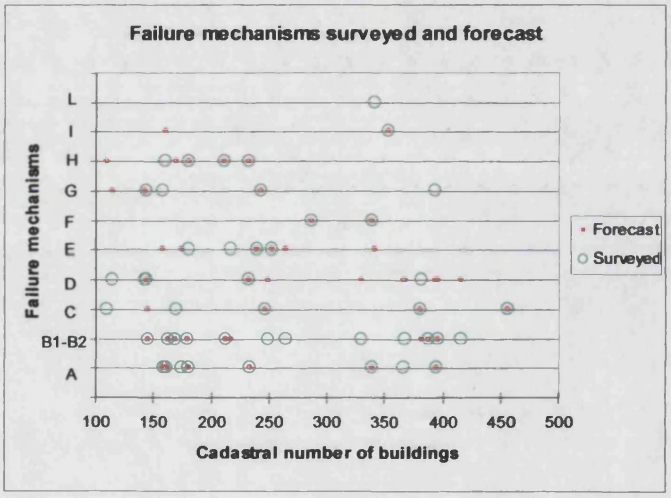

Figure 5- 19 – Failure mechanism surveyed and forecast: check for all the buildings of the stock

5.4 Conclusions

The results achieved by FaMIVE, in terms of μ, failure mechanism likelihood and vulnerability classes enable the following conclusions to be drawn:

- The average μ obtained over the building stock analysed is 0.36. Unlike other statistical methods such as PSI or DPMs (Spence et al.1991, Whitman et al. 1973) the μ distribution does not follow a normal pattern, since it is independent of the observed damage but depends on structural factors interacting with each other;

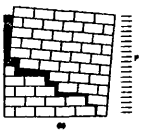

- The correlations between μ values and some structural features such as maintenance levels, masonry fabrics and connections with orthogonal walls are fairly good so that good structural features generally correspond to a rather high μ. Anomalies are due to the several other factors influencing the structural performance of buildings;
- The distribution of seismic vulnerability over the urban layout is able to highlight some typical features such as the increase in vulnerability levels for buildings placed at block edges. However it is not possible to draw definitive conclusions because of the small number of blocks in the sample and the neglect of some important features such as the interaction between adjacent buildings, which could be included in future development of the method;
- The distribution of the Structural and Failure Extent indices in the diagram of Figure 5- 13 shows some empty areas which could be attributed to the small number of buildings considered in the sample or to a certain dependence between the two indices which could mean that buildings with high Structural index and low Failure Extent index are unlikely;
- The correlation between strengthening devices and vulnerability classes is rather good. However, reinforcements are considered as always effective, i.e. ring beams always anchored to walls and ties never failing under tension. This assumption could produce final predicted vulnerability evaluations slightly lower than the one leading to the observed damage;
- The correlation between observed and forecast damage levels is carried out by setting up fragility curves (Figure 5-16), relating earthquake severity to damage levels, as defined by EMS'98, for building classes characterised by similar μ. The pattern of vulnerability curves is optimised by maximising the correlation factor between observed and predicted damage levels of Figure 5- 15.
- The correlation between observed and predicted failure mechanisms highlights that the procedure tends to choose some mechanisms in preference of others. This is attributed to the fact that the decision criteria is not necessarily associated with the highest vulnerability of the building, but to the lowest μ of the structure.

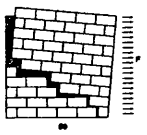

CHAPTER 6

CONCLUSIONS

6.1 Overview

A simple evaluation method has been developed in order to forecast the seismic vulnerability of historic masonry buildings.

The method is based on the identification of feasible collapse mechanisms of the most vulnerable wall of the building and on the calculation of its associated load factors. The mechanical performance is defined by a model of frictional behaviour developed specifically, on the basis of which the failure mechanisms are formulated.

The main advantages of the method can be summarized as follows:

- The method is simple allowing the evaluation of a large number of buildings without neglecting important features such as structural characteristics and mechanical performance of buildings;
- The procedure is based on simplified analytical models based on limit states analysis, requiring elementary input data which can be surveyed from the street. The interface with the computer program is very quick, so that the time required for investigating one building front can be estimated averagely around 20 minutes (assumed that the preliminary survey of §3.3.3 has been carried out);
- A mechanical formulation on purpose developed for ashlars masonry, enables the modelling of the shear strength acting along bedding surfaces, as well as the modelling of the in-plane failure of walls. The same model also allows the restraint action acting at wall intersections to be formulated and quantified, and on the basis of this more realistic failure mechanism can be developed;
- The seismic vulnerability is defined as independent from the earthquake severity and depending on the expected mechanical performance of the wall under examination, defined by the smallest load factor of the wall under examination which is associated with a given type of failure mechanism as well as with the number of storeys most likely involved;

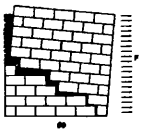

- The method also allows the level of reliability of information to be estimated on the basis of which upper and lower boundaries of the seismic vulnerability levels are defined;
- It could represent a useful tool for urban planning and strengthening policies at urban scale, carried out by Town Councils, and could be easily connected to a GIS (Geographic Information System).

It should be stressed that although the method takes in exam the peculiarities of each individual building, it can be considered more feasible to highlight the vulnerability distribution at a large target area in order to allow the extrapolation of the results for the use in statistical elaborations and earthquake scenario projects.

Notwithstanding the accuracy of the survey phase as well as of the analytical models, some simplifications were necessary in order to reduce the time expenditure. These simplifications particularly concern:

- Some internal structures, such as staircases and thrusting vaults, are neglected. However the presence of vaults has to be recorded during the survey phase in order to be implemented in further developments of the method, after which data previously processed could be re-examined to observe the influence of these structural systems;
- The interaction between adjacent buildings is neglected. The results achieved in §5.2.2, show that some salient features of the vulnerability distribution in the urban layout of Nocera are highlighted, though a greater accuracy in the results could be achieved by modelling this feature in a cluster analysis;
- Soils and foundations are not considered. These type of information are generally very difficult to obtain, unless carrying out local trials and investigations. Consequently the analytical model is assumed independent from these features, and hence it is not able to consider soil amplification factors;
- The frictional model developed in §2.2 relates to an ideal prototype of masonry ("opus quadratum"), which can be easily adapted to analyse very regular fabric layouts, such as dry ashlars masonry. The same model used for analysing very irregular fabric, where the presence of mortar is relevant, such as rubble, is undoubtedly less appropriate. This can lead to misevaluation of the total shear strength and consequently of the final vulnerability;

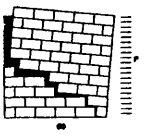

The results achieved in the application of the method in the historic centre of Nocera Umbra (Chapter 4 and 5), have highlighted the following limitations concerning the applicability of the method:

- The level of knowledge and experience required for carrying out the type of survey introduced in Chapter 2, especially in post-earthquake situations, requires the presence of specialised professionals, while less qualified operators, usually working in emergency situations, would not be able to reliably identify mechanisms without appropriate training;
- As highlighted in §4.3.2, the description of each masonry type requires the assignation of a friction coefficient. This process, which should be based on the evaluation of the smoothness level of bedding surface, implies a relatively high level of uncertainty, so that it could lead to unreliable evaluation of the Total Shear Strength introduced at §2.2, which strictly depend on this value. However, in Chapter 2 it was outlined that the stagger ratio s/h and the friction coefficient f, influence in the same way the mechanical performance of the masonry, so that this can be improved either increasing the ratio s/h or the friction coefficient f. Hence, a possible solution to this problem would be to assign pre-defined coefficients f to macro-classes of masonry (such as ashlars masonry, brickwork and so on), which could be carefully estimated on the basis of the literature available, while the stagger ratio s/h, much more easier to be surveyed, would be required during the investigation;
- Some problems concern the strengthening devices recognition and their real effectiveness. During the survey phase, some strengthening devices such as ring beams or metallic anchors can go unobserved since hidden by plaster or placed behind the masonry wall. On the other hand, the strengthening devices visible from the street, could have lost their effectiveness and hence should not be considered. The results produced by the method in both cases could hence loose in reliability, as the screening phase of §3.4.3 strictly depends on the strengthening devices layout;
- As highlighted in §4.5, failure mechanisms exhibits different level of recognition feasibility. To make an example, failure F can be recognised only if horizontal deformation along the wall together with the presence of one horizontal and two vertical cracks at its extremities are observed. In the case that the wall to be observed is rather

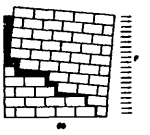

high to allow for an accurate inspection of the upper part, and also the damage is quite low, this particular mechanism can go unobserved. This issue can lead to wrong evaluations of damage occurred and consequently to unreliable correlations between observed and forecast damage;

Some further limitation of the method concerning the evaluation of the seismic vulnerability can be summarised as follows:

- The Vulnerability level is described in a qualitative way as combination between the two indices defined in §3.5.1, while a numerical value would allow more effective correlations and statistical elaborations;
- The Vulnerability level mainly relies on the value of the ultimate load factor of the wall under examination, rather than on the combination between the two indices defined in §3.5.1. This can lead in some cases to setting a final vulnerability level which is not necessarily the highest associated with the wall under examination.

6.2 Possible developments of the research

Beyond the limitations above mentioned which could be refined in a future development of the work, further objectives of a possible upgrade of the method are represented by:

- Laboratory tests on different masonry samples should be carried out in order to define in a more reliable way the friction coefficients and the effective sliding surface. This would enable to set up a range of likely values for each general masonry class (as dry ashlars masonry, rubble, brickwork and so on);
- Laboratory tests on different masonry samples should be carried out in order to analyse the role of mortar along joints and its influence in the mechanical performance of the masonry. The results could be used for setting up a more reliable criterion for calibrating the ideal "opus quadratum model" with different masonry fabrics realised by thick mortar joints;
- Set up of a criterion in order to take into exam the likelihood of ineffective strengthening devices. This should lead to define wider gaps between lower and upper boundaries defining the seismic vulnerability;

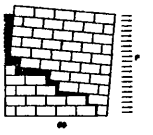

- Development of a screening process of the two Indices I_s and I_f in order to be associated always with the highest level of vulnerability;
- Set up of a criterion for describing the final seismic vulnerability through a numerical value rather than on qualitative descriptions.
- Set up of a integrated procedure in order to correlate the database of FaMIVE to a GIS, such to become a powerful tool for analysing the vulnerability at urban scale, and to automatically create damage scenarios;
- Elaboration of more sophisticated fragility curves based on probabilistic criteria, also taking into account the treatment of uncertainty according to the theory of fuzzy set (Blockley, 1992, Ballocco et al.2003, Carpignano et al.2002);
- Quantification of economical losses;
- Identification of strengthening patterns in order to mitigate the damage and reduce the associated vulnerability.

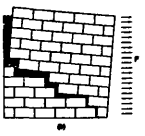

Bibliography

Albini A., Alinaghi H., Azzaro R., Barbano M.S., Camassi R., Carocci C., et al. (ING); Cecic I. (Geophisical Survey of Ljubljana, Slovenja) (1997). Rilevamenti macrosismici dell'area interessata da danni agli edifici in occasione di recenti terremoti: interventi congiunti GNDT-ING-SSN per scopi di protezione civile. Il terremoto Umbro Marchigiano del 26 settembre 1997. Technical Report for the Department for Civil Protection, GNDT/SSN/ING, Milano-Macerata-Roma, Italy. 11pp.

Anonymous (1751). Distinta relazione de' danni cagionati dal terremoto nella terra ragguardevole di Gualdo di Nocera, seguito la notte 26 del Luglio 1751, printed in Foligno.

Anthoine A. (1991). In-plane behaviour of masonry: a literature review. Report EUR 13840 EN, Commission of the European Communities, JRC- ISPRA SITE.

Applied Technology Council, ATC-13 (1985). Earthquake damage evaluation Data for California, ATC-13, Applied Technology Council, ATC-13. Redwood City California.

Applied Technology Council, ATC-14 (1985). Evaluating the seismic resistance of existing buildings, ATC-14. Redwood City California.

Augusti G., Ciampoli M., Giovenale P. (2001). Seismic vulnerability of monumental buildings. In: Structural Safety, 23. pp.253-274.

Baggio C., Giuffrè A., Masiani R. (1990). Seismic Response of Mechanisms of Masonry Assemblages. In: Proceedings of the 9 World Conference on Earthquake Engineering, Moscow, pp.221-230.

Baggio C., Trovalusci P. (1993). Discrete models for joined block masonry walls. In: Proceedings of the 6th North American Masonry Conference. Philadelphia, pp.939-949.

Baggio C., Carocci C. (2000). Valutazione della qualità meccanica delle murature. In: La Vulnerabilità degli edifici: valutazione a scala nazionale della vulnerabilità sismica degli edifici ordinari. Edited by GNDT-CNR.

Ballocco G., Carpignano A., Gargiulo M., Piccini M. (2003) Merging Cut Sets Methods and Reliability Indexes for Reliability and Availability Analysis of Highly Meshed Networks. In: proceedings of European Safety and Reliability Conference (ESREL 2003), Maastricht, Belgium.

Baratta A., Bernardini A., Dolce M., Goretti A., Masi A., Zuccaro G. (1997). Danneggiamento degli edifici indotto dagli eventi sismici successivi al 26 Settembre 1997 in Umbria e Marche. In: "Ingegneria Sismica",XIV, n.3, Sept-Dec. pp.27-56.

Beconcini M.L., Caramelli S., Favilli A. (1984). Metodi di rilevamento della vulnerabilità sismica di centri edificati. In: Proceedings of the Italian Congress "L'Ingegneria Sismica in Italia", Rapallo, Italy, 6-9 June.

Benedetti, D., Petrini V. (1984a). Sulla Vulnerabilita' sismica di Edifici in muratura: un metodo di valutazione . In: L'industria italiana delle costruzioni, n.149. pp.66-74.

Benedetti D., Benzoni G.M. (1984b). A Numerical model for seismic analysis of masonry buildings: experimental correlations In: Earthquake Engineering and Structural Dynamics, vol.12, 817-831.

Benedetti D., Benzoni G., Parisi M. (1988a). Seismic Vulnerability and Risk Evaluation for Old Urban Nuclei. In: Earthquake Engineering& Structural Dynamics. Feb, vol.16, n.2, pp 183-201.

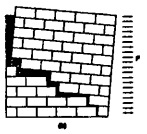

Benedetti D., Carydis P., Pezzoli P. (1998b). Shaking table tests on 24 simple masonry buildings. In: Earthquake Engineering and Structural Dynamics, vol. 27, pp.67-90.

Bernardini A., Modena, C. (1986). The vulnerability of masonry buildings typologies in a seismic area. In: Proceedings of the 8th European Conference on Earthquake Engineering, Lisbon, pp.2.3/57-62.

Bernardini A., Modena C. (1987). Un modello per le analisi di vulnerabilita' sismica di gruppi di edifici in muratura. In: Proceedings of the 3rd Italian Congress "L'Ingegneria Sismica in Italia", Rome. Vol.I, pp.59-70.

Bernardini, A., Modena C., Gori, R. (1988). Valutazioni di resistenza di nuclei di edifici in muratura per analisi di vulnerabilita' sismica. Internal Report of the Department of "Scienza e Tecnica delle Costruzioni", Univeristy of Padova, 2/88.

Bernardini, A., Gori, R., Modena C. (1989). A structural model for continous masonry building systems in historical centres. In: Proceedings of the International Technical Conference "Structural Conservation of Stone Masonry", Athens.

Bernardini, A., Gori, R., Modena C. (1992). Fuzzy measures in the knowledge based diagnosis of seismic vulnerability of masonry buildings. In: Probabilistic mechanics and structural and geothecnical Reliability, Proceedings of the 6th Conference, July 8-10 1992, Denver, Colorado.

Bernardini A. (1999). Qualitative and quantitative measures in seismic damage assessment and forecasting of masonry buildings. In: Seismic Damage to Masonry Buildings. Bernardini ed. Balkema, Rotterdam.

Binda L., Modena C., Baronio G., Abbaneo S. (1997). Repair and Investigation techniques for stone masonry walls. In: Construction and Building Materials, vol.11, n.3, pp.133-142.

Binda L., Gambarotta L., Lagomarsino S., Modena C. (1999). A multilevel approach to the damage assessment and the seismic improvement of masonry buildings in Italy. In: In: Seismic Damage to Masonry Buildings. Bernardini ed. Balkema, Rotterdam.

Binia A. (1751). Ragionamento sopra la cagione de' terremoti ed in particolare di quello della terra di Gualdo di Nocera nell'Umbria. In: Perugia, per li Costantini e Maurizi. pp.48.

Blockley D.I (1992). Structural Safety, Mc Graw-Hill, Berkshire, England.

Borgia A. (1910). La Cronaca della Diocesi Nocerina nell'umbria translated and published, by A.Alfieri, Rome.

Boschi E., Guidoboni E., Ferrari G., Valensise G. & Gasperini P. (EDS) (1997). Catalogo dei forti terremoti storici in Italia dal 461aC al 1990. vol.2. (ING-SGA). Bologna, Italy. p.644.

Braga F., Dolce M., Liberatore O. (1982a). A statistical study on damaged buildings review of the MSK-76 scale. In: Proceedings of the Conference of the European Association of Earthquake Engineering, Athens.

Braga F., Dolce M., Liberatore D. (1982b), Southern Italy November 23, 1980 Earthquake: A Statistical Study on Damaged Buildings and an Ensuing Review of the M.S.K.-76 Scale. CNR-PFG Edition. n.503, Roma.

Braga F., Liberatore O. (1984). Fast and reliable damage estimation for optimal relief operations. In: International Symposium on Earthquake Relief in Less Industrialized Areas, Zurich, 28-30 March. pp.145-151.

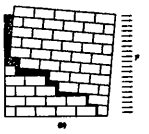

Braga F.,Dolce M., Liberatore O. (1987). Statistical calibration of second level seismic vulnerability of buildings. pp. 1069-1076. Proceedings of the 5th international conference on applications of statistics and probability in soil and structural engineering, Vancouver.

Braga F., Gavarini C. (1997a). Futuro per la Normativa Sismica Italiana. In: Proceedings of the 8th National Conference "L'Ingegneria Sismica in Italia". Taormina, 21-24 Sept.. Pp.739-746.

Braga F., Di Pasquale G., Dolce M., Liberatore D., GNDT Basilicata, Servizio Sismico Nazionale, (1997b). Terremoto del 26.9.97 e giorni seguenti in Umbria e Marche. Ispezione sui danneggiamenti verificatisi alle costruzioni situate nel centro storico di Sellano, rapporto sintetico.

Calabrese G. (1990). Caratteri della sismicità Umbra dai dati del catalogo ING dall'anno 1000. Ed. Graphos, Italy.

Calvi G.M. (1999). A displacement based approach for vulnerability evaluation of classes of buildings. In: Journal of Earthquake Engineering, Vol.3. pp.411-438.

Capotorti F., Monachesi G., Mucciarelli M., Sano' T., Trojani L. (1997). Danneggaimenti ed effetti di sito nel terremoto umbro-marchigiano del settembre 1997. In: "Ingegneria Sismica", vol. 14, n.3 Sept-Dec. Pp.12-21.

Carocci C. (1996). Conservazione dei centri storici in area sismica: Vulnerabilità e Mitigazione. PhD thesis, University of Rome "La Sapienza", Faculty of Architecture.

Carpignano A., Piccini M., Gargiulo M., Ponta A. (2002). Reliability and Availability for Highly Meshed Network Systems: Status of the Art and New Perspectives. In: Proc. Ann. Reliability & Maintainability Symp. (RAMS 2002), Seattle, Washington, USA, January 28-31.

Casolo S., Naumair S., Parisi M.A., Petrini V. (2000). Analysis of Seismic Damage Patterns in Old Masonry Church Facades. In: Earthquake Spectra, Vol.16, n.4. November.

Ceradini V. (1992). Modellazione, sperimentazione per lo studio della della struttura muraria storica. PhD thesis, University of Rome "La Sapienza", Faculty of Architecture.

Ceradini V. (1993). Qualità meccaniche e meccanismi di danno. In: A.Giuffrè, Sicurezza e conservazione dei centri storici. Il caso di Ortigia, Bari, Italy. pp.132-141.

Chiostrini S., Maestrelli L., Vignoli A. (1994). Numerical simulation of destructive tests on a full scale brick-masonry prototype.

CNR-GNDT (1993). Rischio Sismico di Edifici Pubblici, aspetti metodologici. Rome. part I.

CNR-GNDT (1999). The Catania Project: earthquake scenarios for a high risk area in the Mediterranean. Editors: Faccioli E., Pessina V. Rome.

CNR-GNDT (2000). Progetto Catania: indagine sulla risposta sismica di due edifici in muratura. Rome. Edited by: D.Liberatore.

Cobourn A.W. Earthen Buildings in Seismic Areas. (1984a) Proposal for international Standardisation of Recording Earthquake Damage to Earthen Buildings. The Martin Centre for Architectural and Urban Studies, Univ. of Cambridge, Dept. of Architecture.

Cobourn A.W., Kubin J., Spence R.J.S. (1984b). Vulnerability and Seismic Risk reduction for Rural Houses in Turkey. Proc.8thWorld Conference on Earthquake Engineering, San Francisco.

Cobourn A., Spence R. (1992). Earthquake Protection, Chichester, Wiley ed.

Colozza R., Dolce M. (1995). Vulnerabilità e rischio di danneggiamento di edifici, Il Centro Storico. Istituto Poligrafico dello Stato, Rome. pp.497-547.

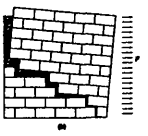

Corsanego A. (1985). A review of methodologies for seismic vulnerability assessment.. In: Restoration and Urban Planning of towns and regions in Seismic Prone Areas, International Conference on Reconstruction, November 5-9, Skopie, Yugoslavia.

D'Ayala D., Spence R. (1995). Vulnerability of Buildings in historic town centres. In: Proceedings of the 7th National Conference "L'Ingegneria Sismica in Italia", Siena, Italy, pp.363-372.

D'Ayala D., Spence R., Oliveira C. (1996). TOSQA Project, Earthquake protection for the Historic Town Centres: the case of the Alfama, Lisbon, September.

D'Ayala D., Spence R., Oliveira C., Pomonis A. (1997). Earthquake Loss Estimation for Europe's Historic Town Centres. In: Earthquake Spectra, November.

D'Ayala D. (1998). Correlation of seismic vulnerability and damage between classes of buildings: Churches and houses. In: Proceedings of the International Workshop on measures of Seismic Damage to Masonry Buildings. Monselice, Padova, Italy. 25-26 June.

D'Ayala D., Spence R. (1998). Earthquake damage and vulnerability assessment for historic masonry structures. In: Proceedings of the SISM-98. Workshop on Reducing earthquake risk to structures and monuments in the European Union. 26-27 Nov. Cambridge.

D'Ayala D. (1999). Correlation of seismic vulnerability and damage between classes of building: Churches and houses. In: Seismic Damage to Masonry Buildings. Bernardini ed. Balkema, Rotterdam.

D'Ayala D., Speranza E. (1999). Identificazione dei Meccanismi di Collasso per la stima della Vulnerabilità Sismica di Edifici nei Centri Storici. In: Proceedings of the 9th National Conference "L'Ingegneria Sismica in Italia" –20-23 Sept, Torino, Italy.

D'Ayala D., Speranza E. (2000) Seismic Vulnerability of historic centres: the case study of Nocera Umbra, Italy. Proceedings of the UNESCO Congress "More than two thousand years in the history of architecture", October, Paris, France.

D.D'Ayala, E.Speranza (2001). A procedure for evaluating the seismic vulnerability of historic buildings at urban scale based on mechanical parameters. Proceedings of the 2nd International Congress "Studies in Ancient structures", Yildiz, Turkey, July.

D'Ayala D., Speranza E. (2003). In plane and out of plane failure mechanisms on the basis of an opus quadratum mechanical formulation of the wall. Earthquake Spectra, August 2003.

De Buhan P., De Felice G. (1997). A homogenisation approach to the ultimate strength of brick masonry. In: J.Mech.Phys.Solids. Vol.45.N.7. pp.1085-1104.

Decanini L., Di Pasquale G., Orsini G., (1997). Considerazioni sui danneggiamenti osservati a seguito del terremoto 15.10.96 in Emilia Romagna. In: Proceedings of the 8th National Conference "L'Ingegneria Sismica in Italia". Taormina, 21-24 Sept.. Pp.209-216.

De Felice G., Carocci C. (1998). The code of Practice as guide for the safety and conservation of Palermo's historic centre. In: Proceedings of the SISM-98. Workshop on Reducing earthquake risk to structures and monuments in the European Union. 26-27 Nov. Cambridge.

De Felice G. (1999). Le strutture murarie: dall'osservazione alla previsione del danno sismico. In: Codice di Pratica per la Sicurezza e la Conservazione del Centro Storico di Palermo. Edited by Giuffrè A. and Carocci C. (Laterza, Bari).pp.99-120.

De Felice G., Giannini R., (1999). Assessment of seismic vulnerability to out-of-plane collapse of masonry walls. In: 12th WCEE.

De Felice G., Giannini R. (2000). Out of plane seismic resistance of masonry walls. In: Journal of Earthquake Engineering. Imperial College.

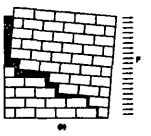

Dialer C. (1991). Some remarks on the strength and deformation behaviour of shear stressed masonry panles under static monolitic loading. In: Proceedings of the 9th International Brick Masonry Conference. October, Berlin, Germany.

Di Pasquale G, Serra C., Ferito R. (1999). Distribuzione del danno fra elementi strutturali di edifici in muratura danneggiati dal sisma. Internal Report of the SSN, Italy. SSN/RT/99/03.

Doglioni F., Moretti A., Petrini V. (1994). Le chiese ed il terremoto. Dalla vulnerabilita' constatata nel terremoto del Friuli al miglioramento antisismico nel restauro, verso una politica di prevenzione. Trieste, LINT editions.

Dolce M. (1996). Vulnerability Evaluation and Damage Scenarios. Proc. US-Italian Workshop on Seismic Evaluation and Retrofit, December, New York City.

Dolce M. (1997). La valutazione di Vulnerabilità per le analisi di Rischio Sismico e gli scenari di danno. In: Atti dell'8th ANIDIS International Congress " L'Ingegneria Sismica in Italia", Taormina, 21-24 Sept. Pp.217-226.

Dolce M., Marino M., Masi A., Vona M. (2000). Seismic Vulnerability Analysis and Damage Scenarios of Potenza Town, International Workshop on Seismic Risk and Earthquake Damage.

EERI Committee on Seismic Risk (1984). Glossary of Terms for Probabilistic Seismic-Risk and Hazard Analysis. In: Earthquake Spectra, vol.1. p.33.

EERI (1997). Special Earthquake Report, Reconnaissance Report on The Umbria Marche, Italy, Earthquakes of 1997.

EERI (2002). Encyclopaedia of Housing Types in Seismically Prone Areas of the World. www.world-housing.net.

Faccioli E., Pessina V., Calvi G.M., Borzi B. (1999). In: A study on damage scenarios for residential buildings in Catania city. In: Journal of Seismology, Vol. 3,No.3.

Fäh D., Kind F., Lang K., Giardini D. (2001): Earthquake scenarios for the city of Basel. In: Soil Dynamics and Earthquake Engineering, Vol. 21, pp. 405- 413.

FEMA (1988). Rapid Visual Screening of Buildings for Potential Seismic Hazards: A Handbook. FEMA 154, Washington.

FEMA (1988). Rapid Visual Screening of Buildings for Potential Seismic Hazards: Sup-porting Documentation. FEMA 155, Washington.

FEMA, NEHRP (1992). Guidelines for the Seismic Rehabilitation of Buildings. FEMA178, Washington.

FEMA, NEHRP (1997). Handbook for the Seismic Evaluation of Existing Buildings.FEMA 273, Washington, 1997.

FEMA, NEHRP (1998). Handbook for the Seismic Evaluation of Existing Buildings – a Pre-standard. FEMA 310, Washington.

Gambarotta L., Lagomarsino S. (1994). Modelling un-reinforced brick masonry walls. In: Proceedings of the U.S. Italy Workshop on Guidelines for Seismic Evaluation and Rehabilitation of Un-reinforced Masonry Buildings, Pavia (Italy) 22-24 June. Chapter 4, pp.17-29.

Ganze H.R. (1989). Failure criteria for masonry. Proc. Of the 5th Canadian Masonry Symposium. Vancouver.

Giovannini G. (1998). Un popolo nella prova. Bastia Umbra (PG).Di emme editions.

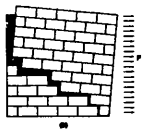

Giuffrè A. (1989). Mechanics of historical masonry and strengthening criteria. In: XV° Regional Seminar on Earthquake Engineering, Ravello, Italy, 18-23 September. Pp.61-91.

Giuffrè A. (1991). Letture sulla meccanica delle murature storiche. Kappa Ed., Rome.

Giuffrè A. (1993). Sicurezza e conservazione dei centri storici. Il caso di Ortigia, Bari, Italy.

Giuffrè A., Carocci C., De Felice G., Tocci C. (1994). Actuality and modelling of historical masonry. In: Proceedings of the U.S. Italy Workshop on Guidelines for Seismic Evaluation and Rehabilitation of Un-reinforced Masonry Buildings, Pavia, Italy. 22-24 June. Chapter I, pp.17-29.

Giuffrè A. and Carocci C. (1999). Codice di Pratica per la Sicurezza e la Conservazione del Centro Storico di Palermo. Laterza, Bari, Italy.

GNDT (1998). Progetto microzonazione sismica Umbria Marche- Analisi del danneggiamento. Cd-rom 1.

Grunthal G. (edited by) (1993). European Macroseismic scale 1992, Council of Europe. Luxembourg.

Grunthal G. 1998. European Macroseismic Scale 1998 , Cahiers du Centre Europ. de Géodyn. et de Séismlogie vol 15: 1-99.

Guagenti, E., Petrini, V. (1989). Il caso delle vecchie costruzioni: verso una nuova legge danni-intensità. In: Proceedings of the 4th National Conference "L'Ingegneria Sismica in Italia", Milano, 4-6 October. Pp.145-153

Hamid A.A., Drysdale R.G. (1981). Proposed failure criteria for concrete block masonry under biaxial stress. Journal of the Structural Division, ASCE, 107 (ST8).

Heyman J. (1966). The stone skeleton. In: Int. J. Solids and Structures. Vol.2. n.2 April. pages.249-279.

Kuobaa B., Nappi A., Papa E. (1994). Numerical analysis of masonry structures by using material models based on damage mechanics.

Lagomarsino S., Brencich A., Bussolino F., Moretti A., Pagnini L.C., Podesta' S. (1997). Una nuova metodologia per il rilievo del danno alle chiese. In: Ingegneria Sismica, XIV, n.3, Sept-Dec. pp-70-82.

Lagomarsino S., Doglioni F. (1998). La scheda per il rilievo dei danni sismici alle chiese nell'emergenza post terremoto. In: Rilievo dei danni e valutazione dell'agibilita' nell'emergenza post terremoto. Esperienze a confronto. Regione Emilia Romagna, Bologna, Italy. pp.I,38-49.

Lang K. (2002). Seismic vulnerability of existing buildings. Doctoral thesis of the Institute of Structural Engineering Swiss Federal Institute of Technology, Zurich, February.

Lewand T.K., Takahashi S.K. (1978). Rapid seismic analysis procedure. Report n.51-78-02, Naval Facilities Engineering Command, Port Hueneme, CA.

Livesley R.K (1978). Limit analysis of structures formed with rigid blocks. In: Int. J. Num. Methods. Eng. Vol.12.n.12. pages 1853-1871.

Mann W., Muller H. (1982). Failure of shear-stressed masonry – An enlarged theory, tests and application to shear walls. In: Proc. Of the British Ceramic Society, N.30.

Margottini C., Molin D., and Serva L (1993). Earthquake intensity vs peak ground acceleration in Italy (unpublished ms).

Mascheroni L. (1785). Nuove ricerche sull'equlibrio delle volte, Bergamo, Italy.

Menichelli A., Bontempi M. (1995). Nocera Umbra, Guida Turistica della città e del suo territorio.

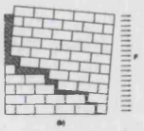

Medvedev S.V. (1965). Engineering Seismology, Jerusalem. Ed. Israel Programs for Scientific Translation.

Mucciarelli M., Monachesi G. (1997a). Evento del 26/9/1997. Scenario speditivo di danno. Preliminary report. Internet, http://www.geofisico.wnt.it/lastnews/970926/scedanni.html

Mucciarelli M., Monachesi G., e Pacor F. (1997b). Rilievi speditivi amplificazione locale e correlazioni con il danno osservato a seguito del terremoto Umbro-Marchigiano del 26 Settembre 1997. In:Prog.STA-2104; Doc.n. RAT-STA-1740/97,26pp.

Murphy J.R., O'Brien L.J. (1977). The correlation of peak ground acceleration amplitude with seismic intensity and other physical parameters. In: Bulletin of the Seismological Society of America.

National Institute of Building Science (NIBS) (1999). Earthquake Loss Estimation Methodology, HAZUS ® 99 Technical Manual. Report prepared for the Federal Emergency Management Agency, Washington D.C., 1999.

Okada S.,Takai N. (2000). Classifications of structural types and damage patterns of buildings for earthquake field investigation. In: Proceedings of 12 WCEE.

Orsini G. (1999). A model for Buildings Vulnerability assessments using the parameterless scale of seismic intensity. In Eartqhquake Spectra, vol.15, n.3. August.

Page A.W. (1981). The biaxial compressive strength of brick masonry. Proc. Instn. Of Civ. Engnrs. 71.

Page A.W. (1982). An experimental investigation of the biaxial strength of brick masonry. In: Proc. Of the 6th I.B. Ma.C. Rome.

Page A.W. (1983). The strength of brick masonry under biaxial tension-compression. In: Journal of Masonry Construction, 3.

Porter K. A., Kiremidjiian A.S., Le Grue J.S (2001). Assembly-based vulnerability of buildings and its use in performance evaluation. In: Earthquake Spectra, vol.17, n.2, May.

Postpischl D. (1986). Progetto finalizzato Geodinamica.

Powell G.H., Allahabadi R. (1988). Seismic damage prediction by deterministic methods: concepts and procedures. In: Earthquake Engineering and Structural Dynamics.vol.16, pp.719-734.

Pujades L.G., Canas J.A., Mena U., Espinoza F., Alfaro A., Caselles J. (2000): Seismic risk evaluation in Barcelona, Spain. Proceedings of the Twelfth World Conference on Earthquake Engineering, Auckland, New Zealand.

Samarasinghe W., Hendry A.W. (1980). The strength of brickwork under biaxial tensile and compressive stress. Proc. Of the 7th Int. Symp. On Load Bearing Brickwork, London

Sandi H. (1986). Vulnerability and Risk analysis for individual structures and systems. In Proceedings of 8th CEEE, Lisbon.

Sarà G., Barbetti G., Boni A., Marilli F., Nudo R., Viti S. (1997). Umbria Marche earthquake of 26 September 1997: damage scenarios and Vulnerability sources in the not-seismic masonry buildings.

Schnedider H., Schnell W. (1978). Versuche uber die Schubtrafahigkeit von Mauerwerk (test on the shear strength of masonry). Betonwerk and Fertigtaeiltechnik.

Sinha B.P. (1978). A simplified Ultimate Load Analysis of Laterally loaded Model Orthotropic Brickwork Panels of Low Tensile Strength. In: Struct.Eng. 56(4), pp.81-4.

Slejko, D., (1999). New seismic hazard maps of the Italian territory, SSN-GNDT, Rome 1999, website http://www.serviziosismico.it/PROG/2000/carte_pericolosita/index.html.

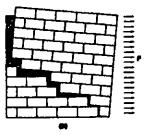

Spence RJS, Cobourn AW, Sakai S., Pominis A. (1991). A parameterless scale of seismic intensity for use in seismic risk analysis and vulnerability assessment. In: Saced ed., Earthquake, Blast and Impact: Measurement and Effects of Vibration. Elsevier Applied Science, Amsterdam.

Spence R., Coburn A. (1992a). Strengthening buildings of stone masonry to resist earthquakes. In: Meccanica 27, 213-221. Kluwer Academic Publisher.

Spence R., Coburn A., Pomonis A., Sakai S. (1992b). Correlation of ground motion with building damage: the definition of a new damaged-based seismic intensity scale. Proceedings of the 10th World Conference on Earthquake Engineering, Madrid.

Spence R., D'Ayala D., Martin B. (1998a). The Umbria-Marche earthquake of September 1997, Istitution of Structural Engineers, London, EEFIT report.

Spence R., D'Ayala D., (1998b). The Umbria-Marche earthquakes of September 1997: Damage Assessment and Preliminary Analysis. In: Structural Engineering International.

Spence R., D'Ayala D. (1999). Damage Assessment and Analysis of the 1997 Umbria Marche Earthquakes. In: Structural Engineering International, n.3.

Tampone G. (1999). Tipologie degli edifici danneggiati dal sisma. In: Manuale per la riabilitazione e la ricostruzione postsismica degli edifici (1999). Regione dell'Umbria. Dei ed.

Thibault C., Velkov P. (1994). Evaluation of seismic vulnerability criteria for the old urban nuclei of Nice. In: Proceedings of the Second International Conference on Earthquake Resistant Construction and Design. Berlin, 15-17 June.

Thibault C., Velkov P. (1995). Evaluation of seismic vulnerability of an urban neighbourhood in Nice. In: Proceedings of fifth international conference on Seismic Zonation. October 17-19, Nice, France.

Tocci C. Carocci C. (1995). La struttura Muraria nell'edilizia storica. Modelli Meccanici elementari. Internal Report of University III of Rome.

Tomazevic M., Turnsek V. (1982). Verification of the seismic resistance of masonry buildings. In: Proceedings of the British Ceramic Society n.30, Shelton House, Stoke on Trent. Str.360-369.

Tomazevic M., Anicic D. (1989). Research, technology and practice in evaluating, strengthening, and retrofitting masonry buildings: some Yugoslavian experiences. In: Proceedings of and International Seminar on Evaluating, Strengthening, and retrofitting Masonry Buildings. October, Arlington, Texas.

Tomazevic, Apih V. (1993). The strengthening of stone-masonry walls by injecting the masonry-friendly grouts. In: European Earthquake Engineering, 1-1993.

Tomazevic M., EERI, Lutman M., Weiss P. (1996). Seismic Upgrading of Old Brick Masonry Urban Houses: Tying of Walls with Steel Ties. In: Earthquake Spectra, Volume 12, No.3, August.

Tomazevic, M. (1999). Earthquake Resistant Design of Masonry Buildings. Imperial College Press, London.

Turnsek V., Cacovic P. (1979). Some experimental results on the strength of brick masonry walls. SIBMAC Proc., Stoke on Trent.

UNDRO (1979). Natural disaster and vulnerability analysis. Report of expert group meeting, U.N. press.

Vitruvius, The Ten Books of Architecture, M.H. Morgan trans., Dover, 1960.

Whitman, R.V., Reed, J.W., Hong S.T. (1973). Earthquake Damage Probability matrices. In: Proc. 5th World Conf. On Earthq. Engng., Rome, vol.1. p.2531.

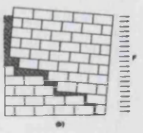

APPENDIX

Computer Program Framework

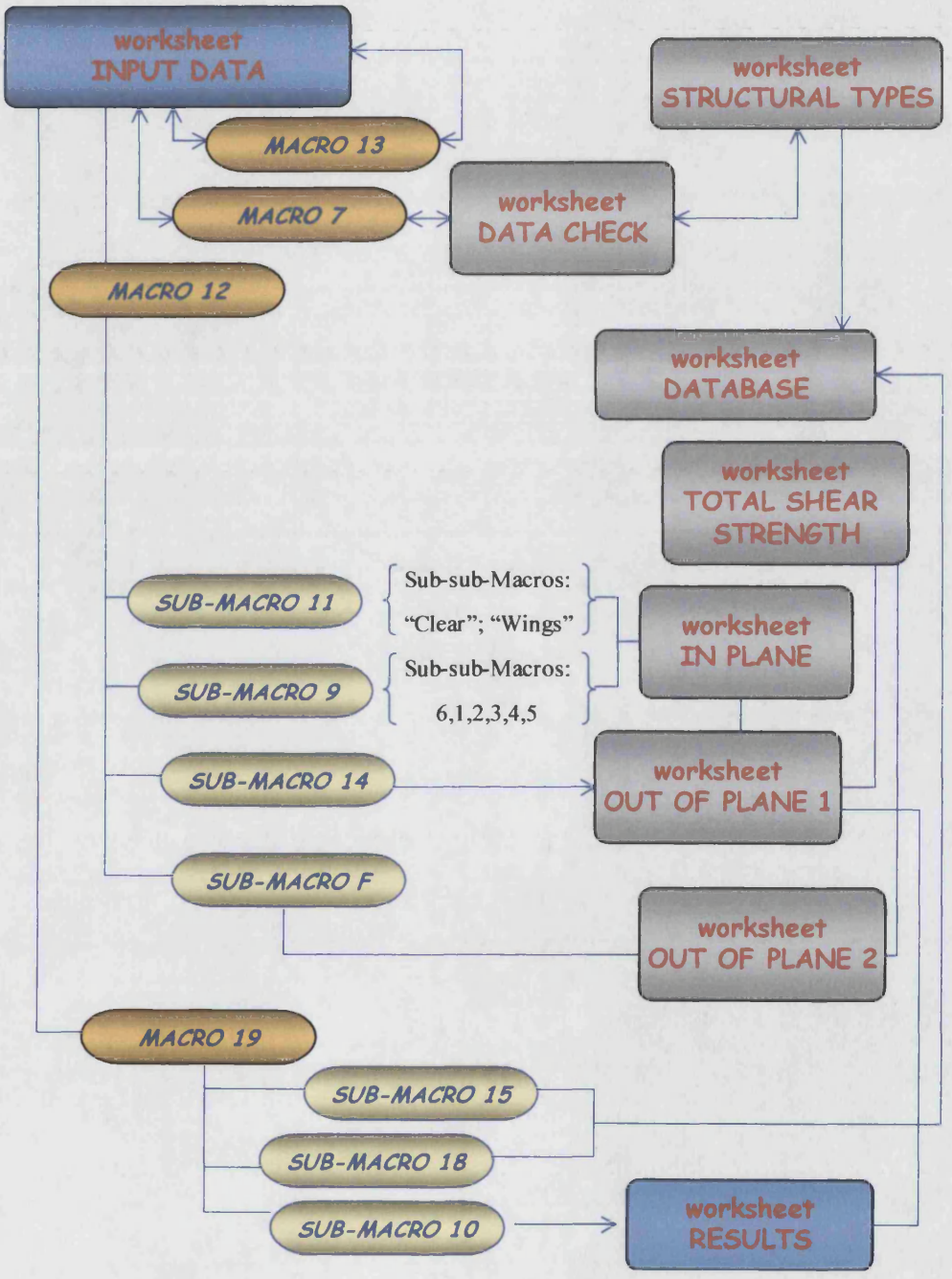

Figure A-1 – Computer program framework

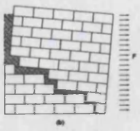

Worksheet Input Data

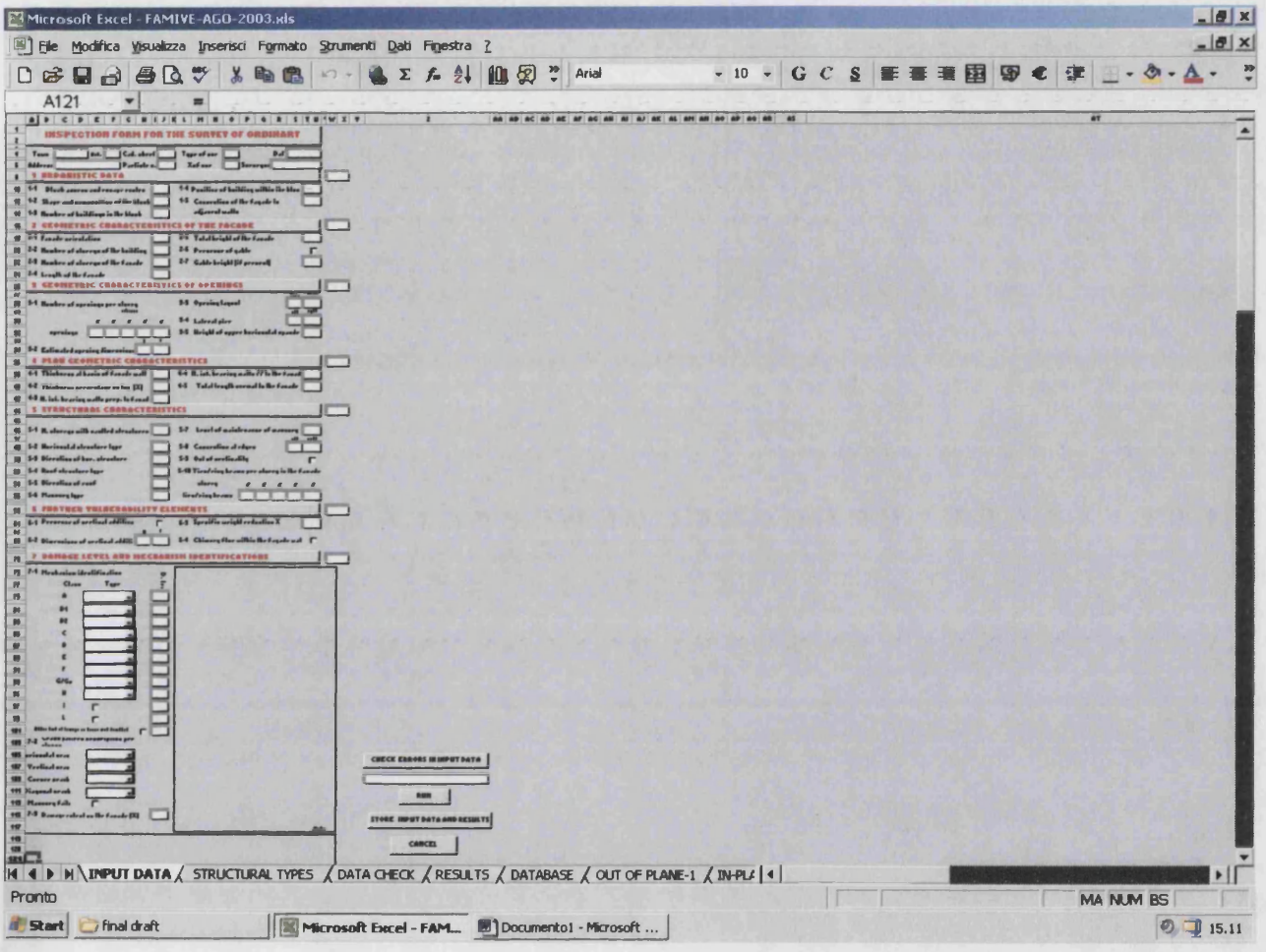

Figure A-2 – Worksheet "Input data"

List of Macros running in worksheet "Input Data":

Macro 13 (runs by intercative button) ⇒ *Clear the on line survey form*

Macro 7 (runs by intercative button) ⇒ *Check errors once the input data have been copied in worksheet "Data Check". Errors are then highlighted in apposite white box in" Input data";*

Macro 12 (runs by intercative button) ⇒ *Run the caluclation of all failure mechanisms, by means of the following sub-macros:*
Sub -Macro 11 *(Runs "In Plane")*
Sub Macro 9 *(Runs "In Plane")*
Sub Macro 14 *(Runs "Out of plane-1")*
Sub Macro F *(Runs "Out of plane 2")*

Macro 19 (runs by intercative button) ⇒ *Stores input data and results in worksheet "Input Data" and "Results" respectively;*

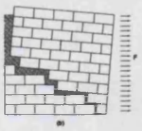

Worksheet Structural Types

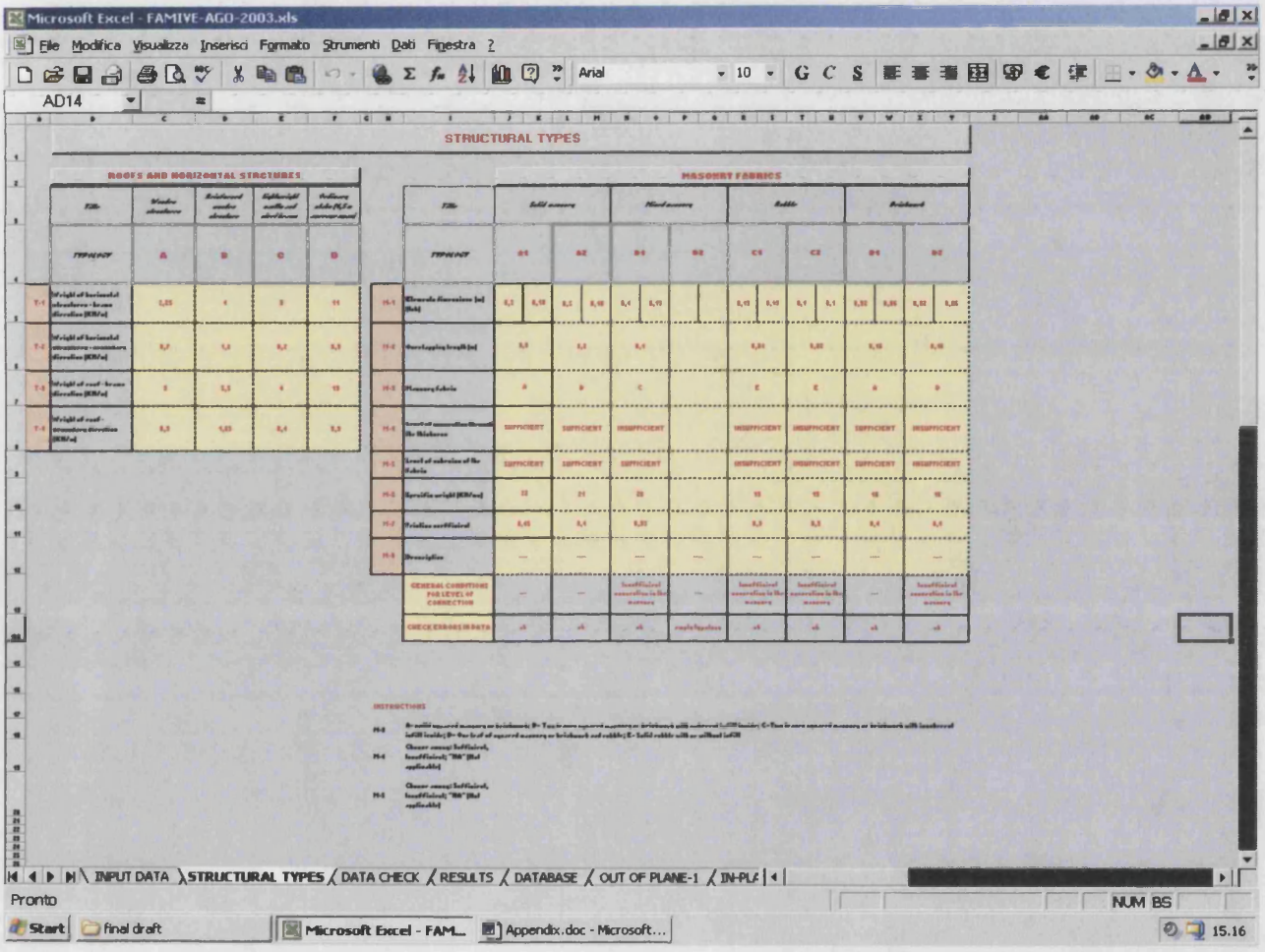

Figure A-3 – Worksheet "Structural Types"

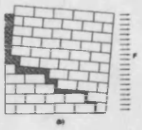

Worksheet Data Check

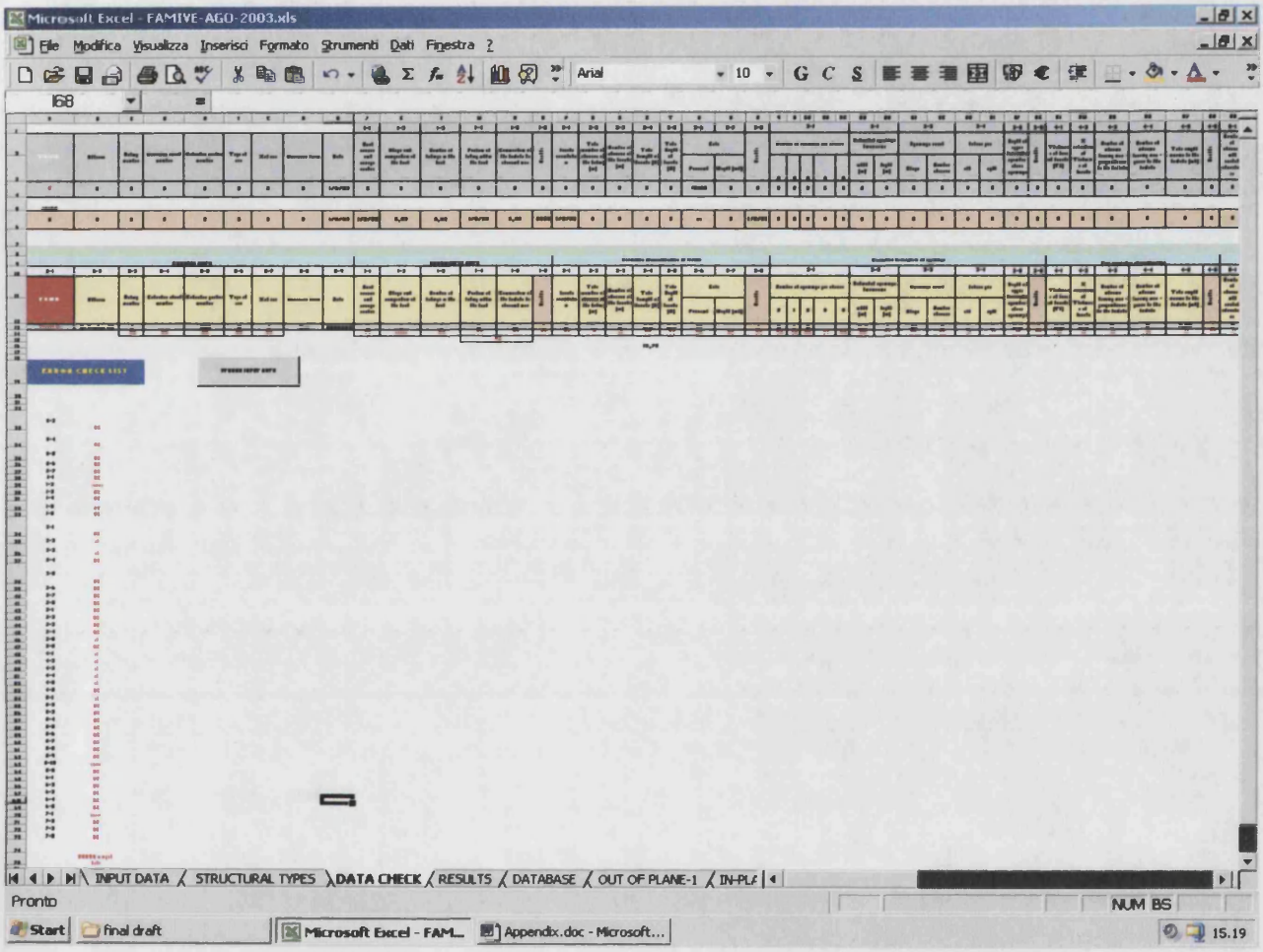

Figure A-4 – Worksheet "Data Check"

Worksheet In Plane

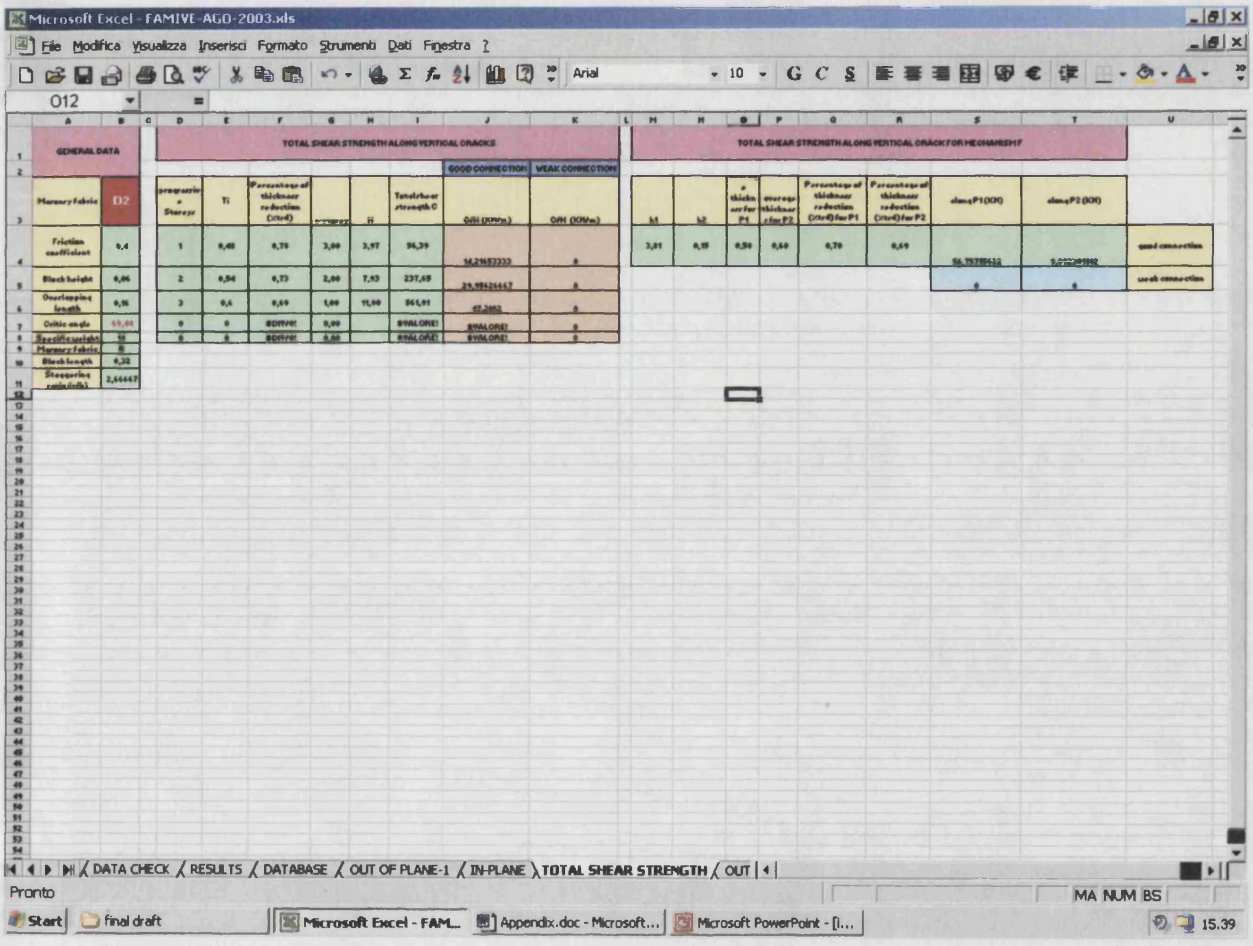

Figure A-5 – Worksheet "In plane"

List of Macros running in worksheet "In plane":

Macro 11 ⇒ *Calulates the crack angles on orthogonal walls by optimisation process. Sub macros:*
Sub Macro Wings
Sub -Macro Clear
Results are then copied in worksheet "Out of plane 1" and are used for calculating failure mechanisms such as C,B1, B2

Macro 9 (runs by intercative button) ⇒ *Calulates crack angles and load factors at every storey of the facade. Sub macros:*
Sub Macro 6,1,2,3,4,5

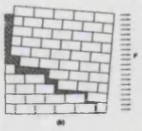

Worksheet Out of Plane 1

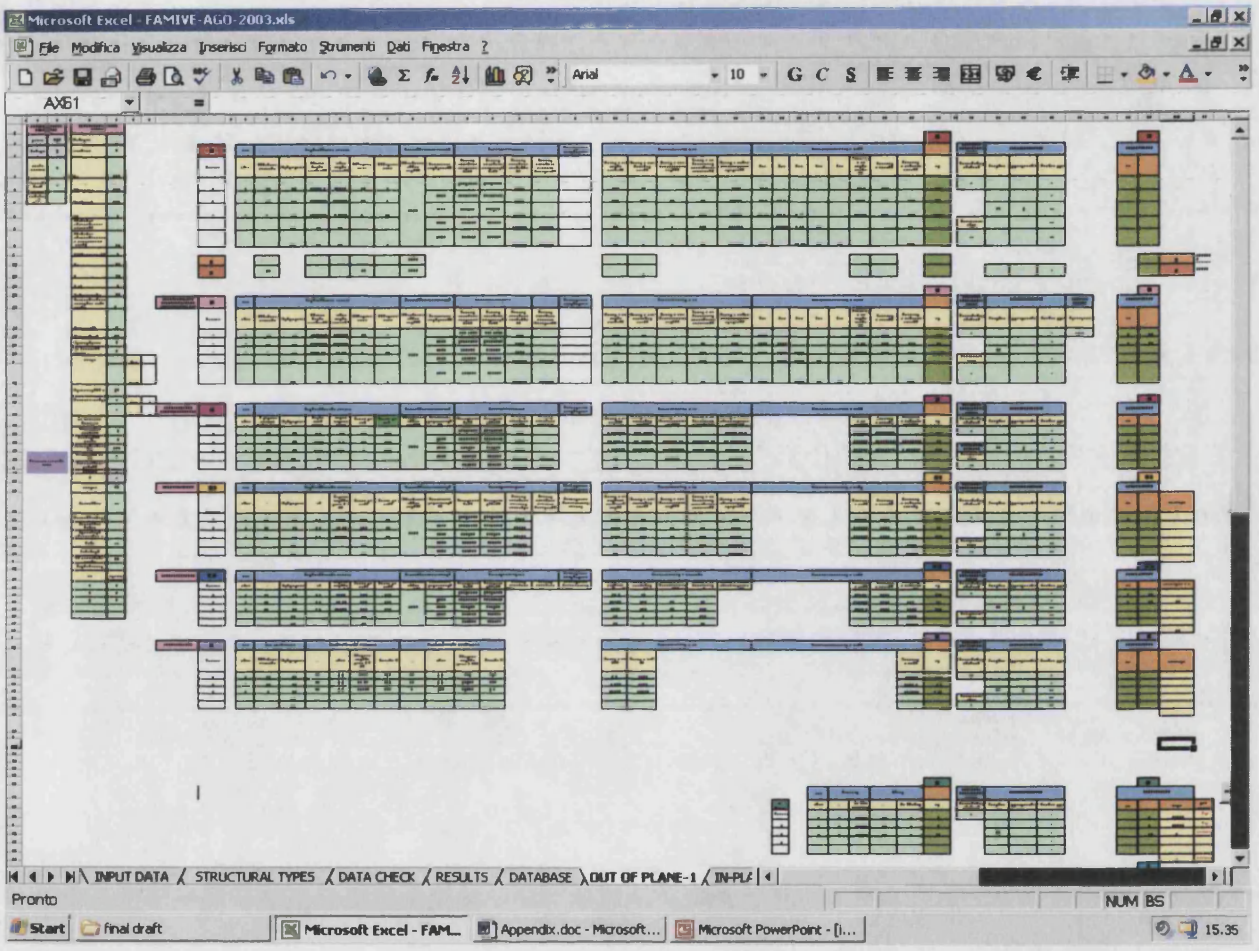

Figure A-6 – Worksheet "Out of plane 1"

List of Macros running in worksheet "Out of plane 1":

Macro 14 ⇒ *Calulates the horizontal arch effect G/Gs*

Failure mechanisms such as A, D,E,I,L are directly calculated in this worksheet without using macros.

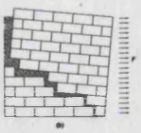

Worksheet Out of Plane 2

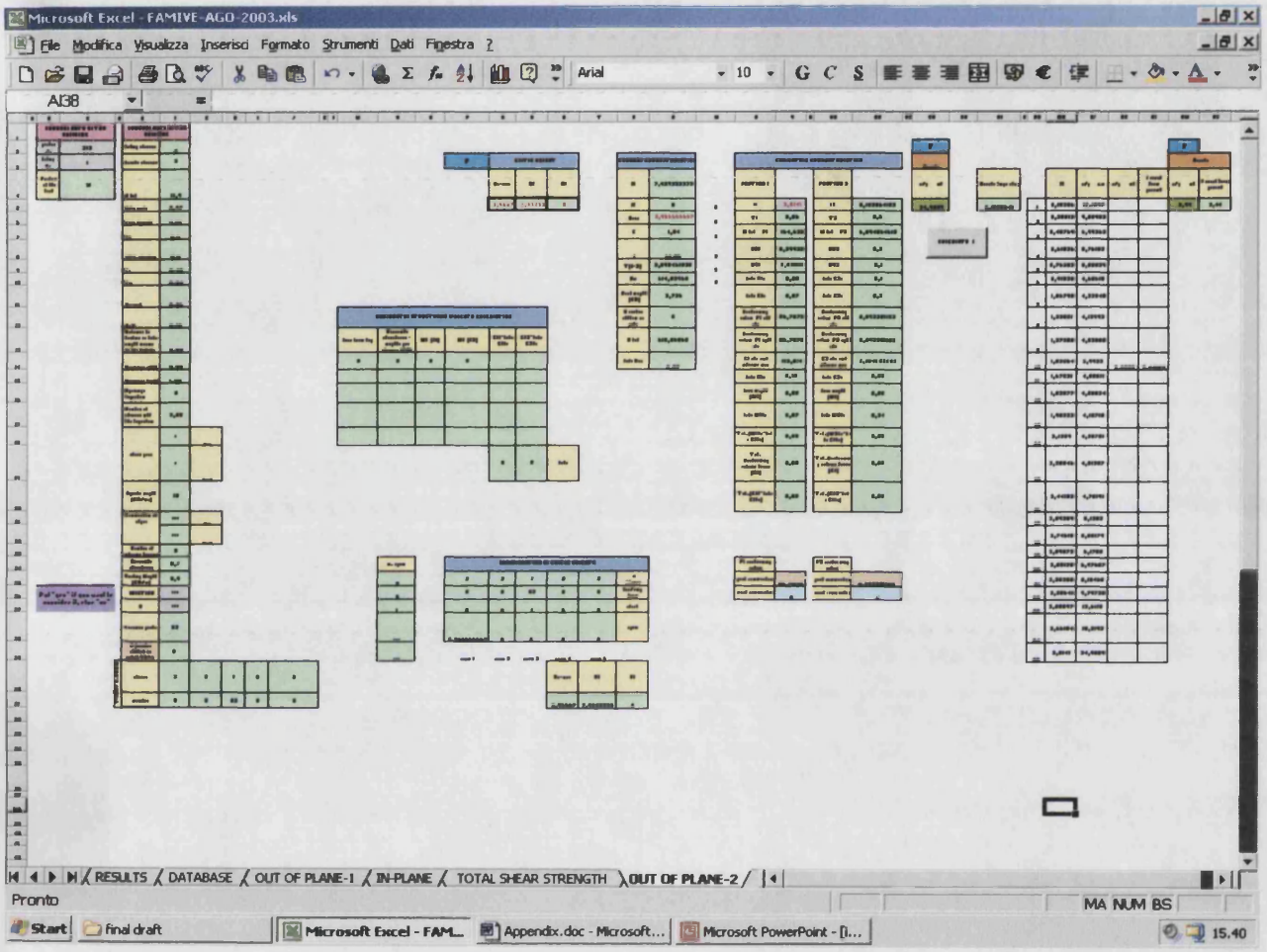

Figure A-7 – Worksheet "Out of plane 2"

List of Macros running in worksheet "Out of plane 2":

Macro F ⇒ *Calulates the vertical arch effect F.*
Results are then copied in Out of Plane 1

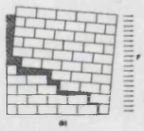

Worksheet Database

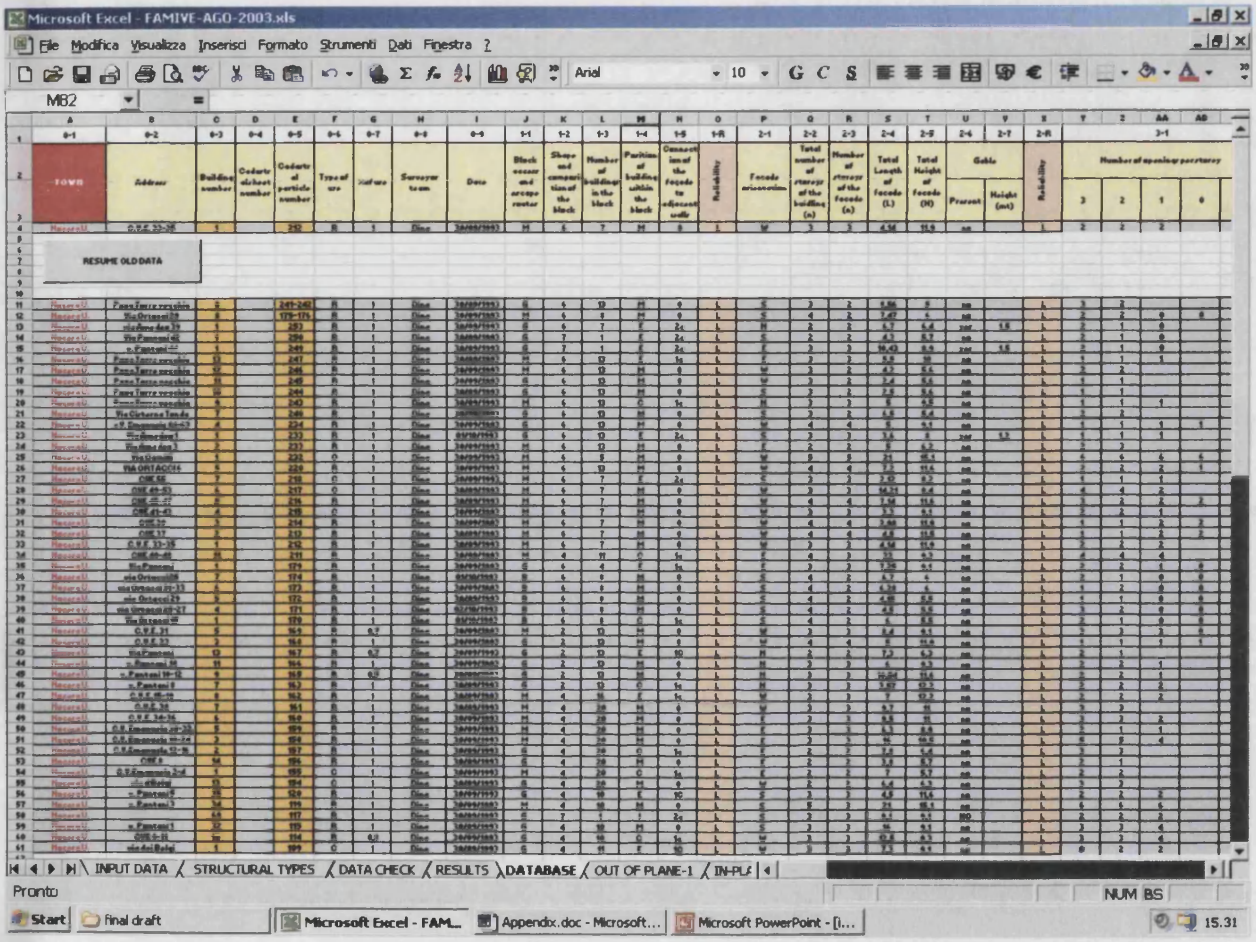

Figure A-8 – Worksheet "Database"

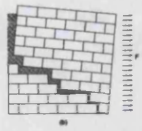

Worksheet Results

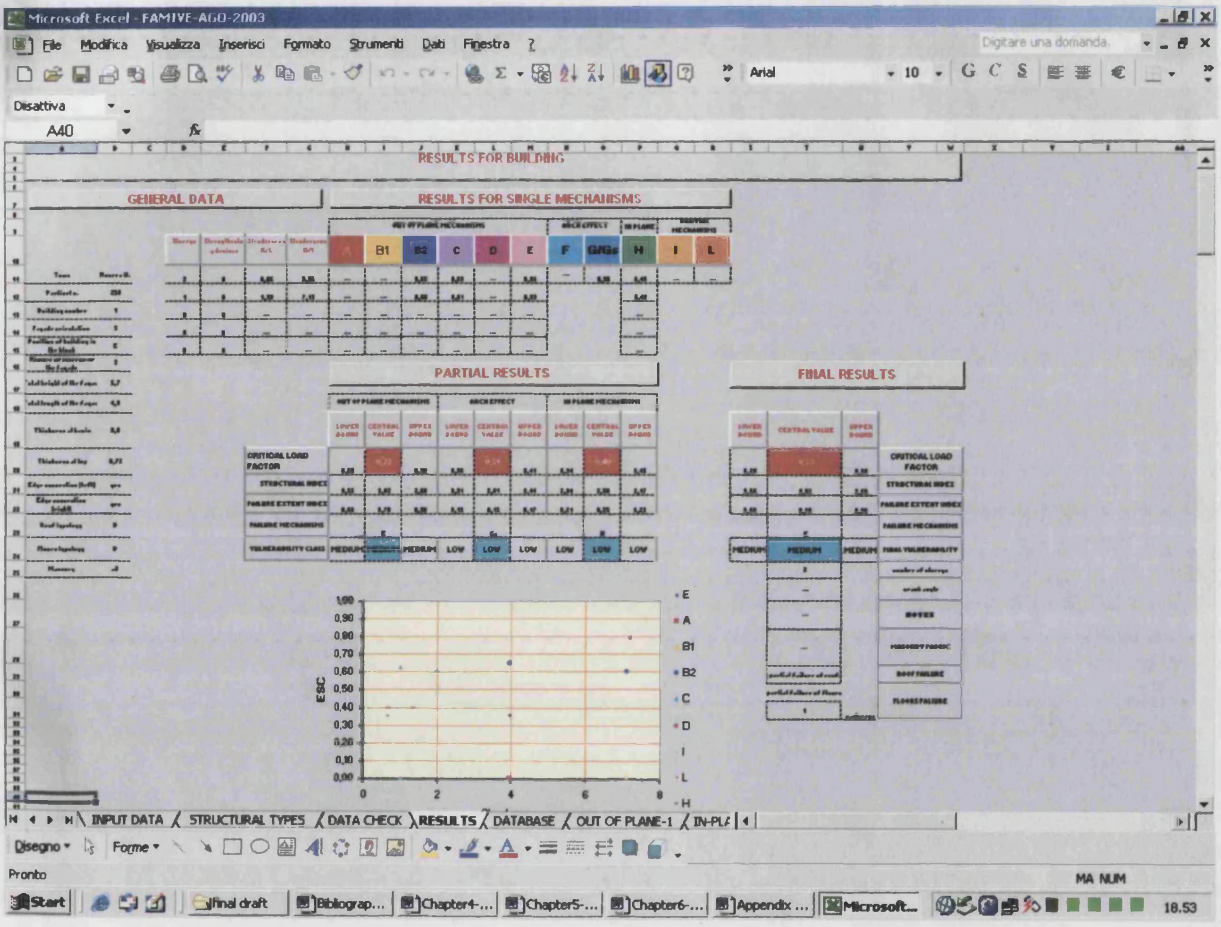

Figure A-9 – Worksheet "Results"